Organizations in supramolecular polymers: from the solution to the bulk behavior

Jessalyn Cortese

▶ To cite this version:

Jessalyn Cortese. Organizations in supramolecular polymers: from the solution to the bulk behavior. Polymers. Université Pierre et Marie Curie - Paris VI, 2013. English. NNT : . pastel-00813603

HAL Id: pastel-00813603
https://pastel.hal.science/pastel-00813603

Submitted on 15 Apr 2013

**THESE DE DOCTORAT DE
L'UNIVERSITE PIERRE ET MARIE CURIE**

Spécialité

Physique et Chimie des Matériaux

Présentée par

Mlle Jessalyn CORTESE

Pour obtenir le grade de

DOCTEUR de l'UNIVERSITÉ PIERRE ET MARIE CURIE

Sujet de la thèse :

**Organisations dans les polymères supramoléculaires :
du comportement en solution au comportement en masse**

soutenue le 15/02/2013

devant le jury composé de :

M. Ludwik LEIBLER	Directeur de thèse
Mme Corinne SOULIÉ-ZIAKOVIC	Co-Directrice de thèse
Mme Bernadette CHARLEUX	Rapportrice
M. Jean-François LUTZ	Rapporteur
Mme Min-Hui LI	Examinatrice
M. E.W. (Bert) MEIJER	Président du jury

Table of contents

Organizations in supramolecular polymers: from the solution to the bulk behavior

Table des matières

Organisations dans les polymères supramoléculaires : du comportement en solution au comportement en masse

Introduction

Supramolecular chemistry (the chemistry of noncovalent bonds) is a powerful tool to create new functional materials.[1] Indeed, since noncovalent interactions are reversible and sensitive to their environment, supramolecular materials can display stimuli-responsive characteristics, such as their size, rheology and viscoelasticity. Therefore, unlike high-molecular-weight covalent polymers, their processing and recycling can be easily achieved. Furthermore, incorporating noncovalent bonds into materials can impart original properties, such as self-healing. As a matter of fact, self-healing and thermoreversible rubbers from supramolecular assembly were developed in the Soft Matter and Chemistry Laboratory.[2]

In these self-healing elastomers, hydrogen bonds between small molecules allow them to self-assemble into three-dimensional networks reminiscent of reticulated polymers.[2] The associations involved are weak but numerous. The unique properties of these materials may be strongly influenced by its suspected nanostructuration, arising from a segregation between the polar hydrogen bonding groups (the stickers) and the apolar linkers between these groups (the spacers).[3,4] Indeed, phase segregation can facilitate hydrogen bonding by locally increasing the sticker concentration.[5] Furthermore, nanodomains are associated with slow diffusion processes, as in block copolymers,[6] and play a part in the healing after damage which implies a reconstruction of the nanostructure.[3,4]

---

[1] Steed, J. W.; Atwood, J. L.; *Supramolecular chemistry, 2nd Edition*; Wiley: Chippenham, UK, **2009**.

[2] Cordier, P.; Tournhilhac, F.; Soulié-Ziakovic, C.; Leibler, L.; **Self-healing and thermoreversible rubber from supramolecular assembly**; *Nature* **2008**, *451*, 977.

[3] Montarnal, D.; *Mise en oeuvre de liaisons réversibles covalentes et non-covalentes pour de nouveaux matériaux polymères recyclables et retransformables*; PhD Thesis, *Université Paris 6*, **2011**.

[4] Maes, F.; Montarnal, D.; Cantournet, S.; Tournilhac, F.; Corte, L.; Leibler, L.; **Activation and deactivation of self-healing in supramolecular rubbers**; *Soft Matter* **2012**, *8*, 1681.

[5] Sivakova, S.; Bohnsack, D. A.; Mackay, M. E.; Suwanmala, P.; Rowan, S. J.; **Utilization of a combination of weak hydrogen-bonding interactions and phase segregation to yield highly thermosensitive supramolecular polymers**; *J. Am. Chem. Soc.* **2005**, *127*, 18202.

[6] Yokoyama, H.; **Diffusion of block copolymers**; *Mater. Sci. Engineer.: R* **2006**, *53*, 199.

Besides, these self-healing rubbers were constructed so that crystallization of the hydrogen bonding groups is inhibited (by cultivating disorder of the linkers). Indeed, crystallization of the stickers in supramolecular polymers is a common phenomena.[7,8]

To investigate the interplay between directional interactions such as hydrogen bonding between the stickers, phase segregation between the spacers and the stickers and crystallization of the stickers, we have chosen to study a model system. This model system consist of noncrystalline poly(propylene oxide) (PPO) chains end-functionalized with complementary stickers: thymine derivative (Thy) and diaminotriazine (DAT). This system combines weak (Thy/Thy and DAT/DAT self-associations) and strong (Thy/DAT complementary association) hydrogen bonding, aromaticity of the stickers, strong repulsion between the polar stickers and the PPO spacers, and very different tendency towards crystallization for Thy and DAT. Indeed, Thy derivatives are prone to crystallization,[9] whereas DAT derivatives are known for their tendency to form glasses instead of crystallizing.[10,11]

In this thesis, we have focused on studying the structuration and rheological properties of this system, in solution and in the bulk.

In chapter I, the concept of supramolecular polymers is explained, put into the context of polymers and supramolecular chemistry, and the literature is reviewed by focusing on relevant examples.

---

[7] Lillya, C. P.; Baker, R. J.; Hutte, S.; Winter, H. H.; Lin, Y. G.; Shi, J.; Dickinson, L. C.; Chien, J. C. W.; **Linear chain extension through associative termini**; *Macromolecules* **1992**, *25*, 2076.

[8] Wietor, J.-L.; van Beek, D. J. M.; Peters, G. W.; Mendes, E.; Sijbesma, R. P.; **Effects of branching and crystallization on rheology of polycaprolactone supramolecular polymers with ureidopyrimidinone end groups**; *Macromolecules* **2011**, *44*, 1211.

[9] Borowiak, T.; Dutkiewicz, G.; Spychaia, J.; **Supramolecular motifs in 1-(2-cyanoethyl)thymine and 1-(3-cyanopropyl)thymine**; *Acta Crystallo. C* **2007**, *63*, 201.

[10] Wang, R.; Pellerin, C.; Lebel, O.; **Role of hydrogen bonding in the formation of glasses by small molecules: a triazine case study**; *J. Mater. Chem.* **2009**, *19*, 2747.

[11] Plante, A.; Mauran, D.; Carvalho, S. P.; Pagé, J. Y. S. D.; Pellerin, C. ; Lebel, O.; **Tg and rheological properties of triazine-based molecular glasses: incriminating evidence against hydrogen bonds**; *J. Phys. Chem. B* **2009**, *113*, 14884.

In <u>chapter II</u>, the functionalization of telechelic diamino PPO with Thy and DAT is described. DAT was grafted through an aromatic nucleophilic substitution, while Thy was grafted through amidation, by heating or with a coupling agent. Homoditopic compounds were synthesized in one step, while heteroditopic compounds were synthesized in four steps through a protection / deprotection pathway.

In <u>chapter III</u>, the solution behavior of our compounds and of their mixture in three solvents of different polarity (DMSO, chloroform and toluene) were studied using spectroscopic and rheological characterizations. The solvent has a tremendous impact on the Thy and DAT stickers association constants and on the supramolecular polymers organization. We show that DMSO is a dissociative solvent of the Thy-DAT hydrogen bonding association, while chloroform and toluene are non-dissociative solvents. Moreover, DMSO is a poor solvent of the PPO chains and a good solvent of the Thy and DAT stickers, while toluene is a poor solvent of the stickers and a good solvent of the PPO chains. The differences in structure and in association constants ($K_{Thy-DAT}^{25°C,toluene} \approx 22 * K_{Thy-DAT}^{25°C,chloroform}$) between toluene and chloroform are suggested to be due to better solvation of the stickers by chloroform and to aromatic interactions, on top of the hydrogen bonds, between the Thy and DAT aromatic cycles in toluene. As a result, our supramolecular polymers seem to form micelles with a PPO core and a Thy, DAT shell in DMSO; inverted micelles with a PPO shell and a Thy, DAT core in toluene; and linear chains through hydrogen bonding between Thy and DAT in chloroform.

In chapters IV and V, the bulk behavior of our compounds and of their mixtures were studied using spectroscopic, structural and rheological characterizations.

In <u>chapter IV</u>, we describe the long-range order and order-disorder transition (ODT) obtained for the main-chain supramolecular polymers based on PPO functionalized on both ends with weakly self-complementary Thy. Below the ODT temperature (T_{ODT}), these compounds exhibit a lamellar structure consisting of alternating 2D-crystallized Thy planes and amorphous PPO layers. Above T_{ODT}, they are amorphous and homogeneous. Macroscopically, the transition is accompanied by dramatic flow and mechanical properties changes. In contrast, the main-chain supramolecular polymers based on PPO functionalized

on both ends with DAT are disordered at all temperatures. Furthermore, we show that optimization of the directional interactions in these systems by strong complementary associations suppresses the mesoscopic order. Indeed, the microphase segregation observed for the self-complementary systems based on Thy (lamellar order and 2D crystallization of Thy) is inhibited by adding the telechelic supramolecular polymers based on PPO and DAT: the strong complementary Thy-DAT interaction inhibits crystallization of thymine in microdomains and lamellar structuration. As a result, the supramolecular polymer with only weakly self-complementary stickers is a solid, whereas the supramolecular polymer with strongly complementary stickers is a liquid.

In <u>chapter V</u>, we study the glass transition of our compounds. We show that grafting Thy and DAT stickers on telechelic PPO oligomers induces a glass transition temperature (T_g) increase that plays an important role on the materials properties. Indeed, as a result the materials based on the short PPO chains are solids at room temperature, whereas the materials based on the long PPO chains are liquids at room temperature. This increase of T_g can be ascribed either to the presence of hydrogen bonds and/or aromatic interactions (π-stacking) slowing down the chain dynamics or to the stiffness of the Thy and DAT stickers.

Parts of this thesis (mostly in chapter IV) were published in reference 12 and 13.[12,13]

---

[12] Cortese, J.; Soulié-Ziakovic, C; Cloitre, M.; Tencé-Girault, S.; Leibler, L.; **Order-disorder transition in supramolecular polymers**; *J. Am. Chem. Soc.* **2011**, 133, 19672.

[13] Cortese, J.; Soulié-Ziakovic, C; Tencé-Girault, S.; Leibler, L.; **Suppression of mesoscopic order by complementary interactions in supramolecular polymers**; *J. Am. Chem. Soc.* **2012**, *134*, 3671.

Acronyms and Abbreviations

ATR	attenuated total reflectance
BHT	butyl-hydroxy-toluene (2,6-di-*tertio*-butyl-4-methylphenol)
BOC	*tertio*-butyloxycarbonyl
COSY	correlation spectroscopy
DAT	2,6-diamino-1,3,5-triazine
DEPT	distortionless enhancement by polarisation transfer
DIEA	diisopropylethylamine
DMF	dimethylformamide
DMSO	dimethylsulfoxyde
DMSO-d_6	deuterated dimethylsulfoxyde
DSC	differential scanning calorimetry
FT-IR	Fourier transform infrared
GC-MS	gas chromatography coupled to mass spectrometry
HMQC	heteronuclear multiple quantum coherence
HOBt	hydroxybenzotriazole
MTBE	methyl-*tertio*-butyl ether
PEO	poly(ethylene oxide)
PPO	poly(propylene oxide)
NMR	nuclear magnetic resonance
TBTU	O-(benzotriazol-1-yl)-N,N,N',N'-tetramethyluronium tetrafluoroborate
TFA	trifluoroacetic acid
T_g	glass transition temperature
THF	tetrahydrofuran
Thy	thymine-1-acetic acid
WLF	Williams-Landel-Ferry

1a-c	NH$_2$-PPO-*X*-NH$_2$
2a-c	DAT-PPO-*X*-DAT
3a-c	Thy-PPO-*X*-Thy
4a-c	50/50-M-*X* (50/50 mixture of **3a-c** and **2a-c**)
5a	25/75-M-2200 (25/75 mixture of **3a** and **2a**)
6a	75/25-M-2200 (75/25 mixture of **3a** and **2a**)
7a-c	NH$_2$-PPO-*X*-BOC
8a-c	Thy-PPO-*X*-BOC
9a-c	Thy-PPO-*X*-NH$_2$
10a-c	Thy-PPO-*X*-DAT

with *X* the PPO chain molecular weight in g.mol^{-1}, **a**: *X* = 2200, **b**: *X* = 460, **c**: *X* = 250.

11a-b	(NH$_2$)$_3$-PPO-*X*
12a-b	DAT$_3$-PPO-*X*
13a-b	Thy$_3$-PPO-*X*
14a-b	50/50-Mtri-*X* (50/50 mixture of **12a-b** and **13a-b**)

with *X* the PPO chain molecular weight in g.mol^{-1}, **a**: *X* = 3000, **b**: *X* = 400.

15a-b	NH$_2$-PPO/PEO-*X*
16a-b	DAT-PPO/PEO-*X*
17a-b	Thy-PPO/PEO-*X*
18a-b	50/50-Mmono-*X* (50/50 mixture of **16a-b** and **17a-b**)

with *X* the PPO/PEO copolymerized [around 90% PPO and 10% PEO] chain molecular weight in g.mol^{-1}, **a**: *X* = 2000, **b**: *X* = 600, and CH$_3$ the other end-group.

<u>Chapter I</u>

From Polymers and Supramolecular Chemistry to Supramolecular Polymers

Polymers are long chains of atoms linked together by covalent bonds. Entanglements and viscoelasticity are a direct result of polymers length. These interesting properties, specific to polymers, explain polymers success in many applications, ranging from cosmetic to automotive, through packaging, electronics, building and medicine. However, polymers length can also hinder their processing and recycling. Supramolecular chemistry, the chemistry of noncovalent bonds, is a convenient tool to make functional materials as it introduces reversibility of the links between atoms and stimuli-responsiveness. To this end, hydrogen bonds are particularly useful. The concept of supramolecular polymers is to build polymers from small molecules and noncovalent directional interactions, thus bringing together the reversibility and stimuli-responsiveness of supramolecular chemistry with the specific polymer properties. Moreover, original properties such as self-healing can also be obtained. In this chapter, the main concepts of polymers and supramolecular chemistry are introduced, and the field of supramolecular polymers is reviewed by focusing on relevant examples.

Chapter I. From polymers and supramolecular chemistry to supramolecular polymers

1. Polymers

a. "Discovery" of polymers

(i) Polymers are macromolecules: many atoms covalently bonded

Polymers are chains of many molecular units, typically between hundreds and hundred-thousands, linked together by covalent bonds (Figure I.1). Staudinger demonstrated, by logical reasoning and experiments, their existence in the early 1920's.[1] However, they were not universally recognized until the 1930's.[2]

$$HO\text{-}(\text{-}CH_2\text{-}CH_2\text{-}O\text{-})_n\text{-}H$$
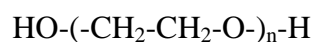
Figure I.1. Representation of a linear polymer: poly(ethylene oxide) (PEO).

(ii) Polymers are <u>not</u> noncovalent aggregates

Indeed, although very high molecular weights had been measured by physical methods, the leading organic chemists believed at the time that noncovalent aggregates of low-molecular-weight compounds caused these apparent high molecular weights.[2]

Definite, more convincing, evidence of polymer existence only came in the 1930's, when Carothers prepared synthetic polymers.[3]

---

[1] Staudinger, H.; **Über polymerisation**; *Ber. Dtsch. Chem. Ges.* **1920**, *53*, 1073.

[2] Presentation Speech by Professor A. Fredga, member of the Nobel Committee for Chemistry of the Royal Swedish Academy of Sciences, Nobel Prize in Chemistry **1953**: H. Staudinger, *Nobel Lectures, Chemistry 1942-1962*, Elsevier Publishing Company, Amsterdam, 1964.

[3] Carothers, W. H.; **Studies on polymerization and ring formation. I. An introduction to the general theory of condensation polymers**; *J. Am. Chem. Soc.* **1929**, *51*, 2548.

b. Specifities of polymers: entanglements and viscoelasticity

(i) Long chains are entangled

If the polymer chains are long enough, they entangle, which means that their motion is topologically restricted by other chains.[4,5,6] Indeed, a polymer chain cannot cross through another chain. To visualize this effect, a common image is that of a spaghetti dish, each spaghetti representing one polymer chain.

Entanglements of polymer chains can occur in the bulk (*i.e.* without solvent) or in concentrated solutions (Figure I.2c). In both cases, the dynamic properties are strongly influenced by the entanglements, because they impose constraints on the chains motions.[4,5,6] Since small molecules do not entangle, polymer melts and concentrated polymer solutions display dynamic properties very different than that of small molecules. Figure I.3 illustrates these differences: the onset of entanglements separates very distinct regimes of linear polymers viscosity behavior in the melt (Figure I.3a) and in solution (Figure I.3b). M_c and C_e represent the onset of entanglement effects, C^* the overlap concentration (Figure I.2). For polymer melts, $\eta \sim M$ for short chains ($M < M_c$) and $\eta \sim M^{3.4}$ for longer chains ($M > M_c$); whereas for polymer solutions, $\eta \sim C$ for low concentrations ($C < C^*$) and $C \sim C^{4.7}$ for higher concentrations ($C > C_e$).
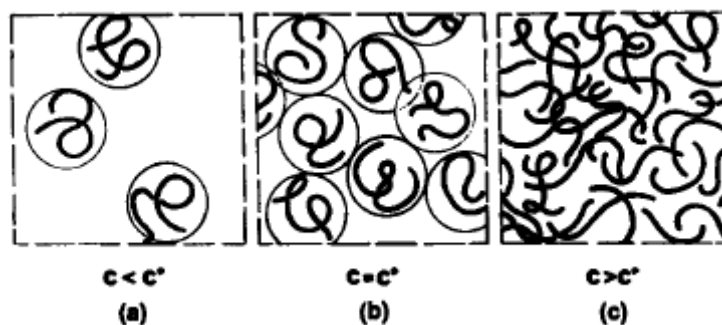
Figure I.2. Cross-over between dilute and semi-dilute solutions of polymers:
(a) dilute, (b) onset of overlap, and (c) semi-dilute, from ref 4.

[4] de Gennes, P.-G.; *Scaling concepts in polymer physics*; Cornell University Press: Ithaca, New York, **1979**.

[5] Doi, M.; Edwards, S.F.; *The theory of polymer dynamics*; Oxford University Press: USA, **1986**.

[6] Rubinstein, M.; Colby, R.; *Polymer physics*; Oxford University Press: USA, **2003**.
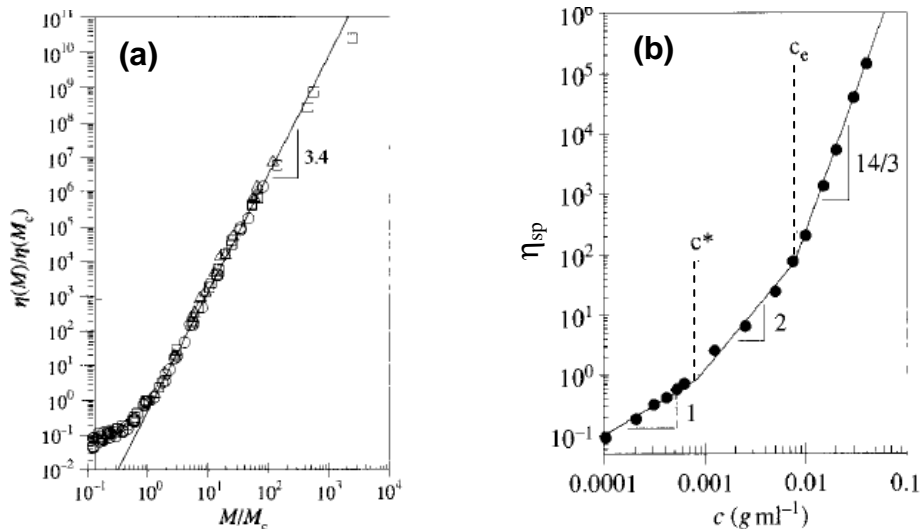
Figure I.3. Viscosity η (or specific viscosity η_{sp}) of linear and flexible polymers as a function of: (a) molar mass M reduced by their critical molar mass M_c [in the melt, for polyisobutylene (M_c = 14 000 g.mol^{-1}), polybutadiene (M_c = 6700 g.mol^{-1}), hydrogenated polybutadiene (M_c = 8100 g.mol^{-1})] and (b) concentration C [for poly(ethylene oxide) (M_w = 5 x 10^6 g.mol^{-1}) in water at 25°C], from ref 6.

(ii) Entanglements are responsible for viscoelasticity

Because of their entanglements, polymers are viscoelastic materials, which means that they combine both viscous (liquid-like) and elastic (solid-like) characteristics under strain or stress.[7] Unlike metals that never deviate far from perfect elasticity and unlike liquids of small molecules exhibiting Newtonian flow, the response of entangled polymers to deformations depends on the solicitation's time scale (Figure I.4).[7] Indeed, an entangled polymer melt presents an elastic response to short time scales (or high frequencies) deformations (Figure I.4b) and a viscous response to long time scales (or low frequencies) deformations (Figure I.4c).[8] At high frequencies, entanglements act as junction points or cross-links, resulting in a temporary network structure which displays elastic solid behavior.[7] At low frequencies, the slow relaxation of whole chains by reptation[4,5] has the time to take place, so the material flows.

---

[7] Ferry, J. D.; *Viscoelastic properties of polymers, 3rd Ed.*; John Wiley and Sons: UK, **1980**.

[8] Coussot, P.; Grossiord, J.-L.; *Comprendre la rhéologie*, *De la circulation du sang à la prise du béton*; EDP Sciences; Tassin, J.-F.; El Kissi, N.; Ernst, B.; Vergnes, B.; *Chapter 2, De la macromolécule aux matières plastiques*, **2002**.
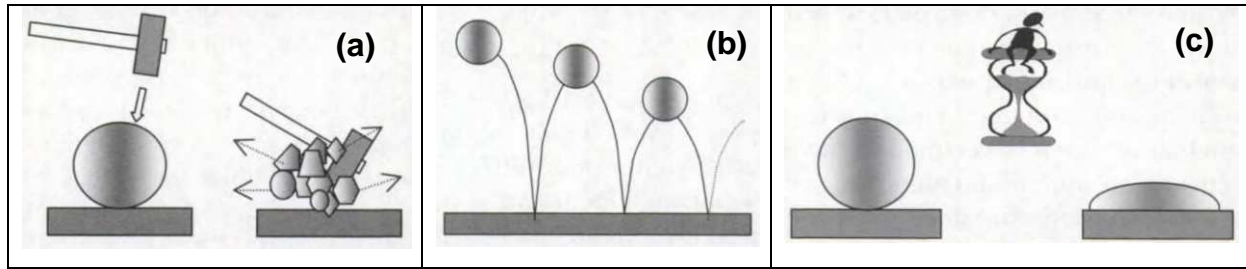
Figure I.4. A high-molecular-weight polymer (silly-putty ball) behaves as:
(a) a glass on very short time scales (very high frequencies ω or very low temperatures T),
(b) an elastic solid on short time scales (high ω or low T),
(c) a viscous liquid at long time scales (low ω or high T); from ref 8.

This behavior dependence on the solicitation frequency is also illustrated in Figure I.5, which shows the storage modulus G' and loss modulus G'' variations of a polymer melt as a function of solicitation frequency. Indeed, under oscillating stress or strain, a viscoelastic polymer concurrently dissipates some energy (represented by the viscous or loss modulus G'') and stores / recovers some energy (represented by the elastic or storage modulus G'). Four zones can be distinguished: (i) terminal regime (liquid flow) for $\omega a_T < 1/\tau_{rep}$ (with τ_{rep} the reptation time of the chain), (ii) plateau zone (rubbery solid) for $1/\tau_{rep} < \omega a_T < 1/\tau_e$ (with τ_R the Rouse time of the chain and τ_e the Rouse time of an entanglement strand), (iii) transition zone from rubberlike to glasslike consistency for $1/\tau_e < \omega a_T < 1/\tau_0$ (with τ_0 the time scale for monomer motion), (iv) glassy zone for $1/\tau_0 < \omega a_T$.[7]
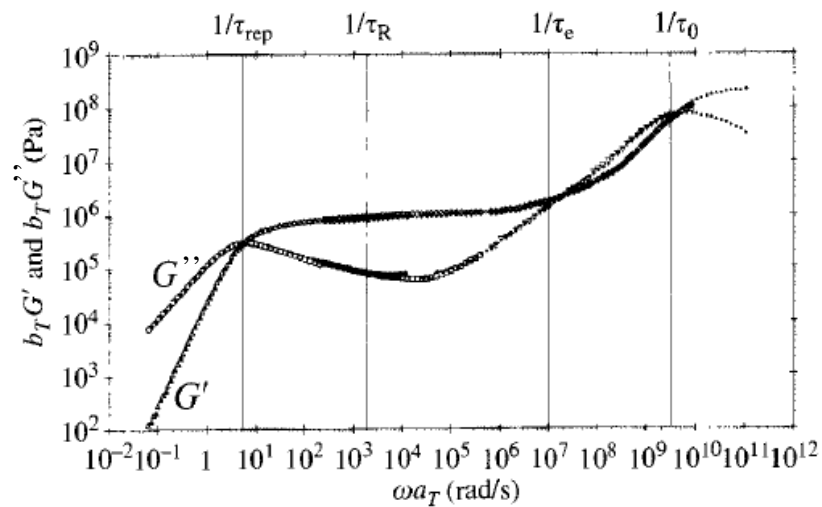
Figure I.5. Master curve from oscillatory shear of a polybutadiene sample ($M_w = 1.3 \times 10^5$ g/mol^{-1}), from ref 4.

The influence of entanglements on the polymers properties can also be underlined by looking at their behavior as a function of temperature (Figure I.6). Indeed, polymers often display time-temperature equivalence.[9] At very low temperatures, as at very high frequencies, polymers are in a glassy state: microscopically with only very limited molecular motions and macroscopically solid, fragile and elastic only for very small deformations. As the temperature increases, polymers undergo a glass transition, followed by a melting transition for semi-crystalline polymers (Figure I.6b). At temperatures above this (these) transition(s), polymers are in a rubbery state. The existence and width of this rubbery state depend on the polymers molecular weight. Indeed, the higher the molecular weight is, the more entanglements there are, and the longer is this rubbery plateau (Figure I.6). Finally, at very high temperatures, as at very low frequencies, linear polymers are in a liquid flow state.
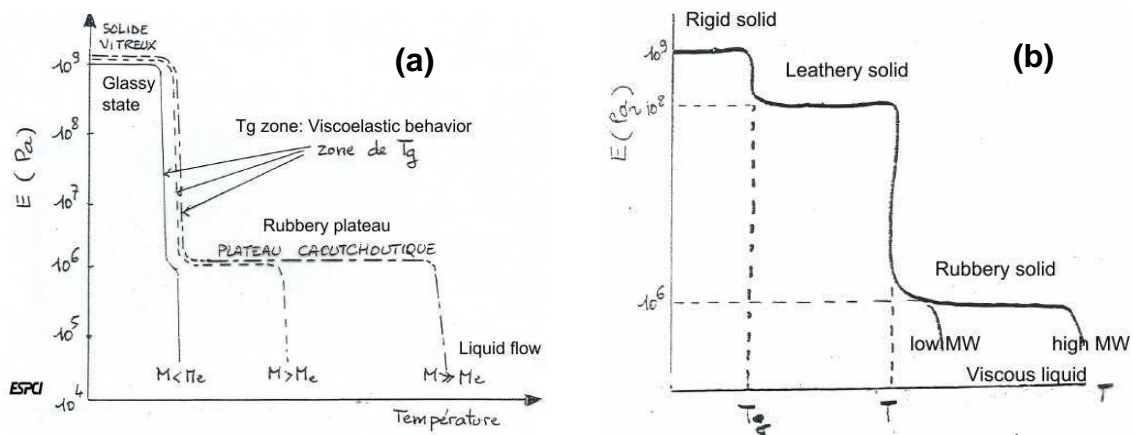
Figure I.6. Storage modulus E of a high-molecular-weight (a) non-crystalline and (b) semi-crystalline polymer as a function of temperature, from ref 9. (a) Four zones: glassy state, glass transition, rubbery plateau, and liquid flow, with M_e the molar mass between entanglements. (b) Six zones: glassy state (rigid solid), glass transition, leathery solid, melting, rubbery plateau, and liquid flow.

So far, we have only considered linear polymers. We have not considered networks of polymers (which are basically just one giant molecule), permanently cross-linked (*e.g.* thermoset elastomers) or reversibly cross-linked (*e.g.* thermoplastic elastomers). Elastomers display rubber elasticity, an elasticity primarily of entropic origins, very specific of polymer networks.

---

[9] Halary, J.L.; Lauprêtre, F.; Monnerie, L.; ***Mécanique des matériaux polymères***; Belin: Paris, **2008**.

(iii) Polymer specificities yield advantages

These properties specific of polymers (entanglements, viscoelasticity, rubber elasticity), as well as their low cost, transparency and low density (lightness) compared to metal, make polymers very important materials used in many applications, ranging from cosmetic to automotive, through packaging, electronics, building and medicine.

(iv) But also drawbacks

However, what makes them so useful is also the source of their major drawbacks. Indeed, very long molecules are generally very difficult to destroy since there are so many covalent bonds to break, which hampers recycling. For instance, thousands of years are necessary for a plastic bag to be destroyed in the wild. Moreover, polymers can be difficult to process (very high temperatures are often necessary) because of their high melt viscosities directly arising from their high molecular weight.

(v) Glass transition: another polymer specificity ?

As we have seen above, polymers undergo a glass transition at low temperatures (Figure I.4a, Figure I.5, Figure I.6), which is sometimes taken as characteristic of polymers.[10,11] However, many small molecules also exhibit glass transition: glycerol, salol, decaline, *m*-toluidine, *o*-terphenyl, *m*-fluoroaniline, 2-biphenylmethanol, propylene carbonate, and propylene glycol;[12] hydroxypentamethyl flavan, glycerol sextol phtalate, and 2-phenyl-3-*p*-tolylindanone;[7] and so on. Therefore, glass transition is actually not a polymer specificity at all. However, some features of polymer glass relaxations may be characteristic of polymers, such as the absence of a relaxation dominant in small molecule glass.[7,12]

---

[10] Wübbenhorst, M.; van Turnhout, J.; Folmer, B. J. B.; Sijbesma, R. P.; Meijer, E. W.; **Complex dynamics of hydrogen bonded self-assembling polymers**; *IEEE Transact. Dielectrics. Electric. Insulation* **2001**, *8*, 365.

[11] Yamauchi, K.; Lizotte, J. R.; Hercules, D. M.; Vergne, M. J.; Long, T. E.; **Combinations of microphase separation and terminal multiple hydrogen bonding in novel macromolecules** *J. Am. Chem. Soc.* **2002**, *124*, 8599.

[12] Dalle-Ferrier, C.; *Transition vitreuse et hétérogénéités dynamiques dans les liquides moléculaires et les polymères*; PhD Thesis, *Université Paris-Sud 11,* **2009.**

2. Supramolecular chemistry

a. The chemistry of noncovalent bonds

(i) Several types of noncovalent bonds

Supramolecular chemistry can be defined as the chemistry beyond the molecules, the chemistry of the noncovalent bonds between molecules.[13,14,15] In particular, it focuses on hydrogen bonding, metal-ligand coordination, aromatic (π-π stacking), Van der Waals, ionic, and hydrophobic interactions. These noncovalent interactions have lower energies than covalent bonds (Table I.1).

Type of force	Strength (kJ/mol)
Van der Waals	1-5
π-donor-acceptor	7-20
hydrogen bonding	10-20
hydrophobic / hydrophilic interaction	12-15
ion-pairing	12-20
coordination bond	40-120
covalent bond	150-1000

Table I.1. Strength of different types of intra- and intermolecular forces, from ref 36.

(ii) Molecular recognition: self- and complementary association

Supramolecular chemistry is at work in molecular recognition, when two (or more) molecular moieties specifically interact with one another through noncovalent bonds. If the two molecular moieties are identical, the association is said to be self-complementary. Otherwise, the association is said to be complementary or host-guest if one of the molecular moieties (the host) is much larger than the other (the guest).

---

[13] The term "supramolecular chemistry" was coined by Jean-Marie Lehn in 1978.

[14] Lehn, J.-M.; *Supramolecular chemistry - Concepts and perspectives*; VCH: Weinheim, Germany, **1995**.

[15] Steed, J. W.; Atwood, J. L.; *Supramolecular chemistry*, *2ⁿᵈ Edition*; Wiley: Chippenham, UK, **2009**.

(iii) Responsible for the self-assembly of molecules

Supramolecular chemistry's noncovalent interactions can induce the self-assembly of molecules into larger objects.[16,17,18] To visualize this effect, a common image is that of a wall where the bricks represent the molecules and the mortar represents the interactions holding the assembly together. Many systems fit that description: from micelles of surfactants (Figure I.7a) to hydrogen-bonded cyclic structures (Figure I.7b),[19] through supramolecular liquid crystals.
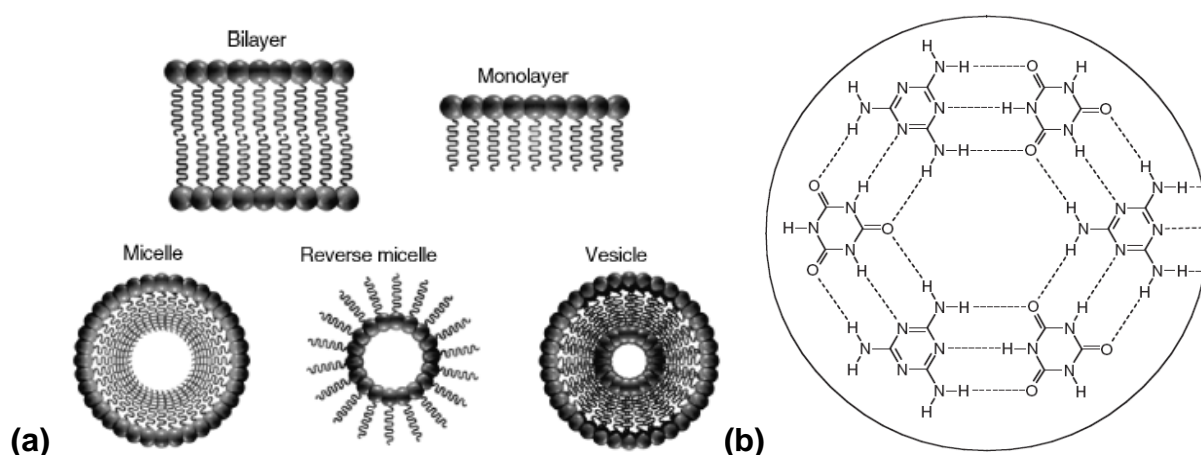
Figure I.7. (a) Ordered surfactant structures in aqueous solution (hydrophilic head group, lipophilic tail), from ref 15. (b) Rosette motif in the solid-state structure of melamine·cyanuric acid, from ref 15.

Very interesting features can arise from the self-assembly of molecules. One example is the emergence of liquid crystallinity from two non-mesogenic components interacting with one another.[20] Moreover, self-assemblies can display functionalities that make them useful for applications such as catalysis[19] or therapeutic delivery.[21]

---

[16] Lawrence, D. S.; Jiang, T.; Levett, M.; **Self-assembling supramolecular complexes;** *Chem. Rev.* **1995***, 95*, 2229.

[17] Whitesides, G. M.; Grzybowski, B.; **Self-assembly at all scales**; *Science* **2002***, 295*, 2418.

[18] Menger, F. M.; **Supramolecular chemistry and self-assembly;** *PNAS* **2002***, 99*, 4818.

[19] Sijbesma, R. P.; Meijer, E. W.; **Self-Assembly of well-defined structures by hydrogen bonding**; *Curr. Opin. Colloid Interface Sci.* **1999***, 4*, 24.

[20] Brienne, M.-J.; Gabard, J.; Lehn, J.-M.; Stibor, I.; **Macroscopic expression of molecular recognition. Supramolecular liquid crystalline phases induced by association of complementary heterocyclic components**; *J. Chem. Soc., Chem. Commun.* **1989***, 24*, 1868.

[21] Branco, M. C.; Schneider, J. P.; **Self-assembling materials for therapeutic delivery**; *Acta Biomater.* **2009***, 5*, 817.

(iv) Paramount in biological systems

Noncovalent interactions, molecular recognition and self-assembly are responsible for the organization of many biological systems.[22] Often, more than one type of noncovalent interactions play a paramount role. A very well known example is DNA, where hydrogen bonding between the base pairs (thymine, adenine, guanine, cytosine) as well as π-π stacking and hydrophobic interactions give DNA its famous double helix structure (Figure I.8c).[15] The recognition between an enzyme and its substrate also relies on intermolecular interactions: an enzyme forms a complex with its substrate because of geometric and interactions matching (Figure I.8a-b, first described by Emil Fischer in 1894).[23] Other examples are lipid bilayers, and folding of proteins into helices or β-sheet stabilized by noncovalent interactions, especially hydrogen bonds.

Therefore, studying noncovalent interactions allows a better understanding of many biological phenomena, such as the link between structure and function of proteins.
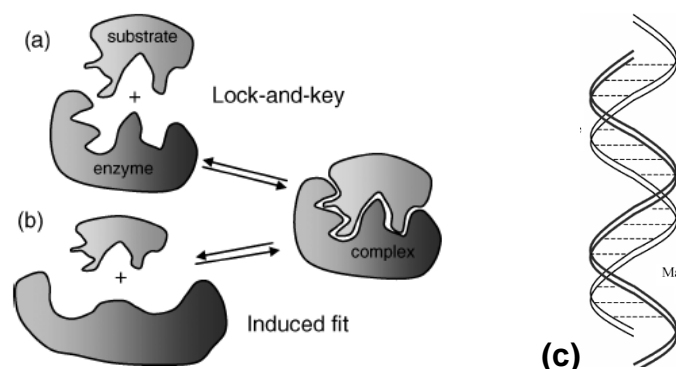
Figure I.8. (a) Rigid lock and key and (b) induced fit models of enzyme-substrate binding, from ref 15. (c) The DNA double helix, from ref 15. Dotted lines represent hydrogen bonded base-pair interactions.

(v) Stimuli-responsiveness

A key feature of self-assemblies, which makes them very useful in applications, is their stimuli-responsiveness. Indeed, because of their sensitivity to various stimuli, such as photo-irradiation, temperature, pH, redox potential, added competitor or voltage, noncovalent interactions can impart stimuli-responsiveness to self-assembled materials.

[22] Grzybowski, B. A.; Wilmer, C. E.; Kim, J.; Browne, K. P.; Bishop, K. J. M.; **Self-assembly: from crystals to cells**; *Soft Matter* **2009**, *5*, 1110.

[23] Fischer, E.; *Ber. Deutsch. Chem. Ges.*, **1894**, *27*, 2985.

b. Hydrogen bonding

(i) A directional and reversible interaction

As we have seen above, hydrogen bonds are particularly important in biology. Perhaps because biologic systems are a major source of inspiration in designing supramolecular assembly, hydrogen bonds are also widely used in synthetic supramolecular systems.[24] Three characteristics of hydrogen bonds explain their success: their directionality (Figure I.9), their reversibility with temperature, and their strength, typically one-tenth of a covalent bond but ten times a Van der Waals interaction (Table I.1).[25]
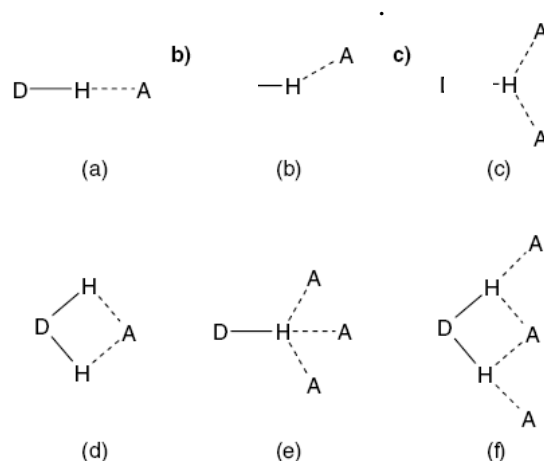
Figure I.9. Various types of hydrogen bonding geometries: (a) linear, (b) bent, (c) donating bifurcated, (d) accepting bifurcated, (e) trifurcated, (f) three centers bifurcated, from ref 15.

(ii) A wide range of strengths and lifetimes

Moreover, the strength of hydrogen bonding interactions $|\Delta G|$ between a host and a guest can range between 2 and 60 kJ/mol, which represents association constants K between 2 and 10^{10} L/mol (equation 1, with R the molar gas constant and T the temperature).

$$K = \exp(-\frac{\Delta G}{RT}) \qquad (1)$$

[24] Zimmerman, S.; Corbin, P.; **Heteroaromatic modules for self-assembly using multiple hydrogen bonds**; *Structure and Bonding* **2000**, *96*, 63.

[25] Jeffrey, G. A.; *An introduction to hydrogen bonding*; Oxford University Press: Oxford, **1997**.

The association constant K of a host-guest complex reflects its thermodynamic stability in a given solvent at a given temperature. The interaction is stronger if there are several hydrogen bonds in parallel. Sartorius and Schneider developed an empirical method to estimate the strength of a hydrogen-bonded array.[26] Actual measurements of the association constant can be performed by any experimental technique that yields the concentration of complex as a function of changing host or guest concentration (NMR spectroscopy,[27,28] spectrophotometry, fluorescence, calorimetry,[29,30] and so on).[15]

However, the properties of a hydrogen bonded host-guest system not only depend on thermodynamic parameters (association constant K), but also depend on dynamic parameters, represented by the lifetime of the association τ and the rates of association k_1 and dissociation k_{-1}. Most of the time, the lifetime of the association increases with the equilibrium constant, but it is not always the case.[35i] Besides, the lifetime of hydrogen bonding interactions also has a wide range. For instance, the preexchange lifetimes of ureidopyrimidinones (UPy) dimers at 298K measured by dynamic NMR spectroscopy were found to be 80 ms in water-saturated-chloroform, 170 ms in chloroform and 1700 ms in toluene.[102]

(iii) A solvent dependant interaction

Hydrogen bonding can occur in solution and in the bulk. In solution, hydrogen bonding association constants (and lifetimes as illustrated above) are higher in apolar and aprotic solvents. Indeed, in protic and polar solvents, and in water in particular, host-guest hydrogen bonding competes with solute-solvent hydrogen bonds.

---

[26] Sartorius, J.; Schneider, H.-J.; **A general scheme based on empirical increments for the prediction of hydrogen-bond associations of nucleobases and of synthetic host-guest complexes;** *Chem. Eur. J.,* **1996***, 2*, 1446-1452.

[27] Fielding, L.; **Determination of association constants (Ka) from solution NMR data**; *Tetrahedron* **2000***, 56*, 6151.

[28] Cohen, Y.; Avram, L.; Frish, L.; **Diffusion NMR spectroscopy in supramolecular and combinatorial chemistry: an old parameter-new insights**; *Angew. Chem. Int. Ed.* **2005***, 44*, 520.

[29] Arnaud, A.; Bouteiller, L.; **Isothermal titration calorimetry of supramolecular polymers;** *Langmuir* **2004***, 20*, 6858-6863.

[30] Turnbull, W. B.; Daranas, A. H.; **On the value of c: can low affinity systems be studied by isothermal titration calorimetry?**; *J. Am. Chem. Soc.* **2003***, 125*, 14859.

However, a strategy to facilitate host-guest hydrogen bonding in aqueous solutions is to create hydrophobic microenvironments where the host-guest hydrogen bonding can take place (an example of this in Figure I.10).[31] Another strategy, inspired by biologic systems, is to use hydrogen bonding in conjunction with other noncovalent interactions such as π-stacking, ionic or solvophobic interactions. Moreover, exclusively hydrogen-bonded supramolecular assemblies in moderately polar solvent such as tetrahydrofuran are possible.[32]
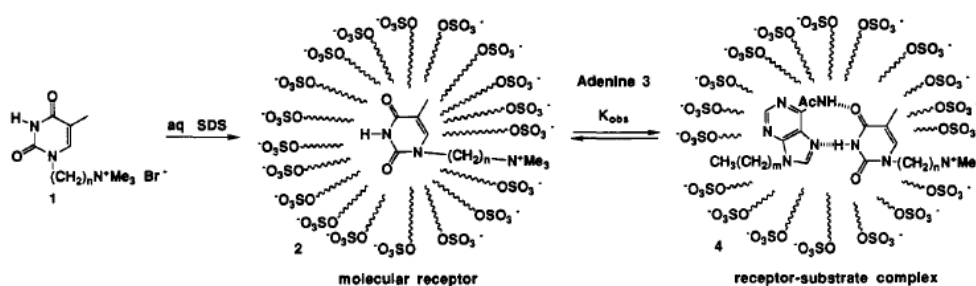
Figure I.10. Incorporation and binding process of thymine and adenine derivatives inside micelles to shield the hydrogen bonds from water, from ref 31.

[31] Nowick, J. S.; Chen, J. S.; Noronha, G.; **Molecular recognition in micelles: the roles of hydrogen bonding and hydrophobicity in adenine-thymine base-pairing in SDS micelles**; *J. Am. Chem. Soc.* **1993**, *115*, 7636.

[32] Ouhib, F.; Raynal, M.; Jouvelet, B.; Isare, B.; Bouteiller, L.; **Hydrogen bonded supramolecular polymers in moderately polar solvents**; *Chem. Commun.* **2011**, *47*, 10683.

3. Supramolecular polymers

a. Polymers and supramolecular chemistry

Supramolecular chemistry plays an important part in the properties of some polymers. For instance, the many hydrogen bonds in polyamide are responsible for their high cohesion energy which results in good mechanical properties and resistance to solvents. Moreover, the unusual strength of poly(1,4-phenylene terephthalamide) (Kevlar) is due to multiple hydrogen bonds and π-stacking. Furthermore, supramolecular chemistry's noncovalent interactions can induce the self-assembly of polymeric molecules. A striking example is the self-assembly of block copolymers into ordered mesophases (Figure I.11).[33,34] Another is thermoplastic elastomers (more details in part e).
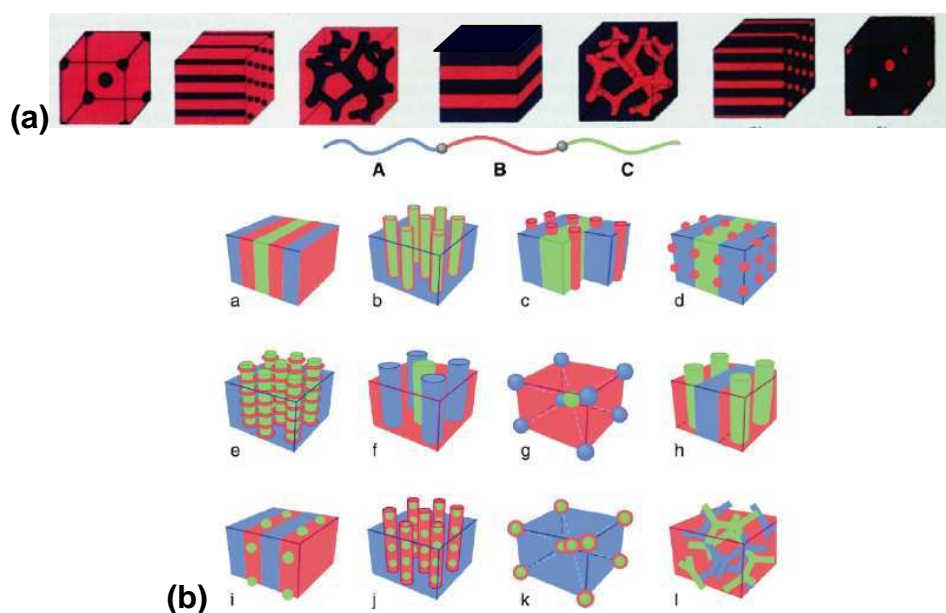
Figure I.11. (a) Morphologies (cubic, cylindrical, gyroid and lamellar) obtained by self-assembly of diblock copolymers, from ref 33. (b) Morphologies obtained by self-assembly of triblock copolymers, from ref 34.

Going one step further, one can use supramolecular chemistry to make polymers, "supramolecular polymers". By using supramolecular chemistry to make polymers, we are in a sense going back to the image of polymers before Staudinger: noncovalent aggregates of low-molecular-weight compounds, with the directionality of the interactions in extra.

---

[33] Bates, F. S.; Fredrickson, G. H.; **Block copolymers-designer soft materials**; *Phys. Today* **1999**, *52*, 32.

[34] Park, C.; Yoon, J.; Thomas, E. L.; **Enabling nanotechnology with self assembled block copolymer patterns**; *Polymer* **2003**, *44*, 6725.

b. Using supramolecular chemistry to make polymers

(i) Building a polymer from small molecules and directional interactions

Based on the principle of supramolecular chemistry, one can build what is called a *supramolecular polymer*,[35] which is basically a polymer where some covalent bonds have been replaced by directional and noncovalent bonds. To ensure the formation of chains, and not three-dimensional arrays, the noncovalent interactions must be directional and the functionality equal to two. Therefore, metal-ion coordination,[36,37] π-stacking,[38] hydrogen bonds,[39] or a combination of these interactions[40] can be used.

---

[35] Reviews: (a) Zimmerman, N.; Moore, J.; Zimmerman, S.; **Polymer chemistry comes full circle**; *Chem. Ind.* **1998**, *15*, 604.

(b) Ciferri, A.; *Supramolecular polymers*; Marcel Dekker: New York, **2000**.

(c) Brunsveld, L.; Folmer, B. J. B.; Meijer, E. W.; Sijbesma, R. P.; **Supramolecular polymers**; *Chem. Rev.* **2001**, *101*, 4071.

(c) Ciferri, A.; **Supramolecular polymerizations**; *Macromol. Rapid Commun.* **2002**, *23*, 511.

(d) Bosnian, A.; Brunsveld, L.; Folmer, B.J.B.; Sijbesma, R.P.; Meijer, E.W. **Supramolecular polymers: from scientific curiosity to technological reality**; *Macromol. Symp.* **2003**, *201*, 143.

(e) Lehn, J.-M.; **Dynamers: dynamic molecular and supramolecular polymers**; *Prog. Polym. Sci.* **2005**, *30*, 814.

(f) Rieth, S.; Baddeley, C.; Badjic, J. D.; **Prospects in controlling morphology, dynamics and responsiveness of supramolecular polymers**; *Soft Matter* **2007**, *3*, 137.

(g) Serpe, M. J.; Craig, S. L.; **Physical organic chemistry of supramolecular polymers**; *Langmuir* **2007**, *23*, 1626.

(h) de Greef, T. F. A.; Meijer, E. W.; **Materials science: supramolecular polymers**; *Nature* **2008**, *453*, 171.

(i) Fox, J. D.; Rowan, S. J.; **Supramolecular polymerizations and main-chain supramolecular polymers**; *Macromolecules* **2009**, *42*, 6823.

(j) de Greef, T. F. A.; Smulders, M. M. J.; Wolffs, M.; Schenning, A. P. H. J.; Sijbesma, R. P.; Meijer, E. W.; **Supramolecular polymerization**; *Chem. Rev.* **2009**, *109*, 5687.

[36] Friese, V. A.; Kurth, D. G.; **From coordination complexes to coordination polymers through self-assembly**; *Curr. Opin. Colloid Interface Sci.* **2009**, *14*, 81.

[37] Whittell, G. R.; Hager, M. D.; Schubert, U. S.; Manners, I.; **Functional soft materials from metallopolymers and metallosupramolecular polymers**; *Nat. Mater.* **2011**, *10*, 176.

[38] Fernandez, G.; Pérez, E.; Sénchez, L.; Martin, N.; **Self-organization of electroactive materials: a head-to-tail donor-acceptor supramolecular polymer**; *Angew. Chem. Int. Ed.* **2008**, *47*, 1094.

[39] Reviews: (a) Farnik, D.; Kluger, C.; Kunz, M. J.; Machl, D.; Petraru, L.; Binder, W. H.; **Synthesis and self-assembly of hydrogen-bonded supramolecular polymers**; *Macromol. Symp.* **2004**, *217*, 246.

(b) Armstrong, G.; Buggy, M.; **Hydrogen-bonded supramolecular polymers: A literature review**; *J. Mater. Sci.* **2005**, *40*, 547.

(c) Bouteiller, L.; **Assembly via hydrogen bonds of low molar mass compounds into supramolecular polymers**; *Adv Polym Sci.* **2007**, *207*, 79.

(d) Binder, W. H.; Zirbs, R.; **Supramolecular polymers and networks with hydrogen bonds in the main- and side-chain**; *Adv. Polym. Sci.* **2007**, *207*, 1.

(e) Shimizu, L. S.; **Perspectives on main-chain hydrogen bonded supramolecular polymers**; *Polym. Int.* **2007**, *56*, 444.

(ii) First advantage: reversibility and responsiveness

The first advantage of this approach to polymers is the reversibility of the noncovalent bonds, in contrast to the permanent nature of covalent bonds. This reversibility of the links means that it is possible to go from an assembly of small molecules, which are easier to process, recycle, and solubilize, to the supramolecular polymer, and vice versa.

The formation and breaking of the noncovalent interactions depend on conditions such as temperature, pH, redox potential or added competitor. For instance, if hydrogen bonds are used, the supramolecular polymer is formed at low temperature and dissociates as the hydrogen bonds break at higher temperatures. Moreover, dissociation of hydrogen-bonded supramolecular polymer can be obtained by addition of monofunctional chain stoppers. Furthermore, depolymerization of hydrogen-bonded supramolecular polymer can also be photoinduced by photochemical formation of end-caps.[41] Besides, in solution, the degree of polymerization of a supramolecular polymer depends on the concentration. Therefore, supramolecular polymers are stimulus-responsive, to a variety of stimuli, tunable and adaptive to the environment.

(iii) Second advantage: unusual properties such as self-healing

The second advantage of supramolecular polymers is that incorporating noncovalent and dynamic bonds into materials can impart original properties, such as elastomer self-healing. Indeed, self-healing thermoreversible rubbers from supramolecular assembly were developed in our group (Figure I.12).[42,43,44,45] When cut in two, a piece of this elastomer can

[40] Gonzalez-Rodriguez, D.; Schenning, A. P. H. J.; **Hydrogen-bonded supramolecular pi-functional materials**; *Chem. Mater.* **2011**, *23*, 310.

[41] Folmer, B. J. B.; Cavini, E.; **Photo-induced depolymerization of reversible supramolecular polymers**; *Chem. Commun.* **1998**, 1847.

[42] Cordier, P.; Tournhilhac, F.; Soulié-Ziakovic, C.; Leibler, L.; **Self-healing and thermoreversible rubber from supramolecular assembly**; *Nature* **2008**, *451*, 977.

[43] Montarnal, D.; Cordier, P.; Soulié-Ziakovic, C.; Tournhilhac, F.; Leibler, L.; **Synthesis of self-healing supramolecular rubbers from fatty acid derivatives, diethylene triamine, and urea**; *J. Polym. Sci., Part A: Polym. Chem.* **2008**, *46*, 7925.

[44] Montarnal, D.; Tournhilhac, F.; Hidalgo, M.; Couturier, J.-L.; Leibler, L.; **Versatile one-pot synthesis of supramolecular plastics and self-healing rubbers**; *J. Am. Chem. Soc.* **2009**, *131*, 7966.

be repaired by simple contact between the broken surfaces and recovers its mechanical properties (Figure I.13). The dynamic of the hydrogen bonds between the self-associating stickers seems to play an important part in the unique properties of these rubbers. Indeed, non-freshly cut surfaces cannot repair.[46] The self-healing ability can be activated by damage of the surface and is related to the presence of many free stickers at broken surfaces.
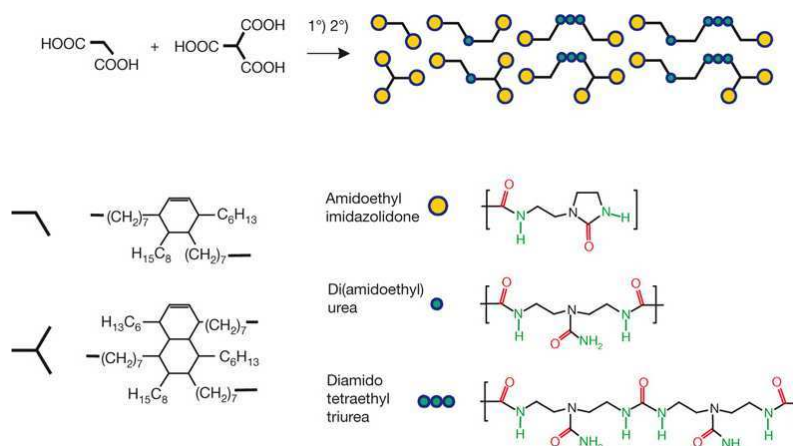
Figure I.12. Synthesis pathway to a self-healing and thermoreversible rubber from supramolecular assembly, from ref 42. A mixture of fatty diacid and triacid is condensed first with diethylene triamine and then reacted with urea giving a mixture of oligomers equipped with complementary hydrogen bonding groups. The hydrogen bond acceptors are shown in red, donors in green.

Figure I.13. Self-healing of the supramolecular elastomer from ref 42. *Photos by Arkema*.

(iv) Third (potential) advantage: self-assembly instead of covalent polymerization

Another advantage of supramolecular polymers is their synthesis using self-assembly as a facile alternative to covalent polymerisation.[15] Of course this is only truly an advantage if the building block are easily synthesized. Moreover, complex architectures, not easily attained by covalent chemistry, can be obtained.[47,48]

---

[45] Montarnal, D.; *Mise en œuvre de liaisons réversibles covalentes et non-covalentes pour de nouveaux matériaux polymères recyclables et retransformables*; PhD Thesis, *Université Paris 6*, **2011**.

[46] Maes, F.; Montarnal, D.; Cantournet, S.; Tournilhac, F.; Corte, L.; Leibler, L.; **Activation and deactivation of self-healing in supramolecular rubbers**; *Soft Matter* **2012**, *8*, 1681.

[47] Ruokolainen, J.; Mäkinen, R.; Torkkeli, M.; Mäkelä, T.; Serimaa, R.; ten Brinke, G.: Ikkala, O.; **Switching supramolecular polymeric materials with multiple length scales**; *Science* **1998**, *280*, 557.

(v) Are supramolecular polymers robust ?

Intrinsically, the question of the robustness of supramolecular polymers arises. Indeed, supramolecular polymers are held by noncovalent bonds, which are much weaker and have much lower lifetimes than covalent bonds. This is in fact what gives supramolecular polymers their advantages. Indeed, if the noncovalent bonds are too strong or too long lived, then the supramolecular polymers cannot be reversible and adaptive. However, if the noncovalent bonds are too weak or if their lifetime is too short, then the supramolecular polymer runs the risk of not being robust enough.[49] As we can see, it is a question of compromise.

A consensus joined by several authors states that association constants K above 10^6 mol/L are required to obtain a significant degree of polymerization,[35,50] unless supramolecular polymerization is enforced by the anisotropy of the medium (which imposes end-to-end association),[51] as for liquid crystals.[19] In terms of hydrogen bonding motifs, the rule has been translated as the need for at least four hydrogen bonds per connection.[15] Indeed, high degrees of polymerization are not readily achieved with low association constants.

However, the rule "K above 10^6 mol/L or else" must be taken with a grain of salt since, in ref 42 the association constants K involved are much lower and still very interesting properties are obtained. Indeed, the associations are weak but numerous.[42] Moreover, the properties of this material may be strongly influenced by its suspected nanostructuration, arising from a segregation between the stickers (polar) and the spacers (apolar).[45,46] Indeed, phase segregation can facilitate hydrogen bonding because the sticker concentration is locally increased.[108] Furthermore, as we will see later on crystallization of the stickers can also complement hydrogen bonds in supramolecular polymers.

---

[48] Ikkala, O.; ten Brinke, G.; **Functional materials based on self-assembly of polymeric supramolecules**; *Science* **2002**, *295*, 2407.

[49] Rybtchinski, B.; **Adaptive supramolecular nanomaterials based on strong noncovalent interactions**; A*CS Nano,* **2011**, *5*, 679.

[50] This value is based on calculations for isodesmic supramolecular polymerization.

[51] Matsuyama, A.; Kato, T.; **Interplay of phase separations and aggregations in solutions of rodlike polymers**; *J. Phys. Soc. Jap.* **1998**, *67*, 204.

c. Building blocks of supramolecular polymers

We have defined supramolecular polymers as polymers where some covalent bonds have been replaced by directional and noncovalent bonds. Therefore, to build a supramolecular polymer a convenient path is to graft stickers onto spacers. The stickers associate reversibly and directionally *via* noncovalent interactions such as hydrogen bonds, while the spacers connect the stickers and afford mobility.

(i) Stickers

The stickers are functional groups that can reversibly and directionally associate with themselves or with another functional group through complementary noncovalent interactions. The stickers can be self-complementary motifs (ureidopyrimidone [UPy],[52] ureidotriazine [UDAT],[53] quadruply hydrogen bonded cytosine module,[54] imidazolidone,[43] perylene derivatives,[55] and so on), complementary motifs (nucleobases,[56] oligonucleotides,[57] 1,3,5-triazine based moieties,[58] guanosine butyl urea [UG] and 2,7-diamido-1,8-naphthyridine [DAN],[59] cyanuric acid and Hamilton wedge receptor,[60] and so on) or host-guest motifs (tetraurea calixarene capsules and *o*-dichlorobenzene,[61] β-cyclodextrin and ferrocene,[62] α-

---

[52] Beijer, F. H.; Sijbesma, R. P.; Kooijman, H.; Spek, A. L.; Meijer, E. W.; **Strong dimerization of ureidopyrimidones via quadruple hydrogen bonding**; *J. Am. Chem. Soc.* **1998**, *120*, 6761.

[53] Hirschberg, J. H. K. K.; Ramzi, A.; Sijbesma, R. P.; Meijer, E. W.; **Ureidotriazine-based supramolecular copolymers**; *Macromolecules* **2003**, *36*, 1429.

[54] Lafitte, V. G. H.; Aliev, A. E.; Horton, P. N.; Hursthouse, M. B.; Golding, K. B. P.; Hailes, H. C.; **Quadruply hydrogen bonded cytosine modules for supramolecular application**; *J. Am. Chem. Soc.* **2006**, *128*, 6544.

[55] Arnaud, A.; Belleney, J.; Boué, F.; Bouteiller, L.; Carrot, G.; Wintgens, V.; **Aqueous supramolecular polymer formed from an amphiphilic perylene derivative**; *Angew. Chem. Int. Ed.,* **2004**, *43*, 1718.

[56] Sivakova, S.; Rowan, S. J.; **Nucleobases as supramolecular motifs**; *Chem. Soc. Rev.,* **2005**, *34*, 9.

[57] Xu, J.; Fogleman, E. A.; Craig, S. L.; **Structure and properties of DNA-based reversible polymers**; *Macromolecules* **2004**, *37*, 1863.

[58] (a) Gamez, P.; Reedijk, J.; **1,3,5-Triazine-based synthons in supramolecular chemistry**; *Eur. J. Inorg. Chem.* **2006**, *1*, 29. (b) Mooibroek, T. J.; Gamez, P.; **The s-triazine ring, a remarkable unit to generate supramolecular interactions**; *Inorg. Chimica Acta* **2007**, *360*, 381.

[59] Park, T.; Todd, E. M.; Nakashima, S.; Zimmerman, S. C.; **A quadruply hydrogen bonded heterocomplex displaying high-fidelity recognition**; *J. Am. Chem Soc.* **2005**, *127*, 18133.

[60] Burd, C.;Weck, M.; **Self-sorting in polymers**; *Macromolecules* **2005**, *38*, 7225.

[61] Castellano, R. K.; Clark, R.; Craig, S. L.; Nuckolls, C.; Julius Rebek, J.; **Emergent mechanical properties of self-assembled polymeric capsules**; *PNAS* **2000**, *97*, 12418.

cyclodextrin and *p-t*-butoxyaminocinnamoylamino group,[63] crown ethers and secondary ammonium ions,[64] crown ethers and paraquats,[65] 2,6-bis(benzimidazolyl)-4-oxypyridine ligand and transition metal ions [Fe^{2+}, Co^{2+}, Zn^{2+}, Cd^{2+}],[66] and so on).

(ii) Spacers

Oligomers (low-molecular-weight polymers), whether rigid or flexible, as well as alkyl chains,[76,100] or fatty acids from vegetable oil,[42-45] are widely used to link the stickers. Oligomers of polyolefins {polybutadiene [PB],[93] polyisobutylene [PIB],[67,105b] poly(ethylene/butylene) [PE-PB][101]}, polyethers {poly(ethylene oxide) and poly(propylene oxide) [PEO-PPO] block copolymers,[100,90] poly(tetrahydrofuran) [pTHF][66,108,115]}, polyesters[101] {poly(butyl acrylate) [PBA],[91] poly(butyl methacrylate) [PBMA],[68] polycaprolactone [PCL][104c,105f]}, polycarbonates,[101] polydimethylsiloxane [PDMS],[69,100] poly(ether ketone) [PEK],[70] polystyrene [PS],[68] polynorbornenes,[60] and so on, have been used to build supramolecular polymers.

[62] Yan, Q.; Yuan, J.; Cai, Z.; Xin, Y.; Kang, Y.; Yin, Y.; **Voltage-responsive vesicles based on orthogonal assembly of two homopolymers**; *J. Am. Chem. Soc.* **2010**, *132*, 9268.

[63] Miyauchi, M.; Takashima, Y.; Yamaguchi, H.; Harada, A.; **Chiral supramolecular polymers formed by host-guest interactions**; *J. Am. Chem. Soc.* **2005**, *127*, 2984.

[64] Cantrill, S. J.; Youn, G. J.; Stoddart, J. F.; Williams, D. J.; **Supramolecular daisy chains**; *J. Org. Chem.* **2001**, *66*, 6857.

[65] Yamaguchi, N.; Nagvekar, D. S.; Gibson, H. W.; **Self-organization of a heteroditopic molecule to linear polymolecular arrays in solution**; *Angew. Chem. Int. Ed.* **1998**, *37*, 2361.

[66] Beck, J. B.; Ineman, J. M.; Rowan, S. J.; **Metal/ligand-induced formation of metallo-supramolecular polymers**; *Macromolecules* **2005**, *38*, 5060.

[67] Binder, W. H.; Kunz, M. J.; Kluger, C.; Hayn, G.; Saf, R.; **Synthesis and analysis of telechelic polyisobutylenes for hydrogen-bonded supramolecular pseudo-block copolymers**; *Macromolecules* **2004**, *27*, 1749.

[68] Park, T.; Zimmerman, S. C.; **Formation of a miscible supramolecular polymer blend through self-assembly mediated by a quadruply hydrogen-bonded heterocomplex**; *J. Am. Chem. Soc.* **2006**, *128*, 11582.

[69] Abed, S.; Boileau, S.; Bouteiller, L.; Lacoudre, N.; **Supramolecular association of acid terminated polydimethylsiloxanes. 1. Synthesis and characterization**; *Polym. Bull.* **1997**, *39*, 317.

[70] Kunz, M. J.; Hayn, G.; Saf, R.; Binder, W. H.; **Hydrogen-bonded supramolecular poly(ether ketone)s**; *J. Polym. Sci. A: Polym. Chem.* **2004**, *42*, 661.

d. Assembling the building blocks to construct supramolecular polymers

We have seen that supramolecular polymers are made of stickers that associate reversibly and directionally *via* noncovalent interactions, and spacers, that connect the stickers and afford mobility. Theses building blocks can be assembled in different ways.[35,39] If the stickers are introduced on both ends of an oligomeric spacer, a main-chain supramolecular polymer is formed. If the stickers are introduced on the side chain of polymers, a side-chain supramolecular polymer is formed. If the linked stickers form the supramolecular backbone, while the spacers act as side-chains, nanotubes are formed.

(i) Main-chain supramolecular polymers

Main-chain supramolecular polymers are made of telechelic molecules linked together by their chain-ends through noncovalent bonds to form a polymer-like assembly. Three constructions of main-chain supramolecular polymers are possible, depending if the stickers are self-complementary (C with C) or hetero-complementary (A with B): self-assembly of an homotelechelic unit (C-spacer-C)$_n$ (Figure I.14a), complementary assembly of two homotelechelic units (A-spacer-A=B-spacer-B)$_n$ (Figure I.14b), or complementary assembly of an heterotelechelic unit (A-spacer-B)$_n$ (Figure I.15).
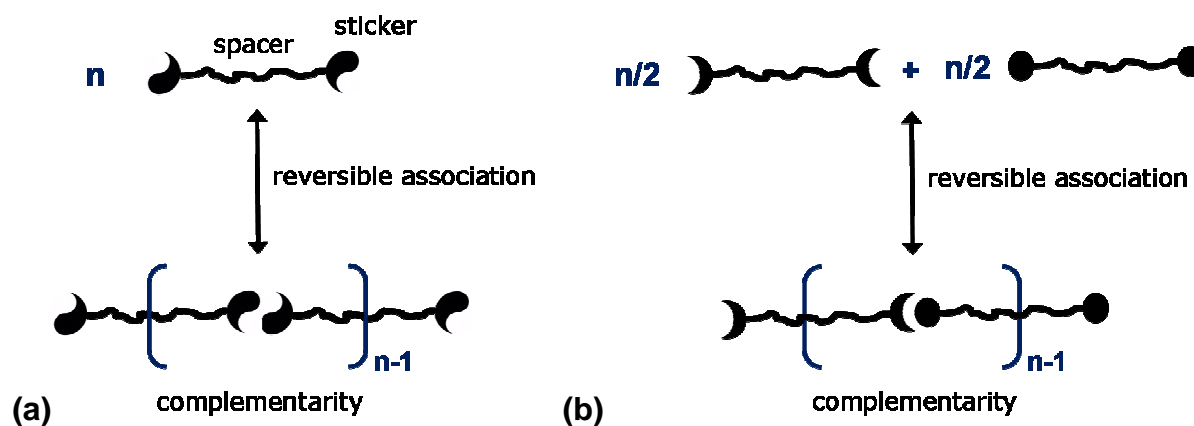
Figure I.14. Main-chain symmetric (or homoditopic) supramolecular polymer: (a) self-complementary and (b) complementary.

To obtain a high degree of polymerization (DP) with homotelechelic blends (A-spacer-A=B-spacer-B)$_n$, the A and B stickers stoichiometry needs to be carefully controlled to 1 to 1, because the excess of one sticker has a chain stopper effect that limits DP.[71] With heterotelechelic unit (A-spacer-B, Figure I.15), stoichiometry is always 1 to 1, so high dimerization constants are no longer needed. However, synthetic pathways are more tedious.
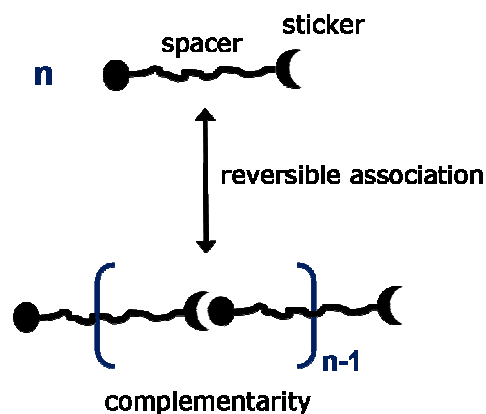
Figure I.15. Main-chain asymmetric (or heteroditopic) supramolecular polymer.

Three main routes have been explored to obtain heteroditopic supramolecular polymers: oligomerization of the spacer from the stickers,[72,73,74] convergent coupling,[57,75] and asymmetric end-functionalization post-oligomerization.[76,77] These strategies will be detailed in Chapter II.

---

[71] Berl, V.; Schmutz, M.; Krische, M. J.; Khoury, R. G.; Lehn, J.-M.; **Supramolecular polymers generated from heterocomplementary monomers linked through multiple hydrogen-bonding arrays formation, characterization, and properties**; *Chem. Eur. J.* **2002***, 8*, 1227.

[72] (a) Ambade, A.; Yang, S.; Weck, M.; **Supramolecular ABC triblock copolymers**; *Angew. Chem. Int. Ed.* **2009***, 48*, 2894. (b) Yang, S. K.; Ambade, A. V.; Weck, M.; **Supramolecular ABC triblock copolymers via one-pot, orthogonal self-assembly**; *J. Am. Chem. Soc.* **2010***, 132*, 1637.

[73] Mansfeld, U.; Winter, A.; Hager, M. D.; Hoogenboom, R.; Gunther, W.; Schubert, U. S.; **Orthogonal self-assembly of stimuli-responsive supramolecular polymers using one-step prepared heterotelechelic building blocks**; *Polym. Chem.* **2012***, 4*, 113.

[74] Lin, I.-H.; Cheng, C.-C.; Yen, Y.-C.; Chang, F.-C.; **Synthesis and assembly behavior of heteronucleobase-functionalized poly(e-caprolactone)**; *Macromolecules* **2010***, 43*, 1245.

[75] Scherman, O. A.; Ligthart, G. B. W. L.; Sijbesma, R. P.; Meijer, E. W.; **A selectivity-driven supramolecular polymerization of an AB monomer**; *Angew. Chem. Int. Ed.* **2006***, 45*, 2072.

[76] Shimizu, T.; Iwaura, R.; Masuda, M.; Hanada, T.; Yase, K.; **Internucleobase-interaction-directed self-assembly of nanofibers from homo- and heteroditopic 1,w-nucleobase bolaamphiphiles**; *J. Am. Chem. Soc.* **2001***, 123*, 5947.

[77] Bertrand, A.; Lortie, F.; Bernard, J.; **Routes to hydrogen bonding chain-end functionalized polymers**; *Macromol. Rapid Comm.* **2012***, 33*, 2062.

(ii) Side-chain supramolecular polymers

Side-chain functionalized supramolecular polymers can form comb-like supramolecular polymers (Figure I.16a).[78]
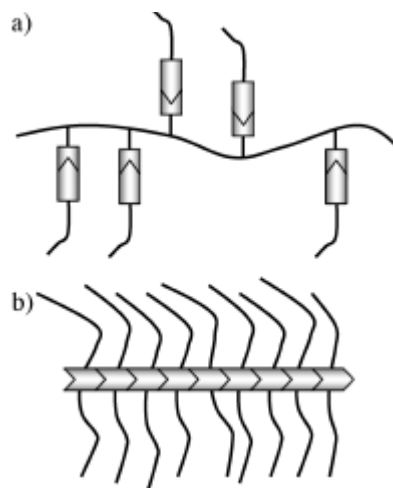
Figure I.16. Schematic structure of a comb-shaped supramolecular polymer with (a) a covalent or (b) a dynamic backbone, from ref 82.

(iii) Nanotubes supramolecular polymers

Nanotubes supramolecular polymers (Figure I.16b) also form comb-like supramolecular polymers.[79] However, unlike side-chain functionalized supramolecular polymers, the backbone is not covalent but dynamic since it is formed of the linked stickers. Bouteiller and his coworkers have extensively studied nanotubular supramolecular polymers.[55,80,81,82]

---

[78] Weck, M.; **Side-chain functionalized supramolecular polymers**; *Polym. Int.* **2007***, 56*, 453.

[79] Bong, D. T.; Clark, T. D.; Granja, J. R.; Ghadiri, M. R.; **Self-assembling organic nanotubes**; *Angew. Chem. Int. Ed.* **2001***, 40*, 988.

[80] Lortie, F.; Boileau, S.; Bouteiller, L.; Chassenieux, C.; Demé, B.; Ducouret, G.; Jalabert, M.; Lauprêtre, F.; Terech, P.; **Structural and rheological study of a bis-urea based reversible polymer in an apolar solvent**; *Langmuir* **2002***, 18*, 7218.

[81] Simic, V.; Bouteiller, L.; Jalabert, M.; **Highly cooperative formation of bis-urea based supramolecular polymers**; *J. Am. Chem. Soc.* **2003***, 125*, 13148.

[82] Pensec, S.; Nouvel, N.; Guilleman, A.; Creton, C.; Boué, F.; Bouteiller, L.; **Self-assembly in solution of a reversible comb-shaped supramolecular polymer**; *Macromolecules* **2010***, 43*, 2529.

e. Properties of supramolecular polymers: examples from the literature

Supramolecular polymers materials can be liquid crystalline, viscoelastic, or gel-like.

(i) Supramolecular liquid crystalline polymers

The first supramolecular polymer described as such in the literature is a liquid crystal.[83] Indeed, Lehn and his coworkers reported from 1990 on liquid crystalline supramolecular polymers made of telechelic spacers functionalized with uracyl and complementary 2,6-diaminopyridine (DAP) stickers (Figure I.17, Figure I.18).[83,84,85] Liquid crystallinity was obtained because the spacers used were rigid (tartaric acid[83,84] or a 9,10-dialkoxyanthracenic derivative[85]). In fact, many main-chain supramolecular polymers based on rigid rod spacers are liquid crystals.[86,87]
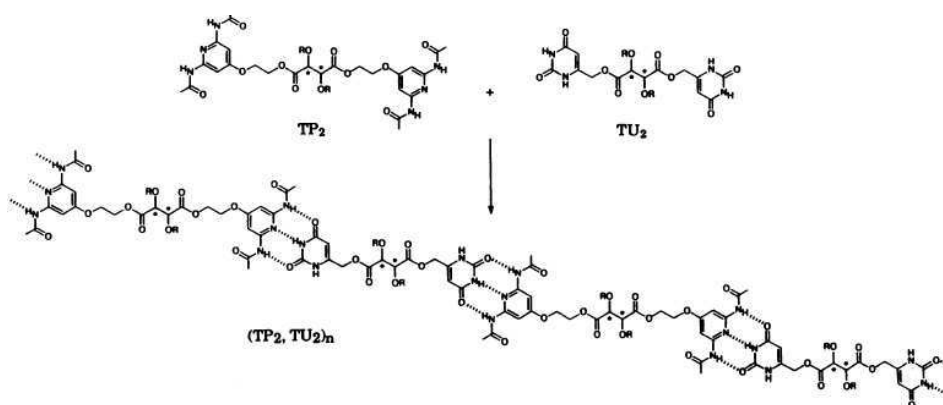
Figure I.17. Self-assembly of the polymolecular supramolecular species (TP$_2$, TU$_2$)$_n$ from the chiral components TP$_2$ and TU$_2$ *via* hydrogen bonding, from ref 84. T represents L-, D-, or *meso*-tartaric acid; R is C$_{12}$H$_{25}$.

[83] Fouquey, C.; Lehn, J.-M.; Levelut, A.-M.; **Molecular recognition directed self-assembly of supramolecular liquid crystalline polymers from complementary chiral components**; *Adv. Mater.* **1990***, 2*, 254.

[84] Gulik-Krzywicki, T.; Fouquey, C.; Lehn, J.-M.; **Electron microscopic study of supramolecular liquid crystalline polymers formed by molecular-recognition-directed self-assembly from complementary chiral components***; Proc. Natl. Acad. Sci. U.S.A.* **1993***, 90*, 163.

[85] Kotera, M.; Lehn, J.-M.; Vigneron, J.-P.; **Self-assembled supramolecular rigid rods**; *J. Chem. Soc.,* **1994***, 2*, 197.

[86] Lee, C.; Griffin, A.; **Hydrogen bonding as the origin of both liquid crystallinity and polymer formation in some supramolecular materials**; *Macromolecul. Symp.* **1997***, 117*, 281.

[87] (a) Sivakova, S.; Rowan, S. J.; **Fluorescent supramolecular liquid crystalline polymers from nucleobase-terminated monomers**; *Chem. Commun.,* **2003***, 19*, 2428. (b) Sivakova, S.; Wu, J.; Campo, C. J.; Mather, P. T. ; Rowan, S. J.; **Liquid-crystalline supramolecular polymers formed through complementary nucleobase-pair interactions**; *Chem. Eur. J.* **2006***, 12*, 446.
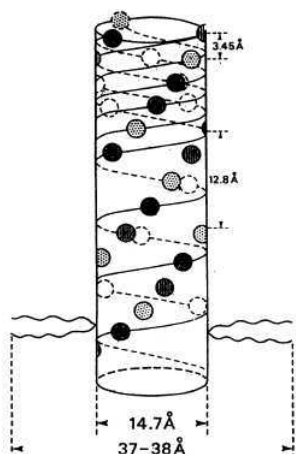
Figure I.18. Schematic representation of the columnar superstructure suggested by the x-ray data for (LP$_2$, LU$_2$)$_n$; each spot represents a PU or UP base pair; spots of the same type belong to the same helical strand of the triple helix; the dimensions indicated are compatible with an arrangement of the PTP and UTU components along the strands; the aliphatic chains stick out of the cylinder, more or less perpendicular to its axis; from ref 84.

Despite having only one, two or three hydrogen bonds per connection, high degrees of polymerization are obtained.[83-87] Indeed, in supramolecular liquid crystalline polymers there is a cooperativity between association and anisotropy: linear association of rigid rods induces anisotropy and reciprocally anistropy increases the degree of polymerization.[86]

As a result of this cooperativity, non-mesogenic compounds can form liquid crystals when mixed with a complementary non-mesogenic compound. For instance, *bis*(4-alkoxy)-substituted bis(phenylethynyl)benzene end-functionalized with thymine or N^6-(4-methoxybenzoyl)adenine do not display any liquid crystalline behavior by themselves, but form a thermotropic liquid crystal upon mixing.[87a]
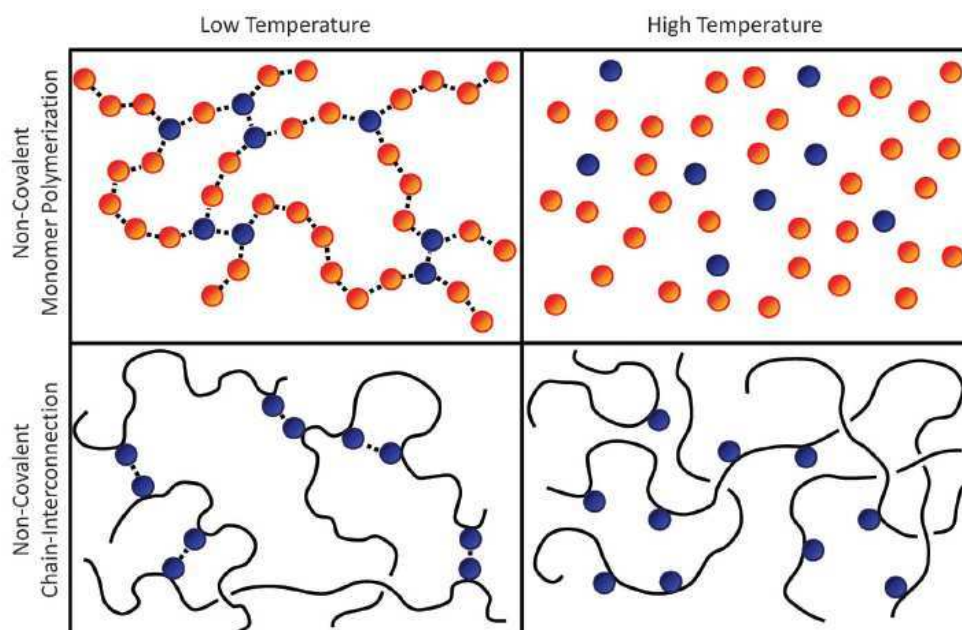
(ii) Supramolecular networks and gels

If branched units (trifunctionnal or more) are used instead of bifunctional units, a network can be formed at low temperatures (Figure I.19 upper row).[88] St. Pourcain and Griffin studied in 1995 such thermoreversible three-dimensional supramolecular networks, made of a mixture of tetrafunctional and bifunctional compounds.[89] Using only trifunctional

---

[88] Seiffert, S.; Sprakel, J.; **Physical chemistry of supramolecular polymer networks**; *Chem. Soc. Rev.* **2012**, *41*, 909.

[89] St. Pourcain, C. B.; Griffin, A. C.; **Thermoreversible supramolecular networks with polymeric properties**; *Macromolecules* **1995**, *28*, 4116.

units, Meijer and his coworkers as well have described networks of this type.[90,100] The self-healing supramolecular rubber already mentioned is also a network of this type, arising from a mixture of difunctional and trifunctional units.[42] Side-chain supramolecular polymers can also form networks (Figure I.19 lower row), belonging to the class of thermoplastic elastomers.[88,91] Stadler and his coworkers in particular pioneered this type of networks, with polybutadienes cross-linked by hydrogen bonding between the side-chain phenyl-urazole functionalities (Figure I.20).[92,93]

Figure I.19. Schematic of two different types of supramolecular polymer networks, from ref 88.
Upper row: supramolecular polymer chains which consist of noncovalently associating monomers. If some of these monomers have a functionality greater than two, a three-dimensional network forms.
Lower row: a network of covalently jointed precursor polymer chains by noncovalent association of suitable side groups. Both systems are in a gel state at low temperatures, where supramolecular association is strong, whereas high temperatures break the supramolecular associates, thereby favoring a sol state.

[90] Lange, R. F. M.; Gurp, M. V.; Meijer, E. W.; **Hydrogen-bonded supramolecular polymer networks** *J. Polym. Sci., Part A: Polym. Chem.* **1999***, 37*, 3657.

[91] Feldman, K. E.; Kade, M. J.; Meijer, E. W.; Hawker, C. J.; Kramer, E. J.; **Model transient networks from strongly hydrogen-bonded polymers**; *Macromolecules* **2009***, 42*, 9072.

[92] Stadler, R.; de Lucca Freitas, L.; **Thermoplastic elastomers by hydrogen bonding 1. Rheological properties of modified polybutadiene**; *Colloid Polym. Sci.* **1986***, 264*, 773.

[93] Hilger, C.; Stadler, R.; **New multiphase architecture from statistical copolymers by cooperative hydrogen bond formation**; *Macromolecules* **1990***, 23*, 2095.
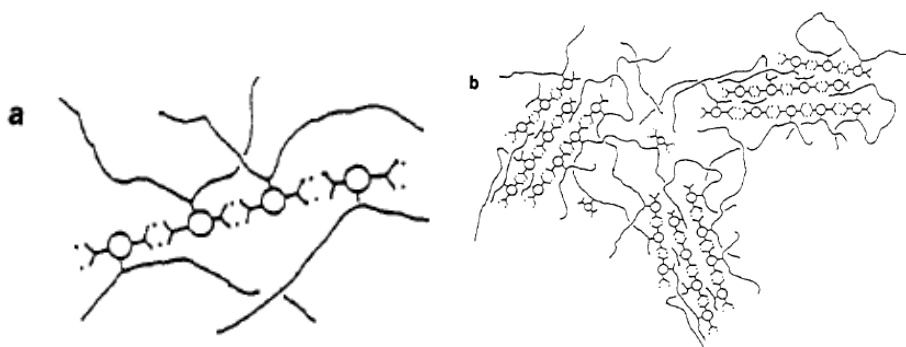
Figure I.20. Schematics of (a) association polymer of difunctional polar groups in a matrix of covalent polymer and (b) phase separation between bundles of association chains and covalent polymer chains, from ref 93.

If the supramolecular associations can maintain in solution, the solvent can swell the network and form a gel,[94,95] a hydrogel[96,97,98] if the solvent is water (Figure I.21, Figure I.22) and an organogel[99] if the solvent is organic.
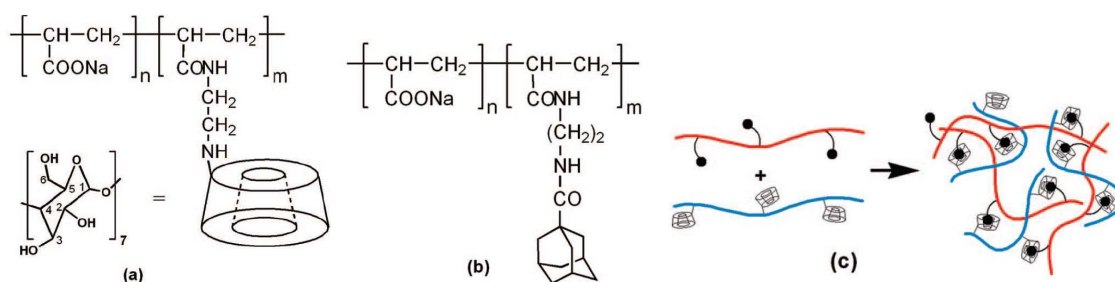
Figure I.21. Chemical and schematic structures of (a) poly(acrylic acid) (PAA) functionalized with β-cyclodextrins, (b) PAA functionalized with adamantyls, and (c) the network formed in aqueous solution by (a) and (b) through host-guest inclusion between adamantyls and β-cyclodextrins , from ref 97.

[94] Noro, A.; Hayashi, M.; Matsushita, Y.; **Design and properties of supramolecular polymer gels**; *Soft Matter* **2012***, 8*, 2416.

[95] Weng, W.; Beck, J. B.; Jamieson, A. M.; Rowan, S. J.; **Understanding the mechanism of gelation and stimuli-responsive nature of a class of metallo-supramolecular gels**; *J. Am. Chem. Soc.* **2006***, 128*, 11663.

[96] Buerkle, L. E.; Li, Z.; Jamieson, A. M.; Rowan, S. J.; **Tailoring the properties of guanosine-based supramolecular hydrogels**; *Langmuir* **2009***, 25*, 8833.

[97] Li, L.; Guo, X.; Wang, J.; Liu, P.; Prud'homme, R. K.; May, B. L.; Lincoln, S. F.; **Polymer networks assembled by host-guest inclusion between adamantyl and β-cyclodextrin substituents on poly(acrylic acid) in aqueous solution**; *Macromolecules* **2008***, 41*, 8677.

[98] Appel, E. A.; Biedermann, F.; Rauwald, U.; Jones, S. T.; Zayed, J. M.; Scherman, O. A.; **Supramolecular cross-linked networks via host-guest complexation with cucurbit[8]uril**; *J. Am. Chem. Soc.* **2010***, 132*, 14251.

[99] Shikata, T.; Nishida, T.; Isare, B.; linares, M.; Lazzaroni, R.; Bouteiller, L.; **Structure and dynamics of a bisurea-based supramolecular polymer in n-dodecane**; *J. Phys. Chem. B* **2008***, 112*, 8459.
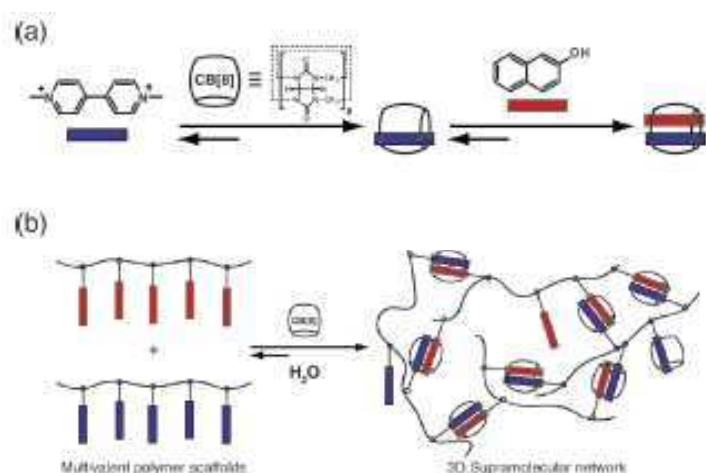
Figure I.22. (a) Schematic of the two-step, three-component host-guest complexation between cucurbit[8]uril, a π-acceptor, and a π-donor, and (b) supramolecular hydrogel preparation through addition of cucurbit[8]uril to a mixture of multivalent first and second guest functional polymers, from ref 98.

### (iii) UPy-based linear supramolecular polymers

A breakthrough in the field of linear "spaghetti-like" non-liquid-crystalline supramolecular polymers came in 1997 through Meijer, his coworkers and their ureidopyrimidinone (UPy) based bifunctional units (Figure I.23, Figure I.24).[100,101] Indeed, UPy is a very strongly self-associating group, dimerizing through four hydrogen bonds, with a very high association constant at 25°C of 6.10^7 L/mol in chloroform and 6.10^8 L/mol in toluene and a relatively long lifetime (0.1 to 1s).[102] Therefore, as pointed out by Lange *et al.*,[90] the UPy unit does not require additional stabilization such as crystallization or other kinds of phase separation, since the dimerization is very strong and unidirectional. As a result, reversible polymer-like properties are obtained in solution and in the bulk, with high degree of polymerization at room temperature.

[100] Sijbesma, R. P.; Beijer, F. H.; Brunsveld, L.; Folmer, B. J. B.; Hirschberg, J. H. K. K.; Lange, R. F. M.; Lowe, J. K. L.; Meijer, E. W.; **Reversible polymers formed from self-complementary monomers using quadruple hydrogen bonding**; *Science* **1997***, 278*, 1601.

[101] Folmer, B. J. B.; Sijbesma, R. P.; Versteegen, R. M.; van der Rijt, J. A. J.; Meijer, E. W.; **Supramolecular polymer materials: chain extension of telechelic polymers using a reactive hydrogen-bonding synthon** *Adv. Mat.* **2000***, 12*, 874.

[102] Söntjens, S. H. M.; Sijbesma, R. P.; van Genderen, M. H. P.; Meijer, E. W.; **Stability and lifetime of quadruply hydrogen bonded 2-ureido-4[1H]-pyrimidinone dimers**; *J. Am. Chem. Soc.* **2000***, 122*, 7487.

Indeed, the viscosity of linear supramolecular polymer increases with the average degree of polymerization, which increases with the thermodynamic association constant of the stickers.[35] For hydrogen-bonded supramolecular polymers, the viscosity decreases as the temperature increases because the hydrogen bonds are released and the association lifetime decreases.[39]
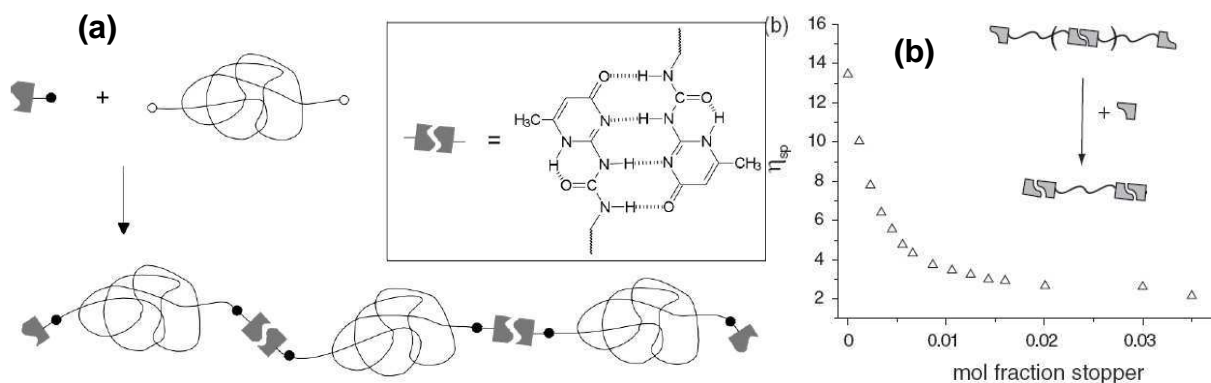
Figure I.23. (a) Schematic drawing of functionalization of telechelic polymers with quadruple hydrogen-bonded ureidopyrimidinone units (UPy), from ref 101. (b) Effect of the addition of a monofunctional UPy compound on the specific viscosity of a 0.04 M solution of a bifunctional UPy compound in CHCl₃, from ref 100.
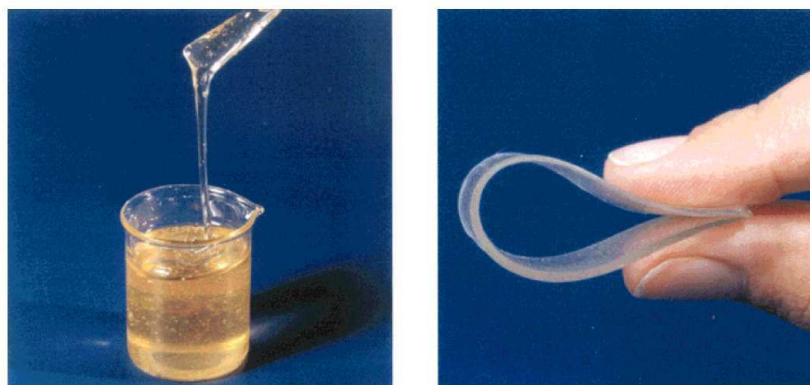

Figure I.24. (left) Poly(ethylene/butylene) with OH end-groups and (right) poly(ethylene/butylene) functionalized with UPy units, from ref 101.

(iv) Clusterization in supramolecular polymers

However, complications can arise from the simple model of linear supramolecular polymers described just above. Indeed, rings and clusters of stickers can form in these supramolecular polymers systems (Figure I.25, Figure I.26, Figure I.27).[103]

---

[103] Manassero, C.; Raos, G.; Allegra, G.; **Structure of model telechelic polymer melts by computer simulation**; *J. Macromol. Sci., Part B: Phys.* **2005**, *44*, 855.
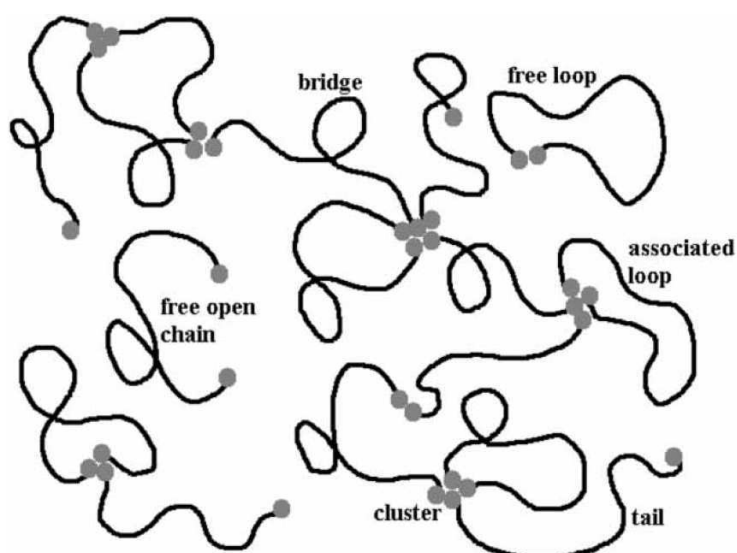
Figure I.25. Schematic representation of the clusters and of the five possible chain states in a telechelic polymer sample, from ref 103.
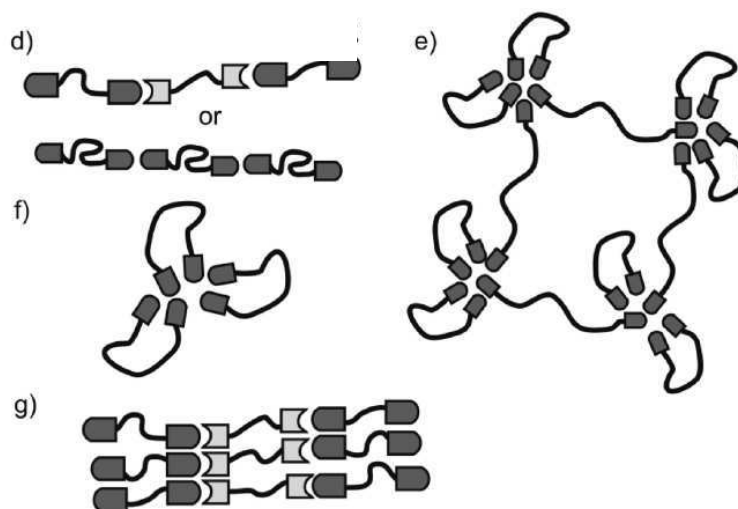
Figure I.26. Possible structures formed by aggregation of bifunctional polymers, from ref 107g.
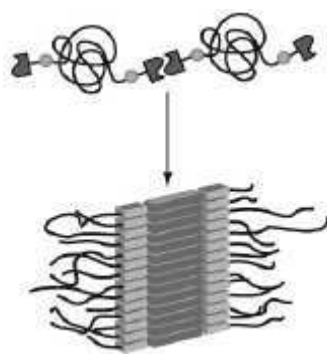
Figure I.27. Schematic representation of the lateral UPy-UPy dimer stacks due to additional hydrogen bonding between the urethane groups (in light grey), from reference 105d.

In the bulk, clusterization of the stickers[11,66,101,104,105,106,107,108] - with[104,105] or without[106] crystallization of the stickers evidenced - has been observed in many supramolecular polymers based on self-complementary associations.

---

[104] Supramolecular polymers with clusterization and crystallization of the stickers:

(a) Hilger, C.; Stadler, R.; **Cooperative structure formation by directed noncovalent interactions in an unpolar polymer matrix. 7. Differential scanning calorimetry and small-angle x-ray scattering**; *Macromolecules* **1992**, *25*, 6670.

(b) Hirschberg, J. H. K. K.; Beijer, F. H.; van Aert, H. A.; Magusin, P. C. M. M.; Sijbesma, R. P.; Meijer, E. W.; **Supramolecular polymers from linear telechelic siloxanes with quadruple-hydrogen-bonded units**; *Macromolecules* **1999**, *32*, 2696.

(c) van Beek, D. J. M.; Spiering, A. J. H.; Peters, G. W. M.; te Nijenhuis, K.; Sijbesma, R. P.; **Unidirectional dimerization and stacking of ureidopyrimidinone end groups in polycaprolactone supramolecular polymers**; *Macromolecules* **2007**, *40*, 8464.

[105] Supramolecular polymers with clusterization and crystallization of the stickers:

(a) Lillya, C. P.; Baker, R. J.; Hutte, S.; Winter, H. H.; Lin, Y. G.; Shi, J.; Dickinson, L. C.; Chien, J. C. W.; **Linear chain extension through associative termini**; *Macromolecules* **1992**, *25*, 2076.

(b) Muller, M.; Dardin, A.; Seidel, U.; Balsamo, V.; Ivan, B.; Spiess, H. W.; Stadler, R.; **Junction dynamics in telechelic hydrogen bonded polyisobutylene networks**; *Macromolecules* **1996**, *29*, 2577.

(c) Colombani, O.; Barioz, C.; Bouteiller, L.; Chanéac, C.; Fompérie, L.; Lortie, F.; Montès, H.; **Attempt toward 1D cross-linked thermoplastic elastomers: structure and mechanical properties of a new system**; *Macromolecules* **2005**, *38*, 1752.

(d) Dankers, P. Y. W.; Zhang, Z.; Wisse, E.; Grijpma, D. W.; Sijbesma, R. P.; Feijen, J.; Meijer, E. W.; **Oligo(trimethylene carbonate)-based supramolecular biomaterials**; *Macromolecules* **2006**, *39*, 8763.

(e) van Beek, D. J. M.; Gillissen, M. A. J.; van As, B. A. C.; Palmans, A. R. A.; Sijbesma, R. P.; **Supramolecular copolyesters with tunable properties**; *Macromolecules* **2007**, *40*, 6340.

(f) Wietor, J.-L.; van Beek, D. J. M.; Peters, G. W.; Mendes, E.; Sijbesma, R. P.; **Effects of branching and crystallization on rheology of polycaprolactone supramolecular polymers with ureidopyrimidinone end groups**; *Macromolecules* **2011**, *44*, 1211.

[106] Supramolecular polymer with clusterization but without crystallization of the stickers: de Lucca Freltas, L.; Burgert, J.; Stadler, R.; **Thermoplastic elastomers by hydrogen bonding**; *Polym. Bull.* **1987**, *17*, 431.

[107] Supramolecular polymer with clusterization of the stickers:

(a) Podesva, J.; Dybal, J., Spevacek, J.; Stepanek, P.; Cernoch, P.; **Supramolecular structures of low-molecular-weight polybutadienes, as studied by dynamic light scattering, NMR and infrared spectroscopy**; *Macromolecules* **2001**, *34*, 9023.

(b) Öjelund, K.; Loontjens, T.; Steeman, P.; Palmans, A.; Maurer, F.; **Synthesis, structure and properties of melamine-based pTHF-urethane supramolecular compounds**; *Macromol. Chem. Phys.* **2003**, *204*, 52.

(c) Mather, B. D.; Elkins, C. L.; Beyer, F. L.; Long, T. E.; **Morphological analysis of telechelic ureidopyrimidone functional hydrogen bonding linear and star-shaped poly(ethylene-co-propylene)s**; *Macromol. Rapid Commun.* **2007**, *28*, 1601.

(d) Botterhuis, N. E.; van Beek, D. J. M.; van Gemert, G. M. L.; Bosman, A. W.; Sijbesma, R. P.; **Self-assembly and morphology of polydimethylsiloxane supramolecular thermoplastic elastomers**; *J. Polym. Sci., Part A: Polym. Chem.* **2008**, *46*, 3877.

(e) Merino, D. H.; Slark, A. T.; Colquhoun, H. M.; Hayes, W.; Hamley, I. W.; **Thermo-responsive microphase separated supramolecular polyurethanes**; *Polym. Chem.* **2010**, *1*, 1263.

(f) Woodward, P. J.; Hermida Merino, D.; Greenland, B. W.; Hamley, I. W.; Light, Z.; Slark, A. T.; Hayes, W.; **Hydrogen bonded supramolecular elastomers: correlating hydrogen bonding strength with morphology and rheology**; *Macromolecules* **2010**, *43*, 2512.

(g) Herbst, F.; Schröter, K.; Gunkel, I.; Gröger, S.; Thurn-Albrecht, T.; Balbach, J., Binder, W. H.; **Aggregation and chain dynamics in supramolecular polymers by dynamic rheology: cluster formation and self-aggregation**; *Macromolecules* **2010**, *43*, 10006.

The fact that there is only one hydrogen-bonding group at the chain ends (telechelic functionality) does not hinder microphase separation.[108] Indeed, stickers, and hydrogen bonding motifs in particular, are often much more polar than the spacer. Furthermore, they are often prone to crystallization. Even the UPy sticker can crystallize[104b,104c,105d,105e,105f] or form stacks[105d,107d] (Figure I.27).

If clusterization of the stickers occurs, the mechanical properties are controlled by this phenomenon. However, the sticker clusterization is not always easy to identify, particularly if the amount of sticker is low (*i.e.* if the spacer are rather long). Moreover, the crystallization process can take quite some time. For instance, in the bulk, the linear supramolecular polymer consisting of two UPy units connected *via* a hexamethylene spacer[100] forms an elastic solid that only crystallises after a few days.[109]

In solution as well clusterization of the stickers can occur. Often, clusterization is induced by aromatic rings stacking, as in the helical columns studied by Hirschberg *et al.*,[110] the fibrillar nanostructure of Kolomiets *et al.*,[111] or the helical nanofibers described by Iwaura *et al.*.[112,113] Interestingly, the nanostructure can be solvent-dependent as in the self-complementary ureidotriazine-based supramolecular polymer that forms random coils *via* hydrogen bonding in chloroform, but helical columns *via* cooperative and solvophobically induced π-stacking of the hydrogen-bonded pairs in dodecane and water.[110,114]

---

[108] Sivakova, S.; Bohnsack, D. A.; Mackay, M. E.; Suwanmala, P.; Rowan, S. J.; **Utilization of a combination of weak hydrogen-bonding interactions and phase segregation to yield highly thermosensitive supramolecular polymers**; *J. Am. Chem. Soc.* **2005**, *127*, 18202.

[109] Hirschberg, J. H. K. K..; *Supramolecular polymers*; PhD Thesis, *Eindhoven University* **2001**.

[110] Hirschberg, J. H. K. K.; Brunsveld, L.; Ramzi, A.; Vekemans, J. A. J. M.; Sijbesma, R. P.; Meijer, E. W.; **Helical self-assembled polymers from cooperative stacking of hydrogen-bonded pairs**; *Nature* **2000**, *407*, 1.

[111] Kolomiets, E.; Buhler, E.; Candau, S. J.; Lehn, J.-M.; **Structure and properties of supramolecular polymers generated from heterocomplementary monomers linked through sextuple hydrogen-bonding arrays**; *Macromolecules* **2006**, *39*, 1173.

[112] Iwaura, R.; Hoeben, F. J. M.; Masuda, M.; Schenning, A. P. H. J.; Meijer, E. W.; Shimizu, T.; **Molecular-level helical stack of a nucleotide-appended oligo(p-phenylenevinylene) directed by supramolecular self-assembly with a complementary oligonucleotide as a template**; *J. Am. Chem. Soc.* **2006**, *128*, 13298.

[113] Iwaura, R.; Iizawa, T.; Minamikawa, H.; Ohnishi-Kameyama, M.; Shimizu, T.; **Diverse morphologies of self-assemblies from homoditopic 1,18-nucleotide-appended bolaamphiphiles: effects of nucleobases and complementary oligonucleotides**; *Small* **2010**, *6*, 1131.

[114] Brunsveld, L.; Vekemans, J. A. J. M.; Hirschberg, J. H. K. K.; Sijbesma, R. P.; Meijer, E. W.; **Hierarchical formation of helical supramolecular polymers via stacking of hydrogen-bonded pairs in water**; *Proc. Natl. Acad. Sci.* **2002**, *99*, 4977.

(v) Supramolecular thermoplastic elastomers from telechelic

As we have seen above, microphase segregation between the spacer and the stickers and crystallization of the stickers into microdomains are not uncommon. As a result, telechelic supramolecular polymers whose stickers clusterize can form supramolecular thermoplastic elastomers (Figure I.28). Indeed, clusterization strongly impacts the mechanical properties of the material: crystalline domains of stickers act as physical cross-links and induce elasticity-dominated rheological behavior;[105] clusters of stickers can also result in a network that allows the formation of mechanically stable films (Figure I.29).[66,108] This phenomenon has been reported as early as in 1992.[105a]
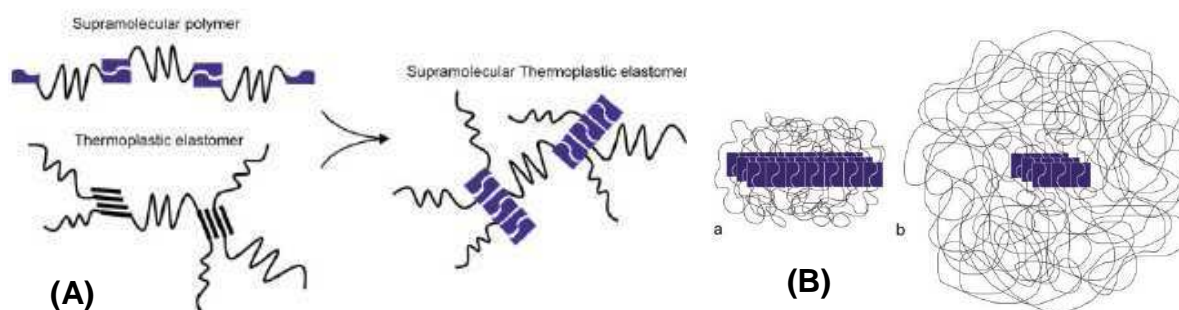
Figure I.28. From reference 107d: (A) schematic overview of the relation between supramolecular polymers, thermoplastic elastomer (TPE), and supramolecular TPEs; (B) cartoon of UPy aggregation in UPy-functionalized siloxane materials: (a) rod-like or (b) spherical.
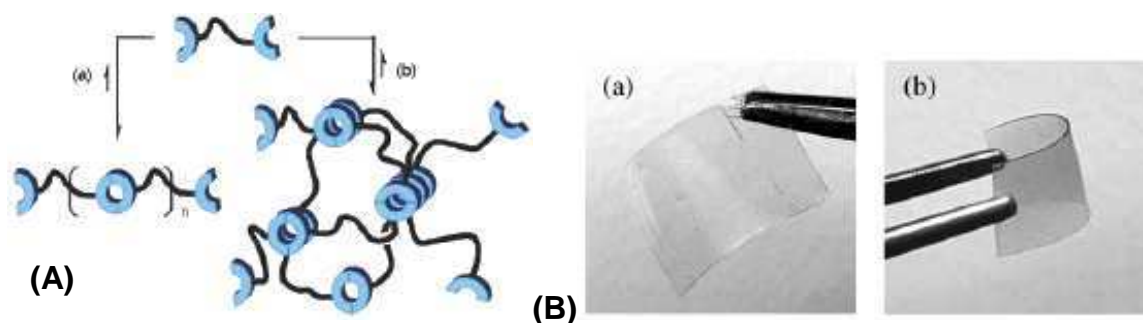
Figure I.29. From ref 108: (A) schematic representation of (a) a linear supramolecular polymer and (b) the use of phase segregation to construct a supramolecular network in the solid state; (B) pictures of the films formed.

Moreover, in Folmer *et al.*'s paper,[101] the time-temperature superposition failure at low frequencies and the presence of a plateau in the storage modulus were suggested to be due to the supramolecular thermoplastic elastomer nature of the UPy-end-capped telechelic compounds, resulting from small clusters of hydrogen-bonded units. The transparent appearance of the material indicated that there were no large clusters.[101]

Rowan and his coworkers have also underlined how phase segregation, combined with weak hydrogen-bonding interactions, can lead to a supramolecular network from telechelic compounds based on adenine or cytosine derivatives (Figure I.29).[108] The presence of π- π stacking between the stickers aromatic rings was also suspected. However, the placement of thymine moiety instead of adenine or cytosine yielded a high melting point solid showing no ability to form mechanically stable films.[115] The authors concluded that there was a complex relationship between the supramolecular assembly of the end group and the phase segregation, and that the right combination of these effects was required to obtain polymeric materials properties.

(vi) Supramolecular polymers based on Thy and DAT

Thymine is often coupled to its complementary nucleobase, adenine,[31,76,87,115,116,117,123] as in DNA. However, diaminopyridine (DAP)[60,118,119] and diaminotriazine (DAT)[107g,120] are also complementary motifs of thymine. Thymine and adenine associate *via* two parallel hydrogen bonds, while thymine and DAT (or DAP) associate *via* three parallel hydrogen bonds. Thymine, adenine, DAP and DAT are aromatic compounds, as illustrated by the fact that, in water, adenine and thymine interact by stacking rather than hydrogen bonding.[31]

[115] Rowan, S. J.; Suwanmala, P.; Sivakova, S.; **Nucleobase-induced supramolecular polymerization in the solid state**; *J. Polym. Sci. A: Polym. Chem.* **2003**, *41*, 3589.

[116] Jacobsen, M. F.; Andersen, C. S.; Knudsen, M. M.; Gothelf, K. V.; **Synthesis of rigid homo- and heteroditopic nucleobase-terminated molecules incorporating adenine and/or thymine**; *Org. Lett.* **2007**, *9*, 2851.

[117] Lutz, J.-F.; Thünemann, A. F.; Rurack, K.; **DNA-like "melting" of adenine- and thymine-functionalized synthetic copolymers**; *Macromolecules* **2005**, *38*, 8124.

[118] Thibault, R. J.; Hotchkiss, P. J.; Gray, M.; Rotello, V. M.; **Thermally reversible formation of microspheres through non-covalent polymer cross-linking**; *J. Am. Chem. Soc.* **2003**, *125*, 11249.

[119] Nandwana, V.; Fitzpatrick, B.; Liu, Q.; Solntsev, K. M.; Yu, X.; Tonga, G. Y.; Eymur, S.; Tonga, M.; Cooke, G.; Rotello, V. M.; **Fluorescence resonance energy transfer in recognition-mediated polymer-quantum dot assemblies**; *Polym. Chem.,* **2012**, *3*, 3072.

[120] Uzun, O.; Frankamp, B. L.; Sanyal, A.; Rotello, V. M.; **Recognition-mediated assembly of nanoparticle-diblock copolymer micelles with controlled size**; *Chem. Mater.* **2006**, *18*, 5404.

f. Differences with other types of self-assembly

Supramolecular polymers are closely related to other types of self-assembly, such as crystals, bolaamphiphiles, block copolymers and other so-called polymerization of molecules in biology. This part aims at clarifying the distinctions between supramolecular polymers and these other self-assembled structures.

(i) Differences with crystals: dynamic

Crystals are also reversibly self-assembled molecules by noncovalent interactions, but unlike supramolecular polymers, the dynamic is frozen in crystals. As a result, crystals form brittle solids.

(ii) Differences with block copolymers: directionality and size

As mentioned before, block copolymers can self-assemble into various morphologies.[121,122] However, unlike supramolecular polymers, block copolymers self-assembly is mostly induced by non-directional interactions (van der Waals, electrostatic, hydrophobic and entropic interactions), although directional interactions such as hydrogen bonding can also control the self-assembly.[123]

Moreover, block copolymers are usually much bigger molecules than supramolecular polymers units. Nevertheless, miniature block copolymers where the blocks are oligomers rather than polymers can also self-assemble. For instance, Stupp and his coworkers reported on the self-assembled nanostructures of miniaturized triblock copolymers consisting of a nine units polystyrene block, a nine units polyisoprene block and a three biphenyl ester units rigid block.[124] Furthermore, Matsushita and his coworkers observed that their triblock copolymers composed of a central polystyrene block (of 11 000 g/mol) and outer oligonucleotide blocks

---

[121] Blanazs, A.; Armes, S. P.; Ryan, A. J.; **Self-assembled block copolymer aggregates: from micelles to vesicles and their biological applications** *Macromol. Rapid Comm.* **2009***, 30*, 267.

[122] Ruzette, A.-V.; Leibler, L.; **Block copolymers in tomorrow's plastics** *Nature Mater.* **2005***, 4*, 19.

[123] Lutz, J.-F.; Pfeifer, S.; Chanana, M.; Thänemann, A. F.; Bienert, R.; **H-bonding-directed self-assembly of synthetic copolymers containing nucleobases: organization and colloidal fusion in a noncompetitive solvent**; *Langmuir* **2006***, 22*, 7411.

[124] Stupp, S. I.; LeBonheur, V.; Walker, K.; Li, L. S.; Huggins, K. E.; Keser, M.; Amstutz, A.; **Supramolecular materials: self-organized nanostructures**; *Science* **1997***, 276*, 384.

of only five thymidine phosphate units microphase-separated in a cylindrical morphology.[125] However, the same compound with only one thymidine unit was disordered and not microphase-separated.[125] In fact, the tendency to microphase-separate of their triblock copolymer series seems to increase with the number of thymidine phosphate units.[125]

(iii) Differences with supramolecular block copolymers: one spacer

The concept of supramolecular block copolymers,[126,127] also called *pseudo* block copolymers,[128] is closely related to that of main-chain supramolecular polymers, except that several types of oligomeric spacers, instead of just one, are used (Figure I.30). The block copolymer aspect allows these materials to microphase-separate while the supramolecular aspect brings responsiveness and reversibility.[129] The simplest form of supramolecular block copolymers results from the self-assembly of two one-end-functionalized polymers into diblock supramolecules (Figure I.31).[130,131,132]
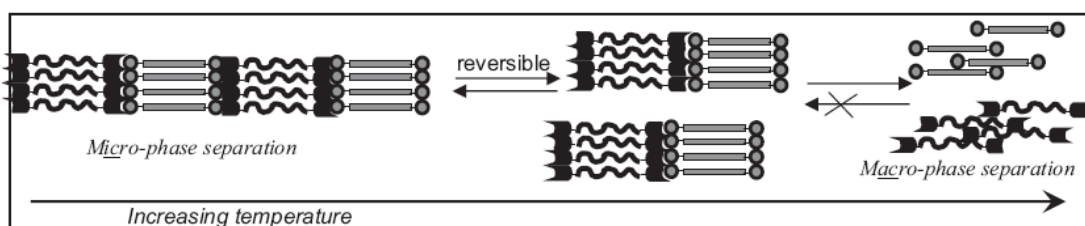
Figure I.30. Self-assembly of telechelic polymers into pseudo block copolymers
by complementary hydrogen bonding associations, from ref 128.

[125] Noro, A.; Nagata, Y.; Tsukamoto, M.; Hayakawa, Y.; Takano, A.; Matsushita, Y.; **Novel synthesis and characterization of bioconjugate block copolymers having oligonucleotides**; *Biomacromolecules* **2005**, *6*, 2328.

[126] Fustin, C.-A.; Guillet, P.; Schubert, U.; Gohy, J.-F.; **Metallo-supramolecular block copolymers**; *Adv. Mater.* **2007**, *19*, 1665.

[127] Yang, S. K.; Ambade, A. V.; Weck, M.; **Main-chain supramolecular block copolymers**; *Chem. Soc. Rev.* **2011**, *40*, 129.

[128] Binder, W.; Bernstorff, S.; Kluger, C.; Petraru, L.; Kunz, M.; **Tunable materials from hydrogen-bonded pseudo block copolymers**; *Adv. Mater.* **2005**, *17*, 2824.

[129] Stuparu, M. C.; Khan, A.; Hawker, C. J.; **Phase separation of supramolecular and dynamic block copolymers**; *Polym. Chem.* **2012**, *3*, 3033.

[130] Huh, J.; ten Brinke, G.; **Micro- and macrophase separation in blends of reversibly associating one-end-functionalized polymers**; *J. Chem. Phys.* **1998**, *109*, 789.

[131] Noro, A.; Nagata, Y.; Takano, A.; Matsushita, Y.; **Diblock-type supramacromolecule via biocomplementary hydrogen bonding** *Biomacromolecules* **2006**, *7*, 1696.

[132] Feldman, K. E.; Kade, M. J.; de Greef, T. F. A.; Meijer, E. W.; Kramer, E. J.; Hawker, C. J.; **Polymers with multiple hydrogen-bonded end groups and their blends**; *Macromolecules* **2008**, *41*, 4694.
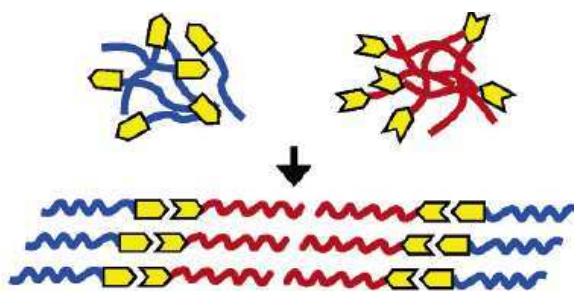
Figure I.31. Schematic illustration for formation of a diblock-type supramacromolecule *via* hydrogen bonding (nanophase separation), from ref 131.

(iv) Differences with bolaamphiphiles, HEUR and ionomers: directionality

Bolaamphiphiles are composed of a central hydrophobic core capped on both ends with a hydrophilic group.[133] Therefore, bolaamphiphiles are basically triblock copolymers where the two end-blocks are comprised of only one monomer. They self-assemble in various supramolecular morphologies (micelles, cylinders, …) because of the incompatibility between the hydrophilic and hydrophobic parts. [133,134] Therefore, unlike the supramolecular polymer concept, the self-assembly of bolaamphiphiles is induced by less specific solvent-surfactants interactions and non-directional interactions, although in some bolaamphiphiles directional hydrogen bonding associations play an important role. It should be noted that the term *bolaamphiphile* is almost always used in the context of aqueous solutions.

Hydrophobically end-capped polymers (such as hydrophobic ethoxylated urethane: HEUR) and ionomers form reversible networks by clustering of the end groups, through hydrophobic and dispersion interactions for HEUR,[135] and through coulomb forces for ionomers.[136] Therefore, unlike the supramolecular polymer concept, the end groups are associated through non-directional interactions.

---

[133] Fuhrhop, J.-H.; Wang, T.; **Bolaamphiphiles**; *Chem. Rev.* **2004**, *104*, 2901.

[134] Shimizu, T.; Masuda, M.; Minamikawa, H.; **Supramolecular nanotube architectures based on amphiphilic molecules** *Chem. Rev.* **2005**, *105*, 1401.

[135] Tam, K. C.; Jenkins, R. D.; Winnik, M. A.; Bassett, D. R.; **A structural model of hydrophobically modified urethane-ethoxylate (HEUR) associative polymers in shear flows**; *Macromolecules* **1998**, *31*, 4149.

[136] Chassenieux, C.; Johannsson, R.; Durand, D.; Nicolai, T.; Vanhoorne, P.; Jérôme, R.; **Telechelic ionomers studied by light scattering and dynamic mechanical measurements**; *Colloids Surf. A* **1996**, *112*, 155.

(vi) Differences with biologist's polymerization

For biochemists and molecular biologists, the word *polymerization* has the meaning of the word *self-assembly*: proteins 'polymerize' (aggregate) into larger structures (microtubules, fibrils, virus particles) and proteins β-sheet structures 'polymerize' into polymeric tapes, gels and membranes through hydrophobic and other noncovalent interactions.[35a]

g. Conclusion

To conclude, scientists like to categorize systems. However, the lines can be blurry and the same system may belong to more than one class. Or a system may sit on the edge, sharing some characteristics, but not quite belonging to any existing (so far) box. Moreover, science fields can be quite compartmentalized, not sharing the same vocabulary for the same underlying physical-chemical phenomena.

Indeed, the telechelic compounds functionalized with hydrogen-bonding stickers and leading to main-chain supramolecular polymers can be considered as miniaturized triblock copolymers (with the outer blocks consisting of only one unit, the sticker), supramolecular multiblock copolymers (with an alternance of very short blocks [the sticker] and longer blocks [the spacer]) or bolaamphiphiles, with the directional interactions between the stickers in extra. These directional interactions are thus always in competition with phase segregation, crystallization, and other potential noncovalent interactions (such as aromatic interactions). Indeed, microphase segregation with only one unit is possible if the incompatibility is high enough.

Therefore, the questions we were interested in are: when a system shares various characteristics, will one of the characteristics take over? Or will a compromise arise, leading to a new type of behavior?

Finally, we were interested in whether the clusterization of stickers occurring because of dispersions interactions or crystallization in supramolecular polymers can lead to long-range order and order-disorder transition as in block copolymers. In other terms do telechelic supramolecular polymers behave as miniaturized block copolymers?

Chapter II

Synthesis

of supramolecular polymers

by grafting

of Thy and DAT stickers

on telechelic PPO chains

Supramolecular polymers are obtained by grafting thymine derivatives (Thy) and/or diamininotriazine (DAT) stickers on the chain ends of telechelic diamino poly(propylene oxide) (PPO). DAT was grafted through an aromatic nucleophilic substitution, while Thy was grafted through amidation, by heating or with a coupling agent. Homoditopic compounds were synthesized in one step, while heteroditopic compounds were synthesized in four steps through a protection / deprotection pathway.

Chapter II. Synthesis of supramolecular polymers by grafting of Thy and DAT stickers on telechelic PPO chains

Chapter II. Synthesis of supramolecular polymers by grafting of Thy and DAT stickers on telechelic PPO chains

To investigate the interplay between hydrogen bonding, phase segregation and crystallization in supramolecular polymers, we have chosen to study a model system. This model system consist of non-crystalline poly(propylene oxide) (PPO) chains end-functionalized with complementary stickers: thymine derivative (Thy) and diaminotrozaine (DAT). This system combines weak (Thy/Thy and DAT/DAT self-association) and strong (Thy/DAT complementary association) hydrogen bonding, aromaticity of the stickers, strong repulsion between the polar stickers and the PPO spacers, and very different tendency towards crystallization for Thy and DAT. Indeed, Thy derivatives are prone to crystallization,[1] whereas DAT derivatives are known for their tendency to form glasses instead of crystallizing.[2]

1. Telechelic PPO chains as spacers between the stickers

a. Amino-terminated PPO chains *1* chosen as linkers

In our model system, the supramolecular stickers associate reversibly and directionally *via* hydrogen bonds, while the spacers connect the stickers and afford mobility.

(i) A low T_g and non-crystalline chain to afford mobility

To afford mobility, the spacers must remain amorphous (non-crystalline) and liquid (non-glassy) in a wide temperature range: typically from - 40 to 200°C would be sufficient for most applications. Indeed, crystalline or glassy spacers would severely reduce the mobility of the system, and thus hinder the stickers association dynamic.

Glassy compounds exhibit a glass transition temperature (T_g): they are glassy below T_g and liquid above T_g. Therefore, a liquid spacer in the temperature range - 40°C to 200°C is a non-crystalline spacer with a T_g below - 40°C.

---

[1] Borowiak, T.; Dutkiewicz, G.; Spychaia, J.; **Supramolecular motifs in 1-(2-cyanoethyl)thymine and 1-(3-cyanopropyl)thymine**; *Acta Crystallo. C* **2007**, *63*, 201.

[2] Wang, R.; Pellerin, C.; Lebel, O.; **Role of hydrogen bonding in the formation of glasses by small molecules: a triazine case study**; *J. Mater. Chem.* **2009**, *19*, 2747.

Oligomers (low-molecular-weight polymers) are perfect candidates to link stickers. Several oligomers are non-crystalline and have a low T_g, for instance:

- branched alcanes such as polyisobutylene (PIB),

- polysiloxanes such as polydimethylsiloxane (PDMS),

- polydisperse or copolymerized poly(ethylene oxide) (PEO),

- poly(propylene oxide) (PPO),

- poly(isoprene) (PI),

- poly(ethylene/butylene) (PE-PB).

PIB have been used to build supramolecular polymers by Stadler and his coworkers,[3] as well as Binder and his coworkers;[4] PDMS by Bouteiller and his coworkers;[5] PPO-PEO block copolymers,[6, 7] PE-PB[8] and PDMS[6, 9, 10] by Meijer, Sijbesma and their coworkers.

Each of these candidates present advantages and drawbacks. For example, PEO are commercial products, available with several end-groups and sizes. However, PEO are very hydrophilic and hygroscopic, so water can easily be absorbed and potentially affect hydrogen bonds. Plus, if not polydisperse enough or too long, PEO crystallizes.

PPO chains are soluble in a wide range of organic solvents, and even in water under their LCST (lower critical solution temperature), around 18°C. Plus, PPO are commercial

---

[3] Muller, M.; Dardin, A.; Seidel, U.; Balsamo, V.; Ivan, B.; Spiess, H. W.; Stadler, R.; **Junction dynamics in telechelic hydrogen bonded polyisobutylene networks**; *Macromolecules* **1996**, *29*, 2577.

[4] Binder, W. H.; Kunz, M. J.; Kluger, C.; Hayn, G.; Saf, R.; **Synthesis and analysis of telechelic polyisobutylenes for hydrogen-bonded supramolecular pseudo-block copolymers**; *Macromolecules* **2004**, *27*, 1749.

[5] Abed, S.; Boileau, S.; Bouteiller, L.; Lacoudre, N.; **Supramolecular association of acid terminated polydimethylsiloxanes. 1. Synthesis and characterization**; *Polym. Bull.* **1997**, *39*, 317.

[6] Sijbesma, R. P.; Beijer, F. H.; Brunsveld, L.; Folmer, B. J. B.; Hirschberg, J. H. K. K.; Lange, R. F. M.; Lowe, J. K. L.; Meijer, E. W.; **Reversible polymers formed from self-complementary monomers using quadruple hydrogen bonding** *Science* **1997**, *278*, 1601.

[7] Lange, R. F. M.; Gurp, M. V.; Meijer, E. W.; **Hydrogen-bonded supramolecular polymer networks** *J. Polym. Sci., Part A: Polym. Chem.* **1999**, *37*, 3657.

[8] Folmer, B. J. B.; Sijbesma, R. P.; Versteegen, R. M.; van der Rijt, J. A. J.; Meijer, E. W.; **Supramolecular polymer materials: chain extension of telechelic polymers using a reactive hydrogen-bonding synthon** *Adv. Mater.* **2000**, *12*, 874.

[9] Hirschberg, J. H. K. K.; Beijer, F. H.; van Aert, H. A.; Magusin, P. C. M. M.; Sijbesma, R. P.; Meijer, E. W.; **Supramolecular polymers from linear telechelic siloxanes with quadruple-hydrogen-bonded units**; *Macromolecules* **1999**, *32*, 2696.

[10] Botterhuis, N. E.; van Beek, D. J. M.; van Gemert, G. M. L.; Bosman, A. W.; Sijbesma, R. P.; **Self-assembly and morphology of polydimethylsiloxane supramolecular thermoplastic elastomers** *J. Polym. Sci. Part A: Polym. Chem.* **2008**, *46*, 3877.

products, available in several sizes and functionality. Moreover, PPO is not hydrophilic, so phase segregation with the stickers might occur and could be studied. Consequently, we have chosen oligomeric PPO as spacer in our model system.

(ii) A primary amine end-functionality to connect the stickers

The spacers must be connected to the stickers, so they need to be at least bifunctional, and preferably with highly reactive functions. That is why we have chosen commercial PPO end-functionalized by primary amine groups, Jeffamine ®, and more specifically Jeffamines ® D Series (bifunctional) and T Series (3-armed branched trifunctional) (Chart II.1, Jeffamines ® M Series [monofunctional] were also used as a control). In this chapter we will focus on the functionalization of Jeffamines ® D Series.

Halogen functionalized stickers can then easily be grafted by nucleophilic substitution, while carboxylic acid functionalized stickers can easily be grafted by amidation.
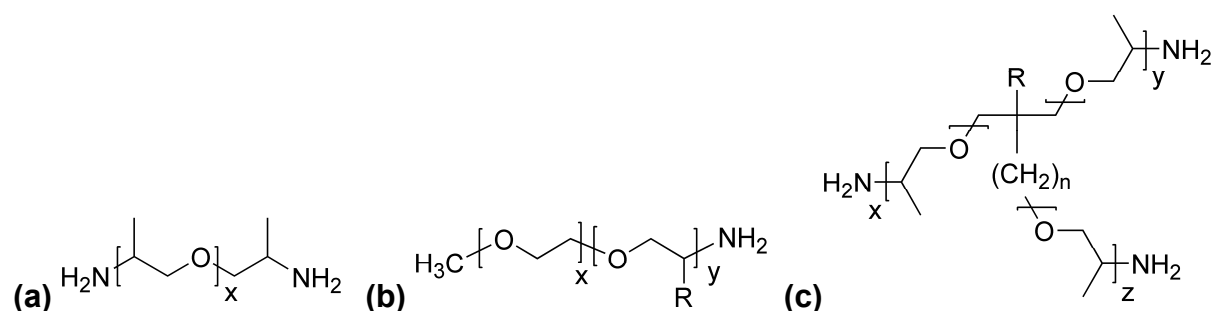
Chart II.1. Chemical structures of Jeffamine ®: (a) D series, (b) M series (R = H or CH$_3$), and (c) T series (R = C$_2$H$_5$ or H, n = 1 or 0).

b. Properties of chosen PPO spacers 1a-c

(i) Number average molecular weight M_n estimated from ^{1}H NMR

^{1}H NMR of commercial Jeffamine ® D-230, D-400 and D-2000, diamine telechelic poly(propylene oxide) (denoted as NH$_2$-PPO-X-NH$_2$, where X is the molecular weight in g/mol), allows the determination of its number average molecular weight (M_n). Indeed, the CH$_3$ protons in α-position of the amine end-groups (**b**, see Chart II.2) are shifted upfield compared to the CH$_3$ protons in the middle of the chain (**a**), as illustrated on the abscissa of Figure II.1. M_n and x ($x = n + 1$) can then be determined by integrating those two ^{1}H NMR

signals (equations 1 and 2, with I_a and I_b the integral of the **a** and **b** signals, respectively). M_n and x values obtained in this fashion are gathered in Table II.1. The values are close to the values from Huntsman technical bulletins.

Given the values of M_n determined by integrating the **a** and **b** ^{1}H NMR signals, Jeffamine D230 will now be denoted as NH_2-PPO-250-NH_2 **1c**, Jeffamine D400 as NH_2-PPO-460-NH_2 **1b**, and Jeffamine D2000 as NH_2-PPO-2200-NH_2 **1a**.

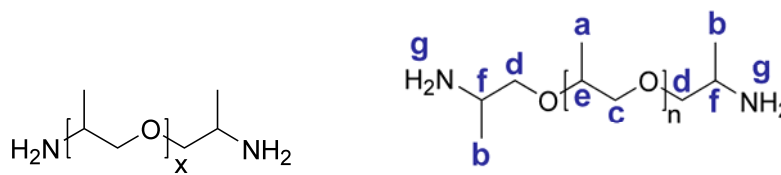**Chart II.2.** Chemical structures of NH_2-PPO-X-NH_2 **1a-c** (Jeffamine D) (n = x -1).
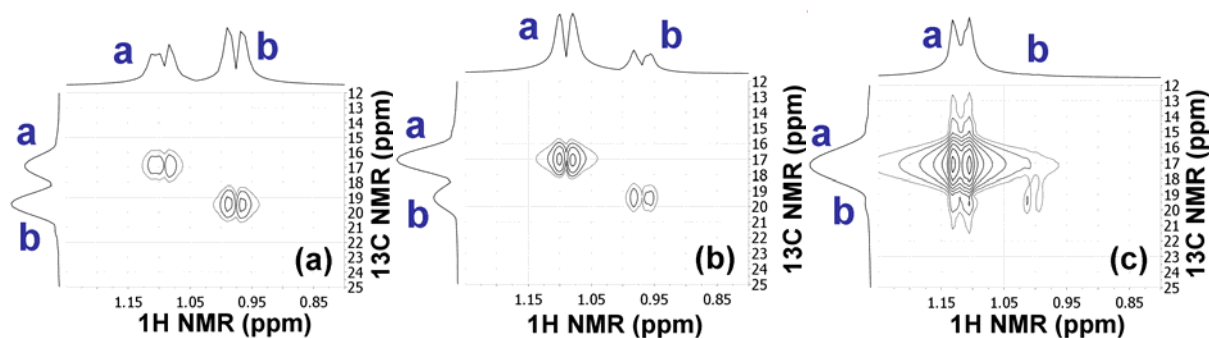
Figure II.1. HMQC (^{1}H-^{13}C 2D NMR) in $CDCl_3$ of NH_2-PPO-X-NH_2 **1** (a) X = 250, (b) X = 460, (c) X = 2200.

$$x = 1 + \frac{2I_a}{I_b} \qquad (1)$$

$$M_n = 58x + 74 \qquad (2)$$

(ii) Polydispersity index I_p estimated from GC-MS and GPC

Gas Chromatography coupled to Mass Spectrometry (GC-MS) was performed on NH_2-PPO-X-NH_2 **1b-c**. Chromatograms reveal NH_2-PPO-250-NH_2 **1c** is constituted of oligomers bearing 2, 3 and 4 repetition units, while NH_2-PPO-460-NH_2 **1b** contains oligomers with 2 to 9 repetition units. Indeed, each oligomer size appears on the GC chromatogram as a distinct peak with tailing characteristic of primary amines (Figure II.2). Peaks were easily attributed thanks to their associated MS spectrum. Indeed, the MS spectra almost all contain the M-1 peak characteristic of primary amines.

Integrating each GC peak's area gives a good estimation of the proportion of each oligomer size. Indeed, although GC is not strictly quantitative since the detector response is compound-dependent, the oligomers' chemical structures are close enough for a quantitative estimation.
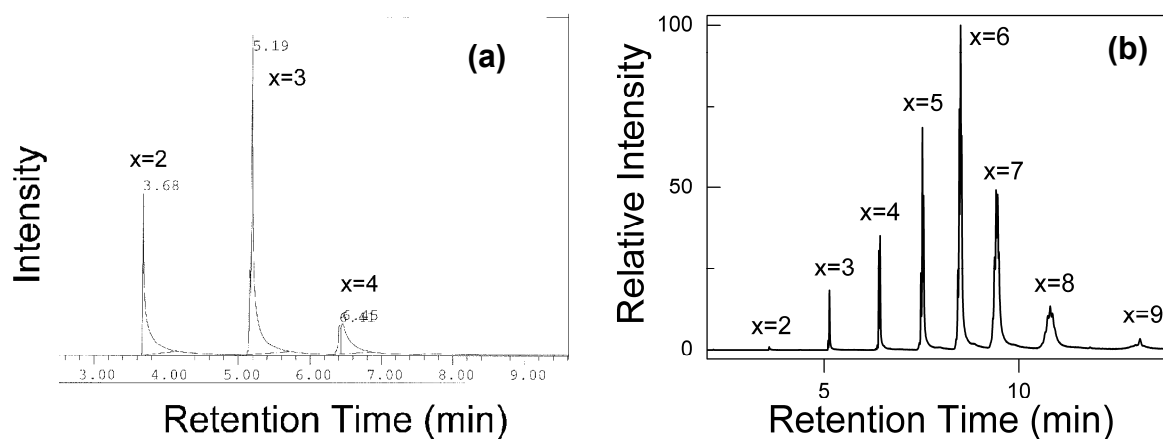
Figure II.2. GC spectrograms of: (a) NH_2-PPO-250-NH_2 **1c**, and (b) NH_2-PPO-460-NH_2 **1b**.

Therefore, M_n, the weight average molecular weight (M_w) and the polydispersity index ($I_p = M_w / M_n$) can be calculated. The values obtained for M_n and I_p are gathered in Table II.1. The values of M_n obtained by GC are close the values obtained by ^{1}H NMR, implying the validity of both methods. M_n of NH_2-PPO-460-NH_2 **1b** from GC is a little underestimated, since oligomers of 10 or more repetition units may be present in NH_2-PPO-460-NH_2 **1b**, but are not detected on the GC spectrogram (Figure II.2b). I_p are quite low.

By zooming on the GC peaks, it appears that they are actually multiple peaks. This multiplicity of peaks, with almost the same retention time, and the same MS spectra, suggests that head-to-head sequences, as well as head-to-tail sequences, were formed during the oligomerization. Indeed, PPO is generally obtained by ring-opening polymerization of 1,2-propylene oxide, and both C-O bonds of the epoxy group may cleave during the polymerization.[11]

NH_2-PPO-2200-NH_2 **1a** molecular weight is too high for the GC-MS column, but gel permeation chromatography (GPC) can be used to estimate I_p. These values are gathered in Table II.1.

---

[11] Schilling, F. C.; Tonelli, A. E.; **Carbon-13 NMR determination of poly(propylene oxide) microstructure**; *Macromolecules* **1986**, *19*, 1337.

(iii) Glass transition temperature T_g measured from DSC

NH_2-PPO-X-NH_2 **1a-c** have been studied by Differential Scanning Calorimetry (DSC). They all display a glass transition step (Figure II.3). The T_g values are gathered in Table II.1.
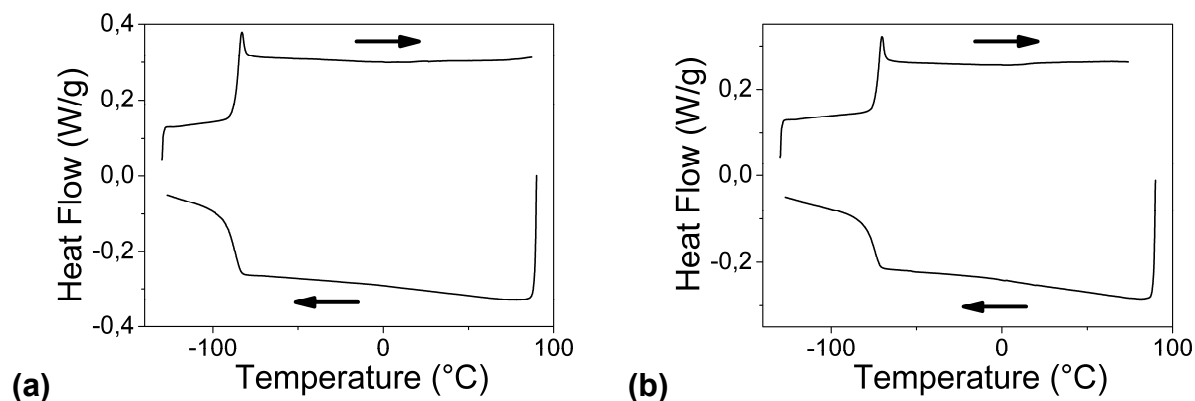

Figure II.3. DSC (exo down) at 10°C/min of (a) NH_2-PPO-250-NH_2 **1c**, and (b) NH_2-PPO-2200-NH_2 **1a**.

T_g increases with the molecular weight, as expected for oligomers because of the free-end effect. Indeed, the lower is the molecular weight, the higher is the proportion of chain ends in a given volume. Chain ends afford free volume, and thus mobility.

The boiling temperature of NH_2-PPO-X-NH_2 **1a-c** (**a**: X = 2200, **b**: X = 460, **c**: X = 250) is announced at 260°C by Huntsman.

(iv) NH_2-PPO-X-NH_2 **1a-c** characteristics recap

JEFFAMINE ®	M_n[a] (g/mol)	x[a]	M_n[b] (g/mol)	x[b]	M_n[c] (g/mol)	I_p	T_g[e] (°C)
D-230	230	~ 2,5	**248**	**3,0**	244	1.029 [c]	- 84,6
D-400	430	~ 6,1	**457**	**6,6**	434 [f]	1.027 [c, f]	- 81,5
D-2000	2000	~ 33	**2220**	**37**	-	1.04 [d]	- 71,8

**Table II.1.** NH_2-PPO-X-NH_2 **1a-c** data
([a] from Huntsman technical bulletin, [b] determined by ^{1}H NMR, [c] determined by GC, [d] determined by GPC, [e] determined by DSC, [f] underestimated since x=10 and higher are not detected).

2. Grafting DAT sticker

a. Grafting DAT via an aromatic nucleophilic substitution

Diaminotriazine (DAT) grafting was achieved *via* an aromatic nucleophilic substitution of amines on the commercial product 2-chloro-4,6-diamino-1,3,5-triazine (DAT-Cl). The reactions were carried out in a water/ethanol mixture (v/v 50/50) under reflux for 20 hrs in the presence of $NaHCO_3$ (adapted from Klenke et al).[12] The chemical structures of the resulting materials were confirmed by ^{1}H NMR, ^{13}C NMR, DEPT 135, ^{1}H-^{1}H correlation NMR (COSY), ^{1}H-^{13}C correlation NMR (HMQC), FT-IR and GC-MS when possible.
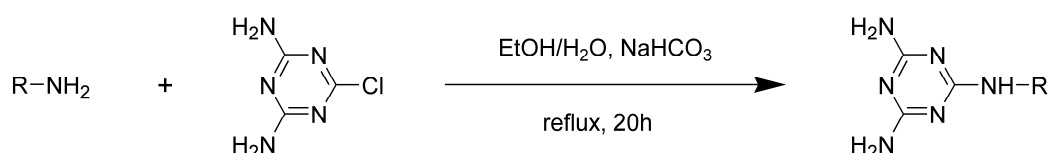
Scheme II.1. Aromatic nucleophilic substitution of an amine on 2-chloro-4,6-diamino-1,3,5-triazine.

b. Reaction efficiency tested by grafting DAT on Dodecylamine

To test this reaction, DAT was grafted on dodecylamine. Since DAT-Cl was only partially soluble in the water/ethanol solvent, the reaction mixture started as a white suspension that transformed into a transparent solution as the reaction progressed. 2-dodecylamine-4,6-diamino-1,3,5-triazine (DAT-C_{12}) was easily retrieved by filtration, since DAT-C_{12} precipitated from the solution at room temperature. The full synthesis protocol and characterization of DAT-C_{12} are in Appendix II.

c. Grafting DAT on diamine telechelic PPO

(i) Same reaction conditions, but adapted purification

The diaminotriazine homoditopic supramolecular polymers DAT-PPO-*X*-DAT **2a-c** (**a**: *X* = 2200, **b**: *X* = 460, **c**: *X* = 250) were synthesized *via* an aromatic nucleophilic

---

[12] Klenke, B.; Stewart, M.; Barrett, M. P.; Brun, R. ; Gilbert, I. H.; **Synthesis and biological evaluation of s-triazine substituted polyamines as new anti-typanosomal drug**; *J. Med. Chem.* **2001**, *44*, 3440.

substitution of the corresponding diamine telechelic poly(propylene oxide) NH_2-PPO-X-NH_2 **1a-c** on DAT-Cl. The reactions were carried out in the same conditions as for dodecylamine (Scheme II.2).
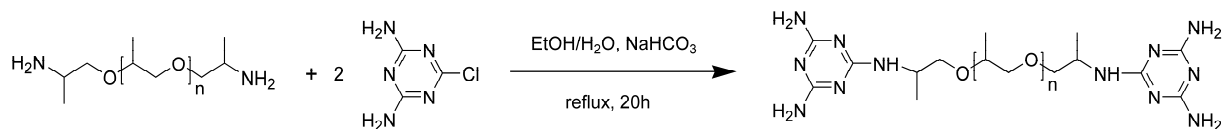
Scheme II.2. DAT-PPO-X-DAT **2a-c** synthesis *via* aromatic nucleophilic substitution of diamine telechelic poly(propylene oxide) NH_2-PPO-X-NH_2 **1a-c** on 2-chloro-4,6-diamino-1,3,5-triazine.

However, the purification procedures were adapted to the length PPO chain. Indeed, all products DAT-PPO-X-DAT **2a-c** are soluble in the water/ethanol mixture at room temperature and thus cannot be obtained by filtration. Therefore, **2a-b** ($X = 2200$, 460) were extracted *via* liquid-liquid extraction after removal of ethanol. In contrast, **2c** ($X = 250$) is not hydrophobic enough to be extracted by a non polar solvent. Indeed, **2c** is insoluble in chloroform, dichloromethane or toluene. Therefore, its purification was achieved by evaporation of solvent, solubilization in a chloroform / methanol mixture (v/v 50/50) under reflux, and filtration to eliminate a precipitate composed of $NaHCO_3$ and DAT-OH. The full experimental protocols are in Appendix II. The syntheses of DAT-PPO-X-DAT **2a-b** (**a**: $X = 2200$, **b**: $X = 460$) were reported in reference 13.[13]

(ii) Characterization of final products

^1H and ^{13}C NMR in DMSO-d_6 showed that the desired product were formed (see Appendix II; for $X = 2200$, see Figure II.4 for ^1H NMR and Figure II.5 for ^{13}C NMR). For instance on the ^1H spectrum of the product, the methine of the PPO backbone closest to the terminal groups were shifted downfield above 4 ppm and the NH_2 on the aromatic ring of DAT were shifted upfield.

---

[13] Cortese, J.; Soulié-Ziakovic, C; Tencé-Girault, S.; Leibler, L.; **Suppression of mesoscopic order by complementary interactions in supramolecular polymers**; *J. Am. Chem. Soc.* **2012**, *134* , 3671.
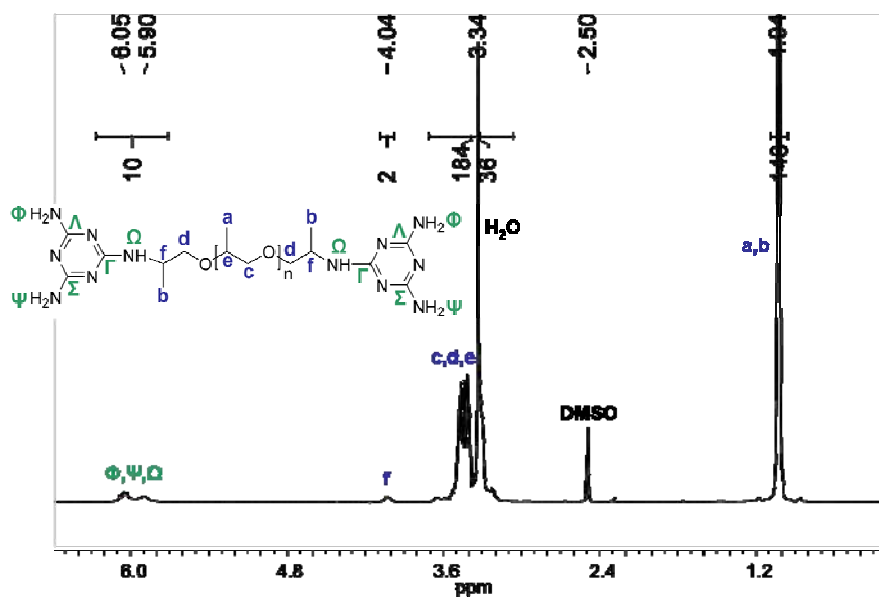
Figure II.4. ^{1}H NMR in DMSO-d_6 of DAT-PPO-2200-DAT **2a**.
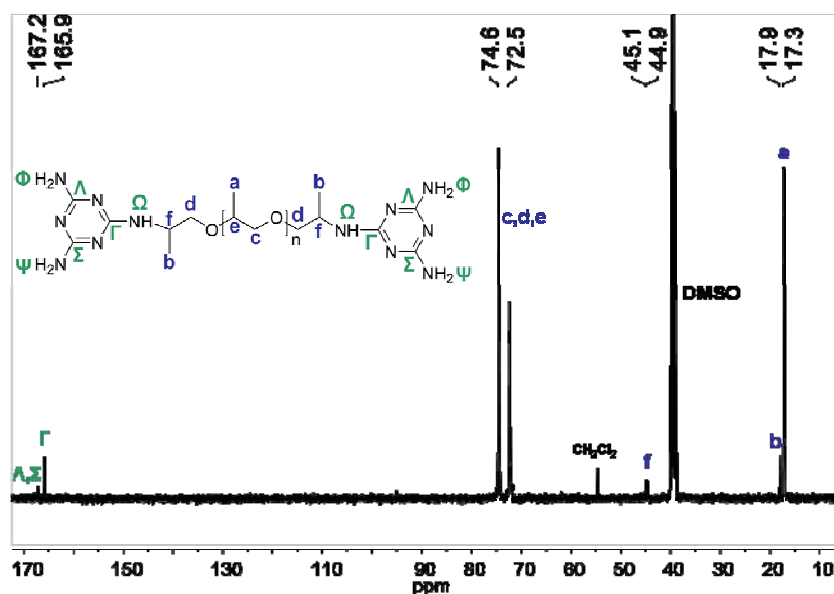
Figure II.5. ^{13}C NMR in DMSO-d_6 of DAT-PPO-2200-DAT **2a**.

GC-MS is not adapted to characterize the products. Indeed, for $X = 460$ and 2200, the molecular weight is too high for the column; and for $X = 250$, high concentrations are needed to observe a signal on the GC spectrum, probably because the DAT groups interact too strongly with the column. However, high concentrations can damage the detector and the column and are thus not recommended.

67

3. Grafting Thy sticker

Thy grafting was achieved *via* amidation of amines by the carboxylic acid functionality of the commercial product thymine-1-acetic acid.

a. Different ways to form an amide bond

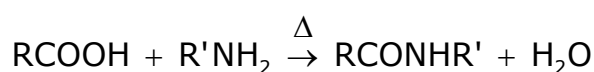Indeed, coupling an amine with a carboxylic acid yields an amide (and water, see Scheme II.3). This reaction, which results from a nucleophilic attack of the amine on the carboxylic acid, can be completed by heating or with coupling reagents.

$$RCOOH + R'NH_2 \xrightarrow{\Delta} RCONHR' + H_2O$$

Scheme II.3. Reaction of a carboxylic acid with an amine to yield an amide (and water).

(i) Amide bond formation by heating

Since amines are bases of pK_a around 10-11, and carboxylic acids are acids of pK_a around 4-5 (pK_a of thymine-1-acetic acid around 3, as measured by NaOH titration), put together they form a salt, with very little amine left at equilibrium to act as the nucleophile in the amidation. However, the amide can still be formed by heating the ammonium salt to high temperatures (160-180°C).

$$RCOOH + R'NH_2 \rightarrow RCOO^- + R'NH_3^+$$
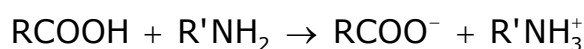
Scheme II.4. Acido-basic reaction of a carboxylic acid with an amine to form an ammonium salt.

Furthermore, the high temperature, accompanied by a nitrogen flow, permits the evacuation of water vapour. Thus, the equilibrium is shifted towards the amide formation. However, high temperatures can be detrimental to the integrity of some substances, even with a nitrogen atmosphere. For instance, high temperature of 160 to 180°C are incompatible with the presence of the *N-tert*-butoxycarbonyl (BOC) protecting group.

(ii) Amide bond formation with coupling agents

Carboxylic acid are not very reactive in nuclepophilic substitution reactions such as amidation, because OH⁻ is a poor leaving group. Therefore, coupling reagents are often used

to activate the acid, by formation of a good leaving group, and thus facilitate the amidation.[14,15] Several types of coupling agents can be used:

- acyl chlorides,

- reagents generating acid halides (such as $SOCl_2$[16] or PCl_5),

- cyanuric chloride,

- carbodiimides,

- triazoles derivatives, …etc …

However, like heat, the strongly acidic conditions induced by acyl chlorides, cyanuric chloride, or reagents generating acid halides induce BOC deprotection. Moreover, acyl chlorides and cyanuric chloride are very toxic.

Besides, the most common carbodiimides, dicyclohexylcarbodiimide (DCC)[17] and diisopropylcarbodiimide (DIC), yield by-products that can be difficult to remove. They can be replaced by water soluble carbodiimides, such as 1-ethyl-3(3'-(dimethylamino)propyl) carbodiimide hydrochloride salt (EDC).[18] However, EDC reacts at low pH, in acidic conditions, which might also induce BOC deprotection.

Hydroxy-benzotriazole (HOBt) and uronium, aluminium and phosphonium salts based on HOBt perform well, and are commonly used for peptide coupling.[14,15] Yet, they can be very expensive and care must be taken because of the explosive properties of HOBt. Indeed, HOBt is explosive when fully dehydrated (but is mostly found hydrated).

(iii) Coupling agent chosen: TBTU

To compromise between reaction speed, purity of the product, ease of by-products purification, efficiency, high conversions, and cost, we have chosen TBTU [O-(benzotriazol-

---

[14] Valeur, E.; Bradley, M.; **Amide bond formation: beyond the myth of coupling reagents**; *Chem. Soc. Rev.* **2009***, 38*, 606.

[15] Montalbetti, C.; Falque, V.; **Amide bond formation and peptide coupling**; *Tetrahedron* **2005***, 61*, 10827.

[16] Cvetovich, R. J.; DiMichele, L.; **Formation of acrylanilides, acrylamides, and amides directly from carboxylic acids using thionyl chloride in dimethylacetamide in the absence of bases**; *Org. Process Res. Dev.* **2006***, 10*, 944.

[17] Chen, G.; Hoffman, A. S.; **Preparation and properties of thermoreversible, phase-separating enzyme-oligo(N-isopropylacrylamide) conjugates**; *Bioconjugate Chem.* **1993***, 4*, 509.

[18] Nakajima, N.; Ikada, Y.; **Mechanism of amide formation by carbodiimide for bioconjugation in aqueous media**; *Bioconjugate Chem.* **1995***, 6*, 123.

1-yl)-N,N,N',N'-tetramethyl uronium tetrafluoroborate] as activating agent of the thymine-1-acetic acid. Indeed, TBTU is the cheapest of the salts based on HOBt {less than 200 euros for 100g, while HATU [O-(7-azabenzotriazol-1-yl)-N,N,N′,N′-tetramethyluronium hexafluoro-phosphate] is at more than 1800 euros for 25g}.

Coupling of thymine-1-acetic acid to an amide with TBTU, in the presence of the non-nucleophilic base DIEA (diiosopropylethylamine) and DMF has been described in the literature.[19] The closely related coupling of thymine-1-acetic acid to an amide with HATU, also in the presence of DIEA and DMF, has also been reported.[20]
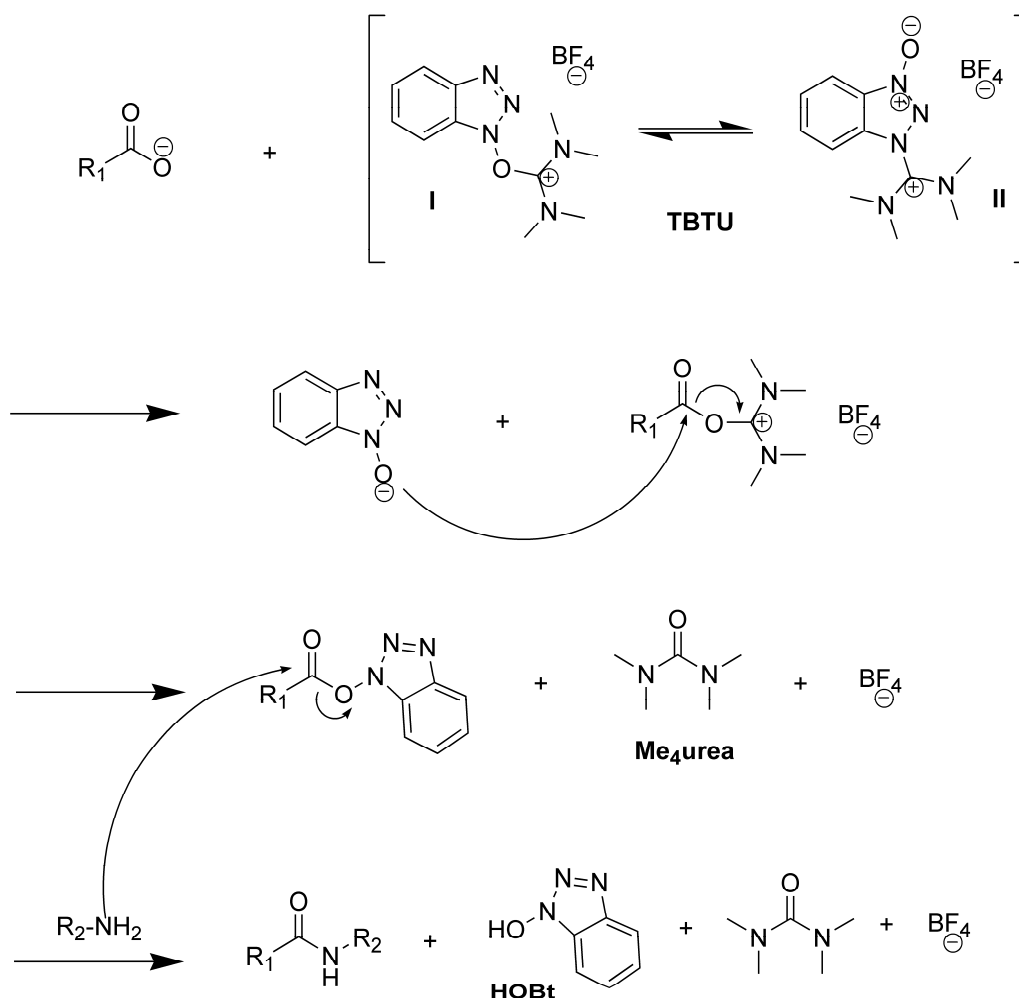

Scheme II.5. Proposed mechanism for the amide bond formation through TBTU activation (**I** and **II** are the two tautomeric forms of TBTU), from ref 21.

---

[19] Corradini, R.; Sforza, S.; Dossena, A.; Palla, G.; Rocchi, R.; Filira, F.; Nastri, F.; Marchelli, R.; **Epimerization of peptide nucleic acids analogs during solid-phase synthesis : optimization of the coupling conditions for increasing optical purity**; *J. Chem. Soc. Perkin Trans. 1* **2001**, *20*, 2690.

[20] Roviello, G.N.; Moccia, M.; Sapio, R.; Valente, M.;Bucci, E. M.; Castiglione, M; Pedone, C.; Peretta, G.; Benedetti, E.; Musumeci, D.; **Synthesis, characterization and hybridization studies of new nucleo-γ-peptides base on diaminobutyric acid**; *J. Peptide Sci.* **2006**, *12*, 829.

Balalaie *et al.* proposed the mechanism reproduced in Scheme II.5 for the amide bond formation, from a carboxylic acid and an amine, with TBTU as the activating agent, in the presence of a non-nucleophilic base.[21] The base, not featured in the mechanism, is here to deprotonate the carboxylic acid and to keep the amine under its basic form -NH$_2$. The protonated base forms a salt with BF$_4^-$ at the end of the reaction. Other by-products from TBTU are tetramethylurea (Me$_4$urea) and HOBt, which will have to be separated from the amide. To simplify purification, polymer-supported coupling reagents can be used.[22]

b. Amidation with TBTU tested by grafting Thy on alkylamines
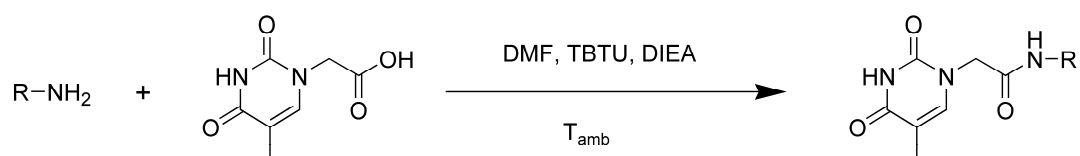
Scheme II.6. Amidification of an amine by thymine-1-acetic acid in solution with a coupling agent.

To test the amidation with TBTU, Thy was grafted on *n*-butylamine, *n*-dodecylamine and *n*-octadecylamine (Scheme II.6 adapted from Corradini *et al.*).[19] N-butyl-thymine-1-acetamide (Thy-C$_4$), N-dodecyl-thymine-1-acetamide (Thy-C$_{12}$), and N-octadecyl-thymine-1-acetamide (Thy-C$_{18}$) were obtained.

The reaction was first performed on butylamine. The Thy-C$_4$ yield was only of 77%, probably due to the fact that TBTU, as other coupling reagents, can degrade when left in solution in the presence of a base. Therefore, to increase the yield, the reactions were subsequently performed with an excess of TBTU. Then, the Thy-C$_{18}$ yield was of 93%. Moreover, for the same reason, the order of mixing is important: first the carboxylic acid is solubilized in DMF, then the amine is added, followed by TBTU, and finally the base (a non nucleophilic amine: diisopropylethylamine [DIEA]).

Other adjustments are made in the protocol depending on the products. For instance, *n*-octadecylamine is scarcely soluble in DMF, so Thy-C$_{18}$ synthesis was done in a

---

[21] Balalaie, S.; Mahdidoust, M.; Eshaghi-Najafabadi, R.; **2-(1H-Benzotriazole-1-yl)-1,1,3,3-tetramethyluronium tetrafluoroborate as an efficient coupling reagent for the amidation and phenylhydrazation of carboxylic acids at room temperature**; *J. Iran. Chem. Soc.,* **2007***, 4*, 364.

[22] Chinchilla, R.; Dodsworth, D. J.; Nájera, C.; Soriano, J. M.; **Polymer-bound TBTU as a new solid-supported reagent for peptide synthesis**; *Tetrahedron Letters* **2000***, 41*, 2463.

toluene/DMF mixture at 60°C. Furthermore, Thy-C$_4$ and Thy-C$_{18}$ were easily retrieved by filtration at room temperature, but Thy-C$_{12}$ did not precipitate from the solution. So, Thy-C$_{12}$ was purified by liquid-liquid extraction. The full synthesis protocols and characterizations of final products are in Appendix 2.

c. Grafting Thy on diamine telechelic PPO

(i) Two synthesis methods

The thymine homoditopic supramolecular polymer **3a-c** (Thy-PPO-X-Thy, **a**: X = 2200, **b**: X = 460, **c**: X = 250) were synthesized *via* amidation of the corresponding diamine telechelic poly(propylene oxide) NH$_2$-PPO-X-NH$_2$ **1a-c** with thymine-1-acetic acid. The reactions were carried out either in the same conditions as for the alkylamines, *ie* in solution with a coupling agent (TBTU, Scheme II.7a); or in bulk at 160°C under a nitrogen flow (Scheme II.7b, adapted from a method by Montarnal *et al.*).[23] The full experimental protocols are in Appendix II. The synthesis of Thy-PPO-X-Thy **3a-b** were reported in reference 24.[24]
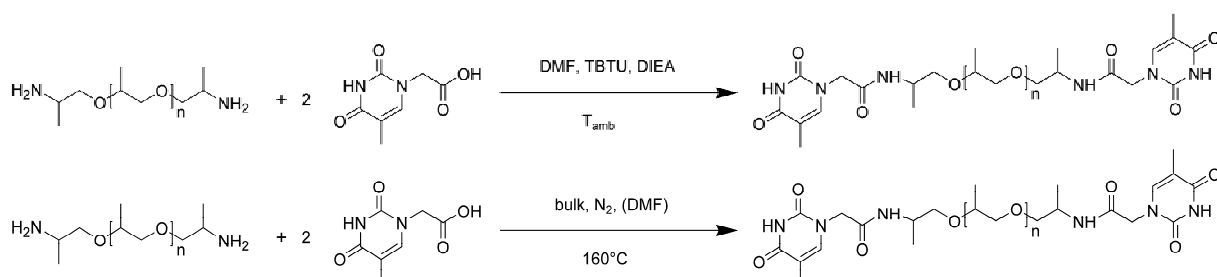
Scheme II.7. Thy-PPO-X-Thy **3a-c** synthesis *via* amidification of diamine telechelic poly(propylene oxide) **1a-c** by thymine-1-acetic acid carried out (a) in solution with a coupling agent, or (b) in the bulk at 160°C under N$_2$.

(ii) With TBTU: same reaction conditions, but adapted purification

With TBTU, the reactions were carried out in the same conditions as for the alkylamines. However, the purification protocols were adapted to the length of PPO chain. Indeed, all products Thy-PPO-X-Thy **3a-c** are soluble in DMF at room temperature and thus

[23] Montarnal, D.; Cordier, P.; Soulié-Ziakovic, C.; Tournhilhac, F., Leibler, L.; **Synthesis of self-healing supramolecular rubbers from fatty acid derivatives, diethylene triamine, and urea**; *J. Polym. Sci., Part A: Polym. Chem.* **2008**, *46*, 7925.

[24] Cortese, J.; Soulié-Ziakovic, C; Cloitre, M.; Tencé-Girault, S.; Leibler, L.; **Order-disorder transition in supramolecular polymers**; *J. Am. Chem. Soc.* **2011**, *133*, 19672.

cannot be obtained by filtration. Therefore, **3a** (X = 2200) was extracted *via* liquid-liquid extraction after addition of water and toluene to the reaction mixture. In contrast, **3c** (X = 250), like DAT-PPO-250-DAT **2c**, is not lipophilic enough to be extracted by a non polar solvent. Indeed, **3c** is insoluble in chloroform, dichloromethane or toluene. Consequently, **3c** was purified by silica column chromatography (eluant MeOH/CHCl₃: 1/9 v/v), which can be done rather easily because of its small size.

The reaction can be followed by ^{1}H and ^{13}C NMR. For instance, as evidenced on Figure II.6, the signal of the methyls in α-position of the amine end-groups (**b**, see Chart II.3) is deshielded as the amine (δ_{b-NH2} = 0.91 ppm) transforms into an amide (δ_{b-Thy} = 1.03 ppm). Moreover, the amino NH₂ signal at 1.57 ppm disappears, while a doublet at 7.98 ppm corresponding to the amide NH appears. The CH₃ (**A**), CH₂ (**B**) and CH (**C**) Thy signals are also shifted upon grafting: they are shielded, because an acid group is more deshielding than an amide group (respectively electron-withdrawing and electron-donating effect) (Figure II.7).
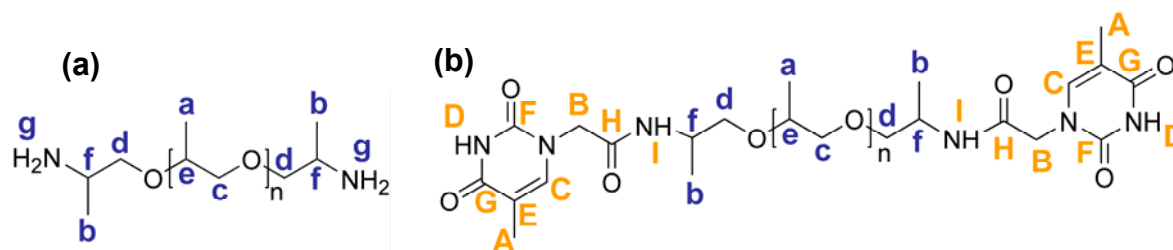

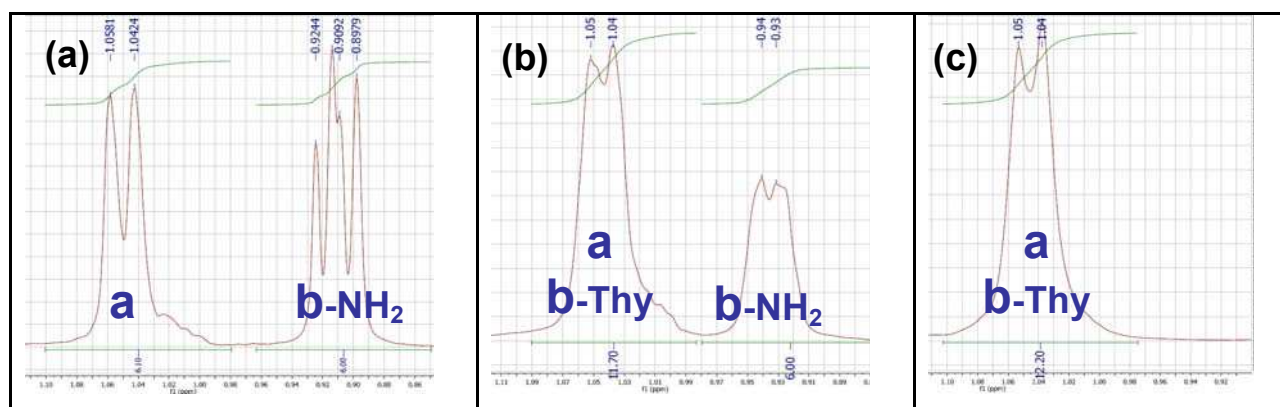**Chart II.3.** Chemical structures of (a) NH₂-PPO-X-NH₂ **1a-c** and (b) Thy-PPO-X-Thy **3a-c**.

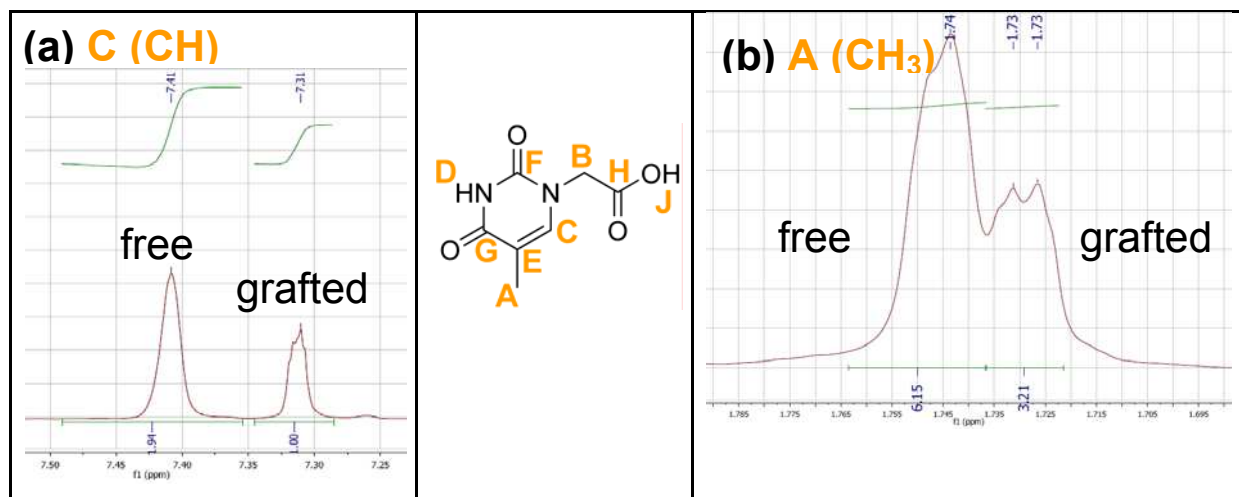**Figure II.6.** ^{1}H NMR in DMSO-d₆ of the methyl region (0.85 -1.11 ppm) of : (a) NH₂-PPO-250-NH₂ **1c**; (b) a mixture of NH₂-PPO-250-NH₂ **1c**, Thy-PPO-250-Thy **3c** and thymine-1-acetic acid (incomplete reaction); (c) Thy-PPO-250-Thy **3c**.

Figure II.7. ^{1}H NMR of a mixture of NH$_2$-PPO-250-NH$_2$ **1c**, Thy-PPO-250-Thy **3c** and thymine-1-acetic acid (incomplete reaction) showing signals of free and grafted Thy: (a) methine proton C region (7.2-7.5 ppm); (b) methyl protons A region (1.69-1.79 ppm).

(iii) By heating

Like the polyamides synthesis often carried out in the lab, Thy grafting can be done in the bulk, *i.e.* without solvent, at 160°C and under a nitrogen flow. In these conditions, thymine-1-acetic acid is soluble in NH$_2$-PPO-*X*-NH$_2$ **1a-c** and these compounds do not oxidize. As mentioned above, the elevated temperature and the nitrogen flow allow evacuation of the water formed by amidation and shifting of the equilibrium toward the amide formation.

However, maintaining a good stirring is difficult with NH$_2$-PPO-250-NH$_2$ **1c**, and gets even harder as the reaction progresses. Indeed, as discussed in Chapter V, the T$_g$ of Thy-PPO-250-Thy **3c** is very high (around 100°C). Thus, its viscosity at 160°C is also quite high. Adding a couple droplets of DMF can help to fluidify the mixture and thus improve the stirring. Indeed, DMF can solubilize thymine-1-acetic acid, and more importantly reduce Thy-PPO-250-Thy's T$_g$ by plasticizing effect.

Furthermore, thymine-1-acetic acid must be added progressively, to limit the NH$_3^+$COO$^-$ salt formation, which blocks stirring by solidification of the solution. As a result, synthesis can take several days, especially for Thy-PPO-250-Thy **3c**.

The reaction can be followed by FT-IR in ATR (attenuated total reflectance) mode. In Figure II.8, salt of NH$_2$-PPO-250-NH$_2$ **1c** and thymine-1-acetic acid was formed immediately

and is characterized by a deformation band δ_{NH3+} at 1608 cm^{-1} and a valence band $\upsilon_{C=O}$ of the carboxylate function at 1694 cm^{-1} (Figure II.8, red curve). When the reaction progresses, the δ_{NH3+} deformation band disappears and the $\upsilon_{C=O}$ valence band shifts towards lower wavenumbers until reaching 1656 cm^{-1}, value of an amide $\upsilon_{C=O}$ (Figure II.8, blue curve).
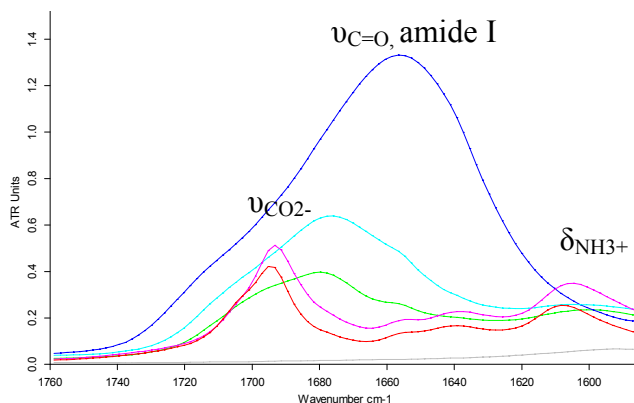
Figure II.8 : ATR FT-IR spectra between 1585 and 1760 cm^{-1} at 25°C with in gray: NH$_2$-PPO-250-NH$_2$; in red: NH$_2$-PPO-250-NH$_2$ + thymine-1-acetic acid salt (1694 cm^{-1},1608 cm^{-1}); in pink: after 45 min at 160°C (1693 cm^{-1},1605 cm^{-1}); in green: after 5h30 (1680 cm^{-1}); in light blue: after 20h (1677 cm^{-1}); in dark blue: Thy-PPO-250-Thy (1656 cm^{-1}).

To sum up, this method is not very convenient for Thy-PPO-250-Thy, but works well for Thy-PPO-2200-Thy, for which stirring is not an issue.

Although the boiling temperature of all NH$_2$-PPO-X-NH$_2$ **1a-c** is around 260°C, some evaporation of NH$_2$-PPO-X-NH$_2$ occurs during the reaction, especially for the shorter oligomers, because of their low vapour pressure and because of the nitrogen stream. Therefore, at the end of the reaction, there is an excess of thymine-1-acetic acid. This excess can either be recrystallized in a CHCl$_3$/MeOH (v /v 50:50) mixture or separated by column chromatography. Thy-PPO-X-Thy **3** migrate almost as fast as the solvent, whereas unreacted thymine acid derivative remains in the column (MeOH/CHCl$_3$: 2/8 v/v).

(iii) Purification efficiency and characterization of final products

The chemical structures of the resulting materials were confirmed by ^{1}H and ^{13}C NMR in DMSO-d$_6$ (see Appendix II; for X = 2200, see Figure II.9 for ^{1}H NMR and Figure II.10 for ^{13}C NMR). Since the end-groups signals can be identified, the molecular weight (M$_n$) can be estimated: 800 g/mol for Thy-PPO-460-Thy **3b** and 2500 g/mol for Thy-PPO-2200-Thy **3a**.

GC-MS is not adapted to characterize the products. Indeed, for $X = 460$ and 2200, the molecular weight is too high for the column; and for $X = 250$, high concentrations are needed to observe a signal on the GC spectrum, probably because the Thy groups interact too strongly with the column. However, high concentrations can damage the detector and the column and are thus not recommended.
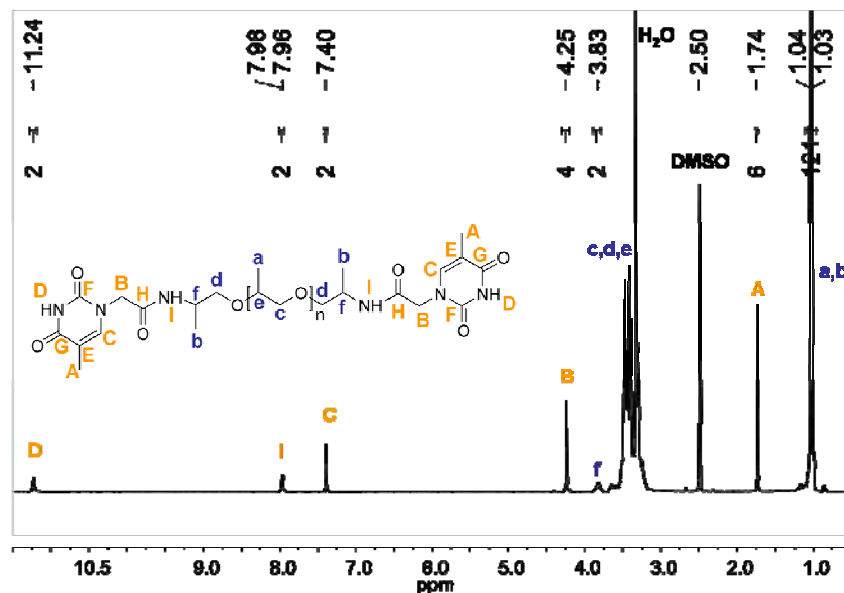

Figure II.9. ^{1}H NMR in DMSO-d_6 of Thy-PPO-2200-Thy **3a**.

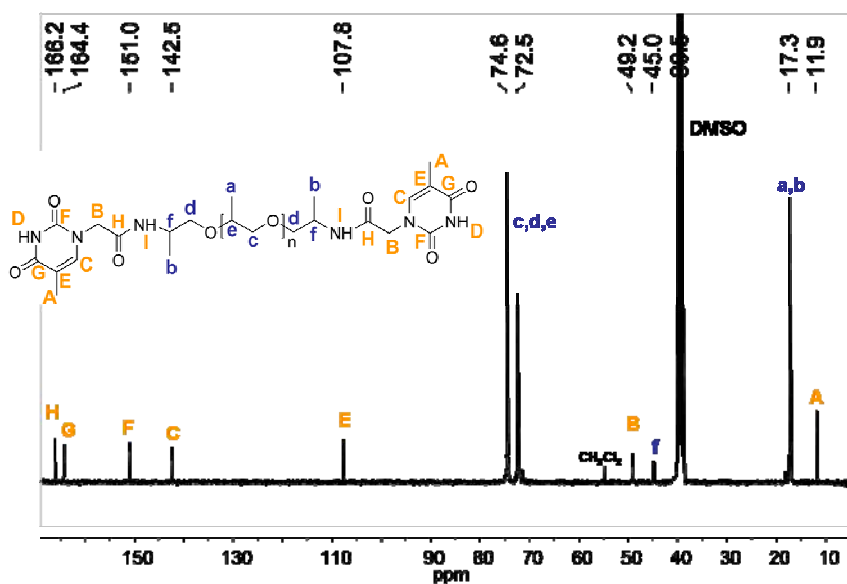**Figure II.10.** ^{13}C NMR in DMSO-d_6 of Thy-PPO-2200-Thy **3a**.

4. Blending Thy-PPO-*X*-Thy **3** with DAT-PPO-*X*-DAT **2**

Thy and DAT can associate with themselves through self-complementary hydrogen bonding, but this self-association is very weak compared to their association with one another through hetero-complementary hydrogen bonding. Therefore mixing Thy-PPO-*X*-Thy with DAT-PPO-*X*-DAT yields a stronger supramolecular polymer.

(i) By solvent cast

Blending Thy-PPO-*X*-Thy **3a-c** with DAT-PPO-*X*-DAT **2a-c** forms homoditopic supramolecular polymers. They are denoted as $\phi/(100-\phi)$-M-*X* **4a-c**, **5a**, and **6a** (**4**: $\phi = 50$, **5**: $\phi = 25$, **6**: $\phi = 75$; **a**: *X* = 2200, **b**: *X* = 460; **c**: *X* = 250) where *X* is still the molecular weight (in g.mol^{-1}) of the PPO spacer, and $\phi/(100-\phi)$-M-*X* indicates a mixture M of ϕ % Thy-PPO-*X*-Thy **3a-c** and $(100-\phi)$ % DAT-PPO-*X*-DAT **2a-c**. $\phi/(100-\phi)$-M-*X* **4a-c**, **5a**, and **6a** were prepared by separately solubilizing **2** and **3** in a good solvent (1:1 CHCl$_3$/MeOH blend or CH$_2$Cl$_2$) and then mixing the two solutions. $\phi/(100-\phi)$-M-*X* were then obtained in the bulk by solvent casting and annealing under vacuum at 100 °C for 3 h.

(iii) Characterization of final products

^{1}H and ^{13}C NMR in DMSO-d$_6$ showed that the desired product were obtained (see Appendix II; for *X* = 2200, see Figure II.11 for ^{1}H NMR and Figure II.12 for ^{13}C NMR).
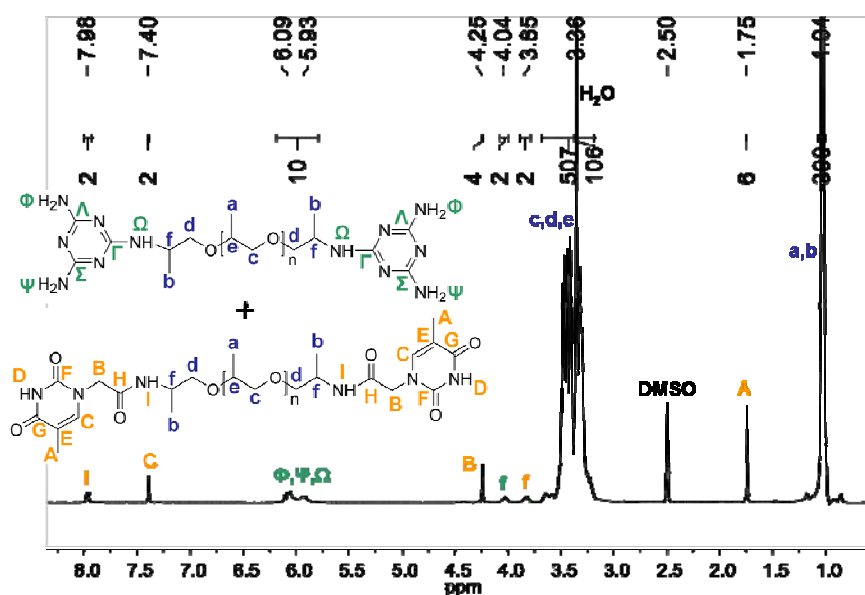
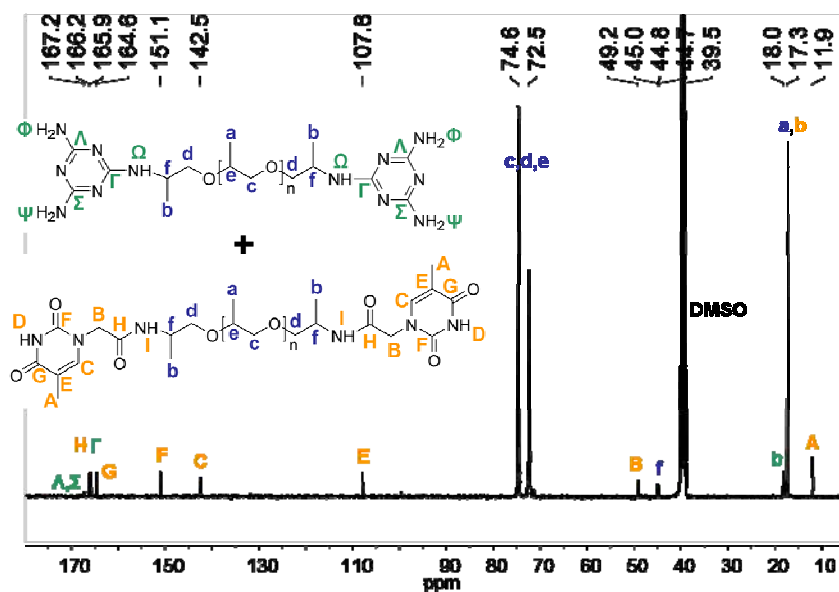

Figure II.11. ^{1}H NMR in DMSO-d$_6$ of 50/50-M-2200 **4a**.

Figure II.12. ^{13}C NMR in DMSO-d$_6$ of 50/50-M-2200 **4a**.

5. Heteroditopic grafting of Thy and DAT (grafting Thy on one side and DAT on the other side)

a. Advantages of heteroditopic supramolecular polymers over blends of homoditopic supramolecular polymers

To obtain a high degree of polymerization (DP) with homotelechelic blends (A-spacer-A=B-spacer-B)$_n$, the A and B stickers stoichiometry needs to be carefully controlled to 1 to 1, because the excess of one sticker has a chain stopper effect that limits DP.[25]

To avoid this issue of stoichiometry in hometelechelic blends, Zimmerman's[26] and Meijer's[27] groups synthesized supramolecular polymers with stickers A not only capable of hetero-complementary association, but also of self-complementary dimerization, *i.e.* both K$_{AB}$

---

[25] Berl, V.; Schmutz, M.; Krische, M. J.; Khoury, R. G.; Lehn, J.-M.; **Supramolecular polymers generated from heterocomplementary monomers linked through multiple hydrogen-bonding arrays formation, characterization, and properties**; *Chem. Eur. J.* **2002**, *8*, 1227.

[26] Park, T.; Zimmerman, S. C.; **Interplay of fidelity, binding strength, and structure in supramolecular polymers**; *J. Am. Chem. Soc.* **2006**, *128*, 14236.

[27] de Greef, T. F. A.; Ercolani, G.; Ligthart, G. B. W. L.; Meijer, E. W.; Sijbesma, R. P.; **Influence of selectivity on the supramolecular polymerization of AB-type polymers capable of both A-A and A-B interaction**; *J. Am. Chem. Soc.* **2008**, *130*, 13755.

and K_{AA} association constants were high. As a result, if A's concentration is higher than B's, DP is still large. The limitation of this strategy is that of course, if it is B that is in excess, chain stopper effect takes place.

With heterotelechelic unit (A-spacer-B), stoichiometry is always 1 to 1, so high dimerization constants are no longer needed. However, synthetic pathways are more tedious.

b. Strategies for asymmetric synthesis of supramolecular polymers

Three main routes have been explored to obtain heteroditopic supramolecular polymers: oligomerization of the spacer from the stickers, convergent coupling, and asymmetric end-functionalization post-oligomerization.

### (i) Oligomerization of the spacer from the stickers

The first path, oligomerization of the spacer from the stickers which are acting as initiators or terminators, has been developed by the Weck group. They used ring-opening methathesis polymerization (ROMP) with a sticker A-functionalized ruthenium initiator (A = Hamilton receptor) and a sticker B-based chain-terminator (B = 2,7-diamido-1,8-naphthyridine (DAN)), to synthesize a heterotelechelic A-poly(norbornene imide)-B.[28] With a similar idea, Mansfeld *et al.* used a heterodifunctionalized alkoxyamine initiator to prepare, *via* nitroxyde-mediated radical polymerization, heterotelechelics bearing the 2-ureido-4[1*H*]-pyrimidinone (UPy) sticker on one side and the terpyridine (tpy) group on the other (Figure II.13).[29]

These elegant routes offer high-yielding preparation of asymmetrically functionalized supramolecular units. However, these approaches require multistep synthesis of the initiators, transfer agents and/or chain terminators. Moreover, the development of these strategies is restricted by the choice of monomers (strained cycles, acrylates, styrenics).

---

[28] (a) Ambade, A.; Yang, S.; Weck, M.; **Supramolecular ABC triblock copolymers**; *Angew. Chem. Int. Ed.* **2009***, 48*, 2894. (b) Yang, S. K.; Ambade, A. V.; Weck, M.; **Supramolecular ABC triblock copolymers via one-pot, orthogonal self-assembly**; *J. Am. Chem. Soc.* **2010***, 132*, 1637.

[29] Mansfeld, U.; Winter, A.; Hager, M. D.; Hoogenboom, R.; Gunther, W.; Schubert, U. S.; **Orthogonal self-assembly of stimuli-responsive supramolecular polymers using one-step prepared heterotelechelic building blocks**; *Polym. Chem.* **2012***, 4*, 113
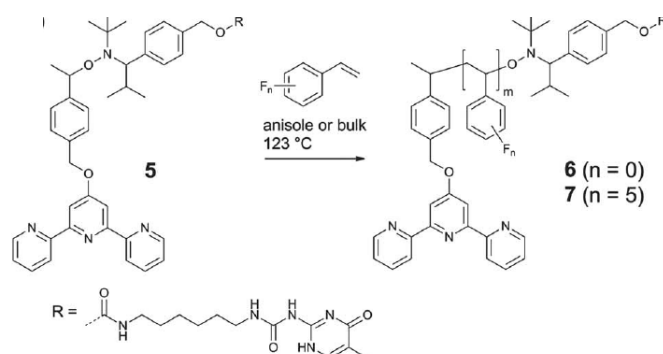
Figure II.13. Schematic representation of the polymerization of styrenic monomers using the heterodifunctional alkoxyamine tpy-TIPNO-UPy **5** as an initiator, from ref 29.

(ii) Convergent coupling

The second route, convergent coupling, has been followed by Xu *et al.*[30] for oligonucleotides and by Scherman *et al.*[31] who used selective olefin cross methathesis coupling of an A functionalized acrylate with a B functionalized olefin (both also obtained by coupling[32]) to obtain heterotelechelic A-spacer-B supramolecular units (A = UPy, B = NaPy). Nevertheless, this pathway shares the same drawbacks as the first one: complicated multistep synthesis and purification of precursors, and limitation of possible chemistries.

(iii) Asymmetric end-functionalization post-oligomerization

The third strategy, asymmetric end-functionalization of an oligomeric spacer, on the contrary, is versatile but not trivial. First of all, oligomer end-functions depend on synthetic pathways, and often have to be modified, along with the stickers, so that they can be reacted together. Furthermore, since spacers are generally larger than 5 carbons, both ends present the same reactivity, and yet, have to be functionalized differently. To circumvent this, Shimizu *et al.*[33] reacted a large excess (10 : 1) of the difunctional spacer with sticker A (A = thymine).

---

[30] Xu, J.; Fogleman, E. A.; Craig, S. L.; **Structure and properties of DNA-based reversible polymers**; *Macromolecules* **2004***, 37*, 1863.

[31] Scherman, O. A.; Ligthart, G. B. W. L.; Sijbesma, R. P.; Meijer, E. W.; **A selectivity-driven supramolecular polymerization of an AB monomer**; *Angew. Chem. Int. Ed.* **2006***, 45*, 2072.

[32] Ligthart, G. B. W. L.; Ohkawa, H.; Sijbesma, R. P.; Meijer, E. W.; **Pd-catalyzed amidation of 2-chloro- and 2,7-dichloro-1,8-naphthyridines**; *J. Org. Chem.* **2006***, 71*, 375.

[33] Shimizu, T.; Iwaura, R.; Masuda, M.; Hanada, T.; Yase, K.; **Internucleobase-interaction-directed self-assembly of nanofibers from homo- and heteroditopic 1,w-nucleobase bolaamphiphiles**; *J. Am. Chem. Soc.* **2001***, 123*, 5947.

Under these conditions, A-bifunctionalized spacer are scarcely formed. Then, they separated the A-monofunctionalized spacer from the excess spacer by column chromatography, and finally reacted it with sticker B (B = adenine), leading to a A-spacer-B heterotelechelic unit. However, they used very well-defined spacers (dodecyl-1,12-diamine, decyl-1,10-diamine, …), convenient for column chromatography purification. Such a purification process is hardly applicable to oligomeric or polymeric spacers, because the polydispersity generally precludes efficient products separation.

Another strategy could be to graft the stickers on already asymmetrical PPO with different reactivity of the chain ends. However, this approach requires multistep synthesis and purifications, as illustrated in Figure II.14.[34]
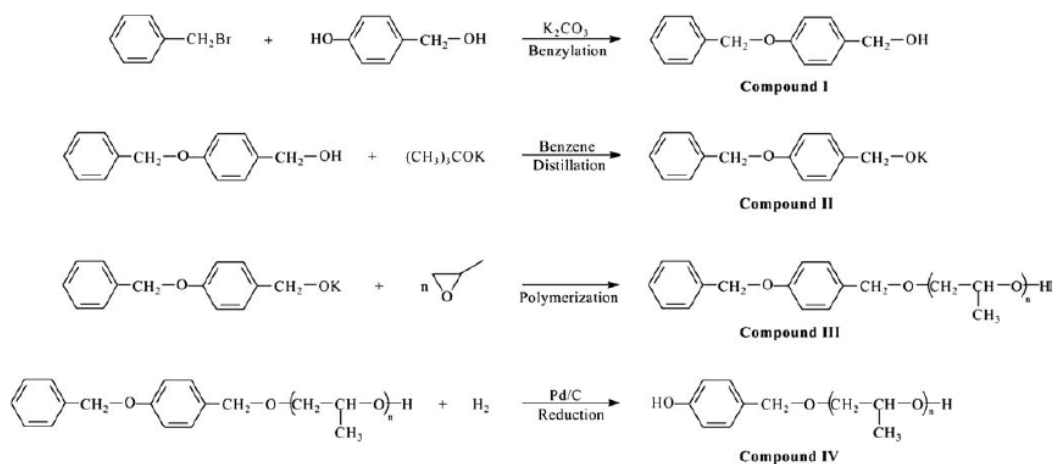

Figure II.14. Synthetic route of asymmetrical poly(propylene oxide), from ref 34.

c. Our Strategy

Our approach to obtain Thy-DAT heterotelechelic supramolecular polymers is to introduce a protection / deprotection pathway, with a very hydrophobic protecting group enabling easy purification, into an asymmetric end-functionalization strategy. The whole chemical pathway is presented in Scheme II.8. We chose this strategy instead of the ones described above because we wanted a simple pathway, starting from commercial products, available in large quantities, and at reasonable costs.

---

[34] Yang, P. F.; Zhu, X. W.; Li, J. Y.; Xia, Y. M.; Li, T. D.; **Synthesis and characterization of linear asymmetrical poly(propylene oxide) diol**; *J. Appl. Polym. Sci.* **2010**, *117*, 1095.
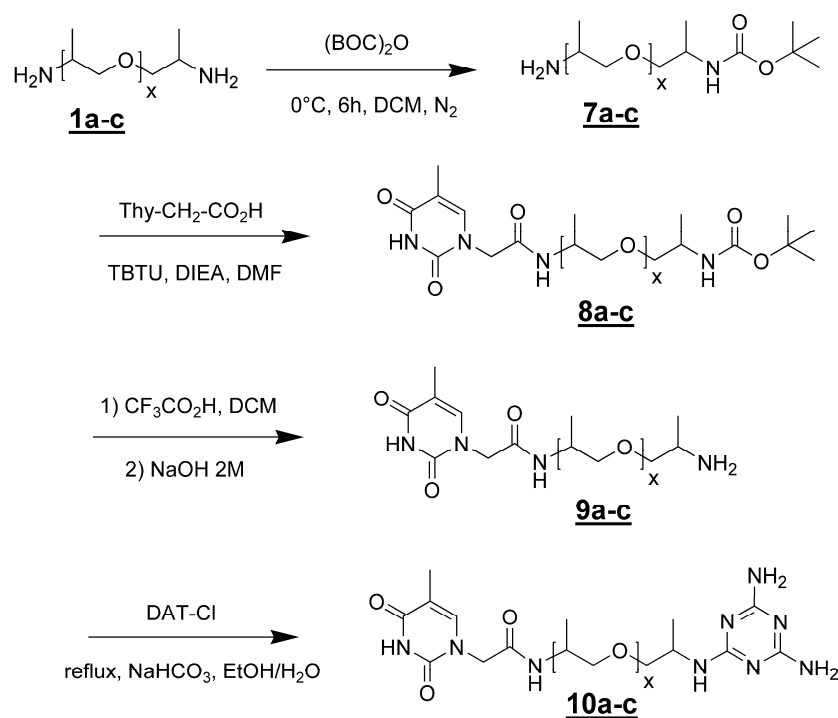
Scheme II.8. Synthesis of heterotelechelic units Thy-PPO-*X*-DAT **10a-c** (**a**: *X* = 2200, **b**: *X* = 460, **c**: *X* = 250).

The first step is the protection by a BOC group of one of the two terminal amine functions of the PPO spacer. Purification is achieved by successive liquid-liquid extractions and aqueous washes. Indeed, since BOC is hydrophobic and amines are hydrophilic, especially at low pH, BOC-PPO-NH$_2$ prefer the organic phase, whereas NH$_2$-PPO-NH$_2$ (or NH$_3^+$-PPO-NH$_3^+$ in acidic conditions) prefer the aqueous phase. However, as evidenced during the purification of Thy-PPO-*X*-Thy **3a-c**, the purification protocol must be adapted to the size of the PPO chain.

After this key step, Thy is grafted by amidation on the unprotected amine, as described above then the protected amine is deprotected, and finally DAT is grafted by an aromatic nucleophilic substitution as already described. This four step synthesis (Scheme II.8) yields a PPO spacer capped with a thymine group (Thy) on one end and a 2,6-diamino-1,3,5-triazine (DAT) on the other (denoted as Thy-PPO-*X*-DAT, **10a-c**, **a**: X = 2200, **b**: X = 460, **c**: X = 250).

d. First step: monoprotection by BOC

(i) *tert*-Butylcarbonylation and purification by extraction

The critical step of our heterotelechelic supramolecular polymer synthesis is the protection of only one of the two symmetrical amino groups, into an *N-tert*-butylcarbamate (BOC) group (Scheme II.9). *tert*-Butylcarbonylation is a very popular protection reaction of amines,[35] including for mono-protection of symmetrical diamines.[36] To increase the yield of mono-BOC protected diamines, as opposed to unreacted and di-BOC protected diamines, several procedures have been developed: low concentrations, prior acid addition, slow addition of di-*tert*-butyl dicarbonate ((BOC)$_2$O) solution and low temperatures.[36,37] Still, a mixture of unreacted, mono-BOC protected and di-BOC protected α,ω-diamines is obtained.
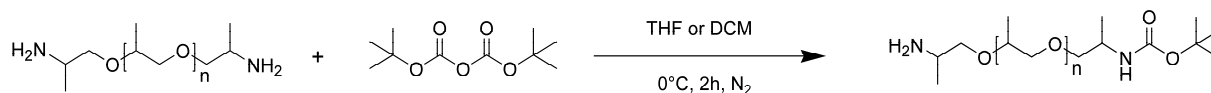
Scheme II.9. NH$_2$-PPO-*X*-BOC **7a-c** synthesis *via* carbamate formation from diamine telechelic poly(propylene oxide) NH$_2$-PPO-*X*-NH$_2$ **1a-c** and (BOC)$_2$O; by-products are *tert*-butanol and CO$_2$.

Unreacted diamines can be separated by taking advantage of their affinity and basic properties differences. Indeed, the BOC group is strongly lipophilic, therefore it enhances the hydrophobic nature of *N*-BOC products. On the other hand, the hydrophilic nature of unreacted diamines is reinforced in acidic aqueous phases, which turn them into ammonium salts. Thus, by successive organic extractions and acidic aqueous washes, unreacted α,ω-diamines mainly go in aqueous phases, while *N*-BOC products mostly go in organic ones.

Di-BOC protected α,ω-diamines are still there, but can be separated after deprotection, also by liquid-liquid extraction. Moreover, the quantity of the di-BOC protected compounds can be reduced by proceeding in dilute media, at low temperature (0°C), without any catalyst,

---

[35] Greene, T. W.; Wuts, P. G. M.; *Protective Groups in Organic Synthesis*, 3rd ed; Wiley-Interscience: New York, **1999**.

[36] (a) Lee, D. W.; Ha, H.-J. ; Lee, W. K.; **Selective mono-BOC protection of diamines**; *Synth. Commun.* **2007**, *37*, 737. (b) Pittelkow, M.; Lewinsky, R. ; Christensen, J. B.; **Selective synthesis of carbamate protected polyamines using alkyl phenyl carbonates**; *Synthesis* **2002**, *15*, 2195.

[37] Krapcho, A. P.; Maresch, M. J.; Lunn, J.; **Mono-(BOC)-protected diamines. Synthesis of tert-butyl-N-alkyl-N-(2-aminoethyl)carbamates and tert-butyl-N-[2-(alkylamino)ethyl] carbamates**; *Synth. Commun.* **1993**, *23*, 2443.

in a short reaction time (6 hours), and by taking advantage of the steric hindrance of the end-chain amine due to the α-methyl of the PPO chain.

The full experimental protocols for X = 2200, 460 and 250 are in Appendix II. Once again, the purification procedures needed to be adapted to the length of PPO chain. The reactions were followed by ^{1}H NMR and ^{13}C NMR for **7a-c**, Maldi-Tof for **7a-b,** and GC-MS for **7b-c**.

(ii) Characterization of NH$_2$-PPO-250-BOC **7c**

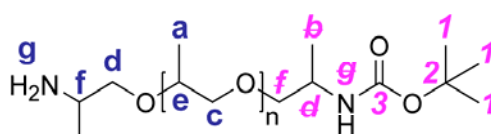**Chart II.4.** NH$_2$-PPO-X-BOC **7**.

^{1}H and ^{13}C NMR in CDCl$_3$ showed that the BOC protection reaction occured. For instance, the ^{13}C NMR of **7c** in CDCl$_3$ features a signal at 155.5 ppm characteristic of the carbamate carbon *3* (the anhydride carbon of di-*tert*-butyldicarbonate would be at 146.8 ppm).

GS-MS indicates that the reaction mixture before purification contains unreacted NH$_2$-PPO-250-NH$_2$ **1c** (with x = n+1 = 2,3,4 cf page 63), monoprotected NH$_2$-PPO-250-BOC **7c** (x = 2,3,4), diprotected BOC-PPO-250-BOC (x = 2,3,4), and butylated hydroxytoluene (BHT), an antioxydant from the THF reaction solvent (Figure II.15b). The GC signals were attributed by MS fragment analysis. The amount of di-BOC protected compounds is limited since the reaction was carried out with an excess of diamines (3 eq.) compared to di-*tert*-butyl dicarbonate (1 eq.). Although GC is not quantitative, because the detector response is compound-dependent and because BOC-deprotection may occur during the injection at 250°C, it indicates whether the protected products were formed or not. It also allows us to follow the reaction by comparing the relative peak intensity.

After washing the reaction mixture with a basic aqueous solution (pH = 14), two phases are obtained. The basic aqueous phase contains unreacted NH$_2$-PPO-250-NH$_2$ (x = 2,3,4) and BHT (Figure II.15c). Conversely, the organic phase (**7c**) contains essentially

monoprotected NH₂-PPO-250-BOC (x=2,3,4), and a few pourcents of diprotected BOC-PPO-250-BOC and BHT (Figure II.15d).
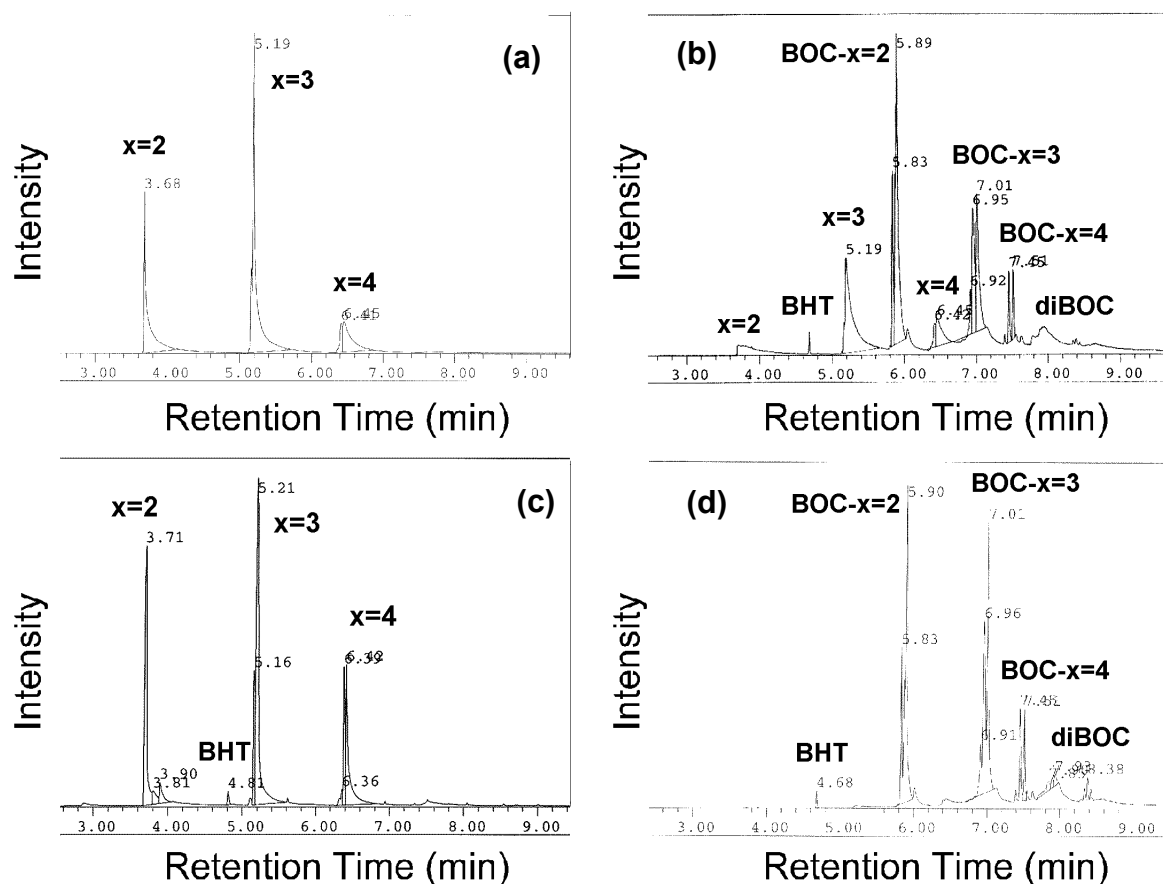

Figure II.15. GC-MS of (a) NH_2-PPO-250-NH_2 (**1c**), (b) reaction mixture after 6h (NH_2-PPO-250-NH_2, NH_2-PPO-250-BOC, BHT and BOC-PPO-250-BOC), (c) aqueous phase (NH_2-PPO-250-NH_2), and (d) organic phase (NH_2-PPO-250-BOC and BOC-PPO-250-BOC) after extraction with DCM.

(iii) Characterization of NH₂-PPO-460-BOC **7b**

For $X = 460$, washing with a basic aqueous solution is not efficient. Indeed, the medium size PPO chain (~ 7 PO monomers) gives NH_2-PPO-460-NH_2 **1b** almost the same affinity for the organic and the basic aqueous phases. More accuratly, the smaller oligomers prefer the basic aqueous phase, whereas the longer oligomers prefer the organic phase. However, washing with an acidic aqueous solution (pH = 3) allows to separate more efficiently monoprotected NH_2-PPO-460-BOC **7b** and unreacted NH_2-PPO-460-NH_2 **1b**, as evidenced by the GC-MS in Figure II.16. Indeed, the protonation of its two amino groups reinforces the hydrophilic nature of the unreacted diamine. Conversely, washing with an

acidic aqueous solution for $X = 250$ would not be efficient, because NH_3^+-PPO-250-BOC
would then be too hydrophilic.
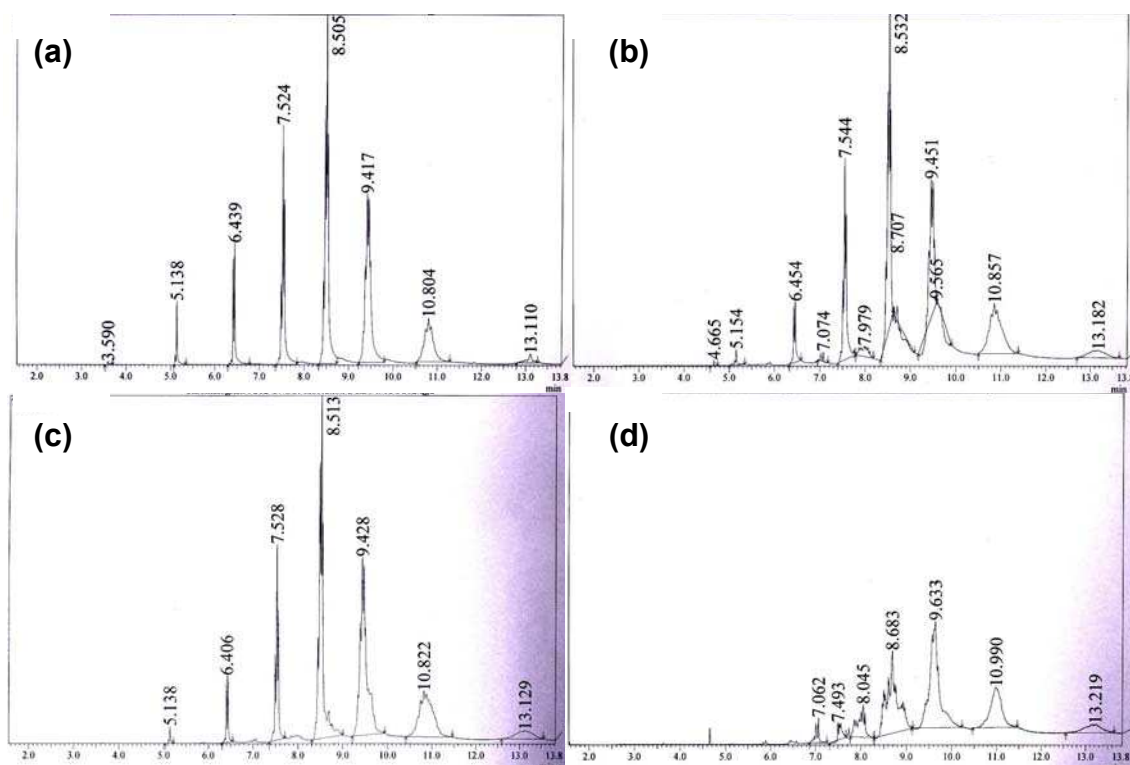
Figure II.16. GC-MS (abscissa: retention time [min], ordinate: intensity [a.u.]) of: (a) NH_2-PPO-460-NH_2 **1b**
x=2-9 (1b), (b) reaction mixture after 6h (NH_2-PPO-460-NH_2 x=2-9, NH_2-PPO-460-BOC x=2-9 and BOC-PPO-
460-BOC x=2-9), (c) acidic aqueous phase, and (d) organic phase (2b).

Still, the longer oligomers of NH_2-PPO-460-NH_2 **1b** partially remain in the organic
phase. To increase the yield and purity, NH_2-PPO-460-NH_2 **1b** can be purified before the
reaction, by liquid-liquid extraction, in order to eliminate the bigger molecules which prefer
the organic phase to the acidic aqueous phase. With this, the yield increases from 14% to 37%
and the purity (determined by ^{1}H NMR) from 78% of NH_2-PPO-460-BOC **7b** (with x ~ 9) to
94% of NH_2-PPO-460-BOC **7b** (with x ~ 6).

Moreover, for $X = 460$, the di-BOC-protected diamine BOC-PPO-X-BOC can be
separated from the mono-BOC-protected diamine NH_2-PPO-X-BOC **7b** by adding water to
the bulk mixture and filtering. Indeed, NH_3^+-PPO-460-BOC solubilizes in the water, but
BOC-PPO-460-BOC does not and can be filtered. This method of separation is efficient only
for $X = 460$. For $X = 230$, the molecules are so small that BOC-PPO-X-BOC can solubilize
(slightly) in water. For $X = 2200$, the molecules are so long that the difference between BOC-

PPO-X-BOC and NH$_3^+$-PPO-X-BOC is not important enough for this method to be really efficient. Plus, micelles can form with $X = 2200$.

Therefore for $X = 460$, the reaction was not carried out with an excess of diamines compared to di-*tert*-butyl dicarbonate, to increase the yield relative to the diamines.

(iv) Characterization of NH$_2$-PPO-2200-BOC **7a**

^{1}H and ^{13}C NMR spectra of **7a** in CDCl$_3$ suggest that the desired product NH$_2$-PPO-2200-BOC was formed. GC-MS could not be performed because the molecular weight is too high for the column.

Integrating the methyl BOC ^{1}H NMR signal (**1**) over the α-methyl of end-function NH$_2$ PPO signal (**b**) (Figure II.17B) shows that the final organic phase **7a** of the protection step contains 1.5 mol% of di-BOC protected amine and no unreacted diamine **1a**. This confirms that di-BOC protection reaction has been limited. As mono-protected amine **7a** is an amphiphilic compound, it is also found in aqueous phases, and reaction yield is estimated at 78 mol% from NH$_2$-PPO-2200-NH$_2$ **1a**.

e. Second step: Thy Grafting

(i) Thy Grafting with TBTU

In the second step, amidation of monoprotected amine **7a-c** by thymine-1-acetic acid is conducted in DMF, in the presence of TBTU as coupling agent.[24] Water is added to the reaction mixture to solubilize hydrophilic products (TEA, DMF, HOBt, tBOH…) and the *N*-BOC/Thy derivative **8a-c** is extracted with toluene. Toluene is now used as the organic extraction solvent, because it induces less emulsions than chloroform or dichloromethane. Purification is facilitated by overall hydrophobicity of thymine moiety. Indeed, even though polar and able to form H-bonds with polar and/or protic solvents (DMSO, methanol…), thymine is only slightly water-soluble, due to the hydrophobic nature of its methyl substituent.[38]

---

[38] Spencer, J. N.; Judge, T. A.; **Hydrophobic hydration of thymine**; *J. Sol. Chem.* **1983**, *12*, 847.

Thy grafting is conducted before DAT grafting because Ph-NH$_2$ derivatives (such as DAT) react with carboxylic acids in the presence of TBTU, to yield Ph-NH-CO-R.[21] Thymine grafting is not done in the bulk at 160°C, to prevent BOC deprotection (carbamates are sensitive to high temperatures).[35]

The full experimental protocols for $X = 2200$, 460 and 250 can be found in Appendix II. From now on characterization will be focused on $X = 2200$.

(ii) Characterization of Thy-PPO-2200-BOC **8a** by NMR

On ^{1}H NMR spectrum of **8a** ($X = 2200$) (Figure II.17C), ratio of BOC (*1*) and α-methyl of end-function NH$_2$ PPO (**b**) signals integrations with the thymine CH$_3$ (**A**) and CH$_2$ (**B**) shows that **8a** is obtained in 90 mol% and that 1.5 mol% of di-protected BOC-PPO-2200-BOC are still present. Indeed, there is an excess of BOC compared to Thy (1.0 BOC for 0.8 Thy).

f. Third step: BOC deprotection

(i) Deprotection reaction by acid treatment

Protected products **8a-c** are deprotected with a trifluoroacetic acid/dichloromethane (DCM) blend, neutralized with a 2M soda solution,[36] and desired product **9a-c** are extracted with toluene. Before neutralization and extraction with toluene, DCM and excess TFA can be evaporated. During neutralization, the product precipitates from the now mostly aqueous solution. After neutralization, the aqueous phase has a pH of 14.

BOC deprotection releases isobutylene vapors and carbon dioxyde, but no by-products. The full experimental protocols for $X = 2200$, 460 and 250 are in Appendix II.

(ii) Characterization of Thy-PPO-2200-NH$_2$ **9a** by NMR

^{1}H NMR spectrum of **9a** ($X = 2200$) (Figure II.17D) confirms that the deprotection reaction is complete since BOC signal (*1*) has disappeared. Yet, ratio of PPO methyl (**a**) signal integration with the thymine CH$_3$ (**A**) and CH$_2$ (**B**) reveal an excess of starting diamine

1a, issuing from deprotection of di-protected diamine (1.5 mol% from step 1) and unreacted mono-protected diamine **7a** (10 mol% from step 2).

g. Final step: DAT Grafting

### (i) DAT Grafting *via* nucleophilic substitution

Finally, the heterotelechelic units Thy-PPO-*X*-DAT **10a-c** are synthesized by nucleophilic substitution of amine end-function of **9a-c** with 2-chloro-DAT in water/ethanol (v/v 1/1) blend.[13] Reaction can easily be followed since, even at reflux, 2-chloro-DAT is insoluble: as reaction takes place, mixture is getting less and less cloudy until it is perfectly clear. Like thymine, even polar and H-bonding able, DAT is roughly hydrophobic due to its aromatic nature. Heterotelechelic unit is thus hydrophobic and is isolated with DCM. The full experimental protocols for X = 2200, 460 and 250 are in Appendix II.

(ii) Characterization of Thy-PPO-2200-DAT **10a** by NMR and Maldi-Tof

^{1}H and ^{13}C NMR in DMSO-d_6 showed that the desired product were formed. ^{1}H NMR spectrum of **10a** (X = 2200) (Figure II.17E) reveals 5.7 mol% excess of DAT moiety. Excess of DAT can be attributed to homotelechelic DAT-PPO-2200-DAT **2a** (*i.e.* 2.8 mol%) issuing from reaction of NH$_2$-PPO-2200-NH$_2$ **1a** recovered by deprotection of *N*-BOC products in step 3. MALDI-TOF confirms that asymetrical Thy-PPO-2200-DAT **10a** was formed.

h. NMR characterizations of **7-10a** and conclusion

Finally, our method to obtain heteroditopic units is somewhat efficient (Figure II.17) since less than a 3% excess of homoditopic compounds is evidenced. However, it is difficult to measure precisely the percentage of homoditopic compounds present with the heteroditopic units. Indeed, the theroretical NMR spectrum of Thy-PPO-DAT is identical to that of a 50:50 mixture of Thy-PPO-Thy and DAT-PPO-DAT, because the chain ends are far from one another. MALDI-TOF as well cannot help to precisely measure the percentage of homoditopic compounds present with the heteroditopic units.
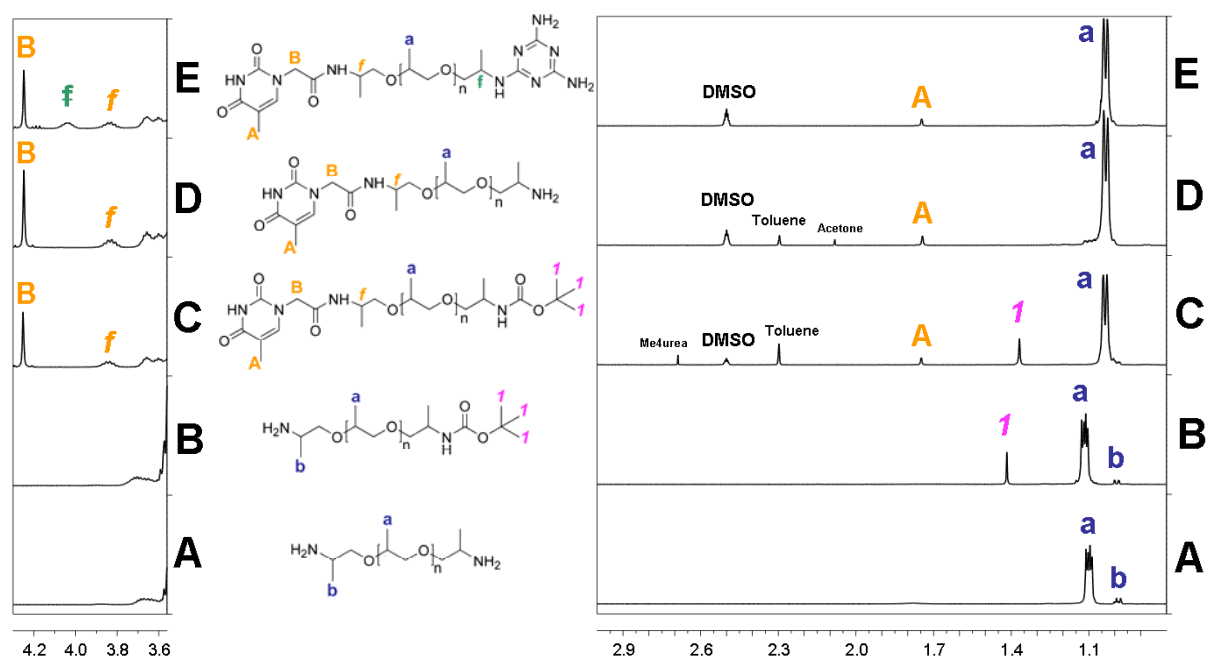
Figure II.17. Partial ^{1}H NMR spectra at 25°C: (A) NH$_2$-PPO-2200-NH$_2$ **1a** (CDCl$_3$); (B) NH$_2$-PPO-2200-BOC **7a** (CDCl$_3$); (C) Thy-PPO-2200-BOC **8a** (DMSO-d$_6$); (D) Thy-PPO-2200-NH$_2$ **9a** (DMSO-d$_6$); (E) Thy-PPO-2200-DAT **10a** (DMSO-d$_6$).

In the next chapters, we will see that the properties of Thy-PPO-2200-DAT **10a** and 50/50-M-2200 **4a** in solution and in the bulk are very similar. Yet, there are some subtle differences. For instance, the viscosity of Thy-PPO-2200-DAT **10a** in toluene and chloroform is slightly higher than that of 50/50-M-2200 **4a**, which suggests a Thy/DAT ratio closer to 1 in **10a**.

Chapter III

Supramolecular polymers
in solution:
solvent dependent behavior

In solution, the solvent has a tremendous influence on the behavior of supramolecular polymers. We have studied our supramolecular polymers in three solvents of different polarity (DMSO, chloroform and toluene), by estimating their association constants through ^{1}H NMR and by monitoring their viscosity and carbon relaxation time. We show that DMSO is a dissociative solvent of the Thy-DAT hydrogen bonding association, while chloroform and toluene are non-dissociative solvents. Moreover, DMSO is a poor solvent of the PPO chains and a good solvent of the Thy and DAT stickers, while toluene is a poor solvent of the stickers and a good solvent of the PPO chains. The differences in structure and in association constants ($K_{Thy-DAT}^{25°C,toluene} \approx 22 * K_{Thy-DAT}^{25°C,chloroform}$) between toluene and chloroform are suggested to be due to better solvation of the stickers by chloroform and to aromatic interactions, in addition to hydrogen bonds, between the Thy and DAT aromatic cycles in toluene. As a result, our supramolecular polymers seem to form micelles with a PPO core and a Thy, DAT shell in DMSO; inverted micelles with a PPO shell and a Thy, DAT core in toluene; and linear chains through hydrogen bonding between Thy and DAT in chloroform.

Chapter III. Supramolecular polymers in solution: solvent dependent behavior

In this chapter, the solution behavior of our compounds and of their mixture in three solvents are studied using spectroscopic and rheological characterizations. The association constants are estimated by ^{1}H NMR and possible structures are suggested.

1. Supramolecular polymers in solution

To begin, theories on supramolecular polymers behavior in solution are presented.

a. Mechanisms of supramolecular polymerization in solution

(i) Thermodynamics of supramolecular polymerization in solution

Solutions of supramolecular polymers have already been extensively studied.[1,2,3] Their properties are influenced by the thermodynamic (association constants K) and kinetic (lifetimes τ of the interactions) parameters of the association process (Scheme III.1).

$$A \ + \ B \ \underset{k_{-1}}{\overset{k_1}{\rightleftharpoons}} \ AB \qquad K_{AB} = \frac{[AB]}{[A][B]} = \frac{k_1}{k_{-1}}$$

Scheme III.1. Association between an A sticker and a B sticker to form an AB complex, with K_{AB} the equilibrium constant of the AB association, k_1 the on-rate constant, k_{-1} the off-rate constant, [AB] the concentration of AB complex, [A] the concentration of free A, and [B] the concentration of free B.

In most cases, a thermodynamic equilibrium takes place between monomers, oligomers and polymers. Supramolecular polymerization is assumed to proceed by successive steps, each associated to an equilibrium constant K_i ($i > 1$, Scheme III.2).

---

[1] Fox, J. D.; Rowan, S. J.; **Supramolecular polymerizations and main-chain supramolecular polymers**; *Macromolecules* **2009**, *42*, 6823.

[2] de Greef, T. F. A.; Smulders, M. M. J.; Wolffs, M.; Schenning, A. P. H. J.; Sijbesma, R. P.; Meijer, E. W.; **Supramolecular polymerization**; *Chem. Rev.* **2009**, *109*, 5687.

[3] Ciferri, A.; **Supramolecular polymerizations**; *Macromol. Rapid Commun.* **2002**, *23*, 511.

$$P_1 + P_1 \leftrightarrows P_2 \qquad \text{step 1, } K_2$$
$$P_2 + P_1 \leftrightarrows P_3 \qquad \text{step 2, } K_3$$
$$\text{.......}$$
$$P_{n-1} + P_1 \leftrightarrows P_n \qquad \text{step n-1, } K_n$$

$$K_i = \frac{[P_i]}{[P_1][P_{i-1}]}$$
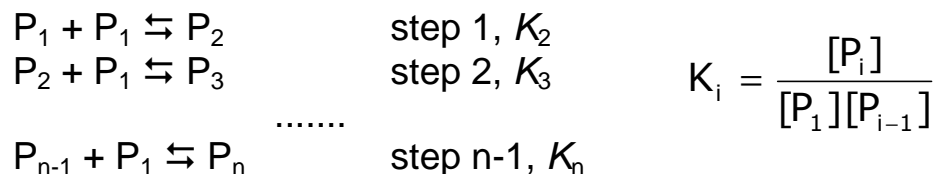
Scheme III.2. Step supramolecular polymerization, with P_i the supramolecular polymer made of i units.

The associations constantly break and reform, but at the same rate. Therefore, although the structures are dynamic and fluctuating, the average degree of polymerization (DP = N) and its distribution are constant at equilibrium. In fact, the average degree of polymerization N and its distribution then depend only on the thermodynamic association constants of the stickers K, on the stickers concentrations C, and on the supramolecular polymerization mechanism.

Indeed, different supramolecular polymerization mechanisms have been envisaged, among them:

- isodesmic with chains (Figure III.1.A.a, Figure III.1.B.a),
- isodesmic with ring-chain equilibrium (Figure III.1.B.b),
- nucleation-elongation (Figure III.1.A.b, Figure III.1.B.c), and
- growth coupled to nematic orientation (Figure III.1.A.c).
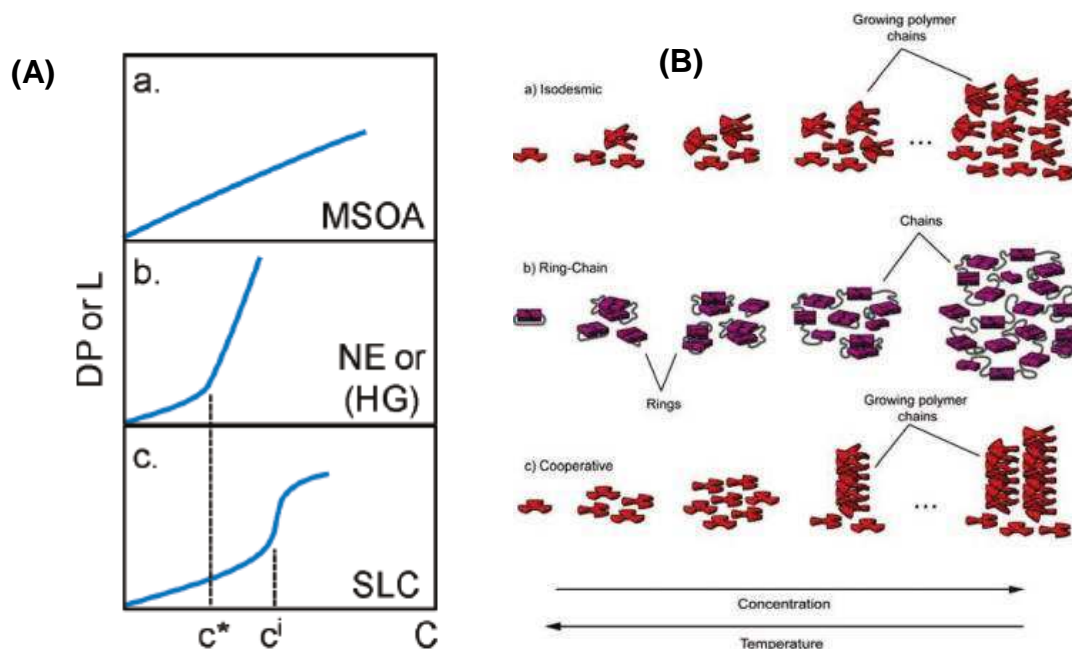
Figure III.1. (A) Schematic representation of the average degree of polymerization DP = N versus monomer concentration C for different supramolecular growth mechanisms : (a) multistage open association (MSOA), (b) nucleation-elongation (NE) or helical growth (HG), and (c) growth coupled to nematic orientation or open supramolecular liquid crystal (SLC). Note the concentration at which helical growth begins (C*) is generally smaller than that of mesophase formation (C^i). Reproduction from ref 1. (B) Graphical representation of : (a) isodesmic, (b) ring-chain mediated, and (c) cooperative, supramolecular polymerizations; from ref 2.

(ii) Isodesmic mechanism with linear chains only

In the isodesmic mechanism (Figure III.1.B.a), also called multistage open association (MSOA),[1] the supramolecular polymer grows under thermodynamic control into a linear chain by a reversible step-growth process, analogous to classical step-growth polymerization (Scheme III.2).[4] Moreover, in the isodesmic mechanism, all the K_i are equal to each other ($K_i = K_2$ for $i>2$) and to the association constant K_{AB} of small model molecules ($K_2 = K_{AB}$, free A and B stickers, not linked by a chain, Scheme III.1). Therefore, the thermodynamic of the isodesmic supramolecular polymerization is governed by a single association constant K. This means K is independent of the chain length of the supramolecular polymer, *i.e.* there is no cooperation, the association constant of two free stickers is the same as the association constant of two stickers already belonging to a long chain.

Consequently, DP increases regularly with concentration, as illustrated in Figure III.1.A.a.[1]. In fact, $N \sim KC$. Moreover, for an isodesmic equilibrium, when the concentration C gets high, the polydispersity index (I_p) approaches 2, as for any step-growth polymerization.[2]

(iii) Isodesmic mechanism with ring-chain equilibrium

If the stickers at each end of a supramolecular chain associate together, a supramolecular polymer ring is formed. Ring formation was neglected in the previous chain isodesmic mechanism, but the proportion of rings can be really high, especially for low concentrations C and high association constant K.[5,6,7,8] Indeed, the ring-chain equilibrium theory developed by Jacobson and Stockmayer for polycondensations applies to isodesmic

---

[4] Schmid, S. A.; Abbel, R.; Schenning, A. P. H.; Meijer, E. W.; Sijbesma, R. P.; Herz, L. M.; **Analyzing the molecular weight distribution in supramolecular polymers**; *J. Am. Chem Soc.* **2009***, 131*, 17696.

[5] Jacobson, H.; Stockmayer, W. H.; **Intramolecular reaction in polycondensations. I. The theory of linear systems**; *J. Chem. Phys.* **1950***, 18*, 1600.

[6] Flory, P. J.; Suter, U. W.; Mutter, M.; **Macrocyclization equilibria. 1. Theory**; *J. Am. Chem. Soc.* **1976***, 98*, 5733.

[7] Petschek, R. G.; Pfeuty, P.; Wheeler, J. C.; **Equilibrium polymerization of chains and rings: A bicritical phenomenon**; *Phys. Rev. A,* **1986***, 34*, 2391.

[8] Ercolani, G.; Mandolini, L.; Mencarelli, P.; Roelens, S.; **Macrocyclization under thermodynamic control. A theoretical study and its application to the equilibrium cyclooligomerization of β-propiolactone**; *J. Am. Chem. Soc.* **1993***, 115*, 3901.

supramolecular polymerization (Figure III.1.B.b),[5] as does Flory's theory of cyclization equilibria.[6]

Experimental studies of supramolecular polymers solutions (concentration-dependent NMR and viscosity measurements) have indicated that rings were indeed favored at low concentrations, while linear chains predominated at high concentrations.[9,10,11,12] Moreover, Pezron *et al.* showed by mean-field approach that in the dilute regime ($C < C^*$) the probability of intrachain association (*i.e.* ring formation) should be proportional to the average concentration in the polymer coil, C^*.[13] As a result, at low concentrations, when mostly intrachain association occur, the ratio of complex to free stickers is independent of the global concentration C, contrary to small molecules association.[13] Concentration dependence only appears in the semidilute regime ($C > C^*$), when interchain association is more likely to occur.[13]

The proportion of rings depends on the entropic cost of closing a chain to form a ring (due to the loss of conformational entropy). Therefore, the size of the resulting ring, the spacer flexibility,[14] and the conformational restrictions[9,15,16] influence the proportion of rings.

[9] Abed, S.; Boileau, S.; Bouteiller, L.; **Supramolecular association of acid-terminated poly(dimethylsiloxane)s. 2. Molecular weight distributions**; *Macromolecules* **2000**, *33*, 8479.

[10] Söntjens, S. H. M.; Sijbesma, R. P.; van Genderen, M. H. P.; Meijer, E. W.; **Selective formation of cyclic dimers in solutions of reversible supramolecular polymers**; *Macromolecules* **2001**, *34*, 3815.

[11] Scherman, O. A.; Ligthart, G. B. W. L.; Sijbesma, R. P.; Meijer, E. W.; **A selectivity-driven supramolecular polymerization of an AB monomer**; *Angew. Chem. Int. Ed.* **2006**, *45*, 2072.

[12] de Greef, T. F. A.; Ercolani, G.; Ligthart, G. B. W. L.; Meijer, E. W.; Sijbesma, R. P.; **Influence of selectivity on the supramolecular polymerization of AB-type polymers capable of both A-A and A-B interactions**; *J. Am. Chem. Soc.* **2008**, *130*, 13755.

[13] Pezron, E.; Leibler, L.; Ricard, A.; Lafuma, F.; Audebert, R.; **Complex formation in polymer-ion solutions. 1. Polymer concentration effects**; *Macromolecules* **1989**, *22*, 1169.

[14] Chen, C.-C. ; Dormidontova, E. E. ; **Ring-chain equilibrium in reversibly associated polymer solutions: Monte Carlo simulations** ; *Macromolecules,* **2004**, *37*, 3905.

[15] Folmer, B. J. B.; Sijbesma, R. P.; Kooijman, H.; Spek, A. L.; Meijer, E. W.; **Cooperative dynamics in duplexes of stacked hydrogen-bonded moieties**; *J. Am. Chem. Soc.* **1999**, *121*, 9001.

[16] ten Cate, A. T.; Kooijman, H.; Spek, A. L.; Sijbesma, R. P.; Meijer, E. W.; **Conformational control in the cyclization of hydrogen-bonded supramolecular polymers**; *J. Am. Chem. Soc.,* **2004**, *126*, 3801.

(iv) Nucleation-elongation mechanism

If an additional supramolecular interaction manifests at high DP (*i.e.* at high concentrations *C*), then a single association constant *K* can no longer describe the system. Indeed, in the nucleation-elongation mechanism, also called helical growth[1] or cooperative supramolecular polymerization (Figure III.1.B.c),[2] secondary binding forces perturb the isodesmic mechanism at high DP, resulting in a cooperative assembly.[17] Several association constants K_i must be used to describe the system, their value increasing with the supramolecular polymer size *i*.

As a result, DP increases sharply above a critical concentration, as illustrated in Figure III.1.A.b.[1] Moreover, non-linear chain structures are formed. For instance, Lehn and his coworkers studied the fibrillar nanostructure in decane of a supramolecular polymer associating primarily *via* six hydrogen bonds and secondly *via* aromatic rings stacking.[18] Other examples also resulting from hydrogen bonds and aromatic rings stacking include the nanofibers described by Shimizu *et al.*[19] and the helical nanofibers described by Iwaura *et al.*.[20,21]

If the association constants K_i decrease when the supramolecular size *i* increases (for entropic reasons for instance), then the mechanism is called the attenuated *K* model.[22]

[17] Zhao, D.; Moore, J. S.; **Nucleation-elongation: a mechanism for cooperative supramolecular polymerization**; *Org. Biomol. Chem.,* **2003***, 1*, 3471.

[18] Kolomiets, E.; Buhler, E.; Candau, S. J.; Lehn, J.-M.; **Structure and properties of supramolecular polymers generated from heterocomplementary monomers linked through sextuple hydrogen-bonding arrays**; *Macromolecules,* **2006***, 39*, 1173.

[19] Shimizu, T.; Iwaura, R.; Masuda, M.; Hanada, T.; Yase, K.; **Internucleobase-interaction-directed self-assembly of nanofibers from homo- and heteroditopic 1,w-nucleobase bolaamphiphiles**; *J. Am. Chem. Soc.* **2001***, 123*, 5947.

[20] Iwaura, R.; Hoeben, F. J. M.; Masuda, M.; Schenning, A. P. H. J.; Meijer, E. W.; Shimizu, T.; **Molecular-level helical stack of a nucleotide-appended oligo(p-phenylenevinylene) directed by supramolecular self-assembly with a complementary oligonucleotide as a template**; *J. Am. Chem. Soc.* **2006***, 128*, 13298.

[21] Iwaura, R.; Iizawa, T.; Minamikawa, H.; Ohnishi-Kameyama, M.; Shimizu, T.; **Diverse morphologies of self-assemblies from homoditopic 1,18-nucleotide-appended bolaamphiphiles: effects of nucleobases and complementary oligonucleotides**; *Small* **2010***, 6*, 1131.

[22] Martin, R. B.; **Comparisons of indefinite self-association models**; *Chem. Rev.* **1996***, 96*, 3043.

(v) Growth coupled to nematic orientation

In the growth coupled to nematic orientation mechanism, also called open supramolecular liquid crystal,[1] the supramolecular polymer growth is coupled to an orientation process at high concentrations. Long-range order is obtained at high concentrations, resulting in a sudden increase in DP (Figure III.1.A.c). Lehn and his coworkers studied such liquid crystalline supramolecular polymers, presenting lyotropic mesophases[23] and columnar organization.[24]

(vi) Solvent-dependent supramolecular polymerization mechanism

Given that the solvent has a huge influence on the strength of the supramolecular interactions,[25] it is not surprising that some supramolecular polymers display solvent-dependent polymerization mechanisms, and thus solvent-dependent organization.

For example, Meijer and his coworkers observed that a self-complementary ureidotriazine-based supramolecular polymer forms random coils *via* hydrogen bonding in chloroform (isodesmic mechanism, Figure III.1.B.a), but helical columns *via* cooperative and solvophobically induced π-stacking of the hydrogen-bonded pairs in dodecane (nucleation-elongation, Figure III.1.B.b).[26] The helical columns are also formed in water (the hydrogen bonds between the ureidotriazine groups are maintained in water thanks to an hydrophobic microenvironment).[27]

---

[23] Kotera, M.; Lehn, J.-M.; Vigneron, J.-P.; **Self-assembled supramolecular rigid rods**; *J. Chem. Soc.,* **1994***, 2*, 197.

[24] Gulik-Krzywicki, T.; Fouquey, C.; Lehn, J.-M.; **Electron microscopic study of supramolecular liquid crystalline polymers formed by molecular-recognition-directed self-assembly from complementary chiral components**; *Proc. Natl. Acad. Sci. USA* **1993***, 90*, 163.

[25] Jonkheijm, P.; van der Schoot, P.; Schenning, A. P. H. J.; Meijer, E. W.; **Probing the solvent-assisted nucleation pathway in chemical self-assembly**; *Science* **2006***, 313*, 80.

[26] Hirschberg, J. H. K. K.; Brunsveld, L.; Ramzi, A.; Vekemans, J. A. J. M.; Sijbesma, R. P.; Meijer, E. W.; **Helical self-assembled polymers from cooperative stacking of hydrogen-bonded pairs**; *Nature* **2000***, 407*, 167.

[27] Brunsveld, L.; Vekemans, J. A. J. M.; Hirschberg, J. H. K. K.; Sijbesma, R. P.; Meijer, E. W.; **Hierarchical formation of helical supramolecular polymers via stacking of hydrogen-bonded pairs in water**; *Proc. Natl. Acad. Sci.* **2002***, 99*, 4977.

(vii) Technical analysis difficulties

As we have mentioned above, the average degree of polymerization N depends on the stickers association constants K, the stickers concentrations C, and on the supramolecular polymerization mechanism. Moreover, the association constants K and the supramolecular polymerization mechanism depend on the solvent and the temperature.

Therefore, the average chain length N changes with concentration, temperature, and solvent. This makes technical analysis somewhat more complicated than for covalent polymers. For instance, one GPC measurement of a covalent polymer allows determination of its molecular weight. For a supramolecular polymer, not only is the analysis dependent on concentration, temperature and solvent, but as the longer chains get separated from the shorter chains, new equilibria arise because of the reversibility of the associations.

Therefore to completely characterize a supramolecular polymer, in a given solvent, concentration- and temperature-dependent measurements are needed. These measurements should permit determination of the supramolecular polymerization mechanism and thermodynamic parameters.[28] However, it is not always so straightforward to distinguish which supramolecular polymerization mechanism is actually occuring.[28]

In this chapter, we have used solvent-, concentration-, and temperature-dependent rheological and ^{1}H NMR measurements to study the supramolecular polymers synthesized in Chapter II. We expect that the solvent will have a strong influence on these solutions behavior.

b. Supramolecular polymers used in this study

The supramolecular polymers used in this study consist of low-molecular-weight (around 2200 g.mol^{-1}) poly(propylene oxide) (PPO) oligomers functionalized on both ends with thymine (Thy) or diaminotriazine (DAT) groups. They are denoted as Thy-PPO-2200-Thy **3a** (Chart III.1a) and DAT-PPO-2200-DAT **2a** (Chart III.1b) for the homotelechelic

---

[28] Smulders, M. M.; Nieuwenhuizen, M. M.; de Greef, T. F.; van der Schoot, P.; Schenning, A. P.; Meijer, E.; **How to distinguish isodesmic from cooperative supramolecular polymerisation**; *Chem.: A Eur. J.* **2010**, *16*, 362.

units, Thy-PPO-2200-DAT **10a** (Chart III.1c) for the heterotelechelic unit, and 50/50-M-2200 **4a** for the 50/50 mixture of Thy-PPO-2200-Thy (**3a)** and DAT-PPO-2200-DAT (**2a**). Their synthesis is described in Chapter II.
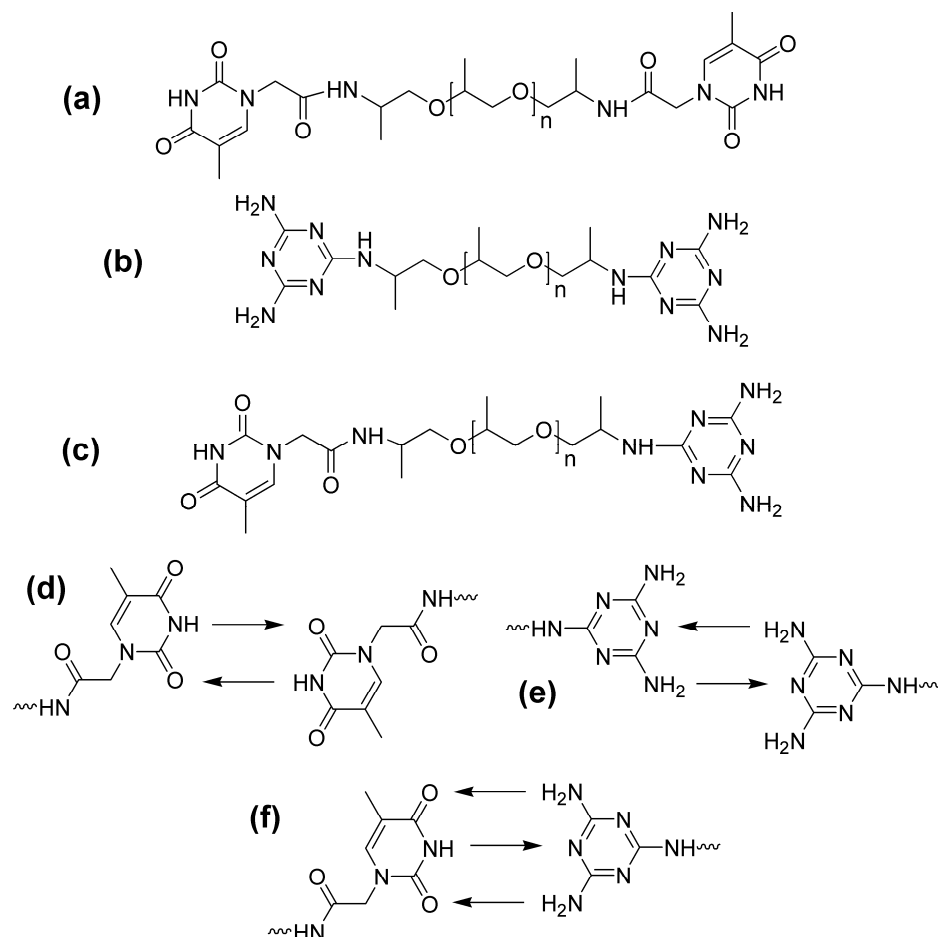
Chart III.1. (a) Thy-PPO-2200-Thy **3a**, (b) DAT-PPO-2200-DAT **2a**, (c) Thy-PPO-2200-DAT **10a**, (d) Thy-Thy self-association, (e) DAT-DAT self-association, and (f) Thy-DAT complementary association.

Thy and DAT can associate with one another through self- and hetero-complementary hydrogen bonding (Chart III.1d,e,f).[29] In chloroform, Thy-DAT complementary association is much stronger than the Thy-Thy and DAT-DAT self-associations, as evidenced by the differences in the thermodynamic binding constants: $K_{Thy\text{-}DAT} = 890$ M^{-1} versus $K_{DAT\text{-}DAT} = 2.2$ M^{-1} and $K_{Thy\text{-}Thy} = 4.3$ M^{-1} (as determined by ^{1}H NMR spectroscopy in CDCl$_3$).[29] Another weak hydrogen bonding association can occur between two amide groups linking the thymine stickers to the PPO spacers, or between one amide group and one thymine motif.

[29] Beijer, F. H.; Sijbesma, R. P.; Vekemans, J. A. J. M.; Meijer, E. W.; Kooijman, H.; Spek, A. L.; **Hydrogen-bonded complexes of diaminopyridines and diaminotriazines: opposite effect of acylation on complex stabilities**; *J. Org. Chem.* **1996**, *61*, 6371.

While Thy and DAT are very polar groups, the PPO-2200 chain is much less polar. As a result, these supramolecular polymers are soluble in a wide range of solvents: from the very polar solvents methanol, dimethylsulfoxyde (DMSO), and dimethylformamide (DMF), thanks to the stickers, to the relatively polar solvents chloroform and dichloromethane, all the way to the apolar toluene, thanks to the PPO-2200 chain. In contrast, the diamine telechic PPO chain (NH$_2$-PPO-2200-NH$_2$ **1a**) is not soluble in DMSO at high concentrations, because it is too apolar/hydropobic; and the small molecules derivatives of Thy and DAT are not soluble in chloroform and toluene. Moreover, the length of the PPO chain (around 2200 g.mol^{-1}) is of importance, not too long and not too short, allowing a good balance with the stickers. Indeed, with short PPO chains (around 250 g.mol^{-1}) the Thy and/or DAT telechelic units are not soluble in apolar solvents at high concentrations and with very long PPO chains they might not be soluble in very polar solvents at high concentrations.

Therefore, hydrogen bonding between the stickers, solvation of the PPO chains, and solvation of the stickers have an influence on the solution properties.

We report in this chapter on the solution behavior of these supramolecular polymers in aprotic solvents of different polarity (DMSO, chloroform and toluene), evidenced by NMR, proton and carbon relaxation times T$_1$, and solution viscosity measurements, all performed at different temperatures and concentrations. Since they are amphiphilic molecules, with polar hydrogen-bonding stickers and a less polar PPO spacer, solvent nature strongly impacts their association constant, supramolecular polymerization mechanism, and structuration.

Moreover, we underline the differences between the solution properties of the heterotelechelic unit Thy-PPO-2200-DAT **10a** and the 50/50 mixture of homotelechelic units Thy-PPO-2200-Thy and DAT-PPO-2200-DAT (50/50-M-2200 **4a**).

c. Determination of association constants by ^1H NMR titration

The association constants of the supramolecular polymers used in this study can be determined by ^1H NMR titration, assuming isodesmic mechanisms.[30,31] Indeed, the chemical shifts of Thy and DAT's protons implicated in the hydrogen bonds (**D**, **Φ**, **Ψ**, Scheme III.3) vary greatly between the free, self-associated, and Thy-DAT associated states. Since equilibria are faster than the NMR spectrocopic time scale, the observed chemical shifts for Thy NH (**D**) and DAT NH$_2$ (**Φ**, **Ψ**) are a weighted average between the chemical shifts of the associated, self-associated, and free states. Thus, Thy-Thy and DAT-DAT self-association constants ($K_{Thy-Thy}$ and $K_{DAT-DAT}$), and Thy-DAT association constant ($K_{Thy-DAT}$), can be obtained by monitoring the Thy NH (**D**) or DAT NH$_2$ (**Φ**, **Ψ**) chemical shift as a function of species concentration. The titration curves are then analyzed by computer fitting with least-squares methods (EQNMR program).[32] More details on this procedure (as well as equations) are available in Appendix I and results are discussed in the following paragraphs.
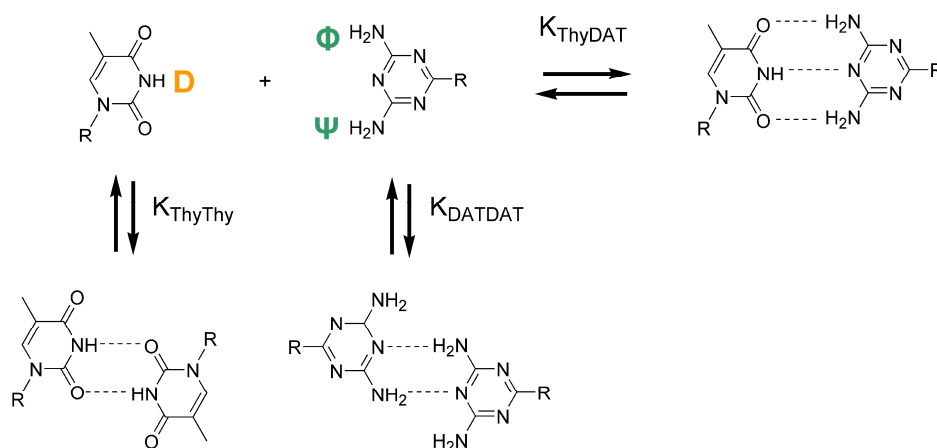
Scheme III.3. Thy-DAT complementary association and Thy-Thy, DAT-DAT self-associations.

[30] Fielding, L.; **Determination of association constants (Ka) from solution NMR data**; *Tetrahedron* **2000**, *56*, 6151.

[31] Steed, J. W.; Atwood, J. L.; *Supramolecular chemistry*, *2nd Edition*; Wiley: Chippenham, UK, **2009**.

[32] Hynes, M. J.; **EQNMR: a computer program for the calculation of stability constants from nuclear magnetic resonance chemical shift data**; J. Chem. Soc. Dalton Trans. **1993**, 2, 311.

2. Supramolecular polymers act as bolaamphiphiles in a dissociative solvent

(i) Very low association constants in DMSO

The Thy-DAT association constant ($K_{\text{Thy-DAT}}$) in DMSO-d$_6$ was determined by ^{1}H NMR titration of N-butyl-thymine-1-acetamide (Thy-C$_4$) by 2-methyl-4,6-diamino-1,3,5-triazine (MeDAT) (Figure III.2).
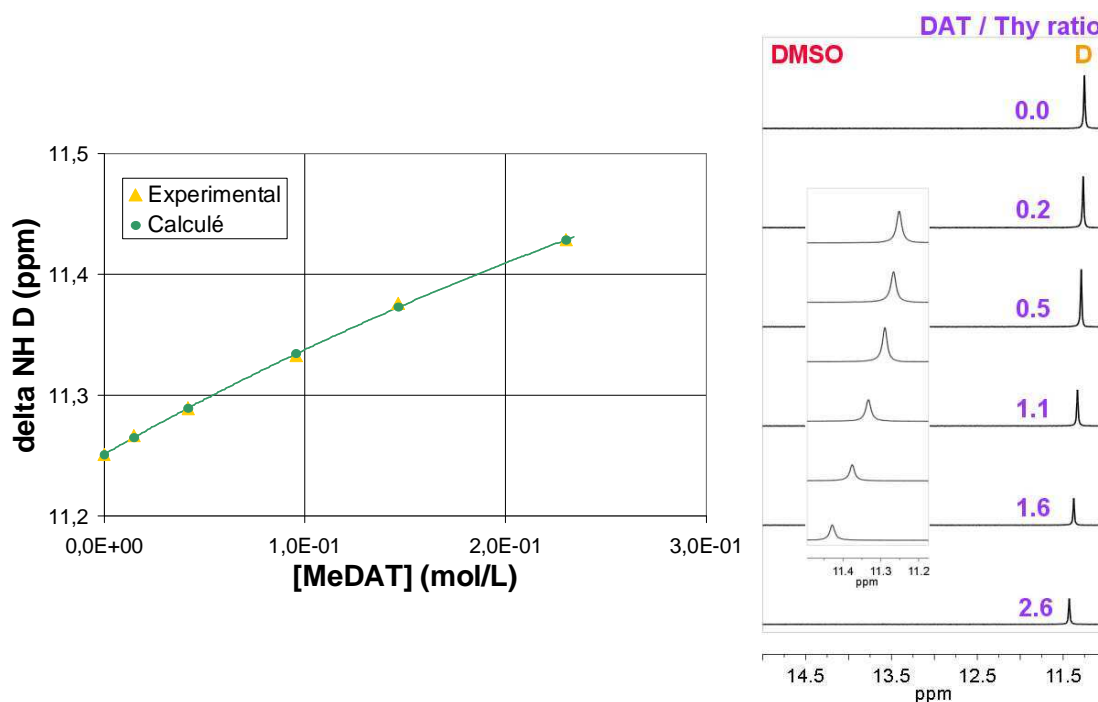
Figure III.2. ^{1}H NMR titration in DMSO-d$_6$ at 25°C of Thy-C$_4$ ($9.0*10^{-2}$ mol/L) by MeDAT (from 0 to $2.3*10^{-1}$ mol/L) ($K_{\text{Thy-DAT}}$ = 1.3 L/mol, δ_{freeThy} = 11.25 ppm, $\delta_{\text{bondedThy}}$ = 12.10 ppm).

As expected, $K_{\text{Thy-DAT}}$ is very low in DMSO-d$_6$ (1.3 L/mol). Indeed, the Thy and DAT hydrogen bonds donors and acceptors are highly solvated in this polar aprotic solvent (dielectric constant $\varepsilon_{\text{DMSO}}$ = 46.7, relative polarity of DMSO = 0.444),[33] and scarcely assemble.[31] DMSO can then be considered as a dissociating solvent of the Thy-DAT association.

Furthermore, the chemical shift of the Thy NH (**D**) proton signal is the same in solutions of Thy-PPO-2200-Thy **3a**, Thy-PPO-2200-DAT **10a** and 50/50-M-2200 **4a** in DMSO-d$_6$ (Figure III.3), and does not vary with concentration (in the error bar). Similarly, the

---

[33] Reichardt, C.; *Solvents and solvent effects in organic chemistry*, 3rd ed; Wiley-VCH Publishers, **2003**.

chemical shift of DAT NH$_2$ (**Φ, Ψ**) is the same in solutions of DAT-PPO-2200-DAT **2a**, Thy-PPO-2200-DAT **10a** and 50/50-M-2200 **4a** in DMSO-d$_6$ (Figure III.3), and also does not vary with concentration (in the error bar). This confirms that DMSO prevents hydrogen bonding between Thy and DAT, and self-association of Thy and DAT (as evidenced by the constant, in the error bar, **D** and **Φ, Ψ** chemical shifts as a function of concentration of a Thy derivative and a DAT derivative, respectively, in DMSO-d$_6$).

So, to sum up, there are no, or very few, hydrogen-bonds between the stickers in DMSO-d$_6$, neither Thy-Thy or DAT-DAT dimerization, nor Thy-DAT association.
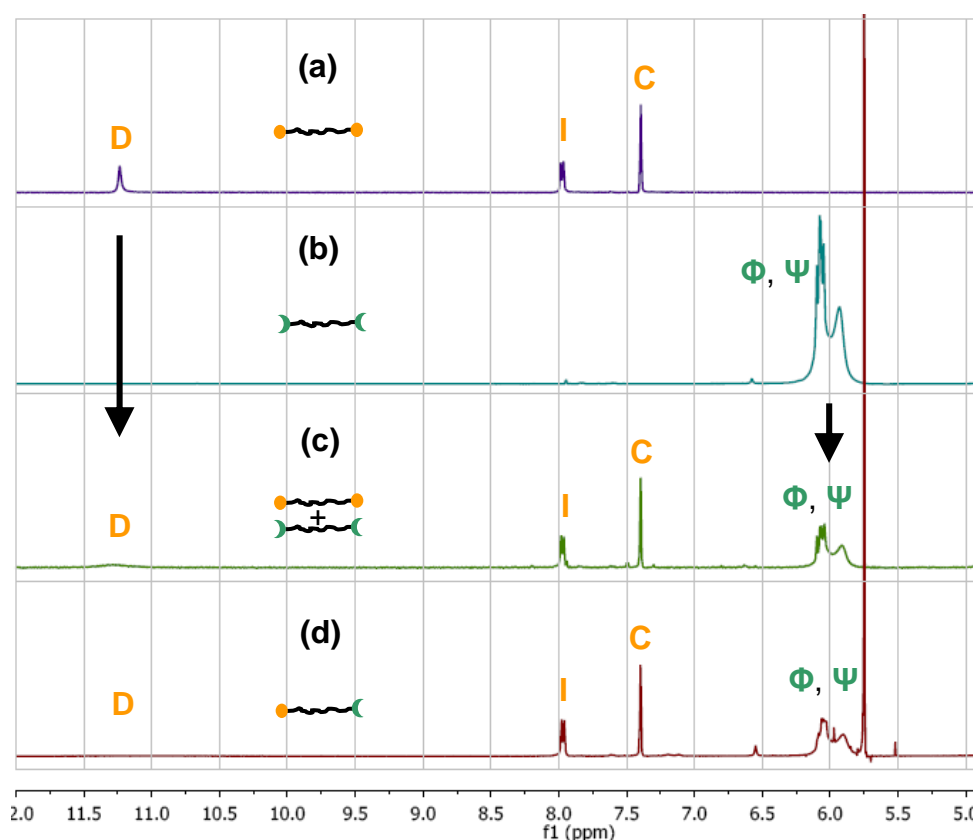

Figure III.3. ^{1}H NMR at 25°C of solutions at 6.6 wt% (0.084 g/cm^3 - 0.034 mol/L) in DMSO-d$_6$ of (a) Thy-PPO-2200-Thy **3a**, (b) DAT-PPO-2200-DAT **2a**, (c) 50/50-M-2200 **4a**, and (d) Thy-PPO-2200-DAT **10a**.

(ii) All samples have the same viscosity in DMSO

In DMSO, 10 wt% (12.2*10^{-2} g/cm^3, 4.9*10^{-2} mol/L) solutions of Thy-PPO-2200-Thy **3a**, DAT-PPO-2200-DAT **2a**, 50/50-M-2200 **4a**, and Thy-PPO-2200-DAT **10a**, all have the same relative viscosity (η_{rel} = 2.0) (Figure III.4). Furthermore, this value of relative viscosity in DMSO is quite lower than in chloroform and toluene at lower concentrations (see part 3 of

this chapter). Therefore, these viscosity measurements confirm the ^{1}H NMR results: DMSO is a dissociating solvent for the Thy-DAT association.
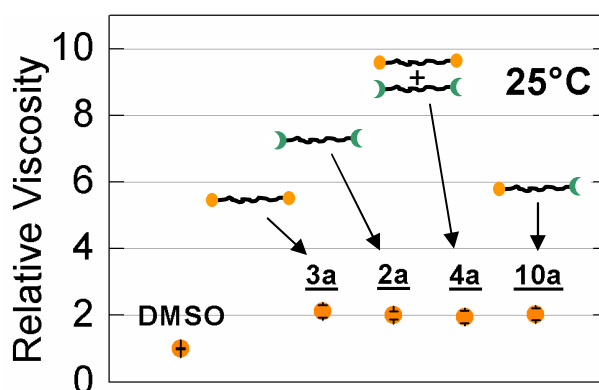
Figure III.4. Relative viscosity in DMSO of 10 wt% ($12.2*10^{-2}$ g/cm^3) solutions of Thy-PPO-2200-Thy **3a**, DAT-PPO-2200-DAT **2a**, 50/50-M-2200 **4a** and Thy-PPO-2200-DAT **10a**.

(iii) PPO chains aggregated in DMSO

However, since DMSO is a polar solvent whereas the PPO chain is mostly non-polar, hydrophobic interactions induce aggregation of the PPO chain. This aggregation can be evidenced by comparing the carbon NMR relaxation times T_1 of Thy-PPO-2200-DAT **10a** and NH$_2$-PPO-2200-NH$_2$ **1a** PPO chain in DMSO-d$_6$, CDCl$_3$ and toluene-d$_8$ (Table III.1). Indeed, T_1 reflects the local mobility of the studied group, and a high T_1 indicates a high mobility. The T_1 results show that chloroform, and especially toluene, are good solvent of the PPO chain, since the T_1 values are rather high. In contrast, the T_1 values in DMSO are much weaker, indicating that the PPO chain mobility is strongly diminished.

		DMSO-d$_6$	CDCl$_3$	Toluene-d$_8$
NH$_2$-PPO-2200-NH$_2$ **1a**	PPO CH$_3$	*insoluble*	1.30	1.46
	PPO CH$_2$	*insoluble*	1.24	1.51
	PPO CH	*insoluble*	0.79	0.93
Thy-PPO-2200-DAT **10a**	PPO CH$_3$	0.73	1.09	1.17
	PPO CH$_2$	0.32	0.66	0.73
	PPO CH	0.51	1.02	1.12

Table III.1. Carbon relaxation time T_1 (in s), measurements performed on $6.7*10^{-2}$ g/cm^3 solutions at 25 °C with an inversion-recovery sequence.

In fact, these results suggest that Thy-PPO-2200-DAT **10a**, 50/50-M-2200 **4a**, DAT-PPO-2200-DAT **2a** and Thy-PPO-2200-Thy **3a** may form micelles in DMSO, with the PPO chains collapsed in the core and the Thy and DAT groups at the surface, solvated by the DMSO. Indeed, DMSO is a good solvent of the polar stickers, but a bad solvent of the hydrophobic PPO chain. This image is consistent with the fact that all compounds have the same relative viscosity.

3. Supramolecular polymers are associated in a non-dissociative solvent

a. High association constants in chloroform and toluene

(i) In chloroform $K_{Thy-DAT}$ ~ 1000 L/mol

The association and dimerization constants of the stickers were determined by ^1H NMR titration in $CDCl_3$ (Figure III.5 to Figure III.8), assuming an isodesmic mechanism. The values obtained are only estimates given the error bars, but are in accordance to what can be found in the literature ($K_{Thy-Thy} = 2$ M^{-1} vs 4.3[ref 29] and 3.8[ref 34]; $K_{DAT-DAT} = 2.8$ M^{-1} vs 2.2[ref 29] and 1.7[ref 34]; $K_{Thy-DAT} = 847 / 1256$ M^{-1} vs 890[ref 29] and 1087[ref 34]).

To correctly fit the experimental data, and thus determine the Thy-DAT association constant $K_{Thy-DAT}$, it was necessary to take the DAT-DAT self-association constant $K_{DAT-DAT}$ into account, even though it is 300 times lower (Thy-Thy self-association can be neglected because DAT is in excess in this set of experiments). If $K_{DAT-DAT}$ is not fixed, the best fit yields $K_{DAT-DAT} = 4.7$ M^{-1} and $K_{Thy-DAT} = 847$ M^{-1} (Figure III.7). When $K_{DAT-DAT}$ is fixed around 2.8 M^{-1} as measured by DAT-PPO-460-DAT **2b** titration, the best fit yields $K_{Thy-DAT} = 1256$ M^{-1} (Figure III.8), which clearly illustrates the uncertainty of the values obtained by this method.
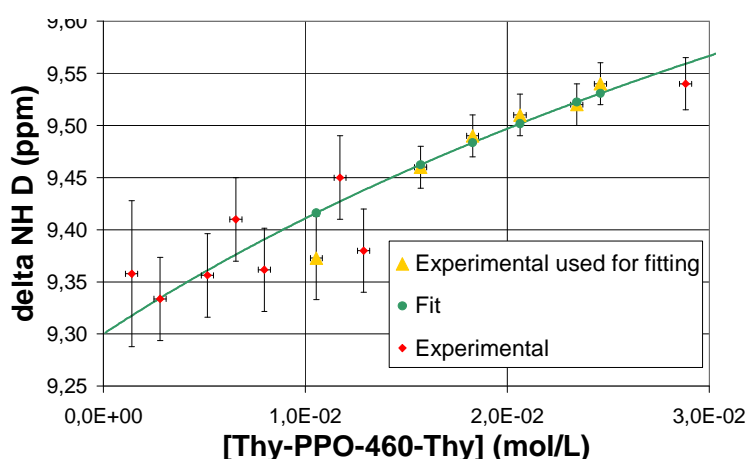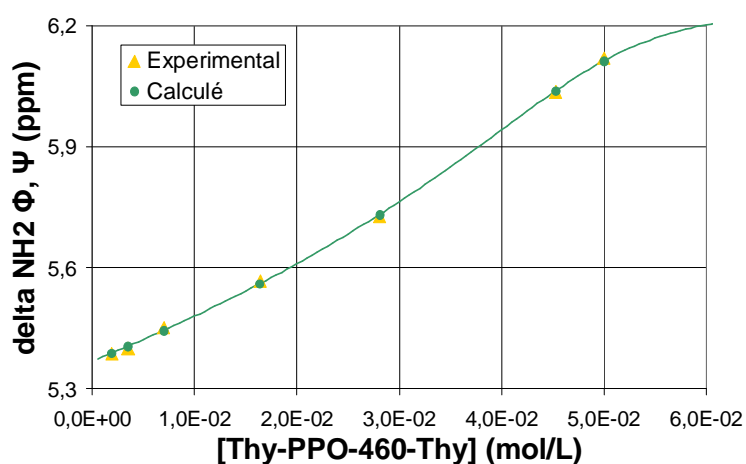

Figure III.5. $K_{Thy-Thy}$ determination by NMR titration in $CDCl_3$ at 25°C of Thy-PPO-460-Thy **3b** ($K_{Thy-Thy} = 2.0$ L/mol, $\delta_{freeThy} = 9.3$ ppm, $\delta_{dimerizedThy} = 10.9$ ppm).

---

[34] Herbst, F.; Schröter, K.; Gunkel, I.; Gröger, S.; Thurn-Albrecht, T.; Balbach, J.; Binder, W. H.; **Aggregation and chain dynamics in supramolecular polymers by dynamic rheology: cluster formation and self-aggregation**; *Macromolecules* **2010**, *43*, 10006.
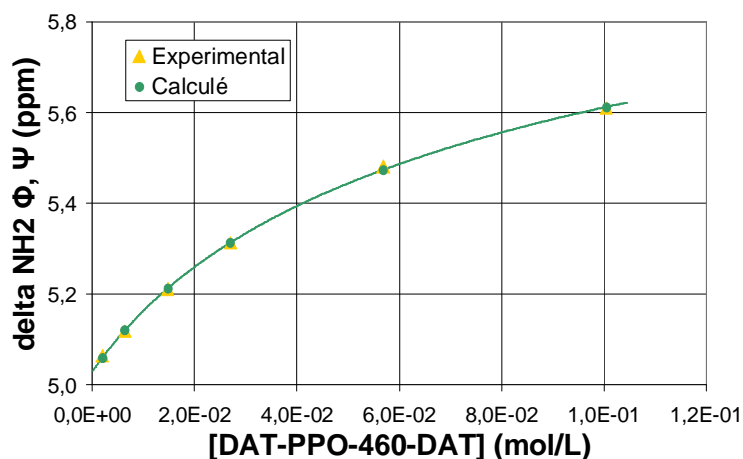
Figure III.6. $K_{\text{DAT-DAT}}$ determination by NMR titration in CDCl$_3$ at 25°C of DAT-PPO-460-DAT **2b** ($K_{\text{DAT-DAT}}$ = 2.8 L/mol, δ_{freeDAT} = 5.03 ppm, $\delta_{\text{dimerizedDAT}}$ = 6.47 ppm).

Figure III.7. $K_{\text{Thy-DAT}}$ determination by NMR titration in CDCl$_3$ at 25°C of DAT-PPO-460-DAT **2b** by Thy-PPO-460-Thy **3b** ($K_{\text{Thy-DAT}}$ = 846.5 L/mol, $K_{\text{DAT-DAT}}$ = 4.7 L/mol, δ_{freeDAT} = 4.52 ppm, $\delta_{\text{dimerizedDAT}}$ = 6.81 ppm, $\delta_{\text{bondedDAT}}$ = 6.28 ppm).
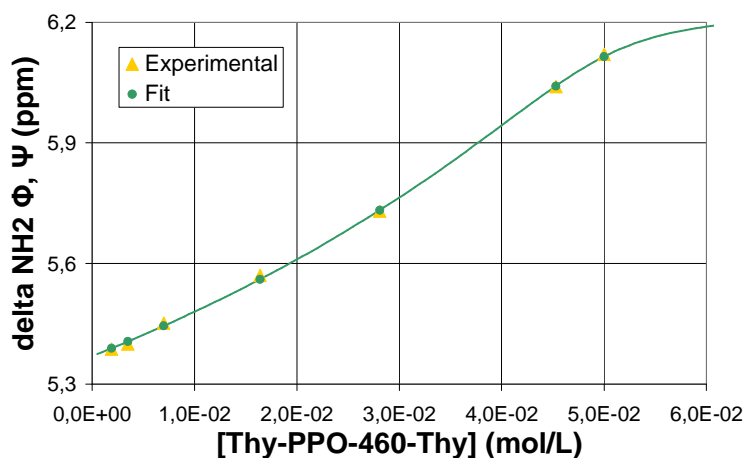

Figure III.8. $K_{\text{Thy-DAT}}$ determination by NMR titration in CDCl$_3$ at 25°C of DAT-PPO-460-DAT **2b** by Thy-PPO-460-Thy **3b** ($K_{\text{Thy-DAT}}$ = 1255.7 L/mol, $K_{\text{DAT-DAT}}$ = 3.2 L/mol, δ_{freeDAT} = 4.70 ppm, $\delta_{\text{dimerizedDAT}}$ = 6.88 ppm, $\delta_{\text{bondedDAT}}$ = 6.24 ppm).

As expected, the Thy-DAT association constant measured is much higher than the measured Thy-Thy and DAT-DAT dimerization constants ($K_{\text{Thy-DAT}} > 300*K_{\text{Thy-Thy}}$ and $K_{\text{Thy-DAT}} > 300*K_{\text{DAT-DAT}}$). This is illustrated in Figure III.9, where the chemical shift of the Thy NH (**D**) proton signal is strongly deshielded in CDCl$_3$ solutions of 50/50-M-2200 **4a** and Thy-PPO-2200-DAT **10a** compared to Thy-PPO-2200-Thy **3a** ($\Delta\delta \sim 4$ ppm). The chemical shift of DAT NH$_2$ and NH (**Φ, Ψ, Ω**) is also shifted downfield in CDCl$_3$ solutions of 50/50-M-2200 **4a** and Thy-PPO-2200-DAT **10a**, compared to DAT-PPO-2200-DAT **2a** ($\Delta\delta \sim 0.9$ ppm).
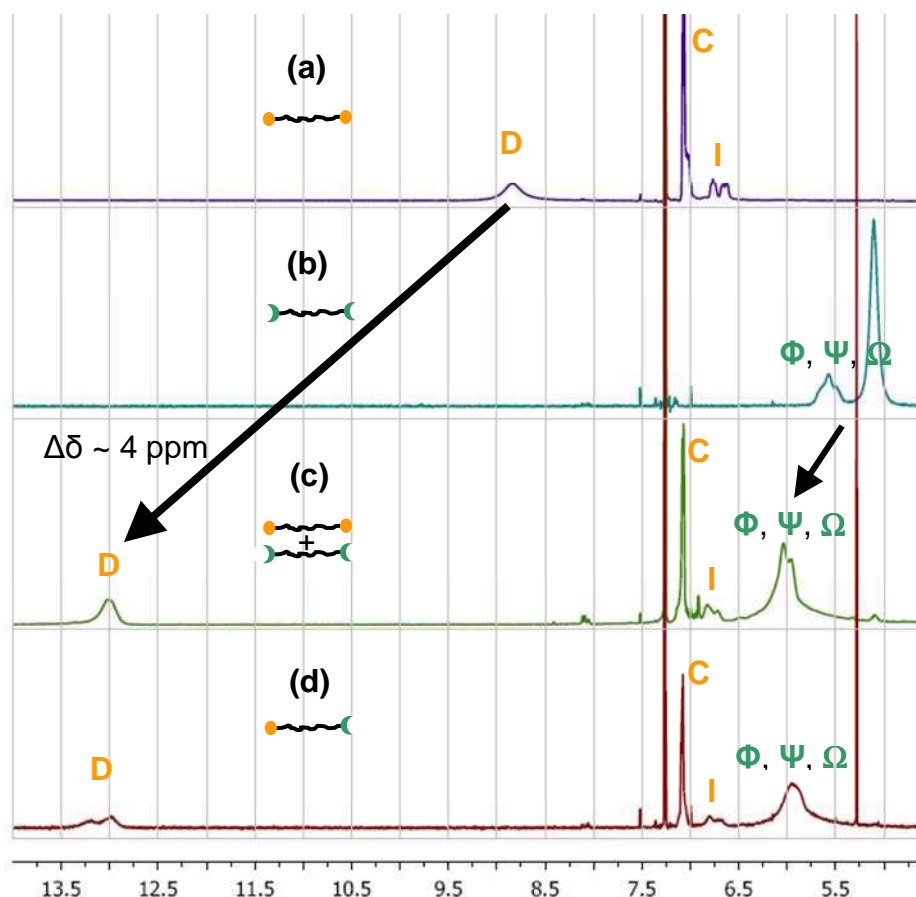
Figure III.9. ^{1}H NMR at 25°C of solutions at 0.06 g/cm^3 in CDCl$_3$ of (a) Thy-PPO-2200-Thy **3a**, (b) DAT-PPO-2200-DAT **2a**, (c)50/50-M-2200 **4a**, and (d) Thy-PPO-2200-DAT **10a**.

A splitting of the thymine NH (**D**) signal is observed on the ^{1}H NMR spectrum of Thy-PPO-2200-DAT **10a** in CDCl$_3$ (Figure III.9d), see part (v) for a tentative explanation.

(ii) In toluene, $K_{\text{Thy-DAT}}$ (Tol) $>>$ $K_{\text{Thy-DAT}}$ (CHCl$_3$)

The Thy-Thy and DAT-DAT self-association constants ($K_{\text{Thy-Thy}}$ and $K_{\text{DAT-DAT}}$) measured in toluene-d_8 by NMR titration (Figure III.10, Figure III.11) are more than 10 times higher than in CDCl$_3$. Therefore, $K_{\text{Thy-DAT}}$ is also crudely expected to be at least 10 times higher in toluene-d_8 than in CDCl$_3$ (*i.e.* over 8.10^3 L/mol).
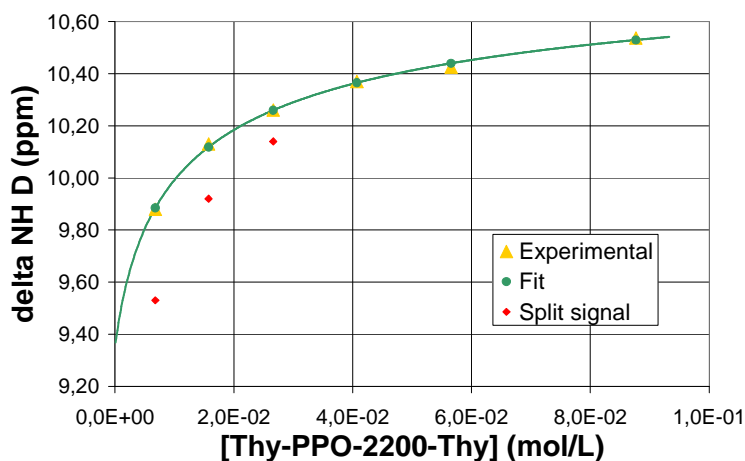
Figure III.10. $K_{\text{Thy-Thy}}$ determination by NMR titration in toluene-d$_8$ at 25°C of Thy-PPO-2200-Thy **3a** ($K_{\text{Thy-Thy}} = 26.5$ L/mol, $\delta_{\text{freeThy}} = 9.35$ ppm, $\delta_{\text{dimerizedThy}} = 10.98$ ppm).
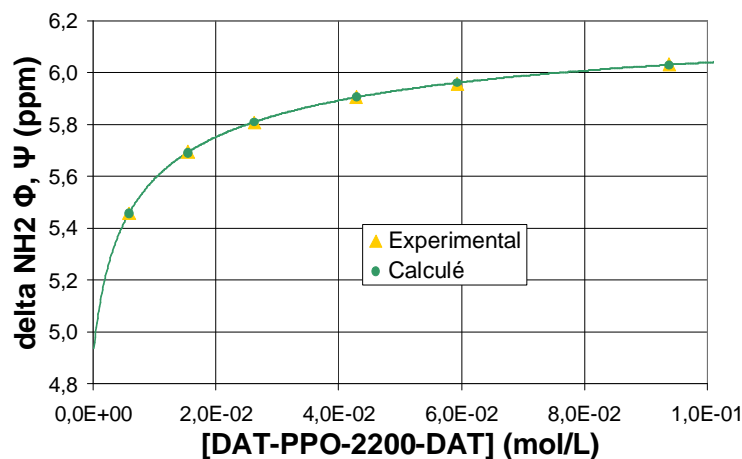
Figure III.11. $K_{\text{DAT-DAT}}$ determination by NMR titration in toluene-d$_8$ at 25°C of DAT-PPO-2200-DAT **2a** ($K_{\text{DAT-DAT}} = 42.5$ L/mol, $\delta_{\text{freeDAT}} = 4.91$ ppm, $\delta_{\text{dimerizedDAT}} = 6.35$ ppm).

However, $K_{\text{Thy-DAT}}$ could not be determined in toluene-d_8 by this NMR titration method. Indeed, the NMR titration method does not allow determination of association constants greater than 10^4 L/mol,[31] 10^5 L/mol.[30]

In toluene-d_8, the Thy NH (**D**) chemical shift is very high and does not vary with DAT concentration above equimolar DAT/Thy ratio, but only starts to shift when Thy is in excess (Figure III.12b). Moreover, the Thy NH (**D**) chemical shift of Thy-PPO-2200-DAT **10a** is independent of concentration in toluene but not in chloroform (Figure III.13). These results confirm that $K_{Thy-DAT}$ is much higher in toluene-d_8 than in CDCl$_3$.
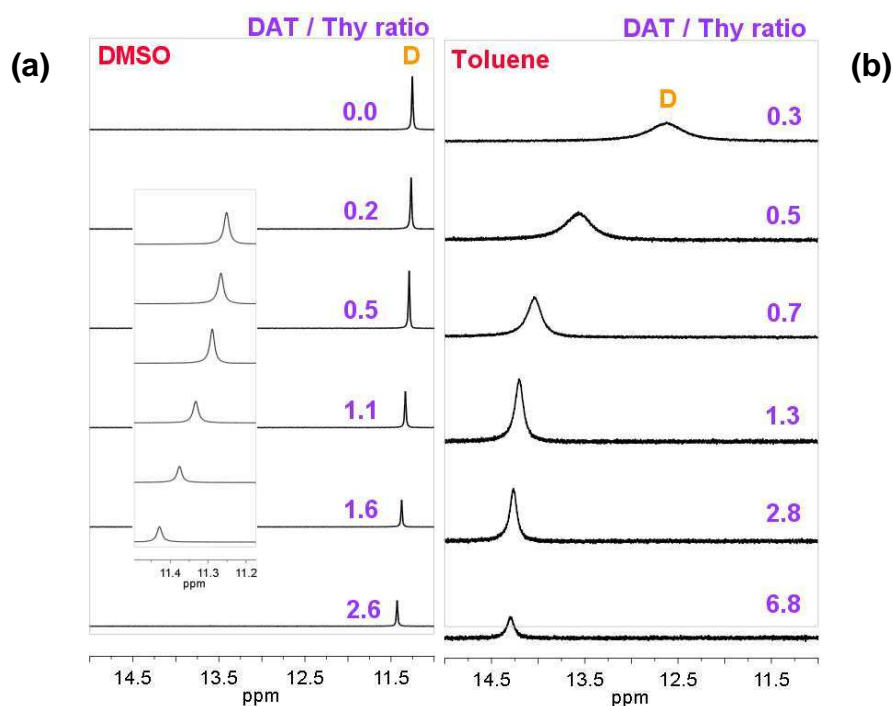
Figure III.12. ^{1}H NMR Spectra at 25°C of (a) BuThy (at 9.0*10^{-2} mol/L) - MeDAT (from 0 to 2.3*10^{-1} mol/L) mixtures in DMSO-d_6, and (b) Thy-PPO-2200-Thy **3a** (from 3.0*10^{-3} to 6.2*10^{-2} mol/L) - DAT-PPO-2200-DAT **2a** (at 2.1*10^{-2} mol/L) mixtures in toluene-d_8.
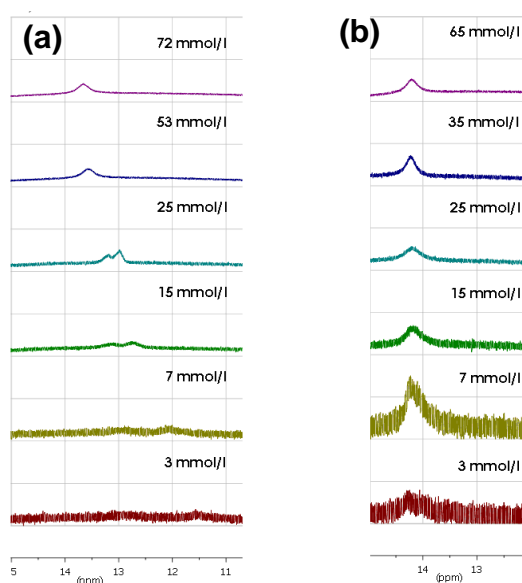
Figure III.13. Concentration-dependent ^{1}H NMR at 24°C of Thy-PPO-2200-DAT **10a** in the Thy NH (**D**) region (a) in CDCl$_3$ and (b) in toluene-d_8.

This could be explain by the fact that hydrogen bonds donors and acceptors are more poorly solvated in the non-polar toluene ($\varepsilon_{toluene}$ = 2.4, relative polarity = 0.099)[33] than in the relatively polar chloroform ($\varepsilon_{chloroform}$ = 4.8, relative polarity = 0.259).[35]

Besides, the Thy-DAT association constant in toluene is much higher than the Thy-Thy and DAT-DAT dimerization constants in toluene. Indeed, as in chloroform solutions, the chemical shift of the Thy NH (**D**) proton signal is strongly deshielded in toluene-d$_8$ solutions of 50/50-M-2200 **4a** and Thy-PPO-2200-DAT **10a** compared to Thy-PPO-2200-Thy **3a** ($\Delta\delta$ ~ 4 ppm, Figure III.14). A similar downfield shift is observed for DAT NH$_2$ and NH (Φ, Ψ, Ω) proton signals ($\Delta\delta$ ~ 0.9 ppm, Figure III.14).
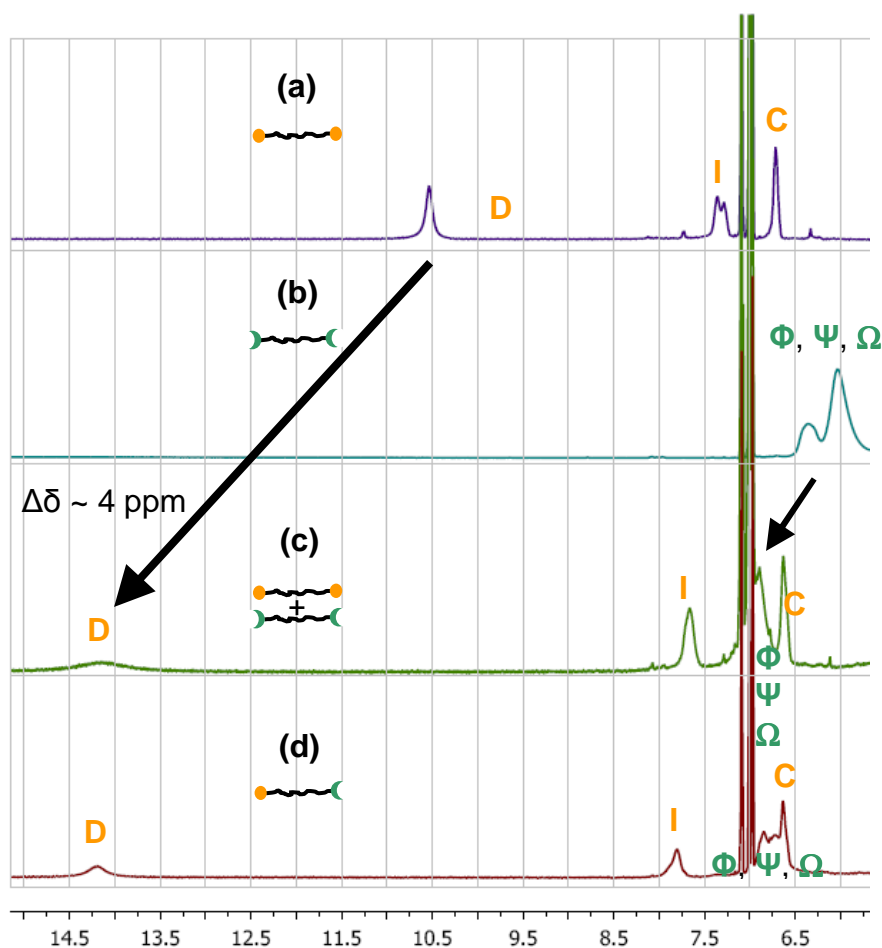

Figure III.14. ^{1}H NMR at 25°C of solutions at 0.2 g/cm^3 in toluene-d$_8$ of (a) Thy-PPO-2200-Thy **3a**, (b) DAT-PPO-2200-DAT **2a**, (c) 50/50-M-2200 **4a**, and (d) Thy-PPO-2200-DAT **10a**.

[35] Zimmerman, S.; Corbin, P.; **Heteroaromatic modules for self-assembly using multiple hydrogen bonds**; *Structure and Bonding* **2000**, *96*, 63.

(iii) Association is temperature-dependent

When a solution of 50/50-M-2200 **4a** is heated from 25 to 50°C, there is an upfield shift of the DAT amine protons (Φ, Ψ, Ω) signal on the ^{1}H NMR spectrum (Figure III.15b), revealing a partial rupture of the hydrogen bonds. Similarly, when a solution of Thy-PPO-2200-Thy **3a** is heated from 25 to 50°C, there is shift of the imide (NH Thy **D**) proton towards higher fields, also indicating rupture of hydrogen bonds under heating (Figure III.15a). After cooling, the initial spectra of both solutions are recovered, demonstrating the reversible nature of the hydrogen bonds (Figure III.15).
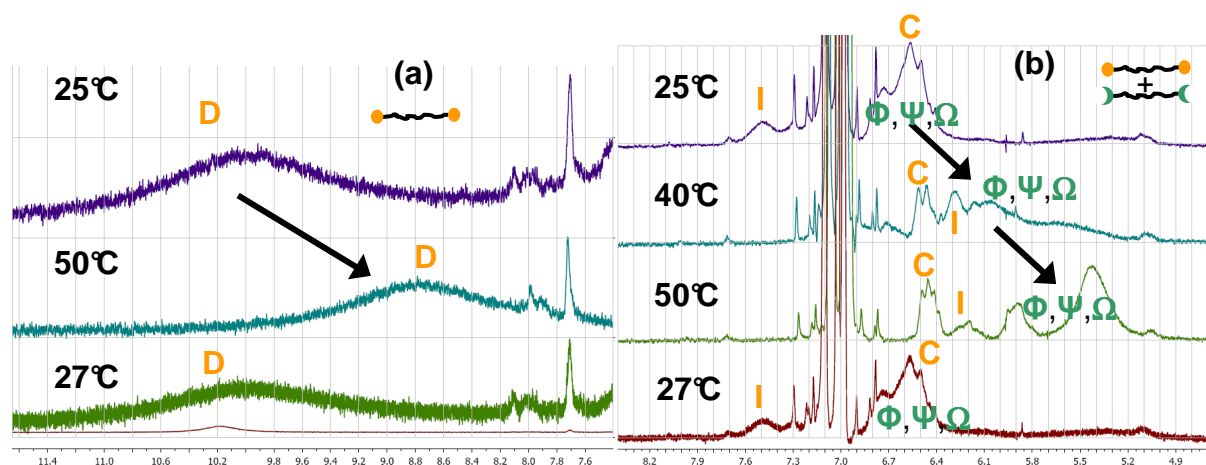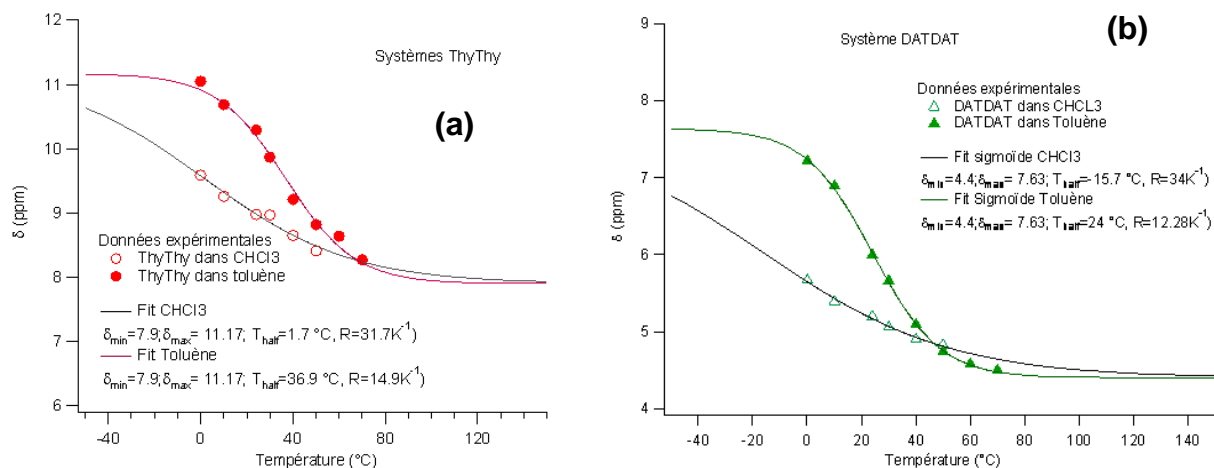

Figure III.15. Temperature-dependent ^{1}H NMR in toluene-d$_8$ of (a) Thy-PPO-2200-Thy **3a** at $6.1*10^{-2}$ g/cm^3 ($2.4*10^{-2}$ mol.L^{-1}) and (b) 50/50-M-2200 **4a** at $2.0*10^{-2}$ g/cm^3 ($8.2*10^{-3}$ mol.L^{-1}).

(iv) Association constant as a function of temperature

Although $K_{Thy-DAT}$ could not be measured in toluene-d$_8$ by NMR titration, temperature-dependent NMR measurements of solutions of Thy-PPO-2200-Thy **3a**, DAT-PPO-2200-DAT **2a**, and Thy-PPO-2200-DAT **10a** allow estimation of $K_{Thy-DAT}$, as well as $K_{Thy-Thy}$ and $K_{DAT-DAT}$, as a function of temperature.

To this end, the extreme chemical shifts of Thy NH (**D**) and DAT NH$_2$ (Φ, Ψ) in the free ($\delta_{free\ Thy}$, $\delta_{free\ DAT}$) and self-associated ($\delta_{dim\ Thy}$, $\delta_{dim\ DAT}$) states (*i.e.* the extreme values, which are temperature-independent and solvent-independent) can be estimated by temperature-dependent ^{1}H NMR measurements of solutions of Thy-PPO-2200-Thy **3a** and DAT-PPO-2200-DAT **2a** (in CDCl$_3$ and in toluene-d$_8$). Indeed, sigmoid fitting on the

observed chemical shift for Thy NH (**D**) ($\delta_{\exp \text{Thy}}^{\text{T,solvent}}$, Figure III.16a) and DAT NH$_2$ (**Φ**, **Ψ**) ($\delta_{\exp \text{DAT}}^{\text{T,solvent}}$, Figure III.16b) in those experiments, yields the values of 7.90 ppm for $\delta_{\text{free Thy}}$, 11.17 ppm for $\delta_{\text{dim Thy}}$, in agreement with literature data,[36] and 4.40 ppm for $\delta_{\text{free DAT}}$, 7.63 ppm for $\delta_{\text{dim DAT}}$.

Figure III.16. Determination of the extreme chemical shifts (temperature-independent and solvent-independent) of: (a) Thy NH (**D**) in the free ($\delta_{\text{free Thy}}$) and self-associated ($\delta_{\text{dim Thy}}$) states by temperature-dependent ^{1}H NMR of Thy-PPO-2200-Thy **3a** in CDCl$_3$ and toluene-d$_8$, and (b) DAT NH$_2$ (**Φ**, **Ψ**) in the free ($\delta_{\text{free DAT}}$) and self-associated ($\delta_{\text{dim DAT}}$) states by temperature-dependent ^{1}H NMR of DAT-PPO-2200-DAT **2a** in CDCl$_3$ and toluene-d$_8$.

Knowing $\delta_{\text{free Y}}$ and $\delta_{\text{dim Y}}$ with Y = Thy or DAT, knowing $\delta_{\exp Y}^{\text{T,solvent}}$ of a Y-PPO-2200-Y solution at a given temperature T and in a given solvent, and knowing the total concentration of Y groups (C_Y) in this solution, one can estimate $K_{Y-Y}^{T,solvent}$ from equations 1, 2, 3 (three equations, three unknowns parameters {[Y], [Y=Y] and $K_{Y\text{-}Y}$}). The resulting values of dimerization constants as function of temperature in toluene (0 to 70°C) and in chloroform (0 to 50°C) are gathered in Table III.2.

$$\delta_{\exp Y}(T) = \frac{[Y]}{C_Y}\delta_{\text{free Y}} + \frac{2[Y=Y]}{C_Y}\delta_{\text{dim Y}} \qquad (1)$$

$$C_Y = [Y] + 2[Y=Y] \qquad (2)$$

$$K_{Y-Y} = \frac{[Y=Y]}{[Y]^2} \qquad (3)$$

[36] Salas, M.; Gordillo, B.; Gonzalez, F.; **Enthalpy and entropy contributions to the equilibrium of the hydrogen bonding interaction between 1-octylthymine and 9-octyladenine**; *ARKIVOC* **2003**, *11*, 72.

With this method, at 24°C, $K_{Thy-Thy}^{24°C}$ is estimated at 7 M^{-1} in CDCl$_3$ and 95 M^{-1} in toluene-d$_8$ and $K_{DAT-DAT}^{24°C}$ at 4 M^{-1} in CDCl$_3$ and 17 M^{-1} in toluene-d$_8$. Values are in the same ballpark but somewhat different than those determined by NMR titration where $\delta_{\text{free Thy}}$, $\delta_{\text{dim Thy}}$, $\delta_{\text{free DAT}}$, $\delta_{\text{dim DAT}}$, $K_{\text{Thy-Thy}}$, and $K_{\text{DAT-DAT}}$ are adjustable parameters.

Following the same method, extreme chemical shifts (temperature-independent and solvent-independent) of Thy NH (**D**) in the Thy-DAT associated ($\delta_{\text{asso Thy}}$) state can be estimated by temperature-dependent ^{1}H NMR measurements on Thy-PPO-2200-DAT **10a** solutions in CDCl$_3$ and toluene-d$_8$. Indeed, sigmoid fitting on the observed chemical shift for Thy NH (**D**) $\delta_{\exp Thy}^{T,solvent}$ in those experiments yields the value of 14.50 ppm for $\delta_{\text{asso Thy}}$ (Figure III.17).
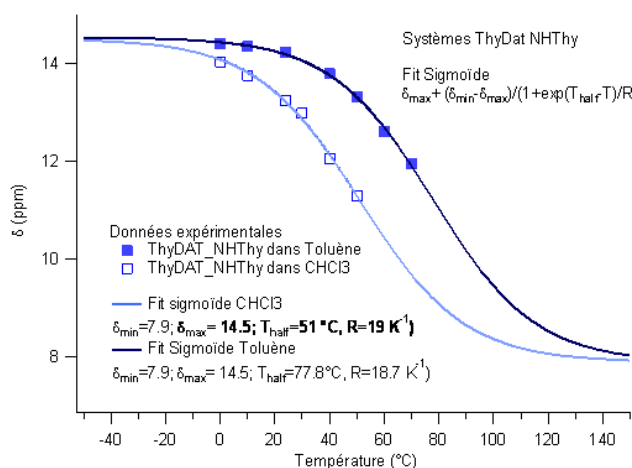
Figure III.17. Determination of the chemical shifts of Thy NH (**D**) in the free ($\delta_{\text{free Thy}}$) and associated with DAT ($\delta_{\text{asso Thy}}$) states by temperature-dependent ^{1}H NMR of Thy-PPO-2200-DAT **10a** in CDCl$_3$ and toluene-d$_8$.

Using previously determined $\delta_{\text{free Thy}}$, $\delta_{\text{dim Thy}}$, and $\delta_{\text{asso Thy}}$, $K_{Thy-Thy}^{T,solvent}$ and $K_{DAT-DAT}^{T,solvent}$ for a given temperature T and in a given solvent, knowing $\delta_{\exp Thy}^{T,solvent}$ in a Thy-PPO-2200-DAT **10a** solution, and knowing the total concentration of Thy and DAT groups in this solution ($C_{\text{Thy}} = C_{\text{DAT}}$), one can estimate, by iteration, $K_{Thy-DAT}^{T,solvent}$ from equations 4, 5, 6, 7, 8, and 9 (six equations, six unknowns parameters {[Thy], [DAT], [Thy=Thy], [DAT=DAT], [Thy=DAT] and $K_{\text{Thy-DAT}}$}). Results as function of temperature in toluene (0 to 70°C) and in chloroform (0 to 50°C) are gathered in Table III.2. At 24°C, we obtained $K_{Thy-DAT}^{24°C,chloroform} = 835$ M^{-1} in

CDCl$_3$, in accordance with our NMR titration (see part 3.a.ii) and with the literature,[29,34] and $K_{Thy-DAT}^{24°C,toluene} = 22061$ M^{-1} in toluene-d$_8$, a very high value as expected.

$$\delta_{exp\,Thy}(T) = \frac{[Thy]}{C_{Thy}}\delta_{freeThy} + \frac{2[Thy = Thy]}{C_{Thy}}\delta_{dim\,Thy} + \frac{[Thy = DAT]}{C_{Thy}}\delta_{assoThy} \qquad (4)$$

$$C_{Thy} = [Thy] + 2[Thy = Thy] + [Thy = DAT] \qquad (5)$$

$$C_{DAT} = [DAT] + 2[DAT = DAT] + [Thy = DAT] \qquad (6)$$

$$K_{Thy-DAT} = \frac{[Thy = DAT]}{[Thy][DAT]} \qquad (7)$$

$$K_{Thy-Thy} = \frac{[Thy = Thy]}{[Thy]^2} \qquad (8)$$

$$K_{DAT-DAT} = \frac{[DAT = DAT]}{[DAT]^2} \qquad (9)$$

	CDCl$_3$			Toluene-d$_8$		
T (°C)	$K_{Thy\text{-}Thy}$	$K_{DAT\text{-}DAT}$	$K_{Thy\text{-}DAT}$	$K_{Thy\text{-}Thy}$	$K_{DAT\text{-}DAT}$	$K_{Thy\text{-}DAT}$
0	21	10	$7.4*10^3$	$6.7*10^3$	493	$3.3*10^5$
10	12	6	$2.7*10^3$	374	134	$8.3*10^4$
24	7	4	835	95	17	$2.2*10^4$
30	7	3	552	36	10	-
40	4	2	174	11	3	$2.9*10^3$
50	2	2	82	5	1	960
60	-	-	-	4	0,6	322
70	-	-	-	1	0,3	152

Table III.2. Association constants (in L/mol), measured by temperature dependent ^{1}H NMR of Thy-PPO-2200-Thy **3a**, DAT-PPO-2200-DAT **2a**, and Thy-PPO-2200-DAT **10a**.

(v) Thymine's NH splitting

The thymine NH (**D**) signal of Thy-PPO-2200-DAT **10a** splits under 0.025 mol/L in CDCl$_3$ at 24°C (Figure III.18a). Binder and his coworkers also observed a splitting of the thymine NH (**D**) signal at low concentrations of a PIB-thymine/PEK-triazine mixture in CDCl$_3$ (Figure III.18b).[37]
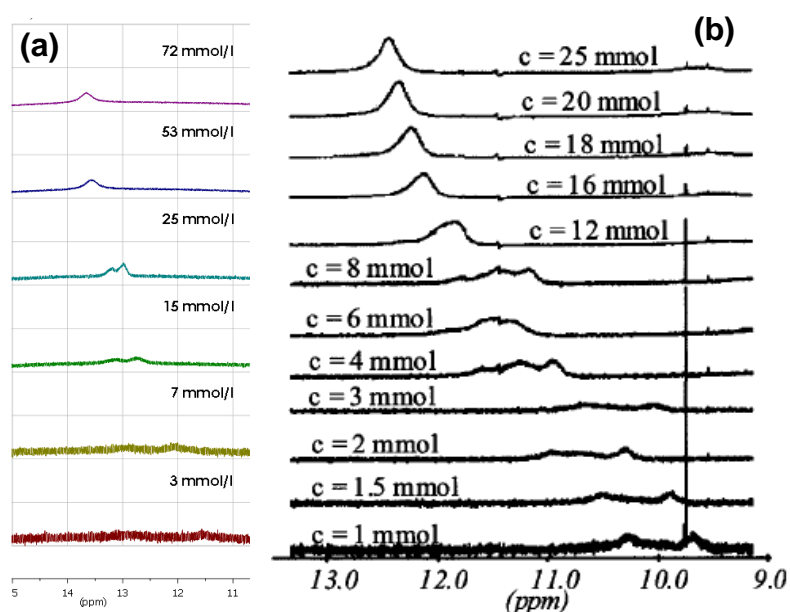
Figure III.18. Concentration-dependent ^{1}H NMR in CDCl$_3$ at 24°C in the Thy NH (**D**) region of (a) Thy-PPO-2200-DAT **10a** and (b) PIB-thymine / PEK-triazine mixture.[37]

^{1}H signal splitting is often encountered in CDCl$_3$ for lactams (such as for the thymine model compound 2-pyridone) and is characteristic of a lactam-lactim tautomerism (Scheme III.4).[38,39] Indeed, both lactam and lactim tautomers of 2-pyridone can occur because their energy difference is relatively small.[38] In fact, thymine, adenine, guanine, and cytosine tautomerism could be responsible of spontaneous mutations in DNA, [40,41] as first suggested by Watson and Crick.[42]

---

[37] Binder, W. H.; Kunz, M. J.; Ingolic, E.; **Supramolecular poly(ether ketone)-polyisobutylene pseudo-block copolymers**; *J. Polym. Sci. A: Polym. Chem.* **2004**, *42*, 162.

[38] Szyc, L.; Guo, J.; Yang, M.; Dreyer, J.; Tolstoy, P. M.; Nibbering, E. T. J.; Czarnik-Matusewicz, B.; Elsaesser, T.; Limbach, H.-H.; **The hydrogen-bonded 2-pyridone dimer model system. 1. Combined NMR and FT-IR spectroscopy study**; *J. Phys. Chem. A* **2010**, *114*, 7749.

[39] Alkorta, I.; Goya, P.; Elguero, J.; Singh, S. P.; **A simple approach to the tautomerism of aromatic heterocycles**; *Natl. Acad. Sci. Lett.,* **2007**, *30*, 139.

[40] Tsuchiya, Y.; Tamura, T.; Fujii, M.; Ito, M.; **Keto-enol tautomer of uracil and thymine**; *J. Phys. Chem.* **1988**, *92*, 1760.
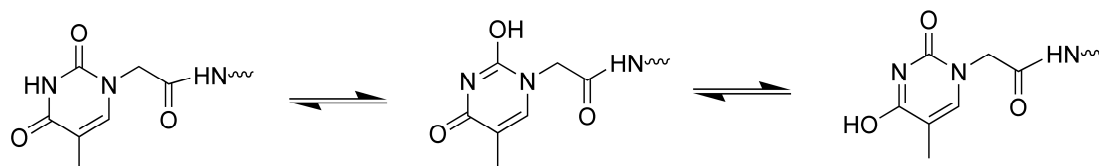
Scheme III.4. Lactam (ceto) - lactim (iminol) tautomerism of Thy (proton exchange between N and O).

As the temperature increases, this equilibrium becomes faster, inducing a coalescence of the split signals (the proton signals are averaged on the NMR time scale).[38] However, this coalescence as the temperature increases is not observed with Thy-PPO-2200-DAT **10a** neither in CDCl$_3$ (at $2.0*10^{-2}$ g/cm^3, Figure III.19a), nor in toluene-d$_8$ (same concentration, Figure III.19c) (splitting is observed at $6.7*10^{-2}$ g/cm^3 in CDCl$_3$ but not in toluene-d$_8$ for the same concentration), nor with Binder's PIB-thymine/PEK-triazine mixture in CDCl$_3$ (Figure III.19b). On the contrary, splitting increases with temperature, and coalescence occurs as the temperature decreases for Thy-PPO-2200-DAT **10a** in toluene-d$_8$ (Figure III.19c).
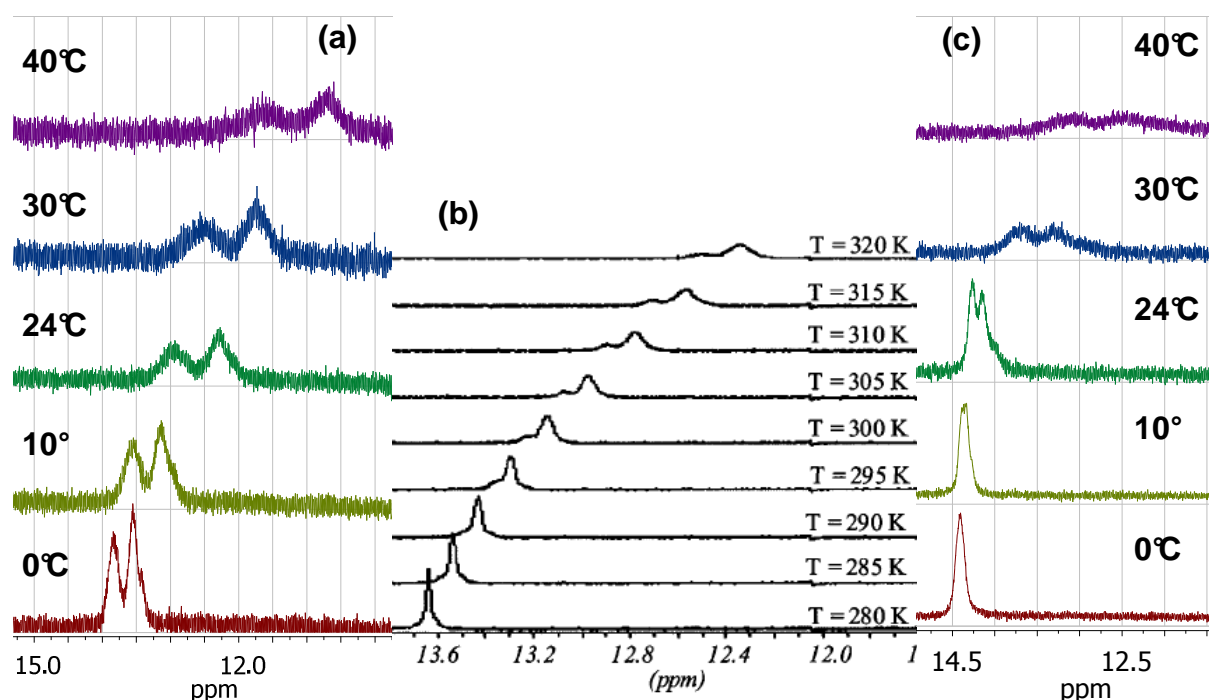
Figure III.19. Temperature-dependent ^{1}H NMR in the Thy NH (**D**) region of (a,c) Thy-PPO-2200-DAT **10a** at $2.0*10^{-2}$ g/cm^3 in: (a) CDCl$_3$, (c) toluene-d$_8$; and (b) PIB-thymine/PEK-triazine mixture in CDCl$_3$.[37]

---

[41] Samijlenko, S. P.; Yurenko, Y. P.; Stepanyugin, A. V.; Hovorun, D. M.; **Tautomeric equilibrium of uracil and thymine in model protein-nucleic acid contacts. Spectroscopic and quantum chemical approach**; *J. Phys. Chem. B* **2010**, *114*, 1454.

[42] Watson, J. D.; Crick, F. H. C.; **Genetical implications of the structure of deoxyribonucleic acid**; *Nature* **1953**, *171*, 964.

Therefore, lactam-lactim tautomerism does not explain the Thy NH (D) signal splitting. For the same reason, transition from a fast exchange to a slow exchange regime with a free and a bonded Thy NH (D) signal does not explain the splitting, because then coalescence should also occur at high temperatures, and the chemical shift would not shift.

Another possible explanation could be that the signal splitting is due to two types of associations, the expected hydrogen bonds and for instance aromatic interactions or a weaker NH_{Thy}---N_{DAT} bond arising at low concentrations or at high temperatures. Indeed, Thy-DAT association is optimal when there are three aligned and parallel H-bonds between Thy and DAT, as it is always drawn in the literature (Chart III.1.f). However, when the temperature increases, the weaker bonds NH_{2DAT}---OC_{Thy} may break while the NH_{Thy}---N_{DAT} bonds holds, allowing the H-bonding units to freely rotate around their bond with the PPO chain. The NH_{Thy}---N_{DAT} bond would then be longer because when the $C=O_{Thy}$ are not implicated in hydrogen bonds, the NH_{Thy} (D) proton acidity decreases,[31] leading to a weaker NH_{Thy}---N_{DAT} bond. This results in the appearance of a shielded signal of imino NH (D). Thus two associated species coexist, one optimal with three parallel H-bonds and one with only one H-bond (Scheme III.5). Relative proportion of the two species (3 H-bonds/1 H-bond) is constant (45/55, according to ^{1}H NMR integration) and depends neither on concentration nor temperature. This is characteristic of an ON/OFF system for which weaker bonded species appears only at a critical concentration for a given temperature. However, NH_{Thy} (D) signal splitting is also observed for homotelechelic Thy-PPO-2200-Thy **3a** at low concentrations in $CDCl_3$ and in toluene-d$_8$. The NH_{Thy}---N_{DAT} bond does not explain this, but aromatic interactions could.
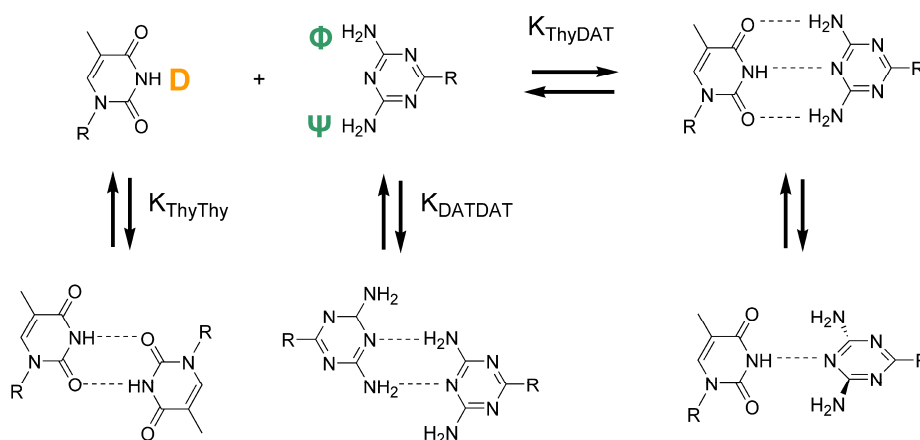
Scheme III.5. Thy-DAT complementary association and Thy-Thy, DAT-DAT self-associations.

b. Impact of the associations on the viscosity

We have evidenced by NMR that hydrogen bonding occurs between the Thy and DAT stickers in chloroform and toluene, with relatively high temperature-dependent association constants. We will now focus on the macroscopic impact of these associations by studying the supramolecular polymers solutions viscosities.

(i) Viscosity higher when Thy and DAT both present
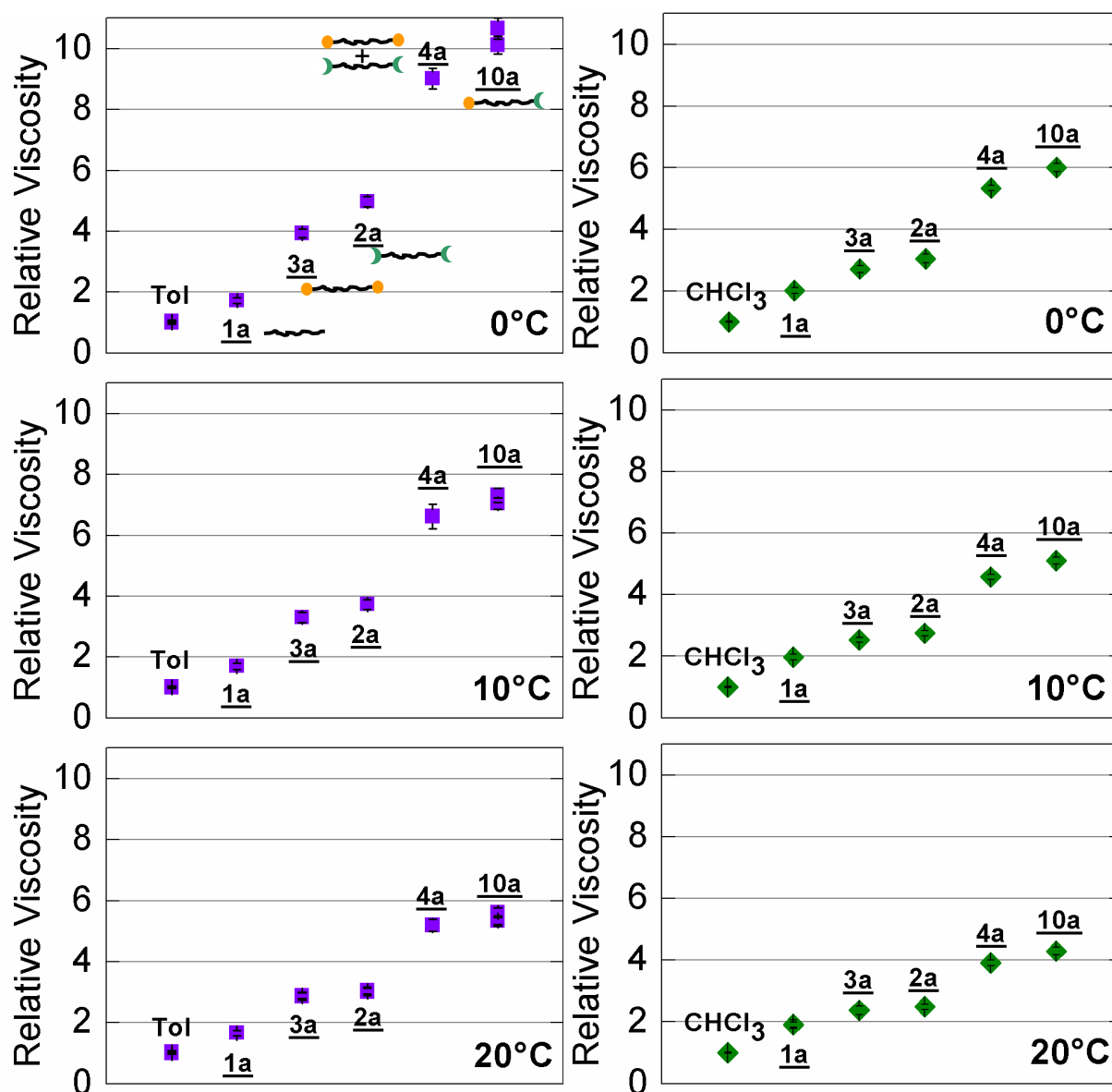
Figure III.20. Relative viscosity of $9.6*10^{-2}$ g/cm^3 solutions of precursor NH$_2$-PPO-2200-NH$_2$ **1a**, homotelechelic units Thy-PPO-2200-Thy **3a** and DAT-PPO-2200-DAT **2a**, 50:50 mixture of Thy-PPO-2200-Thy and DAT-PPO-2200-DAT (50/50-M-2200 **4a**), and heterotelechelic units Thy-PPO-2200-DAT **10a** in: (left) toluene (10 %wt) and (right) CHCl$_3$ (6.1 %wt), at: (top) 0°C, (middle) 10°C, and (bottom) 20°C.

These differences in association and self-association constants ($K_{\text{Thy-DAT}} > 300*K_{\text{Thy-Thy}}$ and $K_{\text{Thy-DAT}} > 300*K_{\text{DAT-DAT}}$) seem to impact the solution properties. Indeed, in toluene and chloroform, the relative viscosities at 0, 10 and 20°C of 0.096 g.cm^{-3} solutions containing both Thy and DAT groups (Thy-PPO-2200-DAT **10a** and 50/50-M-2200 **4a**) are higher than those containing only Thy or only DAT groups (DAT-PPO-2200-DAT **2a** and Thy-PPO-2200-Thy **3a**), which are higher than those containing NH$_2$-PPO-2200-NH$_2$ **1a** (Figure III.20).

These viscosities measurements are thus in agreement with the NMR results: weak Thy-Thy and DAT-DAT self-associations and strong Thy-DAT complementary association, in chloroform and toluene.

Besides, the relative viscosities of 0.096 g.cm^{-3} solutions of 50/50-M-2200 **4a** in toluene or chloroform are slightly lower than that of Thy-PPO-2200-DAT **10a** (Figure III.20). This effect could be due either to a Thy/DAT ratio closer to 1 in the asymmetric Thy-PPO-2200-DAT **10a** than in the mixture 50/50-M-2200 **4a** (stopper effect, explained in Chapter I); or to different structurations.

(ii) Viscosity is temperature-dependent

As visible on Figure III.20, the relative viscosities of all solutions in toluene or chloroform are higher at lower temperature, while that of NH$_2$-PPO-2200-NH$_2$ **1a** are temperature-independent. For instance, the relative viscosity of DAT-PPO-2200-DAT **2a** and 75/25-M-2200 **6a** in toluene decreases as the temperature increases, until a plateau is reached above 40°C (Figure III.21).
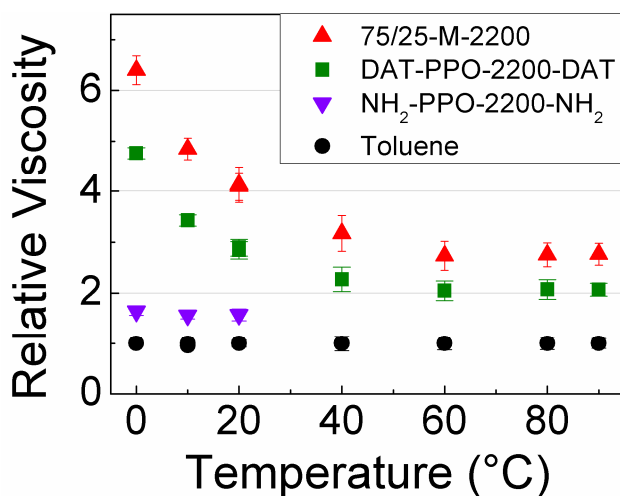
Figure III.21. Relative viscosity as a function of temperature (10%wt - 9.6*10^{-2}g/cm^3) in toluene.

These viscosities measurements are thus also in agreement with the NMR results: Thy-Thy and DAT-DAT self-associations and Thy-DAT complementary association constants in chloroform and toluene decrease as the temperature increases.

## c. Experimental differences between chloroform and toluene

(i) Higher viscosity in toluene than in chloroform due to higher K?

As can be seen on Figure III.20, the relative viscosities of solutions of all compounds are higher in toluene than in chloroform. This is particularly obvious for Thy-PPO-2200-DAT **10a** for which η_{rel} is 10 in toluene *vs* 6 in chloroform at 0°C. This difference is less marked as temperature increases (5 *vs* 4.3 at 20°C). This result could be explained by the higher $K_{Thy-DAT}$, $K_{Thy-Thy}$, and $K_{DAT-DAT}$ in toluene compared to chloroform, leading to larger supramolecular objects in toluene than in chloroform. Furthermore, the temperature dependence could also be explained by lower association constants as demonstrated by ^{1}H NMR measurements.

(ii) Different concentration-dependence in toluene and chloroform

However, concentration-dependent viscosity measurements (Figure III.22) do not seem consistent with this idea, at least on first approach. Indeed, specific viscosity (relative viscosity minus one) of all compounds in toluene and in chloroform are equal at low concentrations. If the higher values of association constants in toluene were responsible for the higher viscosity at 0.096 g.cm^{-3}, one would also naïvely expect higher viscosities in toluene at lower concentrations.

To see if this idea is correct, we have confronted our experimental results with viscosity models of supramolecular polymers.
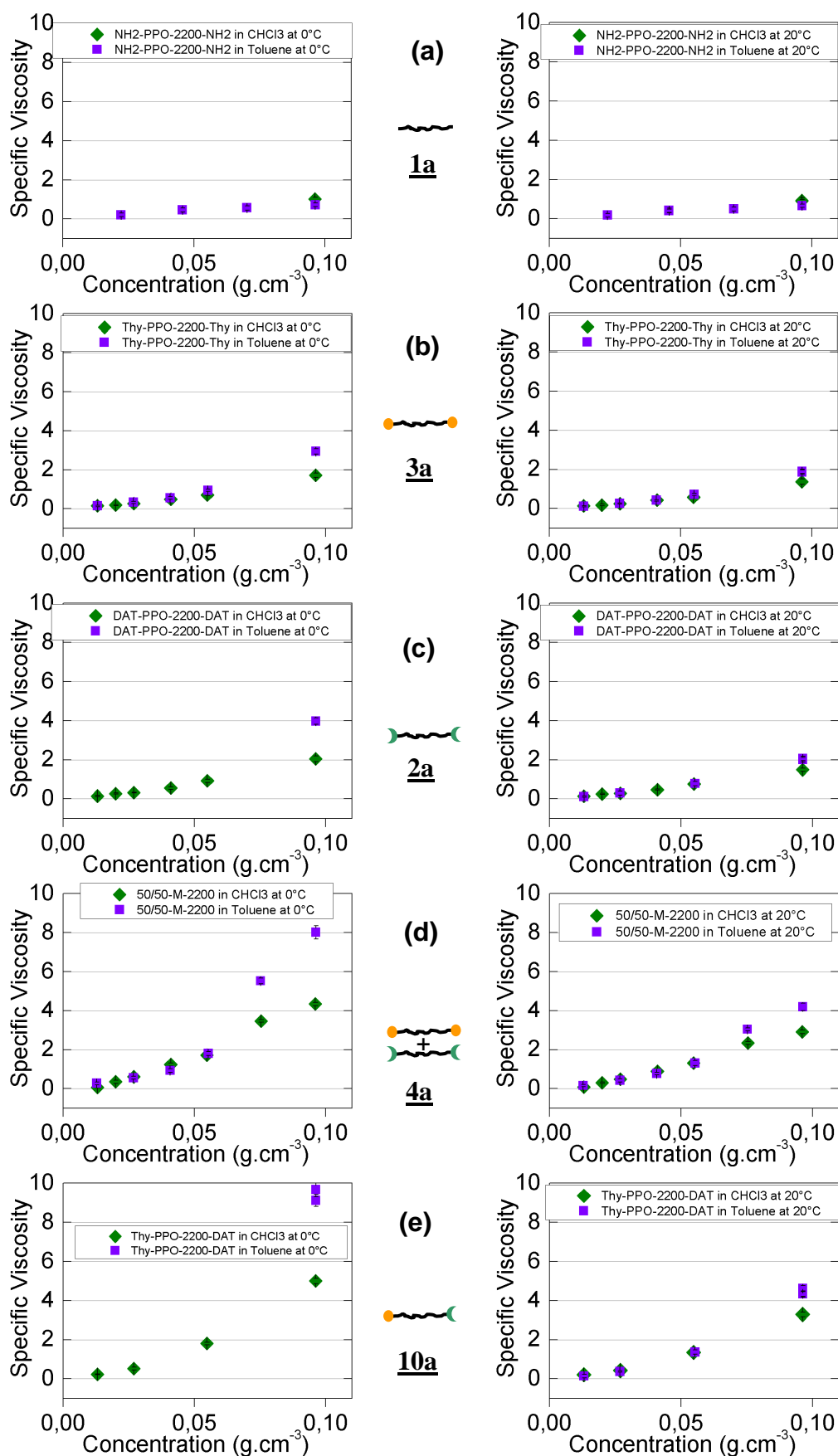
Figure III.22. Concentration-dependent specific viscosity in chloroform (◆) and in toluene (■)
at 0°C (left) and 20°C (right) of (a) NH$_2$-PPO.2200-NH$_2$ **1a**, (b) Thy-PPO-2200-Thy **3a**,
(c) DAT-PPO-2200-DAT **2a**, (d) 50/50-M-2200 **4a**, and (e) Thy-PPO-2200-DAT **10a**.

d. Viscosity models for supramolecular polymers

(i) Viscosity model for linear supramolecular polymers

In the diluted regime, the specific viscosity of a monodisperse polymer solution can be expressed as a function of the polymer radius of gyration R_g, its weight concentration C_g, and its molecular weight M, according to the Zimm model (equation 10, with N_a the Avogadro number and κ a constant, equal to 6.93 according to the original Zimm prediction, or 6.1 from experiments on linear polymers in theta-conditions and more recent theories).[43]

$$\eta_{sp} = \frac{\eta_0 - \eta_s}{\eta_s} = \kappa \frac{C_g N_a R_g^3}{M} \qquad (10)$$

Assuming that the supramolecular polymerization is under thermodynamic control with an isodesmic mechanism, then the average degree of polymerization (DP = N) can be expressed with equations (11) for a self-association (AA) and (12) for a complementary association (AB), C being the concentration of supramolecular solution, and K_{AA} and K_{AB} the association constants.

$$N = \frac{2[AA]}{[A]} + 1 = \frac{8CK_{AA}}{-1 + \sqrt{1 + 16CK_{AA}}} (\approx 2\sqrt{K_{AA}C}) \qquad (11)$$

$$N = \frac{2[AB]}{[A] + [B]} + 1 = \frac{[AB]}{[A]} + 1 = \frac{\beta + 2C - \sqrt{(\beta + 2C)^2 - 4C^2}}{-\beta + \sqrt{(\beta + 2C)^2 - 4C^2}} + 1 \qquad (12)$$

$$\text{with } \beta = \frac{1}{K_{AB}} \qquad (13)$$

The supramolecular polymer size distribution can be expressed with equations (14) for the numbered-average distribution and (16) for the weighted-average distribution, by analogy to step growth polymerization. X_i is the number-fraction, w_i the weight-fraction of supramolecular polymers constituted of i chains, p the extent of reaction (*i.e.* the fraction of stickers that have reacted), and γ a normalization constant fixed by equation (15).[44,45] Indeed,

---

[43] Graessley, W. W.; *Polymer liquids & networks: dynamics and rheology*; Taylor & Francis Group: New York, **2008**.

[44] Flory, P.J.; *Principles of polymer chemistry*; Cornell University Press: Ithaca, NY, **1953**.

[45] Knoben, W.; Besseling, N. A. M.; Stuart, M. A. C.; **Rheology of a reversible supramolecular polymer studied by comparison of the effects of temperature and chain stoppers**; *J. Chem. Phys.* **2007**, *126*, 24907.

although the associations constantly break and reform, the mean size N and the size distribution remain constant at equilibrium.

$$X_i = (1-p)p^{i-1} \approx \frac{1}{\gamma} \exp(\frac{-i}{N}) \tag{14}$$

$$\text{with } \int_1^\infty X_i \approx \int_1^{10000} X_i = 1, \text{ so } \gamma = N(e^{-1/N} - e^{-10000/N}) \tag{15}$$

$$w_i = i(1-p)X_i = \frac{i}{N}X_i \tag{16}$$

The specific viscosity of a supramolecular polymer solution η_{sp} can then be considered to be a weighted sum on all sizes (*i.e.* an integral) of equation (10). This approach yields equation (17) which expresses η_{sp} as a function of the supramolecular polymer's weight concentration C_g and mean size N. Equation (17) also contains a constant α characteristic of the supramolecular polymer unit [equation (18), with M_1 the unit's molecular weight and R_1 the unit's radius of gyration), and a function of N. $f(N)$ is actually an infinite integral that can be approximated to an integral to 10 000 [equation (19)], since there are virtually no supramolecular polymer made of more than 10 000 units given the order of magnitude of our association constants. Besides, υ is equal to 0,5 for short chains or in Θ-solvent.[46]

$$\eta_{sp} = \frac{\alpha C_g}{N\gamma} f(N) \tag{17}$$

$$\text{with } \alpha = \kappa \frac{N_a R_1^3}{M_1} \tag{18}$$

$$\text{with } f(N) = \int_1^{10000} i^{3\upsilon} \exp(\frac{-i}{N})di \tag{19}$$

The specific viscosity η_{sp} can then be calculated as follows. Knowing C and using the values of association constants previously estimated by ^{1}H NMR measurements at room temperature (Table III.3, see parts 2.i and 3.a), N can be calculated from equation (11) or (12). Knowing N, the integral $f(N)$ can be numerically calculated with the mathematical software Maxima. α is estimated from concentration-dependent viscosity measurements of NH_2-PPO-2200-NH_2 **1a**. Indeed, assuming there are no association in NH_2-PPO-2200-NH_2 **1a**, α is the slope of the η_{sp} *vs* C_g linear curve (Figure III.23, without association: $\eta_{sp} = \alpha C_g$).

---

[46] Rubinstein, M.; Colby, R.; *Polymer physics*; Oxford University Press: USA, **2003**.

	DMSO-d_6	CDCl$_3$	Toluene-d_8
$K_{\text{Thy-Thy}}$	-	2.0 [b]	26.5 [e]
$K_{\text{DAT-DAT}}$	-	2.8 [c]	42.5 [f]
$K_{\text{Thy-DAT}}$	1.3 [a]	~ 1000 [d]	~ 22 000 [g]

Table III.3. Association constants (in L/mol), measured by ^{1}H NMR: [a] BuThy with MeDAT; [b] Thy-PPO-460-Thy **3b**; [c] DAT-PPO-460-DAT **2b**; [d] DAT-PPO-460-DAT **2b** with Thy-PPO-460-Thy **3b**; [e] Thy-PPO-2200-Thy **3a**; [f] DAT-PPO-2200-DAT **2a**; [g] Thy-PPO-2200-DAT **10a**.
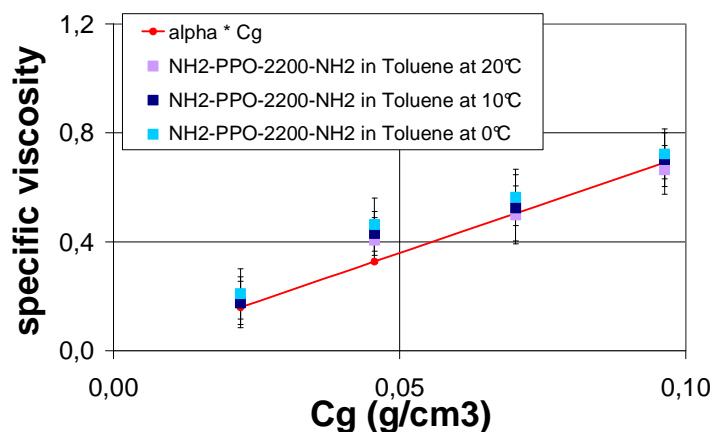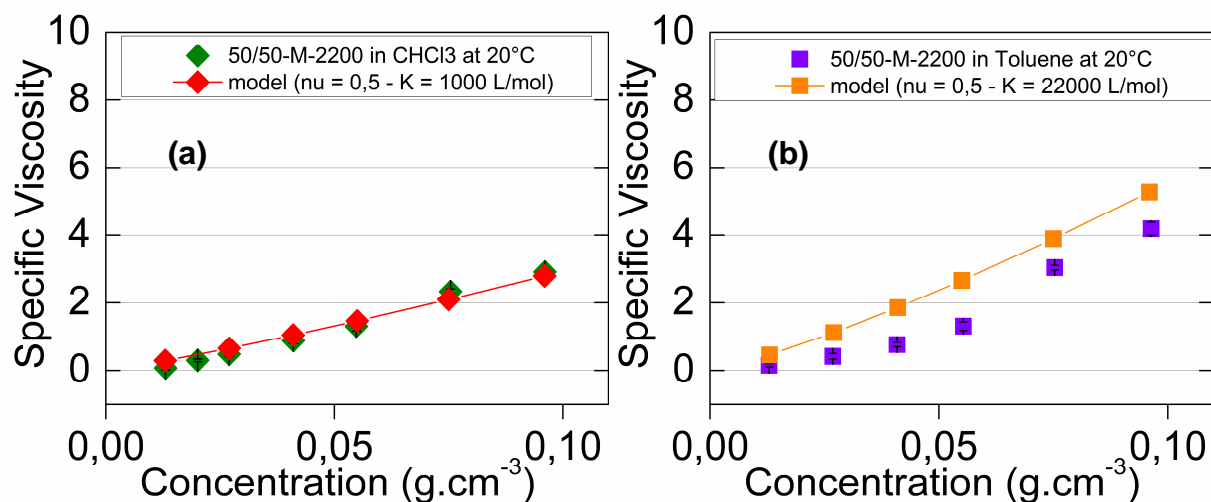

Figure III.23. Concentration-dependent specific viscosity of NH$_2$-PPO-2200-NH$_2$ **1a** in toluene, allowing determination of α as the slope of the linear curve (α = 7.17 cm^3/g).

The results of this simple model which applies mostly at low concentrations (below 0.06 g.cm^{-3}) are plotted in Figure III.24. The fit is good for chloroform (Figure III.24a) but not for toluene (Figure III.24b), since as naïvely expected, a higher association constant yield higher viscosities at any concentration. This very crude model does not consider intrachain associations, which are quite likely at low concentrations. We have confronted our experimental results with a viscosity model of supramolecular polymers with ring-chain equilibrium in the next part.

Another way to modelize viscosity of supramolecular polymers without using the Zimm equation (10) has been illustrated by Bouteiller and his coworker. [47] However, their method requires synthesis of a model covalent polymer to determine its viscosimetric parameters (Mark-Houwink and Huggins constants).

---

[47] Abed, S.; Boileau, S.; Bouteiller, L.; **Supramolecular association of acid terminated polydimethylsiloxanes. 3. Viscosimetric study**; *Polymer* **2001**, *42*, 8613.

Figure III.24. Concentration-dependent specific viscosity of 50/50-M-2200 **4a** at 20°C (a) in chloroform (◆) and (b) in toluene (■). Viscosity model for an isodesmic supramolecular polymerization into linear chains with an association constant of (a) 1000 L/mol (◆) and (b) 22 000 L/mol (■).

(ii) Viscosity for ring supramolecular polymers

Cyclic supramolecular polymers obey the same Zimm equation (10) as linear supramolecular ones. The difference is that, for the same molecular weight, a ring has a lower radius of gyration than a chain [see equations (20),(21), and (22), with a the monomer size, i the number of monomers, and v equal to 0,5 for short chains or in Θ-solvent].

$$R_{g,chain,i} = \frac{a(in)^v}{\sqrt{6}} \qquad (20)$$

$$R_{g,ring,i} = \frac{a(in)^v}{\sqrt{12}} \qquad (21)$$

$$R_{g,ring,i} = \frac{R_{g,chain,i}}{\sqrt{2}} \qquad (22)$$

(iii) Ring-chain equilibrium

The weight fraction of rings ρ_w can be estimated with the Jacobson-Stockmayer theory [equations (23), (25) and (24), with x the fraction of reacted end-groups in the chain fraction, v the number of chain atoms per monomer unit, and b the effective link length of the polymer chain].[5] The function $\phi(x,s)$ can be calculated numerically with the mathematical software

Maxima, using expression (26) more suited for numerical calculation than equation (25).[48] x is assumed to be equal to what it would be without rings, *i.e.* it is just a function of the association constant and of the concentration.
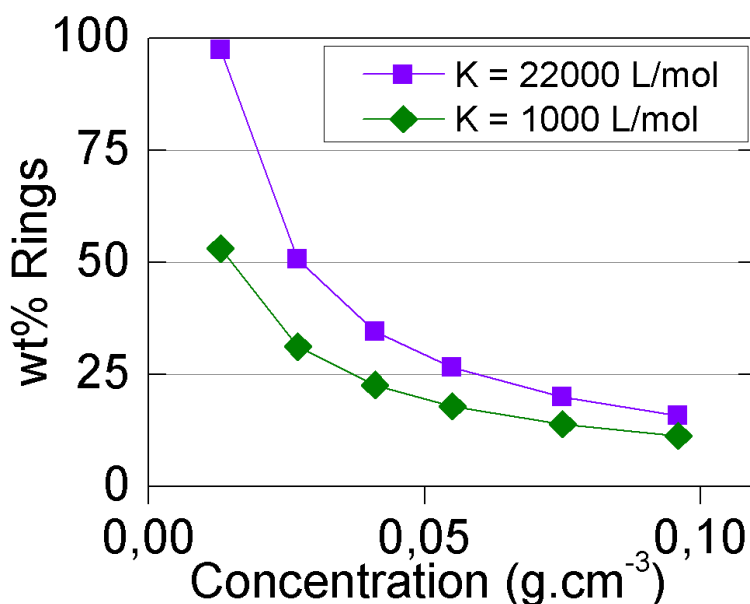
$$\rho_w = \frac{B'}{C} \phi(x, \frac{3}{2}) \tag{23}$$

$$\text{with} \quad B' = \frac{1}{N_A} \left(\frac{3}{2\pi\upsilon} \right)^{\frac{3}{2}} \frac{1}{2b^3} \tag{24}$$

$$\text{and} \quad \phi(x, s) = \sum_{i=1}^{\infty} x^i i^{-s} \tag{25}$$

$$\phi(x, s) = \Gamma(1-s)(-\log x)^{s-1} + \sum_{i=0}^{\infty} \zeta(s-i) \frac{(\log x)^i}{i!} \tag{26}$$

The weight fraction of rings ρ_w is plotted against concentration of the supramolecular polymer in Figure III.25. ρ_w is very high, especially for low concentrations and high association constants.

Figure III.25. Weight fraction of rings as a function of concentration for an association constant of 1000 L/mol (◆) and 22 000 L/mol (■).

Predominance of ring formation at low concentrations should impact the concentration-dependent ^{1}H NMR chemical shift variation. Indeed, for independent self-complementary stickers A or for self-complementary stickers A linked by a chain and having interchain associations only, the concentration of associated stickers [AA] is proportional to

---

[48] Truesdell, C.; **On a function which occurs in the theory of the structure of polymers**; *Ann. Math.* **1945**, *46*, 144.

[A]^2 [equation (27)]. However, as discussed in reference 13, for self-complementary stickers A linked by a chain, if only <u>intra</u>chain associations occur (*i.e.* ring formation), the concentration of complexed stickers [AA] should be proportional to [A] instead of [A]^2. [AA] should also be proportional to C^*, because the probability of intrachain association is proportional to the average concentration in the polymer coil, which is C^* by definition [equation (28)].[49] As a result, in the dilute regime with intrachain association only ($C < C^*$), the chemical shift δ should obey equation (31) (determined from equations 28, 29 and 30) and be independent of the global concentration of sticker A, $C_A = 2C$.

$$K_2^{inter} = \frac{[AA]}{[A]^2} \tag{27}$$

$$K_2^{intra} = \frac{[AA]}{[A]C^*} \tag{28}$$

$$\delta_{exp} = \delta_A \frac{[A]}{C_A} + 2\delta_{AA} \frac{[AA]}{C_A} \tag{29}$$

$$C_A = [A] + 2[AA] \tag{30}$$

$$\delta_{exp} = \frac{(\delta_A + 2\delta_{AA} K_2^{intra} C^*)}{1 + 2K_2^{intra} C^*} \tag{31}$$

Looking back at the ^{1}H NMR titration of Thy-PPO-460-Thy **3b** (Figure III.5), it appears that it could indeed be interpreted that δ is almost independent of concentration at low concentrations (below 0.01 g/cm^2), although the error bar are very high at these low concentrations (Figure III.26). Concentration dependence is much more pronounced in the semidilute regime, where interchain associations occur. The other ^{1}H NMR titration plots (Figure III.6 to Figure III.11) do not contain enough points at low concentrations to distinguish this concentration-independent regime.

---

[49] Pezron, E.; Leibler, L.; Ricard, A.; Lafuma, F.; Audebert, R.; **Complex formation in polymer-ion solutions. 1. Polymer concentration effects**; *Macromolecules* **1989***, 22*, 1169.
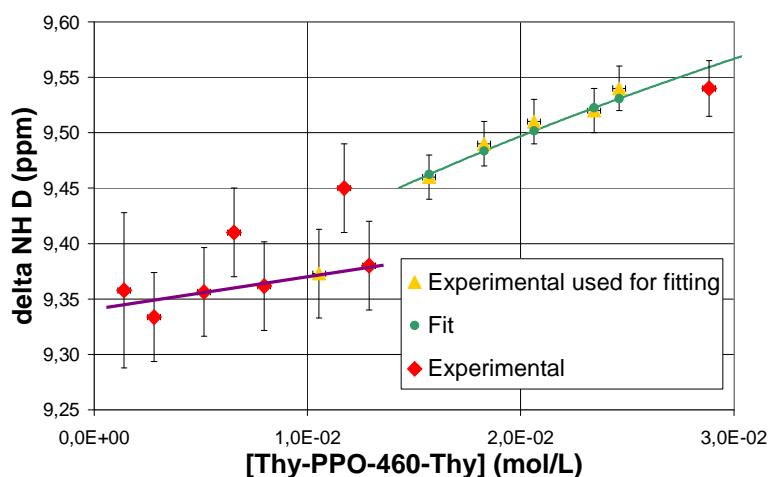
Figure III.26. NMR titration in CDCl$_3$ at 25°C of Thy-PPO-460-Thy **3b** (in green: fit for $K_{\text{Thy-Thy}}$ = 2.0 L/mol, δ_{freeThy} = 9.3 ppm, $\delta_{\text{dimerizedThy}}$ = 10.9 ppm; in purple: concentration independent chemical shift).

(iv) Viscosity for ring-chain equilibrium

Taking into account the presence of rings, the specific viscosity becomes a weighted average following equation (32).[50] The results of this second model, also mostly applying at low concentrations (below 0.06 g.cm^{-3}), are plotted in Figure III.27, assuming all rings are made of the two supramolecular units (by far the predominant form in 50/50-M-2200 **4a**, see Table III.4). Taking into account the presence of rings, the specific viscosity fit is still good for chloroform (Figure III.24a), especially at low concentrations (below 0.06 g.cm^{-3}) where the model applies. Indeed, in this case the ring correction has a limited impact on the specific viscosity. In contrast, in toluene, taking into account the presence of rings significantly lowers the specific viscosity, so the fit is better but not perfect especially at medium concentrations (around 0,05 g.cm^{-3}, Figure III.27b). Moreover, as we will see in the next part, NMR results suggest another interpretation for toluene.

$$\eta_{\text{sp}} = \rho_w \eta_{\text{sp}}^{\text{rings}} + (1 - \rho_w)\eta_{\text{sp}}^{\text{chains}} \qquad (32)$$

---

[50] Jacobson, H.; Beckmann, C. O.; Stockmayer, W. H.; **Intramolecular reaction in polycondensations. II. Ring-chain equilibrium in polydecamethylene adipate**; *J. Chem. Phys.* **1950**, *18*, 1607.
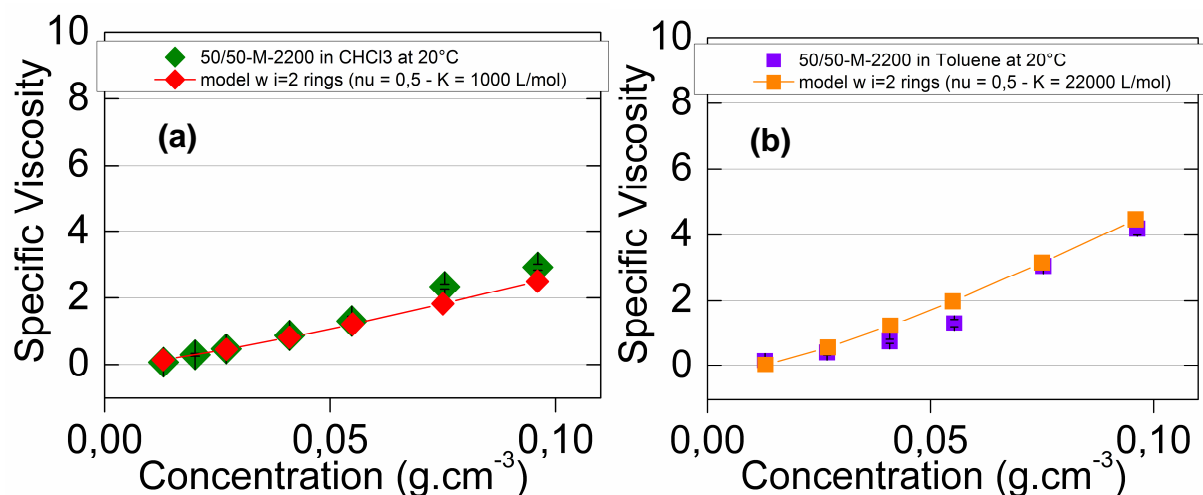
Figure III.27. Concentration-dependent specific viscosity of 50/50-M-2200 **4a** in (a) chloroform (◆) and (b) toluene (■) at 20°C. Viscosity model for a ring-chain equilibrium supramolecular polymerization with an association constant of (a) 1000 L/mol (◆) and (b) 22 000 L/mol (■).

C (g/cm3)	% of i = 2	% of i = 3	% of i = 4	% of i = 5
in chloroform				
0.013	**97.2**	2.5	0.8	0.3
0.027	**94.9**	3.0	1.1	0.5
0.041	**94.1**	3.3	1.3	0.6
0.055	**93.8**	3.5	1.4	0.7
0.075	**93.1**	3.7	1.5	0.7
0.096	**92.7**	3.8	1.6	0.8
In toluene				
0.013	**91.2**	4.2	1.9	1.0
0.027	**90.4**	4.4	2.0	1.1
0.041	**90.0**	4.5	2.1	1.1
0.055	**89.7**	4.5	2.1	1.2
0.075	**89.4**	4.6	2.1	1.2
0.096	**89.3**	4.6	2.2	1.2

Table III.4. Distribution of ring sizes. Percentages are defined as the number of rings made of i supramolecular units divided by the total number of rings.

e. Different aggregation mechanisms in toluene and chloroform ?

An explanation for the differences observed in chloroform and toluene, could be that, not only $K_{\text{Thy-DAT}}$ is higher in toluene than in chloroform, but there also are different aggregation mechanisms in toluene and in chloroform. More specifically, an isodesmic mechanism could take place in chloroform and a nucleation-elongation mechanism in toluene.

(i) Secondary interactions in toluene: π-stacking

A nucleation-elongation mechanism in toluene means that there are secondary interactions that take place in addition to hydrogen bonding. One possible interaction between the Thy and DAT stickers, besides hydrogen bonding, is aromatic stacking, commonly encountered for DNA bases and biological recognition.[51]
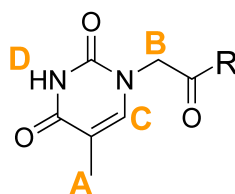

Chart III.2. Thy group.

In fact, Thy's π-stacking in toluene can be evidenced by comparing the ¹H NMR chemical shifts of Thy CH_3 (**A**) and CH protons (**C**) in different solvents (Chart III.2). Indeed, aromatic electrons circulation induces a local magnetic field that shields protons lying above aromatic rings.[52] Methyl (**A**) and CH (**C**) signals are shielded by around 0.4 ppm in toluene-d_8 compared to $CDCl_3$. This suggests that these protons lie above aromatic cycles in toluene, but not in chloroform. Thus, in toluene Thy is believed to π-stack with other aromatic rings (such as: toluene,[53] Thy,[20,54,55] and/or DAT[56]) in an off-centered parallel displaced manner.[57]

---

[51] Tewari, A. K.; Dubey, R.; **Emerging trends in molecular recognition: Utility of weak aromatic interactions**; *Bioorg. Med. Chem.* **2008**, *16*, 126.

[52] Gomes, J. A. N. F.; Mallion, R. B.; **Aromaticity and ring currents**; *Chem. Rev.* **2001**, *101*, 1349.

[53] Rahman, M. H.; Liao, S.-C.; Chen, H.-L.; Chen, J.-H.; Ivanov, V. A.; Chu, P. P. J.; Chen, S.-A.; **Aggregation of conjugated polymers in aromatic solvent**; *Langmuir* **2009**, *25*, 1667.

[54] Surin, M.; Janssen, P. G. A.; Lazzaroni, R.; Leclère, P.; Meijer, E. W.; Schenning, A. P. H. J.; **Supramolecular organization of ssDNA-templated π-conjugated oligomers via hydrogen bonding**; *Adv. Mater.* **2009**, *21*, 1126.

However, small Thy and DAT derivatives (such as thymine-1-acetic acid, thymine, 4,6-diamino-2-methyl-1,3,5-triazine [DAT-Me], 2-chloro-4,6-diamino-1,3,5-triazine [DAT-Cl], as well as 1:1 thymine and 4,6-diamino-2-methyl-1,3,5-triazine mixture) are quasi-insoluble in toluene. Thy-PPO-460-Thy **3b** and 50/50-M-460 **4b** are also quasi-insoluble in toluene (tested down to 0.002 mol/L), but slightly soluble in chloroform (soluble under 0.03 mol/L), although the PPO chain does not have more affinity with chloroform than with toluene (Hildebrand solubility parameters $\delta_{PPO} \cong 18$ (MPa)$^{1/2}$, $\delta_{CHCl3} = 18.9$ (MPa)$^{1/2}$ and $\delta_{toluene} = 18.2$ (MPa)$^{1/2}$).[58] This indicates that Thy and DAT groups have very little affinity with toluene, even when they are associated together via hydrogen bonds, despite the fact that Thy and DAT could *a priori* π-stack with toluene. Indeed, Thy and DAT are polar groups, while toluene is apolar. Therefore, it seems likely that, in toluene, Thy and DAT preferably π-stack with Thy or DAT, rather than toluene. As a result, objects consisting of a PPO shell and a Thy and DAT core, with hydrogen bonds and π-stacking interactions between Thy and DAT, should form in toluene (Figure III.28C). Such inversed micelles (flowers) can connect to each other,[59] especially at high concentration (C > C*), resulting in an increase of viscosity.

(ii) No secondary interactions in chloroform

In contrast, no or much less π-stacking of Thy and DAT seem to occur in chloroform. The reason could be that chloroform solvates better than toluene, not only the hydrogen bonds donors and acceptors as mentioned above, but also the Thy and DAT aromatic cycles, illustrating the connection between solvation and π-stacking. Therefore, the classical vision of linear supramolecular polymers in equilibrium with cycles seems to manifest in chloroform (Figure III.28B).
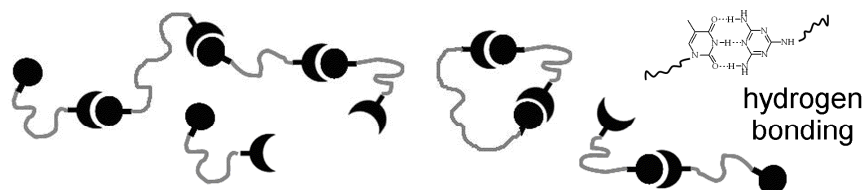
---

[55] Umezawa, Y.; Nishio, M.; **Thymine-methyl interaction implicated in the sequence-dependent deformability of DNA**; *Nucleic Acids Res.* **2002**, *30*, 2183.

[56] Mooibroek, T. J.; Gamez, P.; **The s-triazine ring, a remarkable unit to generate supramolecular interactions**; *Inorg. Chim. Acta* **2007**, *360*, 381.

[57] Meyer, E. A.; Castellano, R. K.; Diederich, F.; **Interactions with aromatic rings in chemical and biological recognition**; *Angew. Chem. Int. Ed.* **2003**, *42*, 1210.

[58] Barton, A. F. M.; ***Handbook of solubility parameters and other cohesion parameters***; CRC Press: Boca Raton, FL, **1991**.

[59] Semenov, A. N.; Joanny, J.-F.; Khokhlov, A. R.; **Associating polymers: equilibrium and linear viscoelasticity**; *Macromolecules* **1995**, *28*, 1066.

(A) In Chloroform: linear supramolecular polymers

hydrogen
bonding

**(B) In Toluene: columns
with a PPO shell and a Thy, DAT core**

hydrogen bonding
and π-stacking
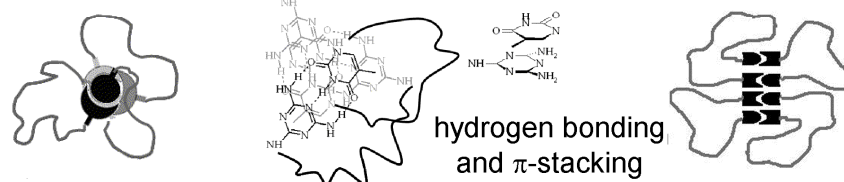
Figure III.28. Thy-PPO-2200-DAT **10a** solution structuration: (A) in chloroform and (B) in toluene.

(iii) Connection between solvation and π-stacking

The higher $K_{Thy-DAT}$ value in toluene, compared to chloroform, may be attributed to poor solvation of the hydrogen bonds donors and acceptors in toluene.[35] However, π-stacking may also be held responsible for the high $K_{Thy-DAT}$ in toluene. Indeed, hydrogen bonds involving its C=O groups cause an increase of thymine's aromatic character.[60] Reciprocally, when the thymine cycle interacts by π-stacking with an aromatic ring, the thymine cycle's aromaticity increases, resulting in more basic C=O, and a more acidic NH. Moreover, π-stacking may induce a parallel alignment of Thy and DAT, with an optimal NH_2 and C=O relative orientation.[31] Therefore, the supramolecular Thy-DAT hydrogen bonding association is reinforced when Thy and DAT interact by π-stacking with an aromatic cycle.

Furthermore, π-stacking and solvation are connected. π-stacking may occur between Thy and DAT in toluene and not in chloroform because chloroform better solvates Thy and DAT rings.

---

[60] Cyranski, M. K.; Gilski, M.; Jaskolski, M.; Krygowski, T. M.; **On the aromatic character of the heterocyclic bases of DNA and RNA**; *J. Org. Chem.* **2003**, *68*, 8607.

f. Viscosity model for colloidal supramolecular polymers

If our supramolecular polymers do form colloidal objects in toluene as suggested by NMR and described above, then we should be able to fit their viscosity with a model for colloids. Equation (33) is a commonly used semi-empirical relation for colloidal suspensions,[61] with Φ the particle volume fraction and Φ_{max} the maximum value of the particle volume fraction.

$$\eta_{sp} = -1 + (1 - \frac{\Phi}{\Phi_{max}})^{-2} \qquad (33)$$

$$\text{with} \quad \Phi = \frac{CN_a V}{Mp} \qquad (34)$$

$$\text{then} \quad \eta_{sp} = -1 + (1 - \frac{CN_a}{M} \frac{V}{p\Phi_{max}})^{-2} \qquad (35)$$

Φ can be expressed by equation (34) with C the supramolecular polymers concentration in g.cm^{-3}, N_a the Avogadro number, V the volume of one colloidal object, M the molecular weight of one unit (here, $M = 2500$ g.mol^{-1}), and p the number of units in one colloidal object.

The specific viscosity of 50/50-M-2200 **4a** can thus be expressed as a function of the concentration C through equation (35) which comprise only one fitting parameter: $\frac{V}{p\Phi_{max}}$.

The best fit is plotted in Figure III.29 and is obtained for $\frac{V}{p\Phi_{max}} = 2.5 * 10^{-20}$ cm^3, which corresponds for instance to the very reasonable parameters $\Phi_{max} = 0.68$, $p = 6$, and $V = 1.02 * 10^{-19}$ cm^3, the volume of a sphere of radius 2.9 nm. Indeed, according to the slope value of the η_{sp} *vs* C_g linear curve of NH$_2$-PPO-2200-NH$_2$ **1a** (Figure III.23) and to equation (18), the radius of gyration of NH$_2$-PPO-2200-NH$_2$ **1a** is 16 Å and its end-to-end radius is 39 Å. Therefore, the radius of the inversed micelles with the Thy, DAT core and PPO shell is expected to be around 39 Å divided by √2, that is to say around 2.8 nm.

---

[61] Mewis, J.; Wagner, N. J.; *Colloidal suspension rheology*; Cambrigde University Press: Cambridge, **2012**.

Finally, the colloid model with these reasonnable parameters fits relatively well the specific viscosity of 50/50-M-2200 **4a** from 0 to 0.1 g.cm^{-3} in toluene (Figure III.29b) but not in chloroform (Figure III.29a). Therefore, the model of colloidal inversed micelles in toluene is consistent with the viscosity results as well as the NMR results, unlike the ring-chain equilibrium model in toluene (Figure III.27b). Still, the ring-chain equilibrium specific viscosity model in toluene is relatively good because rings have a size comparable to the colloidal inversed micelles. In fact, the specific viscosity models by themselves cannot distinguish between the two interpretations, but the NMR and viscosity results together point toward the colloidal model in toluene and ring-chain equilibrium model in chloroform.
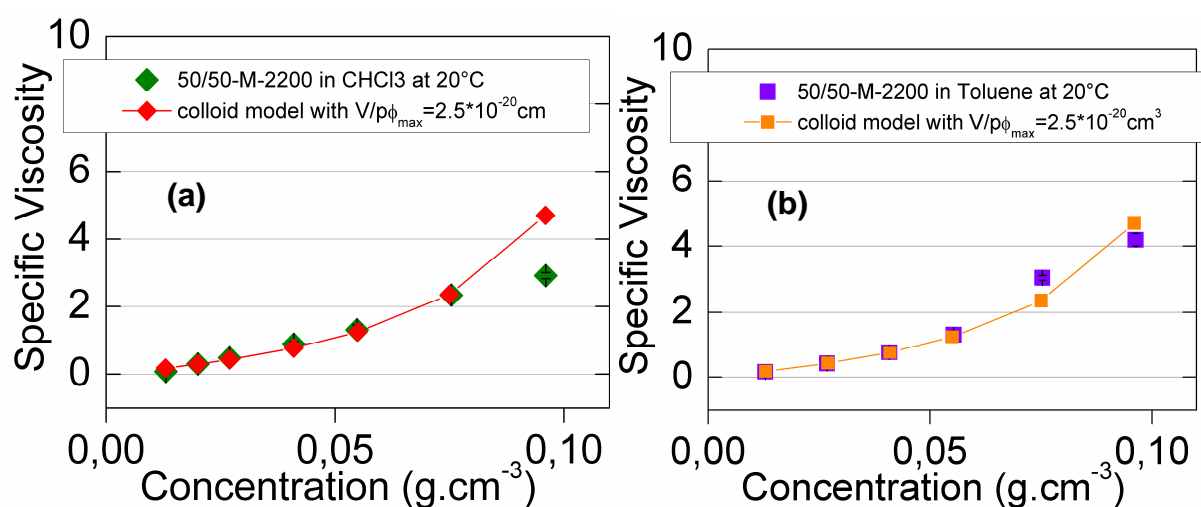

Figure III.29. Concentration-dependent specific viscosity of 50/50-M-2200 **4a** in (a) chloroform (◆) and (b) toluene (■) at 20°C. Viscosity model for colloidal supramolecular polymers (◆) (■).

4. Conclusions and perspectives

(i) Conclusion: importance of solvation

In this chapter, we have studied supramolecular polymers in solution using viscosity (some results are highlighted in Figure III.30) and NMR measurements (association constants results are gathered in Table III.3).
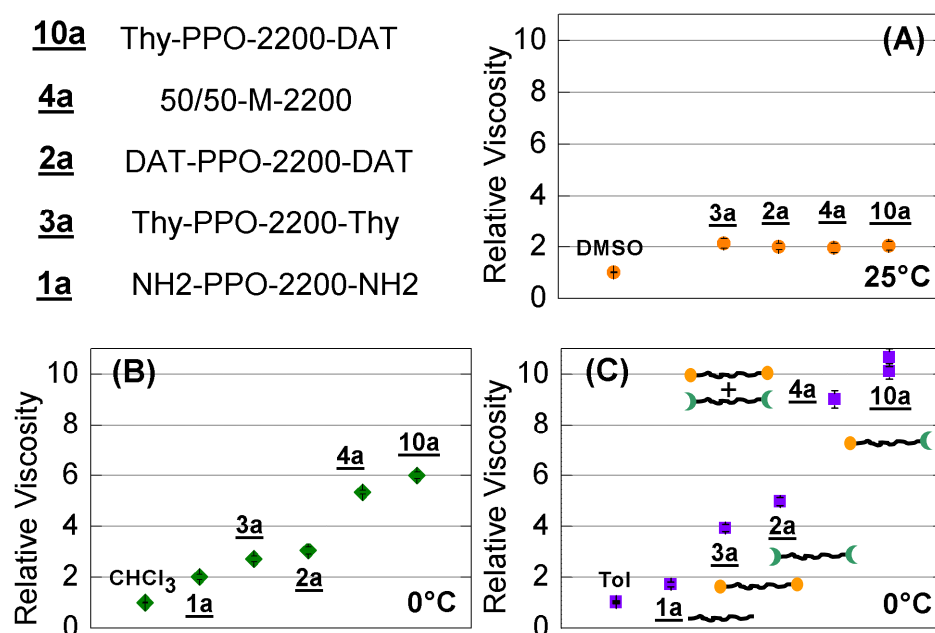
Figure III.30. Relative viscosity of heterotelechelic unit Thy-PPO-2200-DAT **10a**, homotelechelic units Thy-PPO-2200-Thy **3a** and DAT-PPO-2200-DAT **2a**, 50/50-M-2200 **4a** and precursor NH_2-PPO-2200-NH_2 **1a** solutions in: (A) DMSO at $12.2*10^{-2}$ g/mL and 25°C, (B) chloroform at $9.6*10^{-2}$ g/mL and 0°C, and (C) toluene at $9.6*10^{-2}$ g/mL and 0°C.

We conclude that the solvent has a tremendous impact on the supramolecular polymers sizes and structures (Figure III.31). In the polar dissociating DMSO, micelles with a PPO core and a Thy, DAT shell seem to form. In the less-polar non-dissociating chloroform, linear supramolecular polymers form through hydrogen bonding between Thy and DAT, in equilibrium with ring supramolecular polymers. In the apolar non-dissociating toluene, inversed micelles with a PPO shell and a Thy, DAT core seem to form, also with hydrogen bonds between Thy and DAT, as well as aromatic interactions.

(A) In DMSO: micelles
with a PPO core and a Thy, DAT shell

(B) In Chloroform: linear supramolecular polymers

hydrogen
bonding

(C) In Toluene: columns
with a PPO shell and a Thy, DAT core

hydrogen bonding
and π-stacking
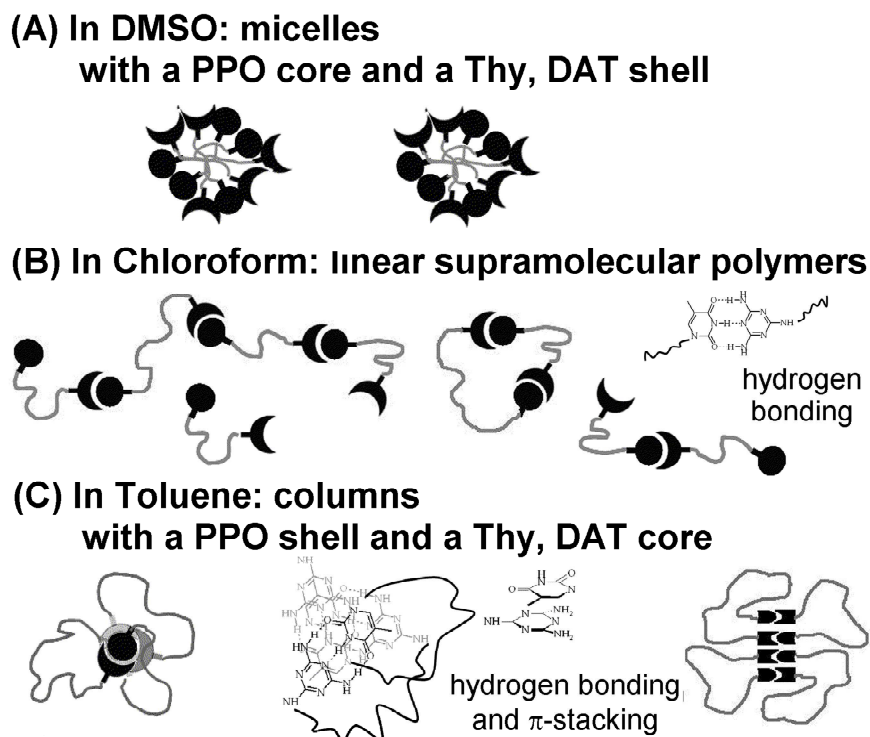
Figure III.31. Thy-PPO-2200-DAT **10a** solution structuration: (A) in DMSO, (B) in chloroform, (C) in toluene.

Such solvent-dependant organization and driving force of the assembly had already been observed, notably by Bouteiller and his coworkers,[62] as well as Meijer and his coworkers on a self-associative homotelechelic system.[26] It is interesting to find the same solvent effect for a complementary heterotelechelic system, Thy-PPO-2200-DAT **10a**.

(ii) Confirmation of structure

Confirmation of the micellar structures in DMSO and toluene and linear structure in chloroform could theoretically be obtained by neutron scattering, circular dichroism,[26] or dynamic light scattering measurements (DLS). However, toluene is not a suitable solvent for circular dichroism measurements of our compounds and our compounds are insoluble in dodecane. Furthermore, the contrast between the PPO chains (refractive index n_D(PPO) = 1.45) and DMSO (n_D(DMSO) = 1.48) or chloroform (n_D(chloroform) = 1.44) are not high enough, so DLS measurements in DMSO and chloroform yielded no result.

---

[62] Obert, E.; Bellot, M.; Bouteiller, L.; Andrioletti, F.; Lehen-Ferrenbach, C.; Boué, F.; **Both water- and organo-soluble supramolecular polymer stabilized by hydrogen-bonding and hydrophobic interactions**; *J. Am. Chem. Soc.* **2007**, *129*, 15601.

Preliminary results of DLS of $9.6*10^{-2}$ g/mL 50/50-M-2200 **4a** in toluene seem rich. The contrast between the PPO chains and toluene (n_D(toluene) = 1.49) is not very high, but sufficient for the measurements of concentrated solutions. The correlation functions can be fitted by the sum of three exponentials, each corresponding to a relaxation time (τ_1, τ_2, τ_3). The two highest relaxation times (the slow mode τ_1 and the the fast mode τ_2) correspond to diffusive modes. Indeed, diffusive modes obey equation (36), with D the diffusion coefficient and q the wave vector defined by equation (37) (with n the refractive index of the solvent, λ the laser wavelength, and θ the scattering angle). The diffusion coefficient of the slow mode τ_1 is $D_{\text{slow}} = 9,5.10^{-9}$ cm^2.s^{-1} and that of the fast mode τ_2 is $D_{\text{fast}} = 1,1.10^{-6}$ cm^2.s^{-1}. In contrast, the lowest relaxation mode τ_3 is a non-diffusive mode and is only measured for low scattering angles (below 90°).

$$\frac{1}{\tau} = Dq^2 \qquad (36)$$

$$q = \frac{4\pi n}{\lambda} \sin(\frac{\theta}{2}) \qquad (37)$$

(iii) Perspective: trifunctional supramolecular polymers yield higher viscosity

Solutions of trifunctional Thy$_3$-PPO-3000 **13a** and DAT$_3$-PPO-3000 **12a** in toluene have higher viscosities than solutions of difunctional Thy-PPO-2200-Thy **3a** and DAT-PPO-2200-DAT **2a** in toluene. However, what is much more striking is the very high viscosity of the 50/50 mixture of Thy$_3$-PPO-3000 and DAT$_3$-PPO-3000 in toluene (Figure III.32), for instance, at 0°C, 60 *vs* 9 for the 50/50 mixture of Thy-PPO-2200-Thy and DAT-PPO-2200-DAT in toluene. This effect remains to be investigated, but one may hypothesize that such a high viscosity is due to an increase in bridging with trifunctional supramolecular polymers.[63] However, a gel does not form probably because the lifetime of the association is too short.

---

[63] Versteegen, R. M.; van Beek, D. J. M.; Sijbesma, R. P.; Vlassopoulos, D.; Fytas, G.; Meijer, E. W.; **Dendrimer-based transient supramolecular networks**; *J. Am. Chem. Soc.,* **2005***, 127*, 13862.
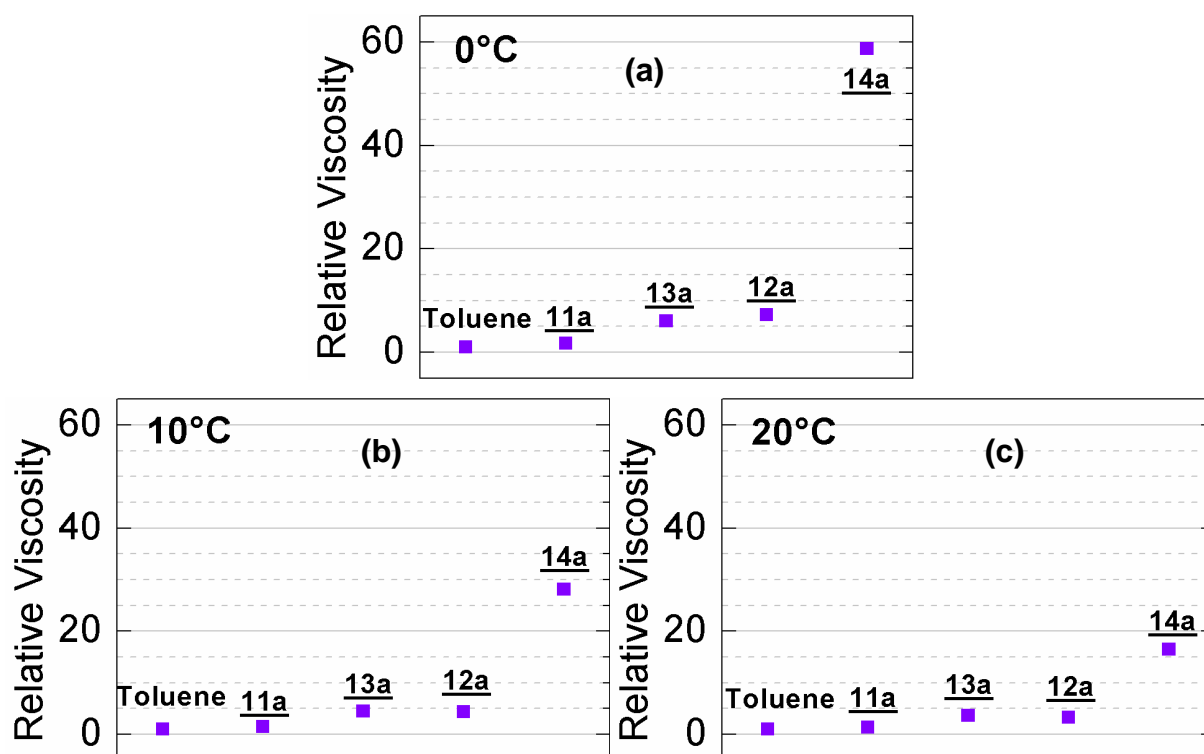
Figure III.32. Relative viscosity of $9.6*10^{-2}$ g/mL solutions of Jeffamine T-3000 **11a**, Thy$_3$-PPO-3000 **13a**, DAT$_3$-PPO-3000 **12a**, 50/50-MT-3000 **14a** (50/50 mixture of Thy$_3$-PPO-3000 **13a** and DAT$_3$-PPO-3000 **12a**) in toluene at: (a) 0°C, (b) 10°C, and (c) 20°C.

(iv) Perspectives: studies in solution to better understand the melt state

Often, studies of supramolecular polymers in solution, particularly association constants measurements, are used to better understand the melt state.[34] Indeed, measuring association constants in solution, by NMR or UV for instance, is a convenient method. However, behavior in the melt state can be quite different than in solution, in the same way that a supramolecular polymer can behave very differently in two different solvents.

As we will see in Chapter IV and V, in the melt state, phase separation also needs to be taken into account in addition to the directional interactions, as well as an additional effect in the bulk: crystallization.

142

.

<u>Chapter IV</u>

Order and disorder in bulk supramolecular polymers
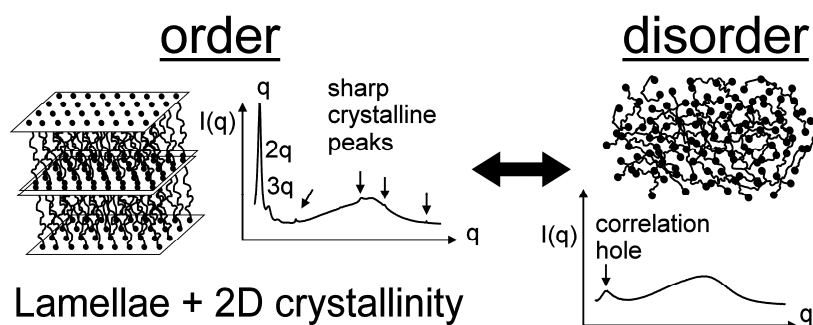
In supramolecular polymers, directional interactions control the constituting units connectivity, but dispersion forces may conspire to make complex organizations. We report here on the long-range order and order-disorder transition (ODT) of main-chain supramolecular polymers based on poly(propylene oxide) (PPO) spacers functionalized on both ends with a thymine derivative (Thy). Below the ODT temperature (T_{ODT}), these compounds are semicrystalline with a lamellar structure, showing nanophase separation between crystallized Thy planes and amorphous PPO layers. Above T_{ODT}, they are amorphous and homogeneous even though their X-ray scattering spectrum reveals a peak. This peak is due to correlation hole effect resulting from contrast between end-functional groups and spacer. Macroscopically, the transition is accompanied by dramatic flow and mechanical properties changes. In contrast, main-chain supramolecular polymers based on PPO spacers functionalized on both ends with diaminotrizaine (DAT) are disordered at all temperatures.
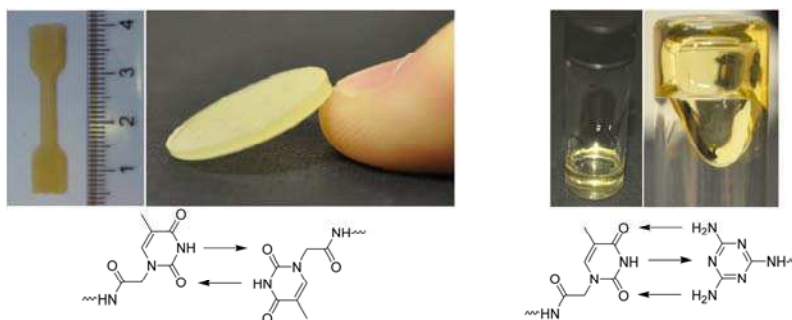
Moreover, we show here that optimization of the directional interactions in these systems by strong complementary associations suppress the mesoscopic order and thus lead to a counterintuitive change in material properties. Indeed, the microphase segregation observed for the self-complementary systems based on Thy is inhibited by addition of DAT: the strong complementary Thy-DAT interaction inhibits crystallization of thymine in microdomains and lamellar structuration. As a result, the supramolecular polymer with only weakly self-complementary stickers is a solid, whereas the supramolecular polymer with strongly complementary stickers is a liquid.

Chapter IV. Order and disorder in supramolecular polymers

1. Order-disorder transition (ODT) in supramolecular polymers

This part was partially published in reference 1.[1]

a. ODT and supramolecular polymers□organization in the bulk

(i) Can supramolecular polymers display an ODT like block copolymers ?

Block copolymers have attracted a great deal of interest in part because long-range ordered mesophases (such as lamellar, cylindrical, cubic or gyroid morphology) and order-disorder transition (ODT) can be achieved by simple control of the molecular parameters (degree of polymerization N and interaction parameter χ).[2] These two features are of great importance in technological applications ranging from cutting-edge electronic to bitumen additives.[3] The ability of a block copolymer to go from elastomeric-like (in its ordered state) to liquid-like (in its disordered state) properties by varying the temperature is particularly interesting.[4]

Since long-range ordered mesophases and ODT are also observed for liquid crystals[5] and supramolecular liquid crystals,[6] the question of the existence and of the manifestations of long-range order and ODT in supramolecular polymers arises.

[1] Cortese, J.; Soulié-Ziakovic, C; Cloitre, M.; Tencé-Girault, S.; Leibler, L.; **Order-Disorder Transition in Supramolecular Polymers**; *J. Am. Chem. Soc.* **2011**, 133, 19672.

[2] (a) Leibler, L.; **Theory of Microphase Separation in Block Copolymers**; *Macromolecules* **1980**, *13*, 1602. (b) Fredrickson, G. H.; Helfand, E.; **Fluctuation effects in the theory of microphase separation in block copolymers**; *J. Chem. Phys.* **1987**, *87*, 697. (c) Bates, F. S.; Rosedale, J. H.; Fredrickson, G. H.; **Fluctuation effects in a symmetric diblock copolymer near the order-disorder transition**; *J. Chem. Phys.* **1990**, *92*, 6255.

[3] (a) Lodge, T. P.; **Block Copolymers: Past Successes and Future Challenges**; *Macromol. Chem. Phys.* **2003**, *204*, 265. (b) Park, C.; Yoon, J.; Thomas, E. L.; **Enabling nanotechnology with self assembled block copolymer patterns**; *Polymer* **2003**, *44*, 6725.

[4] Bates, F. S.; Fredrickson, G. H.; **Block Copolymer Thermodynamics: Theory and Experiment**; *Annu. Rev. Phys. Chem.* **1990**, *41*, 525.

[5] De Gennes, P. ; Prost, J.; *The Physics of Liquids Crystals*; Oxford University Press: Oxford, **1993**.

In this part, we report on the long-range order lamellar structure and ODT of a main-chain supramolecular polymer.

(ii) Clusterization in supramolecular polymers

Main-chain supramolecular polymers are typically made of telechelic molecules (A-spacer-A) linked together through noncovalent bonds to form a polymer-like assembly (A-spacer-A)$_n$.[7] The self-complementary binding stickers (A) are often hydrogen bonding motifs such as nucleobases[8] or ureidopyrimidinone,[9] while the spacer is generally an oligomer.[10]

In these systems, microphase segregation between the spacer and the stickers,[11,12,13] as well as crystallization of the stickers into microdomains[14,15] can occur (Figure IV.1, Figure IV.2, Figure IV.3).

[6] (a) Kato, T.; Frechet, J. M. J.; **A new approach to mesophase stabilization through hydrogen bonding molecular interactions in binary mixtures**; *J. Am. Chem. Soc.* **1989**, *111*, 8533. (b) Kato, T.; Frechet, J. M. J.; **Hydrogen bonded liquid crystals built from hydrogen bonding donors and acceptors Infrared study on the stability of the hydrogen bond between carboxylic acid and pyridyl moieties**; *Liq. Cryst.* **2006**, *33*, 1429.

[7] (a) Lehn, J.-M.; **Dynamers: dynamic molecular and supramolecular polymers**; *Prog. Polym. Sci.* **2005**, *30*, 814. (b) Fox, J. D.; Rowan, S. J.; **Supramolecular Polymerizations and Main-Chain Supramolecular Polymers**; *Macromolecules* **2009**, *42*, 6823. (c) de Greef, T. F. A.; Smulders, M. M. J.; Wolffs, M.; Schenning, A. P. H. J.; Sijbesma, R. P.; Meijer, E. W.; **Supramolecular Polymerization**; *Chem. Rev.* **2009**, *109*, 5687. (d) Serpe, M. J.; Craig, S. L.; **Physical Organic Chemistry of Supramolecular Polymers**; *Langmuir,* **2007**, *23*, 1626.

[8] Sivakova, S.; Rowan, S. J.; **Nucleobases as supramolecular motifs**; *Chem. Soc. Rev.* **2005**, *34*, 9.

[9] Sijbesma, R. P.; Beijer, F. H.; Brunsveld, L.; Folmer, B. J. B.; Hirschberg, J. H. K. K.; Lange, R. F. M.; Lowe, J. K. L.; Meijer, E. W.; **Reversible Polymers Formed from Self-Complementary Monomers Using Quadruple Hydrogen Bonding**; *Science* **1997**, *278*, 1601.

[10] (a) Binder, W. H.; Zirbs, R.; **Supramolecular Polymers and Networks with Hydrogen Bonds in the Main- and Side-chain**; *Adv. Polym. Sci.* **2007**, *207*, 1. (b) Bouteiller, L. ; **Assembly via Hydrogen Bonds of Low MolarMass Compounds into Supramolecular Polymers**; *Adv Polym Sci.* **2007**, *207*, 79.

[11] Herbst, F.; Schröter, K.; Gunkel, I.; Gröger, S.; Thurn-Albrecht, T.; Balbach, J., Binder, W. H.; **Aggregation and Chain Dynamics in Supramolecular Polymers by Dynamic Rheology: Cluster Formation and Self-Aggregation**; *Macromolecules* **2010**, *43*, 10006.

[12] (a) de Lucca Freltas, L.; Burgert, J.; Stadler, R.; **Thermoplastic elastomers by hydrogen bonding**; *Polym. Bull.* **1987**, *17*, 431. (b) Folmer, B. J. B.; Sijbesma, R. P.; Versteegen, R. M.; van der Rijt, J. A. J.; Meijer, E. W.; **Supramolecular Polymer Materials: Chain Extension of Telechelic Polymers Using a Reactive Hydrogen-Bonding Synthon**; *Adv. Mater.* **2000**, *12*, 874. (c) Yamauchi, K.; Lizotte, J. R.; Hercules, D. M.; Vergne, M. J.; Long, T. E.; **Combinations of Microphase Separation and Terminal Multiple Hydrogen Bonding in Novel Macromolecules**; *J. Am. Chem. Soc.* **2002**, *124*, 8599. (d) Öjelund, K.; Loontjens, T.; Steeman, P.; Palmans, A.; Maurer, F.; **Synthesis, Structure and Properties of Melamine-Based pTHF-Urethane Supramolecular Compounds**; *Macromol. Chem. Phys.* **2003**, *204*, 52. (e) Mather, B. D.; Elkins, C. L.; Beyer, F. L.; Long, T. E.; **Morphological Analysis of Telechelic Ureidopyrimidone Functional Hydrogen Bonding Linear and Star-Shaped Poly(ethylene-co-propylene)s**; *Macromol. Rapid Commun.* **2007**, *28*, 1601. (f) Botterhuis, N. E.; van
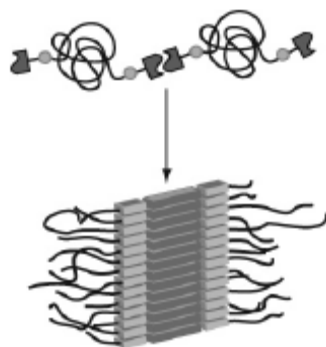
Figure IV.1. Schematic representation of the lateral UPy-UPy dimer stacks due to additional hydrogen bonding between the urethane groups, from reference 15d.

Indeed, hydrogen-bonding motifs are usually more polar than the spacer and are prone to crystallization. These two phenomena strongly impact the mechanical properties of the material: crystalline domains of stickers function as physical cross-links and induce elasticity-dominated rheological behavior;[15] clusters of stickers can also result in a network that allows the formation of mechanically stable films.[13]

Beek, D. J. M.; van Gemert, G. M. L.; Bosman, A. W.; Sijbesma, R. P.; **Self-assembly and morphology of polydimethylsiloxane supramolecular thermoplastic elastomers**; *J. Polym. Sci., Part A: Polym. Chem.,* **2008**, *46*, 3877. (g) Merino, D. H.; Slark, A. T.; Colquhoun, H. M.; Hayes, W.; Hamley, I. W.; **Thermo-responsive microphase separated supramolecular polyurethanes**; *Polym. Chem.* **2010**, *1*, 1263. (h) Woodward, P. J.; Hermida Merino, D.; Greenland, B. W.; Hamley, I. W.; Light, Z.; Slark, A. T.; Hayes, W.; **Hydrogen Bonded Supramolecular Elastomers: Correlating Hydrogen Bonding Strength with Morphology and Rheology**; *Macromolecules* **2010**, *43*, 2512. (i) Manassero, C.; Raos, G.; Allegra, G.; **Structure of Model Telechelic Polymer Melts by Computer Simulation**; *J. Macromol. Sci. B* **2005**, *44*, 855. (j) Podesva, J.; Dybal, J., Spevacek, J.; Stepanek, P.; Cernoch, P.; **Supramolecular Structures of Low-Molecular-Weight Polybutadienes, as Studied by Dynamic Light Scattering, NMR and Infrared Spectroscopy**; *Macromolecules* **2001**, *34*, 9023.

[13] (a) Sivakova, S.; Bohnsack, D. A.; Mackay, M. E.; Suwanmala, P.; Rowan, S. J.; **Utilization of a Combination of Weak Hydrogen-Bonding Interactions and Phase Segregation to Yield Highly Thermosensitive Supramolecular Polymers**; *J. Am. Chem. Soc.* **2005**, *127*, 18202. (b) Beck, J. B.; Ineman, J. M.; Rowan, S. J.; **Metal/Ligand-Induced Formation of Metallo-Supramolecular Polymers**; *Macromolecules* **2005**, *38*, 5060.

[14] (a) Hilger, C.; Stadler, R.; **Cooperative structure formation by directed noncovalent interactions in an unpolar polymer matrix. 7. Differential scanning calorimetry and small-angle x-ray scattering**; *Macromolecules* **1992**, *25*, 6670. (b) Hirschberg, J. H. K. K.; Beijer, F. H.; van Aert, H. A.; Magusin, P. C. M. M.; Sijbesma, R. P.; Meijer, E. W.; **Supramolecular Polymers from Linear Telechelic Siloxanes with Quadruple-Hydrogen-Bonded Units**; *Macromolecules* **1999**, *32*, 2696. (c) van Beek, D. J. M.; Spiering, A. J. H.; Peters, G. W. M.; te Nijenhuis, K.; Sijbesma, R. P.; **Unidirectional Dimerization and Stacking of Ureidopyrimidinone End Groups in Polycaprolactone Supramolecular Polymers**; *Macromolecules* **2007**, *40*, 8464.

[15] (a) Lillya, C. P.; Baker, R. J.; Hutte, S.; Winter, H. H.; Lin, Y. G.; Shi, J.; Dickinson, L. C.; Chien, J. C. W.; **Linear chain extension through associative termini**; *Macromolecules* **1992**, *25*, 2076. (b) Muller, M.; Dardin, A.; Seidel, U.; Balsamo, V.; Ivan, B.; Spiess, H. W.; Stadler, R.; **Junction Dynamics in Telechelic Hydrogen Bonded Polyisobutylene Networks**; *Macromolecules* **1996**, *29*, 2577. (c) Colombani, O.; Barioz, C.; Bouteiller, L.; Chanéac, C.; Fompérie, L.; Lortie, F.; Montès, H.; **Attempt toward 1D Cross-Linked Thermoplastic Elastomers: Structure and Mechanical Properties of a New System**; *Macromolecules* **2005**, *38*, 1752. (d)
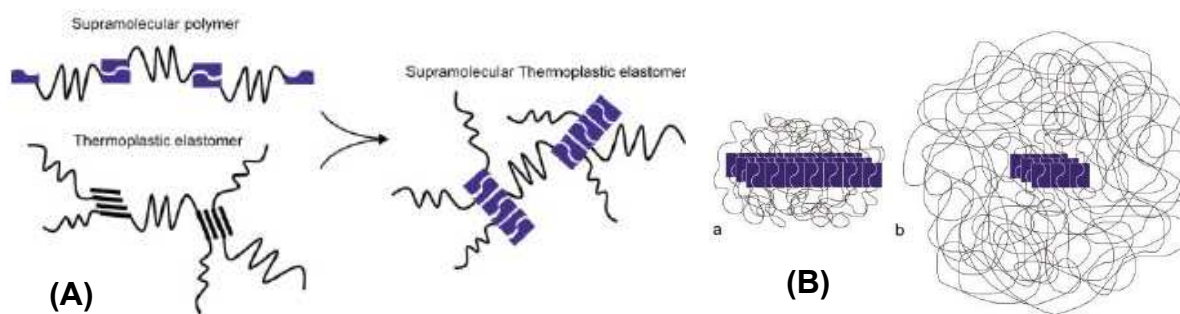
Figure IV.2. From reference 12f: (A) schematic overview of the relation between supramolecular polymers, thermoplastic elastomer (TPE), and supramolecular TPEs; (B) cartoon of UPy aggregation in UPy-functionalized siloxane materials: (a) rod-like or (b) spherical.
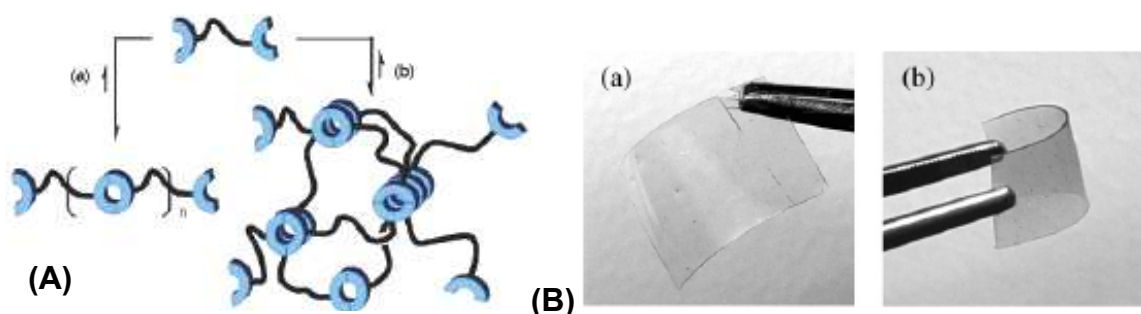
Figure IV.3. From ref. 13a: (A) schematic representation of (a) a linear supramolecular polymer and (b) the use of phase segregation to construct a supramolecular network in the solid state; (B) pictures of the films formed.

Cluster of stickers have sometimes been evidenced in the literature by a broad peak in the small angle X-ray scattering (SAXS) pattern, attributed to the microphase separation between the stickers and the spacers (Figure IV.4).
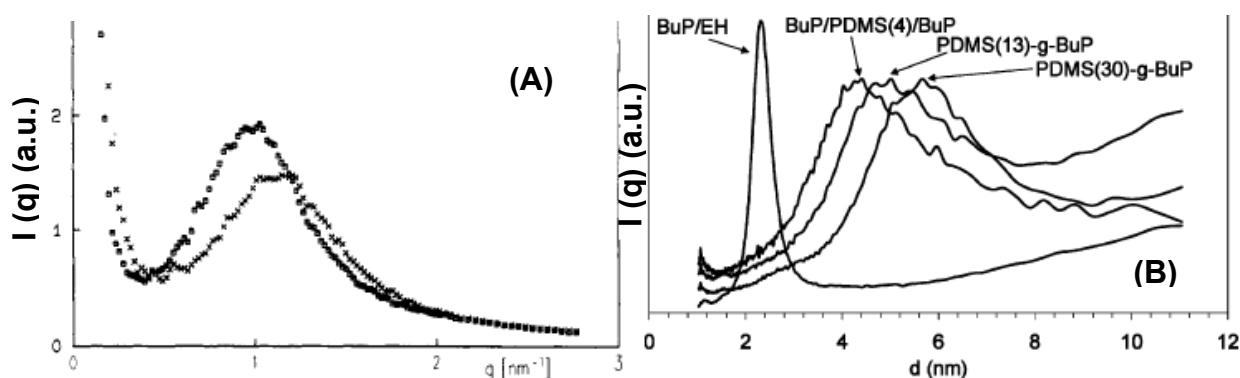
Figure IV.4. Supramolecular polymers' SAXS patterns of (A) polybutadienes bearing urazoylbenzoic acid groups from reference 14a; (B) bis-urea functional PDMS and model bis-urea from reference 15c.

Dankers, P. Y. W.; Zhang, Z.; Wisse, E.; Grijpma, D. W.; Sijbesma, R. P.; Feijen, J.; Meijer, E. W.; **Oligo(trimethylene carbonate)-Based Supramolecular Biomaterials**; *Macromolecules* **2006***, 39*, 8763. (e) van Beek, D. J. M.; Gillissen, M. A. J.; van As, B. A. C.; Palmans, A. R. A.; Sijbesma, R. P., **Supramolecular Copolyesters with Tunable Properties**; *Macromolecules* **2007***, 40*, 6340. (f) Wietor, J.-L.; van Beek, D. J. M.; Peters, G. W.; Mendes, E.; Sijbesma, R. P., **Effects of Branching and Crystallization on Rheology of Polycaprolactone Supramolecular Polymers with Ureidopyrimidinone End Groups**; *Macromolecules* **2011***, 44*, 1211.

(iii) Nonordered vs ordered microphase separation

The microphase segregation phenomenon can manifest either as a clustering of the stickers[12] or as an ordered microphase separation as observed for block copolymers.[2]

In fact, the telechelic molecule A-spacer-A can be seen as a triblock copolymer with the two outer blocks containing only one monomer. Cylindrical morphology has been reported for triblock copolymers with outer blocks containing nucleobase functionalities by Long[16] or oligonucleotides by Matsushita.[17] We anticipate that if incompatibility between the spacer and the sticker is strong, ordered mesophases should occur even for a single hydrogen-bonding group at both chain ends. Binder and his co-workers[11] described the body-centered cubic (BCC) morphology of polyisobutylene monofunctionalized with diaminotriazine. The BCC structure was evidenced by regular peaks in the small-angle X-ray scattering pattern that disappeared above 90°C. However, mesophases were not observed for the main-chain supramolecular polymer, polyisobutylene difunctionalized with diaminotriazine.[11]

Different scenarios of disorder-order transition (DOT) from a homogeneous melt to an organized mesophase can be envisaged for main-chain supramolecular polymers (Figure IV.5). In the ordered state, various mesophases with segregated end-functional groups can be obtained. Depending on the system, the stickers atoms can present liquid-like correlations (Figure IV.5A and B) or long-range order, *i.e.* crystallization (Figure IV.5C). When the DOT is driven by the tendency of end-groups to crystallize, lamellar structure should be favored. In the disordered state, the scattering pattern is expected to display a low intensity peak (Figure IV.5D). The existence of such a peak does not imply local phase separation or clustering, but results from correlation hole effect (see part e).

---

[16] Mather, B. D.; Baker, M. B.; Beyer, F. L.; Berg, M. A. G.; Green, M. D.; Long, T. E.; **Supramolecular Triblock Copolymers Containing Complementary Nucleobase Molecular Recognition**; *Macromolecules* **2007**, *40*, 6834.

[17] Noro, A.; Nagata, Y.; Tsukamoto, M.; Hayakawa, Y.; Takano, A.; Matsushita, Y.; **Novel Synthesis and Characterization of Bioconjugate Block Copolymers Having Oligonucleotides**; *Biomacromolecules* **2005**, *6*, 2328.
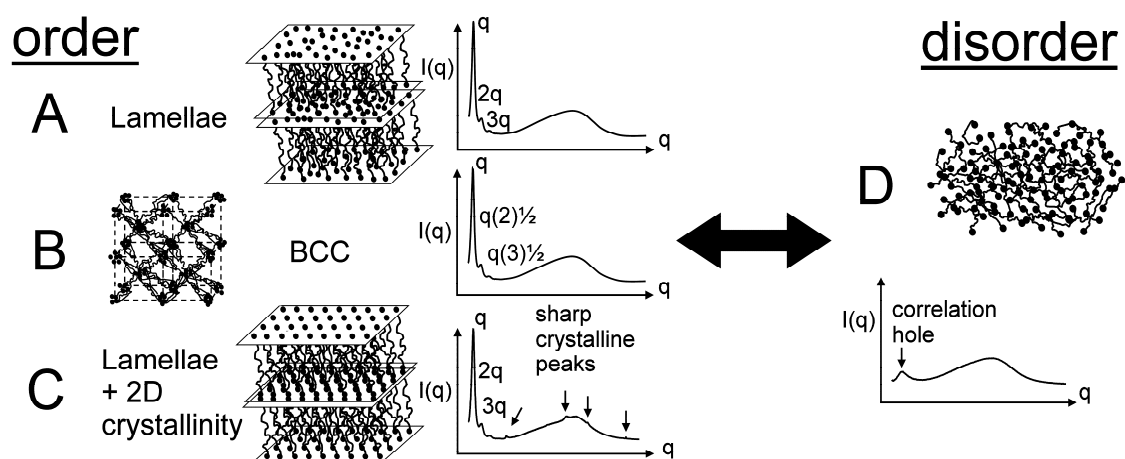
Figure IV.5. Possible scenarios for ODT in main-chain telechelic self-complementary supramolecular polymers and associated X-ray spectra. Ordered mesophase in a lamellar (A) or BCC (B) morphology with liquid-like correlations of the stickers atoms inside the structure. Ordered mesophase in a lamellar morphology with crystallinity of the stickers atoms inside the lamellar planes (C). Disordered state (D).

b. Supramolecular polymers used in this study: Thy-PPO-X-Thy **3a-b**, *Thy₃-PPO-X* **13a-b**, *and Thy-PPO/PEO-X* **17a-b**

The supramolecular polymers used in this study consist of low glass transition temperature (T_g), low-molecular-weight (between 400 and 3000 g.mol^{-1}) and noncrystalline poly(propylene oxide) (PPO) oligomers functionalized on each end with thymine groups. They are denoted as Thy-PPO-X-Thy **3a-b** (**a**: X = 2200, **b**: X = 460) for the linear difunctional (Chart IV.1a) and Thy₃-PPO-X **13a** (**a**: X = 3000) for the 3-armed branched trifunctionalized (Chart IV.1b), where X is the molecular weight (in g/mol) of the PPO spacer. The monofunctional Thy-PPO/PEO-X **17a-b** (**a**: X = 2000, **b**: X = 600) is also studied (Chart IV.1c). They were synthesized via amidation of monoamine, diamine or triamine telechelic PPO with thymine-1-acetic acid (see Chapter II).

Thymine stickers can associate with one another through two hydrogen bonds (Chart IV.1d). Thymine dimerization is quite weak, as evidenced by its low thermodynamic association constant ($K_{Thy-Thy}$ = 4.3 M^{-1}, as determined by ^{1}H NMR in CDCl₃).[49] Another weak hydrogen bonding association can occur between two amide groups linking the thymine stickers to the PPO spacers, or between one amide group and one thymine motif. While the PPO chain is hydrophobic, thymine is polar. Besides, thymine derivatives readily crystallize.[18]

---

[18] Borowiak, T.; Dutkiewicz, G.; Spychaia, J.; **Supramolecular motifs in 1-(2-cyanoethyl)thymine and 1-(3-cyanopropyl)thymine**; *Acta Crystallo. C* **2007**, *63*, 201.
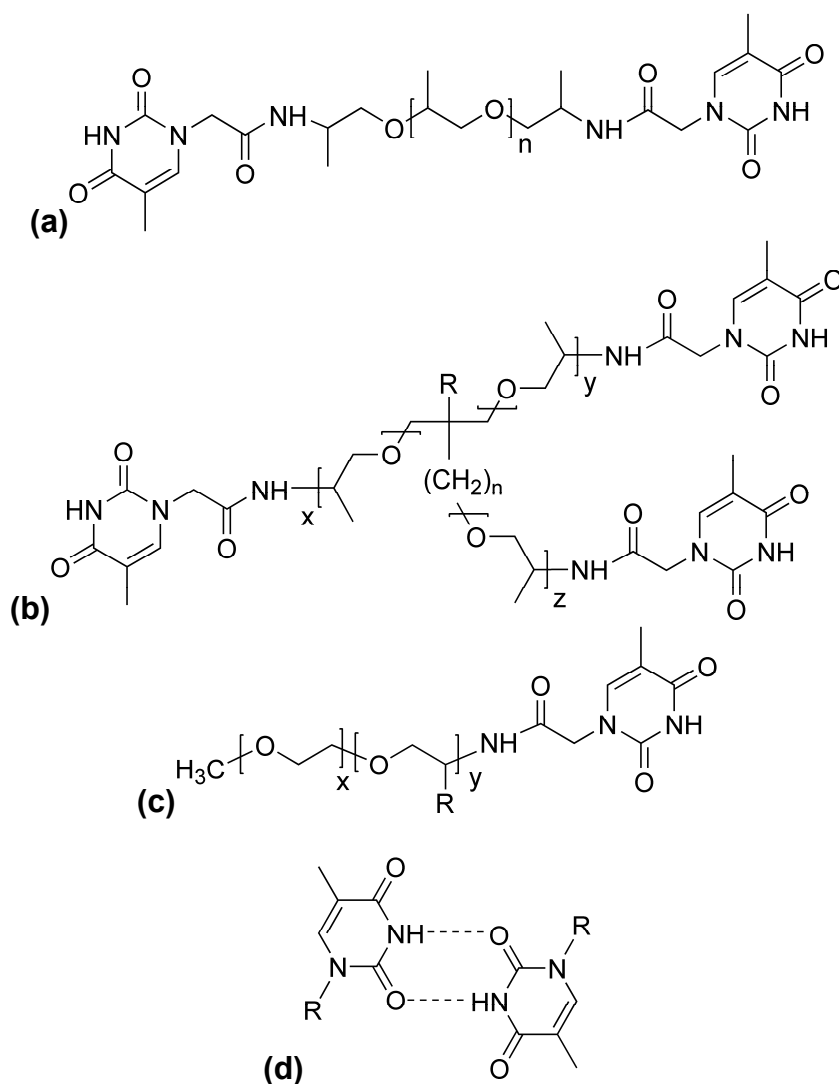
Chart IV.1. (a) Thy-PPO-*X*-Thy **3a-b**, (b) Thy₃-PPO-3000 **13a** (R = H, n = 0, x + y + z = 50), (c) Thy-PPO/PEO-*X* **17a-b** (R = H for EO or CH$_3$ for PO; **a**: *X* = 2000 and 90 PO for 10 EO; **b**: *X* = 600 and 83 PO for 17 EO), and (d) Thy self-association.

Therefore, three different phenomena concur and compete in the bulk: hydrogen bonding, microphase segregation between the PPO chains and the thymine stickers, and crystallization of thymines into microdomains.

The bulk structure and properties of the Thy-PPO-*X*-Thy **3a-b**, Thy$_3$-PPO-3000 **13a**, and Thy-PPO/PEO-*X* **17a-b** compounds were investigated by structural (polarized optical microscopy, X-ray scattering, Fourier transformed infrared [FTIR] spectroscopy), thermal (differential scanning calorimetry [DSC]) and rheological characterizations. X-ray scattering were performed at the SOLEIL Synchrotron source in France with the beamline SWING enabling simultaneous small-angle and wide-angle X-ray scattering measurements.

c. Two thermal transitions: glass transition and melting

### (i) Thermal transitions on DSC

Thy-PPO-*X*-Thy **3a-b**, Thy$_3$-PPO-3000 **13a** and Thy-PPO/PEO-600 **17b** display on DSC (Figure IV.6, Figure IV.8) a glass transition step, an exotherm reminiscent of crystallization, and an endotherm reminiscent of melting.
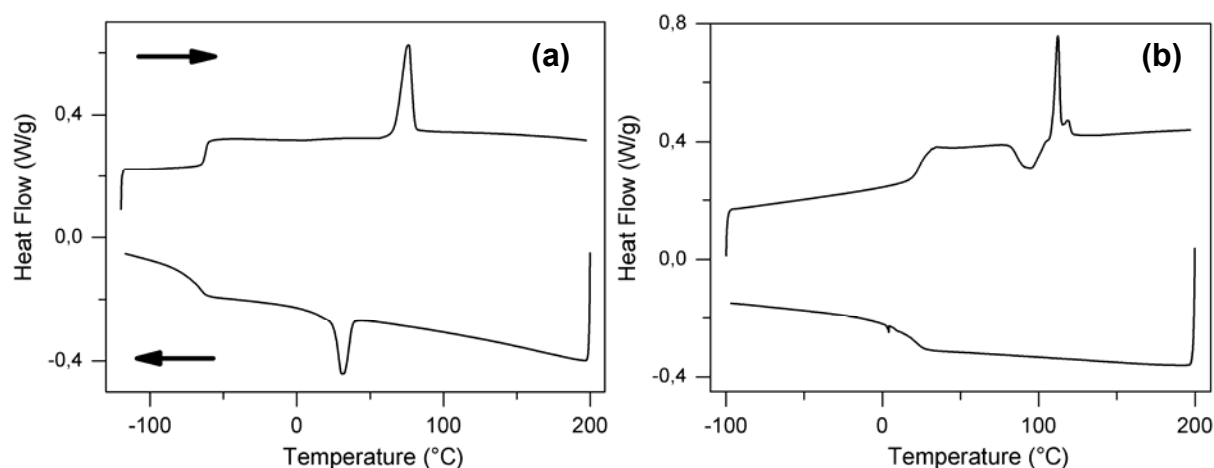
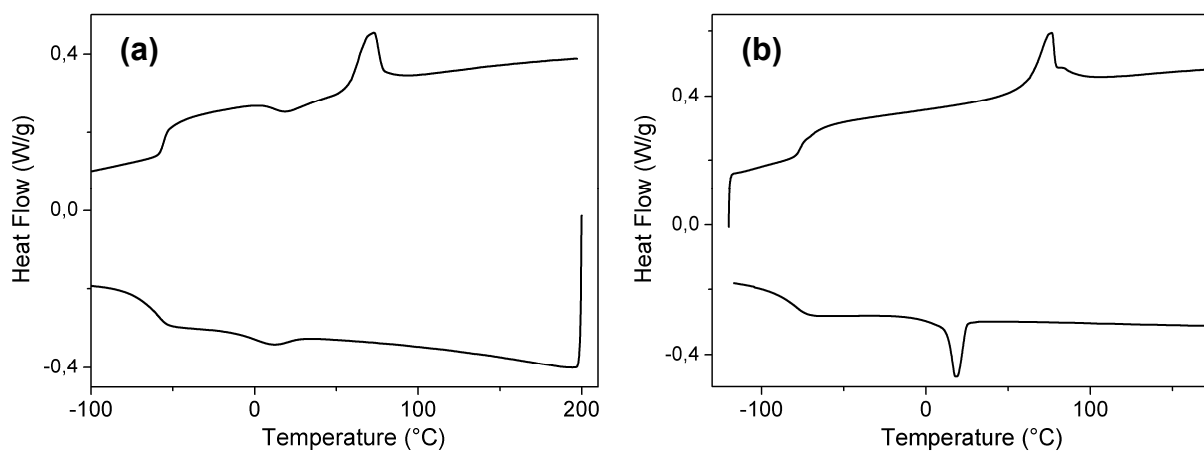**Figure IV.6.** DSC at 10°C/min (exo down) of (a) Thy-PPO-2200-Thy **3a** and (b) Thy-PPO-460-Thy **3b**.

After a heating cycle, Thy-PPO-2200-Thy **3a** (Figure IV.6a) crystallizes during the cooling cycle at 10°C/min, while Thy-PPO-460-Thy **3b** (Figure IV.6b) only crystallizes during the next heating cycle (cold crystallization), revealing that its crystallization is a slower process than that of Thy-PPO-2200-Thy **3a**. Indeed, the T_g of Thy-PPO-460-Thy **3b** is much higher than that of Thy-PPO-2200-Thy **3a**. So, at the same temperature Thy-PPO-2200-Thy **3a** has a higher mobility than Thy-PPO-460-Thy **3b**.

If the materials are given time to anneal at temperatures below the melting temperature ($T_m = 67°C$ for Thy-PPO-2200-Thy **3a** and $T_m = 109°C$ for Thy-PPO-460-Thy **3b**) but above the crystallization temperature, the extent of crystallization increases, as reflected by the enthalpy of fusion (ΔH_f) increase. In fact, ΔH_f increases dramatically for Thy-PPO-460-Thy **3b** (from 9 to 33 J/g), but only slightly for Thy-PPO-2200-Thy **3a** (from 15 to 18 J/g) upon annealing. Moreover, if the cooling cycle is done at a lower rate (0.7°C/min), then Thy-PPO-460-Thy **3b** crystallizes during that cooling cycle (Figure IV.7).
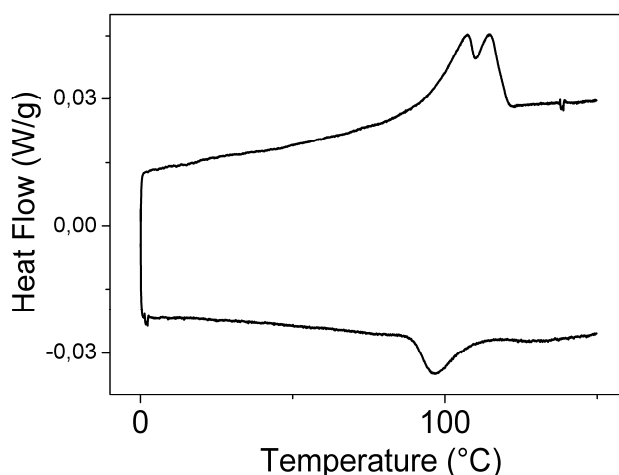
Figure IV.7. DSC at 0.7°C/min (exo down) of Thy-PPO-460-Thy **3b**.

Like Thy-PPO-2200-Thy **3a**, Thy-PPO/PEO-600 **17b** (Figure IV.8b) has a low T_g and thus crystallizes during the cooling cycle at 10°C/min. Thy$_3$-PPO-3000 **13a**'s T_g is a little higher, so it only partially crystallizes during the cooling cycle and continues to crystallize during the next heating cycle (Figure IV.8a).

Figure IV.8. DSC at 10°C/min (exo down) of (a) Thy$_3$-PPO-3000 **13a** and (b) Thy-PPO/PEO-600 **17b**.

(ii) Thermal transitions on IR spectroscopy and polarized optical microscopy

The thermal transitions detected on DSC, T_g and crystallization, can also be evidenced by temperature-dependent FTIR spectroscopy (see Chapter V for T_g). Moreover, crystallization and melting can be observed by temperature-dependent polarized optical microscopy. Indeed, polarized optical microscopy images of these materials at 25°C (Figure

IV.9) show bright spherulite-like spots with a Maltese cross extinction along the polarization axes of the crossed polarizer and analyzer, characteristic of anisotropy. However, as the temperature increases above the melting temperature determined by DSC (T_m), the images become totally black, indicating isotropic phases.
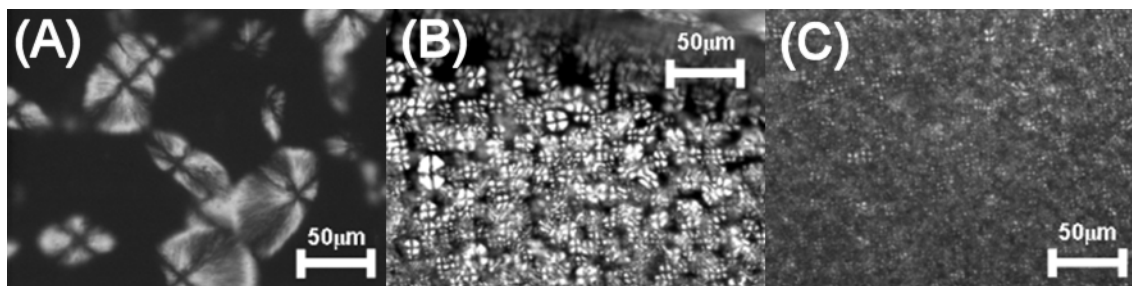
Figure IV.9. Polarized optical microscopy at 25°C of (A) Thy-PPO-460-Thy **3b**, (B, C) Thy-PPO-2200-Thy **3a**.

d. Order at low temperatures

(i) Crystalline order

X-ray scattering spectra at 30°C of Thy-PPO-2200-Thy **3a** (Figure IV.11A and C) and Thy-PPO-460-Thy **3b** (Figure IV.10) show a broad band between $q = 0.6$ Å^{-1} (corresponding to $d = 10.5$ Å) and $q = 2.4$ Å^{-1} ($d = 2.6$ Å) characteristic of nearest neighbors correlation in amorphous phases. Sharp peaks characteristic of crystallinity are surimposed on this broad halo. These results indicate that Thy-PPO-X-Thy **3a-b** are semicrystalline.

The sharp peaks corresponding to d spacing of 4.0, 4.8, and 11.9 Å are common to Thy-PPO-460-Thy **3b** and Thy-PPO-2200-Thy **3a**. We attribute these peaks to the crystallization of thymine end groups in microdomains.[19] Thus, the crystallinity concerns only the thymine moieties, while the rest of the PPO chain remains amorphous. This picture is consistent with the fact that diamine telechelic PPO are amorphous and thymine is crystalline, and with the fact that the value of the enthalpy of fusion ΔH_f of annealed Thy-PPO-460-Thy **3b** is much greater than that of annealed Thy-PPO-2200-Thy **3a** (33 J/g compared to 18 J/g).

---

[19] Shimizu, T.; Iwaura, R.; Masuda, M.; Hanada, T., Yase, K.; **Internucleobase-Interaction-Directed Self-Assembly of Nanofibers from Homo- and Heteroditopic 1,w-Nucleobase Bolaamphiphiles**; *J. Am. Chem. Soc.* **2001**, *123*, 5947.

Indeed, the percentage of thymine moieties is much higher in Thy-PPO-460-Thy **3b** than in Thy-PPO-2200-Thy **3a**.
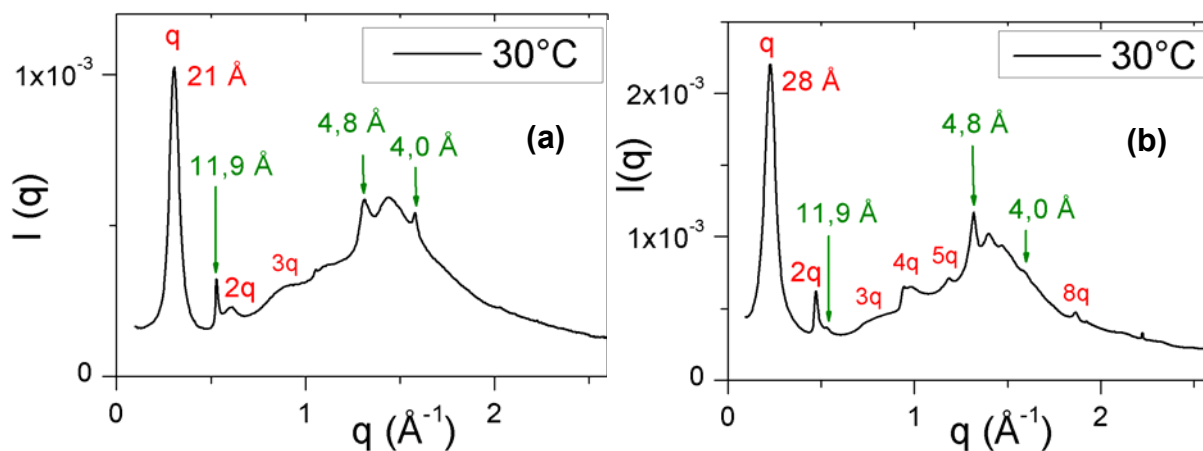
Figure IV.10. X-ray scattering of Thy-PPO-460-Thy **3b** at room temperature
(a) before annealing and (b) after annealing.
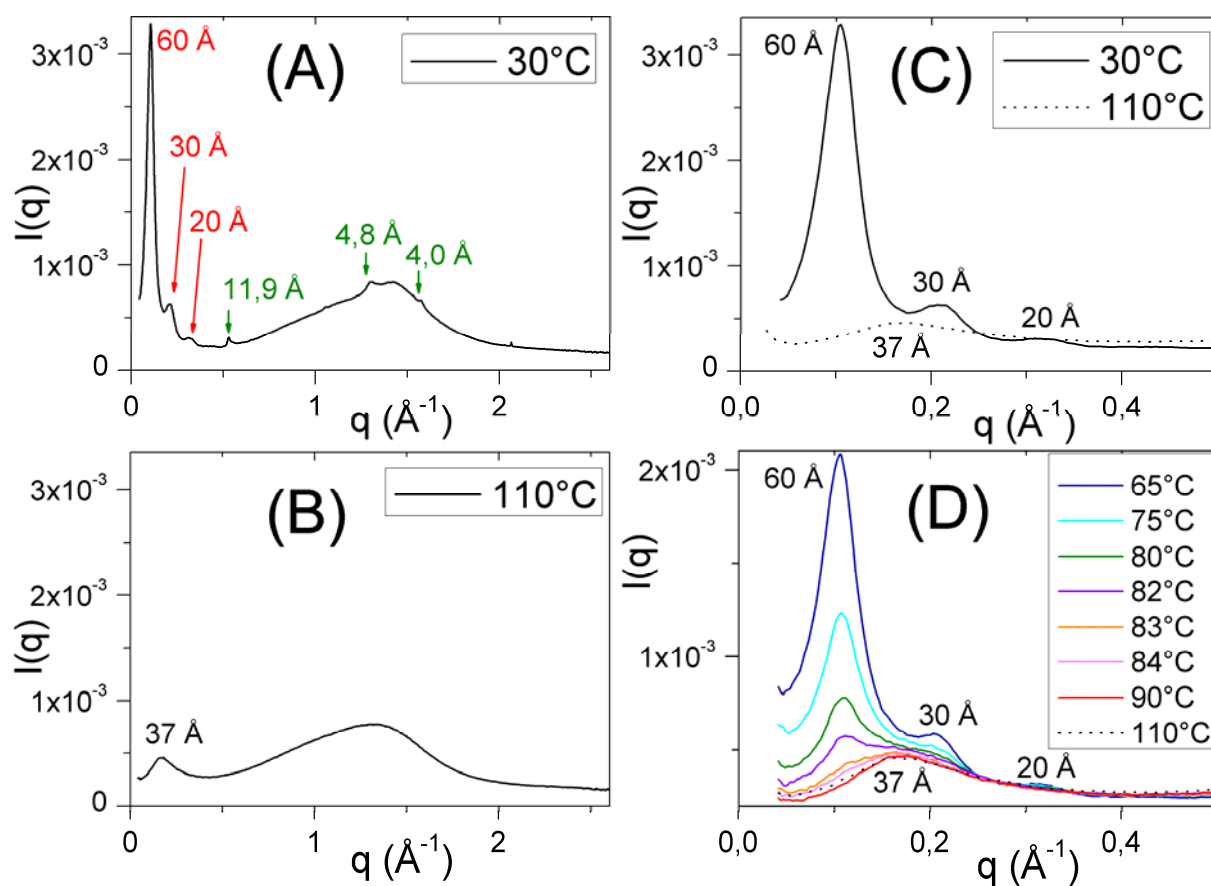
Figure IV.11. X-ray scattering of Thy-PPO-2200-Thy **3a** at 30°C (A), 110°C (B); enlargement of the small q range at 30°C and 110°C (C) and around the ODT ($T_{ODT} = 85$°C) (D).

(ii) Long-range order

In addition to the crystalline order, long-range ordering is also found for Thy-PPO-*X*-Thy **3a-b**. Thy-PPO-2200-Thy **3a** reveals peaks corresponding to 60 Å (*q*), 30 Å (*2q*), 20 Å (*3q*), and 15 Å (*4q*), that are consistent with a lamellar order of spacing $d = 60$ Å (Figure IV.11A and C). This value of lamellar spacing (60-61 Å) is comparable to the one observed in layered silicates intercalated with telechelic diamine PPO of the same molecular weight.[20] Annealed Thy-PPO-460-Thy **3b** (Figure IV.10b) displays peaks corresponding to 27.7 Å (*q*) and 13.3 Å (*2q*) clearly defined, as well as 8.6 Å (*3q*), 6.7 Å (*4q*), 5.3 Å (*5q*), and 3.4 Å (*8q*) less defined. The regular spacing is consistent with a lamellar order of spacing $d = 27.7$ Å. Without annealing, the peaks corresponding to the lamellar order are shifted to shorter distances, whereas the peaks corresponding to the crystalline order remain at the same position. The lamellar *d* spacing of Thy-PPO-460-Thy **3b** increases from 20.6 to 27.7 Å after annealing at 100°C (Figure IV.10).

(iii) PPO chain extension from the disordered to the lamellar state

The ratio L/r_0 of the average end-to-end length L of PPO in the ordered lamellar state versus the end-to-end distance r_0 in the disordered melt is approximately 60 / 50 = 1.2 for Thy-PPO-2200-Thy **3a** and 27.7 / 22.4 = 1.2 for Thy-PPO-460-Thy **3b**.

The volume V of one PPO chain can be estimated from the PPO density and molecular weight to be $3.7*10^{-27}$ m^3 for Thy-PPO-2200-Thy **3a** and $7.6*10^{-28}$ m^3 for Thy-PPO-460-Thy **3b**. The PPO chain extension required to accommodate the lamellar morphology is determined by the crystal packing of the 2D crystallized thymine plane. Assuming incompressibility of the system, the volume V of one PPO chain is then equal to $L*\Sigma$, where Σ is the area of the thymine plane occupied by one chain. This area is related to the distance d between two crystallized thymines by $d = \sqrt{\Sigma} = \sqrt{(V/L)}$. The estimations obtained for $\sqrt{\Sigma}$ (7.9 Å for Thy-PPO-2200-Thy **3a** and 5.2 Å for Thy-PPO-460-Thy **3b**) are compatible with distances between two thymines in the crystallized state.

---

[20] Lin, J.-J.; Cheng, I.-J.; Wang, R., Lee, R.-J.;**Tailoring Basal Spacings of Montmorillonite by Poly(oxyalkylene)diamine Intercalation**; *Macromolecules* **2001**, *34*, 8832.

(iv) Two distinct orders

To conclude, under T_m Thy-PPO-X-Thy **3a-b** are semicrystalline and exhibit two distinct orders: a crystalline order and a lamellar order. The lamellar structure is constituted of alternating two-dimensional (2D) crystallized thymine planes and amorphous PPO layers (Figure IV.5C). Additional hydrogen bonding between the amide groups linking the thymine to the PPO chain may further stabilize this organization. The annealing allows the PPO chains to stretch more and thus increases the lamellar spacing. Yet, the chains remain partially folded and stay amorphous.

Moreover, Thy-PPO/PEO-X **17a-b**, Thy$_3$-PPO-3000 **13a** and Thy-PPO-4000-Thy **3d** also seem to exhibit this crystallinity and long-range lamellar structure, showing nanophase separation between crystallized thymine planes and amorphous PPO layers (Figure IV.12, Figure IV.13, Figure IV.14).
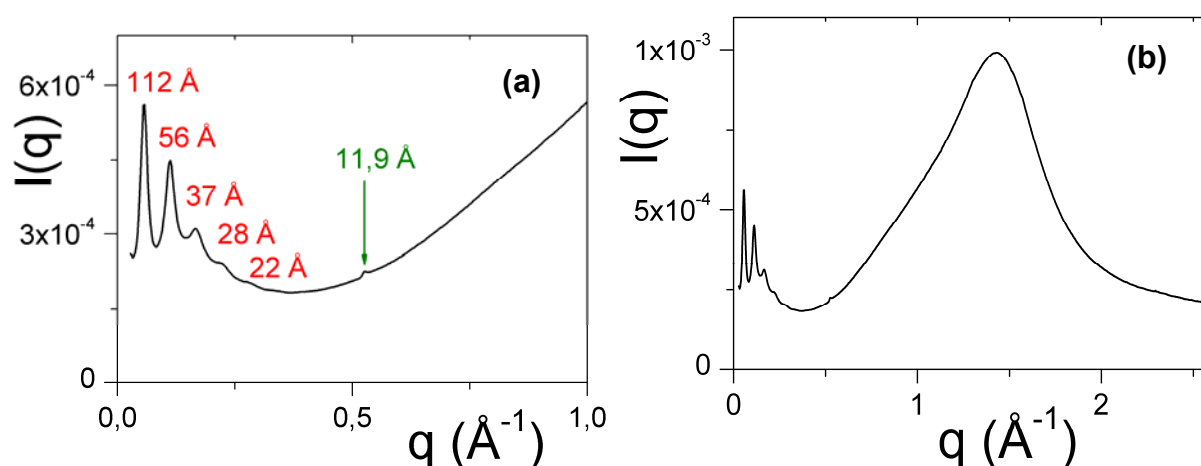

Figure IV.12. X-ray scattering at 25°C of (a, b) Thy-PPO/PEO-2000 **17a**.

For the monofunctionals Thy-PPO/PEO-X **17a-b** the lamellar spacings correspond to double layers of molecules (Figure IV.12a,b and Figure IV.13a). For the trifunctional Thy$_3$-PPO-3000 **13a** (Figure IV.13b) the third arm does not seem affect ordering and crystallization of the thymines. For the difunctional Thy-PPO-4000-Thy **3d** (Figure IV.14) the lamellar order is not very long-range since only two reflections are visible, and the crystallinity peak is also weak. The decreased percentage of Thy in this last compound can be held responsible of the ill-definition of the orders.
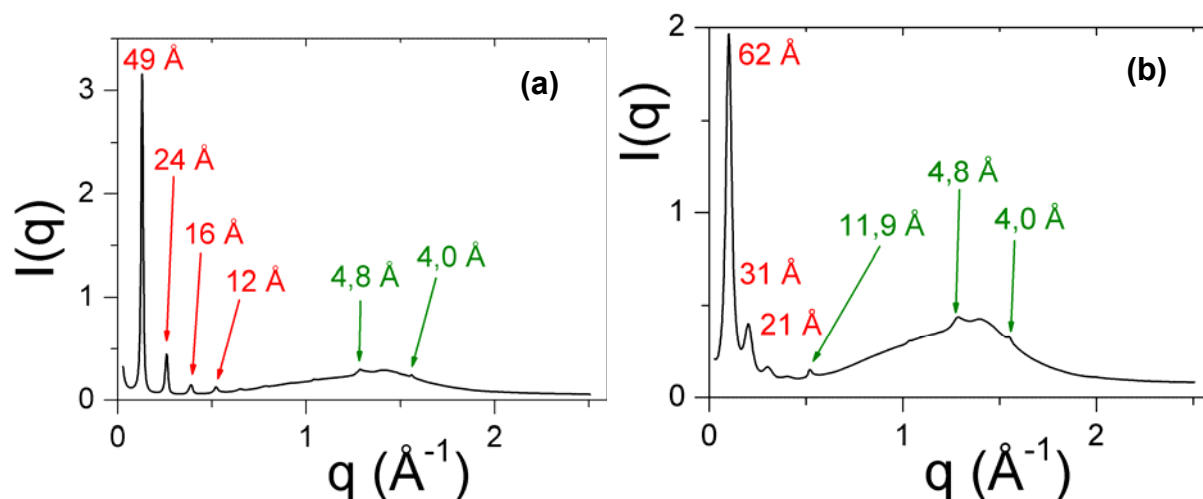
Figure IV.13. X-ray scattering at 25°C of (a) Thy-PPO/PEO-600 **17b** and (b) Thy$_3$-PPO-3000 **13a**.
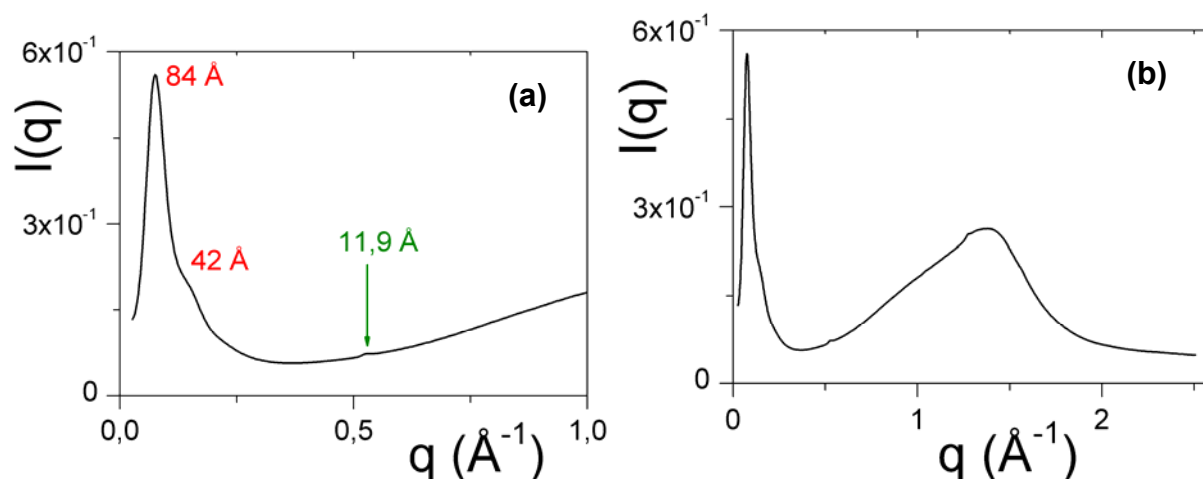
Figure IV.14. X-ray scattering at 25°C of (a,b) Thy-PPO-4000-Thy **3d**.

e. Disorder at high temperatures

(i) Low-intensity peak

At higher temperature, above T_m, in addition to the nearest neighbors correlation halo, a peak that scales with the chain length is observed on the X-ray scattering spectra of Thy-PPO-2200-Thy **3a** (Figure IV.11B and D, Figure IV.15a) and Thy-PPO-460-Thy **3b** (Figure IV.15b). This peak is clearly not a sign of a long-range correlated nanostructure, since it is broad and there are no higher order reflections. However, it could still be argued that it reflects a short-range fluctuating nanoscale segregation, *i.e.* it indicates microphase separation.
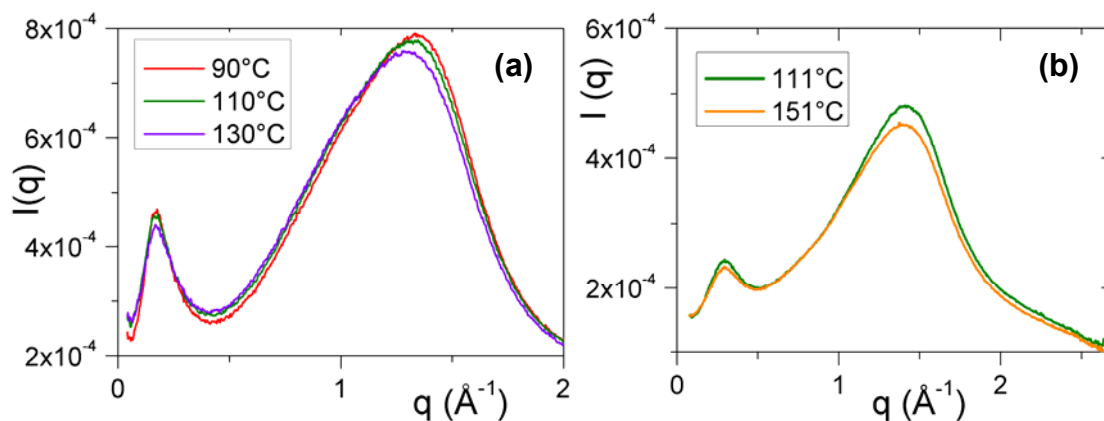
Figure IV.15. X-ray Scattering above ODT of (a) Thy-PPO-2200-Thy **3a** (T_{ODT} = 85°C) and (b) Thy-PPO-460-Thy **3b** (T_{ODT} = 105°C).

(ii) Correlation hole effect

Yet, we interpret this peak as resulting from the correlation hole effect:[2a,21,22] it reflects the typical distance between strong scattering polar stickers separated by the PPO chain, hence the chain length scaling, but it does not necessarily indicate mesoscopic segregation. Indeed, this peak's intensity is very low compared to the nearest neighbors' correlation halo and its width is very broad compared to the lamellar order Bragg peak.

The correlation hole effect was first explained by De Gennes.[23] Let's follow his demonstration. First, we consider the simple case of chains of end-to-end radius R_0 each labeled at one end (for instance by a deuterated monomer for neutron scattering). The origin is fixed as one such labeled unit (the labels are point-like), and we look at the distribution $S_{11}(r)$ of labeled ends at a distance r from the origin (Figure IV.16a).

For r between 0 and R_0, $S_{11}(r)$ is lower than $S_{11}(\infty)$. Indeed, we have fixed one label at the origin, so there is one chain of radius R_0 near the origin. As a result of the repulsion of the polymer coils (which ensures the incompressibility of the system), the probability of finding other chains inside the sphere of radius (approximately) R_0 around the origin is reduced, so

[21] Bates, F. S.; **Measurement of the correlation hole in homogeneous block copolymer melts**; *Macromolecules* **1985**, *18*, 525.

[22] Huh, J.; Ikkala, O.; ten Brinke, G.; **Correlation Hole Effect in Comblike Copolymer Systems Obtained by Hydrogen Bonding between Homopolymers and End-Functionalized Oligomers**; *Macromolecules* **1997**, *30*, 1828.

[23] de Gennes, P.-G.; ***Scaling Concepts in Polymer Physics***; Cornell University Press: Ithaca, New York, **1979**.

the density of other labels is also reduced. Therefore, $S_{11}(r)$ has a correlation hole between zero and R_0. Experimentally, it is the scattering intensity that is measured, which is proportional to the Fourier transform of $S_{11}(r)$, that is to say the correlation function $S_{11}(q)$ (Figure IV.16b).

(a)

(b)
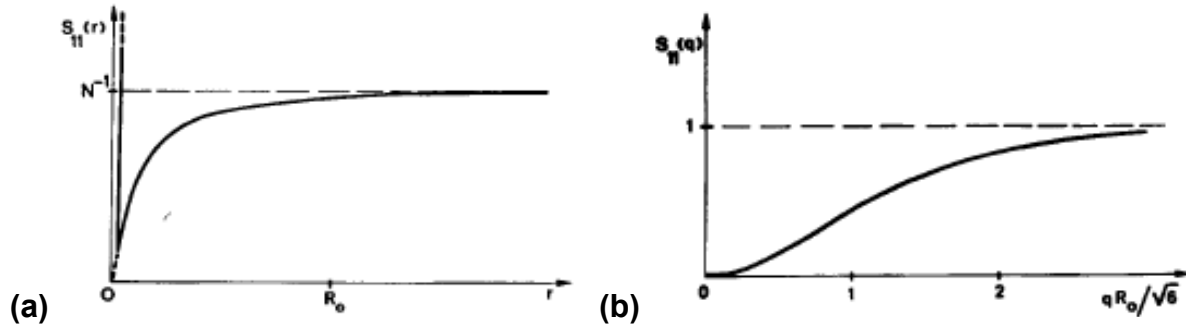
Figure IV.16. For chains labeled at one end, from ref 23: (a) distribution $S_{11}(r)$ of labeled ends at distance r from the origin, with a delta function at the origin (self-correlation), a constant value equal to the average density of labels in the melt at high r, and a correlation hole between 0 and R_0, and (b) correlation function $S_{11}(q)$.

Now, we consider the case where the chains are labeled by a segment instead of a point (for instance by a deuterated block for neutron scattering), with the segment length N_D (number of monomers in the D segment) much smaller than the total length of the chain N (total number of monomers).

In the low q region ($q \ll R_D^{-1}$ with R_D the natural size of the labeled segment $R_D = a\sqrt{N_D}$ with a the monomer size), the D segment can be considered point-like and the scattering intensity $I(q)$ is directly proportional to the correlation function $S_{11}(q)$ from Figure IV.16b. In the high q region, interference between different D segments can be neglected and the intensity is that of a single chain of N_D monomers. Therefore, $I(q)$ shows a broad peak between R_0^{-1} and R_D^{-1} (Figure IV.17), without any segregation effect considered.
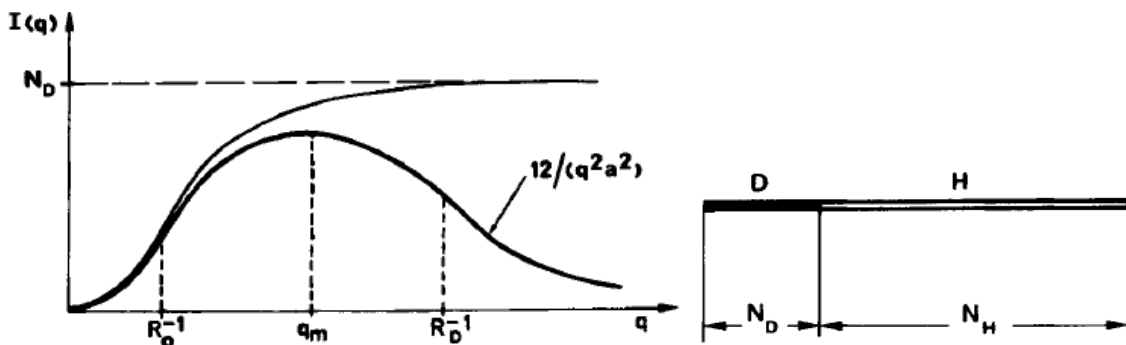
Figure IV.17. Qualitative plot of scattering intensity versus scattering wave vector in a neutron experiment using a melt of polymer chains, each chain being deuterated in one portion of its length as shown, from ref 23.

So, to sum up, the mean-field theory developed by de Gennes[23] and Leibler[2a] predicts a maximum for $qR \sim 1$ in the scattering intensity of block copolymers' disordered state (with q the scattering vector and R the radius of gyration). The existence of this maximum does not result from segregation between the blocks. It results from the correlation hole effect and has been experimentally demonstrated by Bates for diblock copolymers.[21] Triblock copolymers also show a bump resulting from the correlation hole effect on their small-angle scattering spectra, even when there is no phase segregation effect (for instance, on Figure IV.18 for a triblock copolymer comprised of a central deuterated polystyrene block and two outer hydrogenated polystyrene blocks).
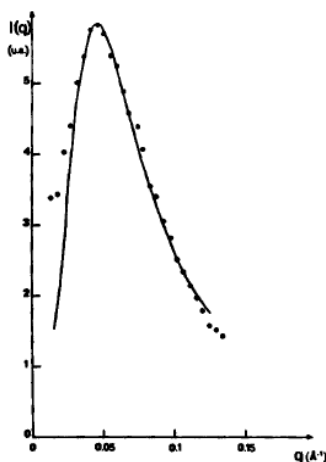

Figure IV.18. Small-angle scattering of neutrons by a melt of triblock copolymers polystyrene H - polystyrene D - polystyrene H (where H stands for hydrogenated and D for deuterated), from ref 23.

So far, we have been focused on the case of neutron scattering, where labelling can be done with minimum modification of the system by deuteration. For X-ray scattering, labelling can be done by heavy atoms, but complications can arise if there are specific associations between them. Following another De Gennes paper,[24] we consider the X-ray scattering intensity of chains carrying a single heavy atom (noted X) at one end (case A, Figure IV.19a) or at both ends (case B, Figure IV.19b). We neglect any specific associations between the atoms X. For the case A we must take into account the individual scattering of the X atoms and the correlation hole effect around one X atom (due to the repulsion between the chains), while for case B we must take into consideration the individual scattering, the correlation hole effect, and the direct correlation between two X atoms belonging to the same chain. Indeed, from an atom X, the probability of finding another atom X at a distance corresponding to the chain size is higher, because two X atoms are connected by the chain. However as can be seen

---

[24] de Gennes, P. G.; **Theory of X-ray scattering by liquid macromolecules with heavy atom labels**; *J. Phys.* **1970**, *31*, 235.

on Figure IV.19b, the correlation hole effect predominates the direct correlation between two X atoms of the same chain.
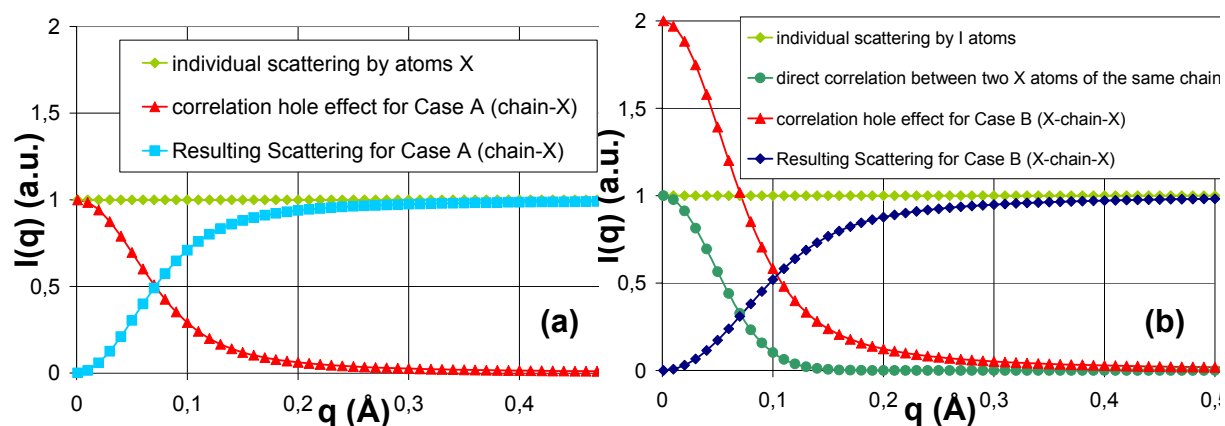

Figure IV.19. Calculated (formulas from ref 24) X-ray scattering intensity for: (a) chains carrying a single heavy atom X at one end (case A) and (b) chains carrying a single heavy atom X at both ends (case B), with an end-to-end mean radius $R_0 = 37$ Å, from ref 23.

If we now consider, like we did before, chains labeled by segments of heavy atoms instead of points, we find again that the scattering intensity $I(q)$ shows a broad peak around R_0^{-1} without any segregation effect considered.

(iii) Importance of synchrotron radiation

It should be stressed here that the visibility of the correlation hole peak depends on the contrast between the spacer and the stickers, and that while with our system this peak is clearly visible with a synchrotron radiation, it was barely noticeable with a sealed tube X-ray generator radiation (Figure IV.20). This underlines the necessity of SOLEIL's short acquisition time to follow the structure evolution with temperature.
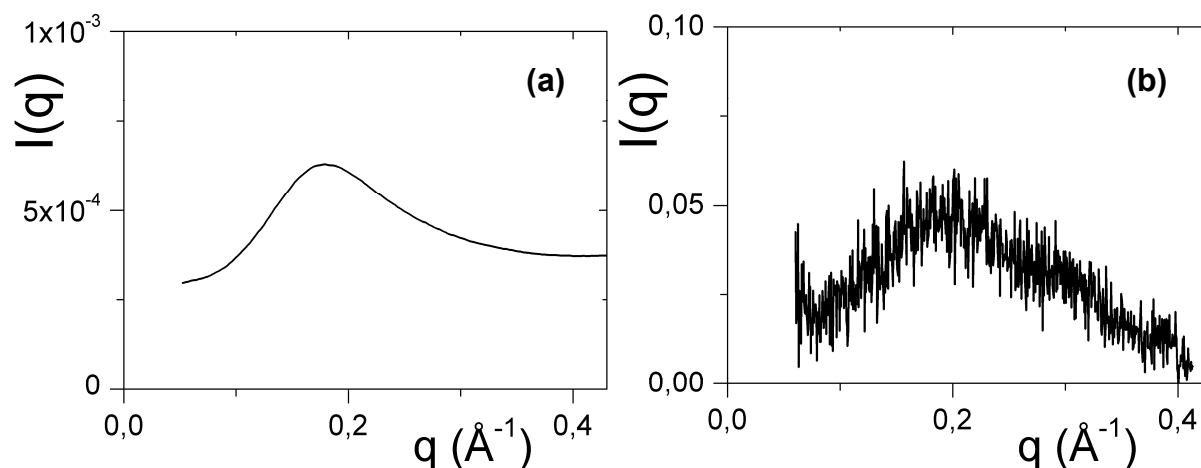

Figure IV.20. X-ray scattering of 50/50-M-2200 **4a** with (a) SOLEIL synchrotron radiation (acquisition time = 1 s) and (b) sealed tube X-ray generator radiation (acquisition time = 14 h).

(iv) Correlation hole effect modelization

Comparison with a simple model[2a] of the correlation hole peaks in corresponding block copolymers seems to further support this interpretation of peaks resulting from the correlation hole effect (Figure IV.21).

The theory developed in reference 2 predicts a maximum in the correlation function $S(q)$ of the disordered state, which is proportional to the scattering intensity.[2] Even though this theory was developed for non-associating diblock copolymers, it can be applied by virtually cutting the molecule in half, as a first approximation for our pseudo-triblock copolymers and associated species. This first approximation allows a relatively good fitting of the shape and position of the experimental peak, for both Thy-PPO-460-Thy **3b** and Thy-PPO-2200-Thy **3a**, using reasonable molecular parameters. The intensity is renormalized to fit the experimental curve.

The visibility of the correlation hole peak depends on the contrast between the spacer and the stickers. The contrast between the PPO chain and the stickers is quite high, since the sticker electron density is 20% higher than the PPO electron density. Still, the correlation hole intensity is very low, lower than the nearest neighbors' correlation halo intensity.
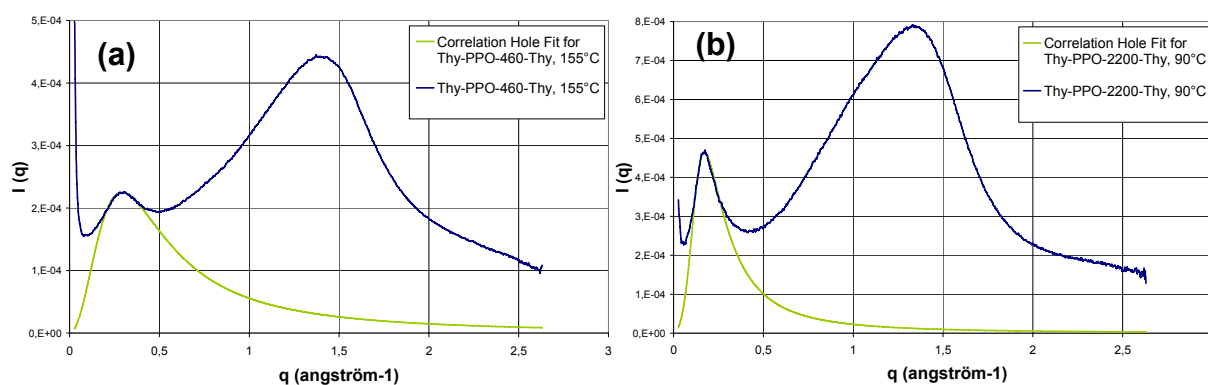
**Figure IV.21.** Correlation hole modelization of (a) Thy-PPO-460-Thy **3b** at 155°C and (b) Thy-PPO-2200-Thy **3a** at 90°C. Parameters: PPO monomer size: $a = 3.6$ Å, Thymine size: $d_{Thy} = 3$ Å; for $X = 460$: fraction: $f_{Thy} = 0.233$, number of PPO monomer unit $n = 6.6$, $C_\infty = 4.7$ for PPO chain, $\chi N_k = 1$; for $X = 2200$: $f_{Thy} = 0.048$, $n = 40$, $C_\infty = 7.4$, $\chi N_k = 15$.

f. Order-Disorder Transition

(i) Order-disorder transition

Consequently, Thy-PPO-X-Thy **3a-b** are in a disordered state above T_m. The transition at T_m is then an ODT that takes place in just a few degrees as evidenced by the dramatic evolution of the X-ray scattering spectra in the small q range during an heating ramp at 10°C per minute (Figure IV.11D, Scheme IV.1). The slight shift in temperature compared to the DSC T_m is related to the set-up and thermoinertia resulting from the ramp.
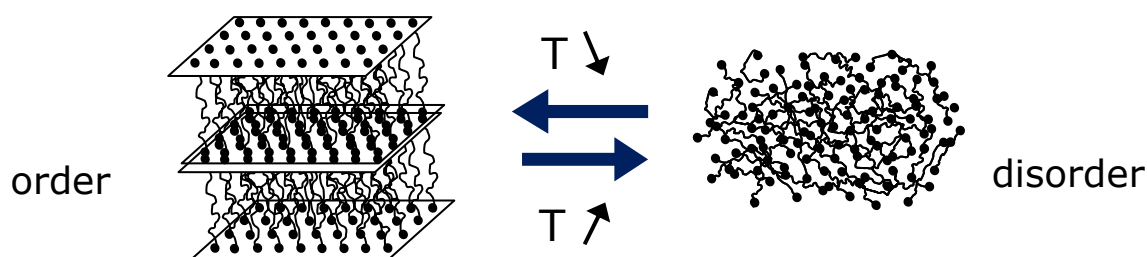

order   T↘   disorder
               T↗

**Scheme IV.1.** ODT: lamellar and crystalline order under T_{ODT}, disorder above T_{ODT}.

(ii) Thymine crystallization and lamellar organization seem to disappear and reappear together

Temperature-dependent X-ray scattering measurements of Thy-PPO-X-Thy **3a-b** (Figure IV.22, Figure IV.23) show that the two orders, crystalline and lamellar, disappear together on heating around the DSC melting temperature T_m. The transition is reversible upon cooling, with the two orders also reappearing together. So, the DSC melting endotherm and crystallization exotherm can be attributed to the simultaneous (on the time scale of our temperature dependent XRD experiments) destruction and formation, respectively, of these two orders. So, it seems that, in analogy with block copolymers consisting of amorphous and crystallizable blocks, the crystallization is localized in the lamellar planes not because the melt morphology was retained during crystallization but because of crystallization-driven microphase segregation.[25]

---

[25] (a) Xu, J.-T.; Turner, S. C.; Fairclough, J. P. A.; Mai, S.-M.; Ryan, A. J.; Chaibundit, C.; Booth, C.; **Morphological Confinement on Crystallization in Blends of Poly(oxyethylene-block-oxybutylene) and Poly(oxybutylene)**; *Macromolecules* **2002**, *35*, 3614. (b) Rangarajan, P.; Register, R. A.; Adamson, D. H.; Fetters, L. J.; Bras, W.; Naylor, S.; Ryan, A. J.; Dynamics **of Structure Formation in Crystallizable Block Copolymers**; *Macromolecules* **1995**, *28*, 1422.
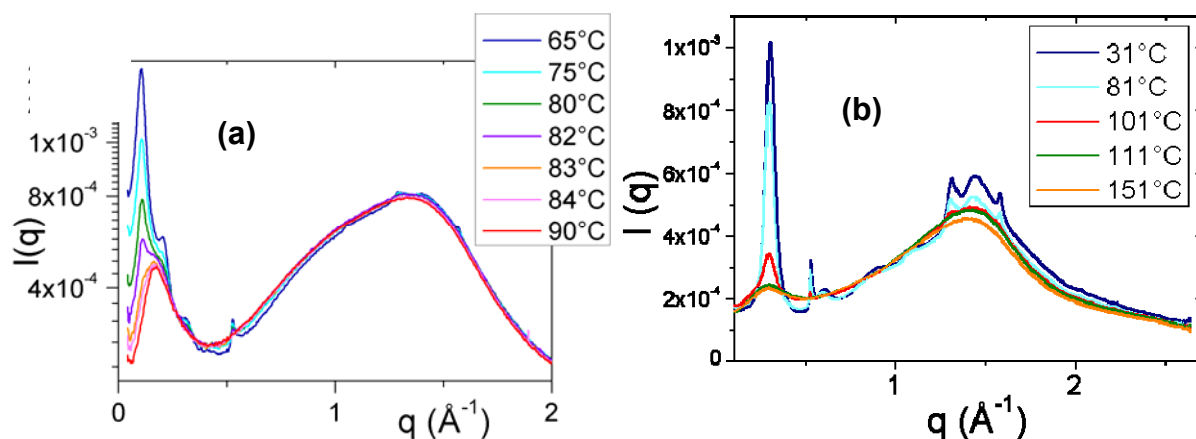
Figure IV.22. X-ray Scattering around ODT during heating of (a) Thy-PPO-2200-Thy **3a** (T_{ODT} = 85°C) and (b) Thy-PPO-460-Thy **3b** (T_{ODT} = 105°C).
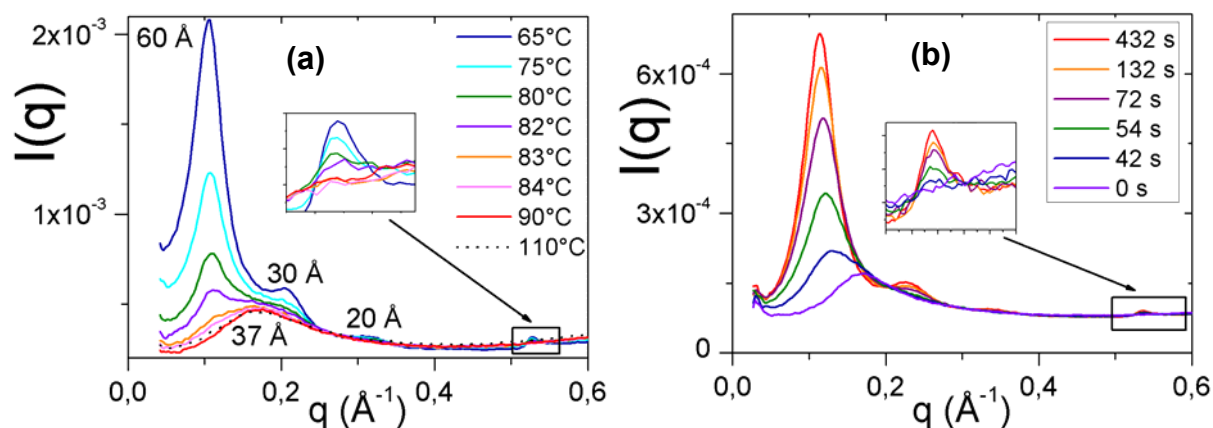
Figure IV.23. X-ray scattering of Thy-PPO-2200-Thy **3a** (a) at different temperatures during heating and (b) isothermal at 18°C after temperature jump from 100°C.

(iii) Impact on rheological and mechanical properties

This image of ODT is nicely confirmed by the rheological study and supports an analogy with crystallizable block copolymers.[26,27] Indeed, the frequency sweep of Thy-PPO-2200-Thy **3a** above 70°C, in the molten disordered state, is characteristic of a viscous fluid in the terminal flow regime (Figure IV.24a). However, a transition from viscous flow to elastic behavior is observed in a few minutes after a temperature jump from 70°C to 60°C (Figure IV.24a, Figure IV.25). At 60°C, under T_{ODT} = 67°C, the storage modulus *G'* becomes higher than the loss modulus *G''*. The transition is reversible upon heating. The same behavior is

---

[26] Hamley, I.; **Crystallization in Block Copolymers**; *Adv. Polym. Sci.* **1999**, *148*, 113.

[27] Deplace, F.; Wang, Z.; Lynd, N. A.; Hotta, A.; Rose, J. M.; Hustad, P. D.; Tian, J.; Ohtaki, H.; Coates, G. W.; Shimizu, F.; Hirokane, K.; Yamada, F.; Shin, Y.-W.; Rong, L.; Zhu, J.; Toki, S.; Hsiao, B. S.; Fredrickson, G. H. ; Kramer, E. J.; **Processing-structure-mechanical property relationships of semicrystalline polyolefin-based block copolymers**; *J. Polym. Sci. B: Polym. Phys.* **2010**, *48*, 1428.

observed Thy-PPO-460-Thy **3b** on temperature sweeps (Figure IV.24b). These results suggest that crystalline planes of thymine act as physical cross-links, causing rheological behavior typical of a thermoplastic elastomer.
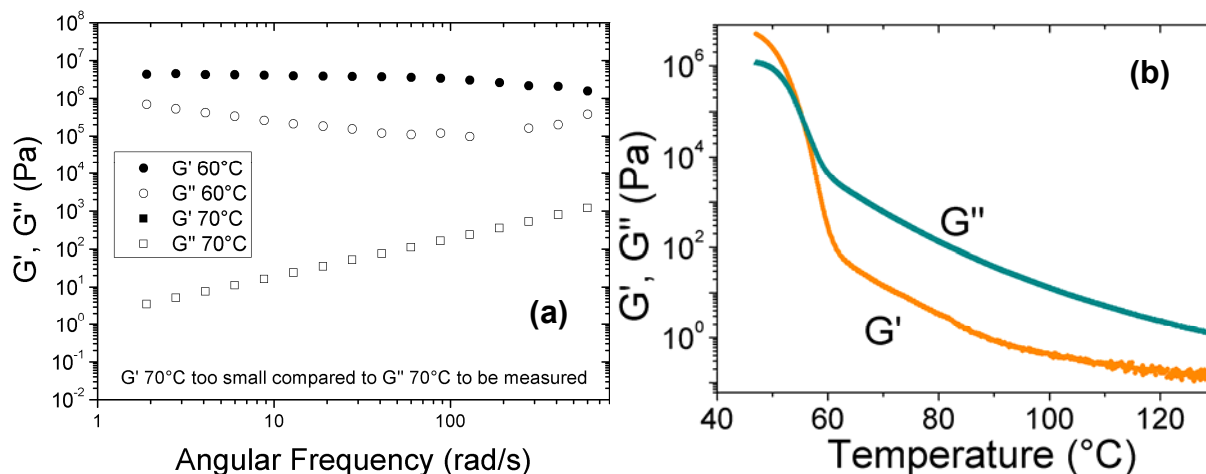
Figure IV.24. (a) Frequency sweep of Thy-PPO-2200-Thy **3a** at 60°C (elastic solid) and 70°C (viscous fluid), (b) Temperature sweep of Thy-PPO-460-Thy **3b** at 0.7°C/min, from 130°C to 50°C.
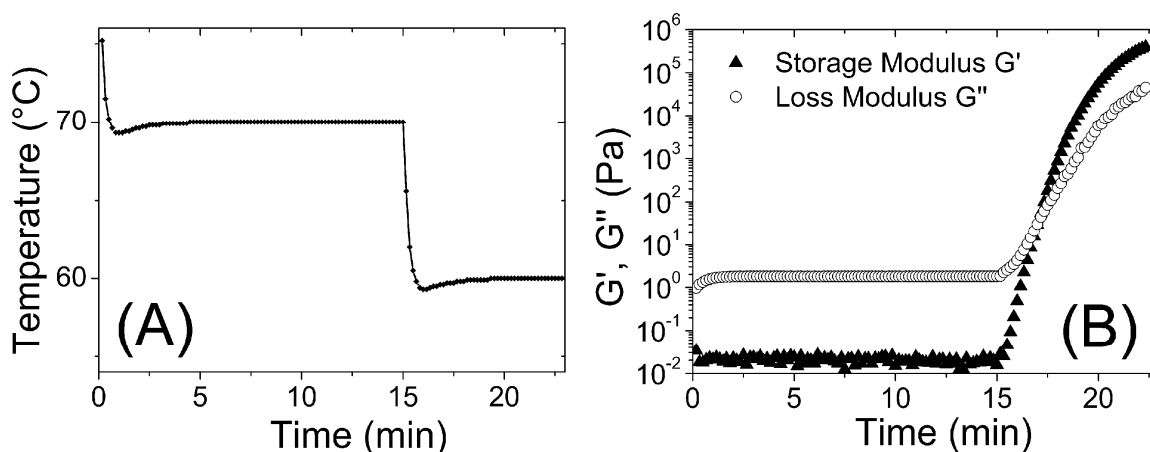
Figure IV.25. Rheology of Thy-PPO-2200-Thy **3a** during a temperature jump: (A) temperature jump from 70 to 60°C and (B) transition from viscous flow to elastic behavior after the temperature jump from 70 to 60°C.
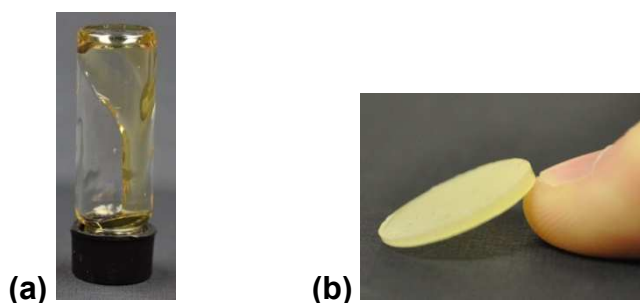
Figure IV.26. Picture of Thy-PPO-2200-Thy **3a** (a) above T_{ODT} and (b) below T_{ODT}.

As a result, these materials are solid below T_{ODT} (Figure IV.26b), even above their glass transition temperature ($T_g = 24°C$ for $X = 460$, $-62°C$ for $X = 2200$). At T_{ODT}, a transition to a disordered sta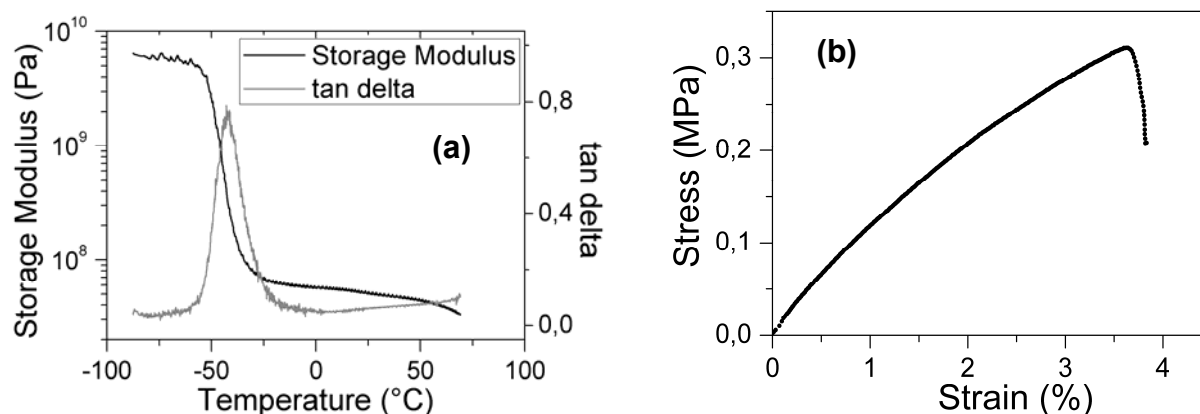te occurs and these materials become liquid (Figure IV.26a). Dynamic mechanical analysis (DMA) and tensile tests of Thy-PPO-2200-Thy **3a** confirm these observations (Figure IV.27).

Figure IV.27. (a) Dynamic Mechanical Analysis (DMA) and (b) tensile test at 25°C and 2mm/min, of Thy-PPO-2200-Thy **3a**.

g. Conclusion and perspectives

(i) Summary

In summary, we have demonstrated the existence of a long-range order and of an order-disorder transition in a telechelic supramolecular system. Under T_{ODT}, a lamellar structure with alternating amorphous chains and 2D crystallized stickers plane is formed. This organization is favorable as it allows microphase segregation of the hydrophobic spacers and polar stickers, as well as dimerization of the stickers by hydrogen bonding and their 2D-crystallization. Because of this structuration, the material behaves like a semicrystalline polymer: liquid over T_{ODT} and viscoelastic solid below. Besides, we have underlined the importance of taking into account the correlation hole effect to interpret X-ray scattering spectra of the disordered state, to avoid confusion between a cluster peak and a homogeneous state correlation hole peak.

(ii) Why is Thy-PPO-250-Thy **3c** different ?

Thy-PPO-250-Thy **3c** is not ordered at room temperature like Thy-PPO-460-Thy **3b** and Thy-PPO-2200-Thy **3a** (Figure IV.28a). Moreover, this compound does not display on DSC, up to 300°C, any exotherm reminiscent of crystallization or any endotherm reminiscent of melting; only a glass transition step is visible on Figure IV.28b. That glass transition temperature (T_g) is quite high (around 100°C), which explains why Thy-PPO-250-Thy **3c** does not organize at room temperature. However, annealing above the T_g (at 120, 140 and 160 °C) still does not allow Thy-PPO-250-Thy **3c** to crystallize and to microphase separate.
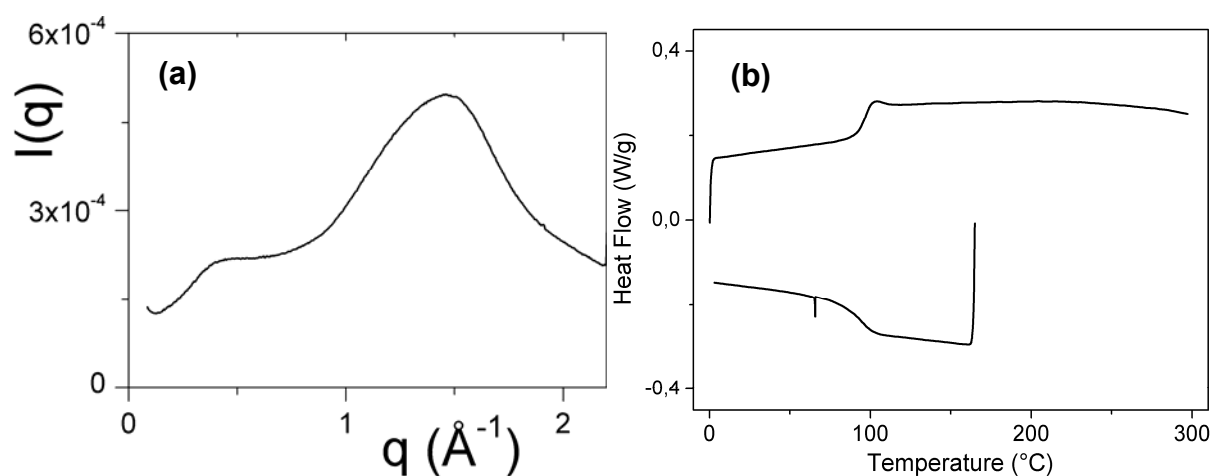
Figure IV.28. (a) X-ray scattering at 25°C and (b) DSC at 10°C/min after annealing at 160°C (exo down), of Thy-PPO-250-Thy **3c**.
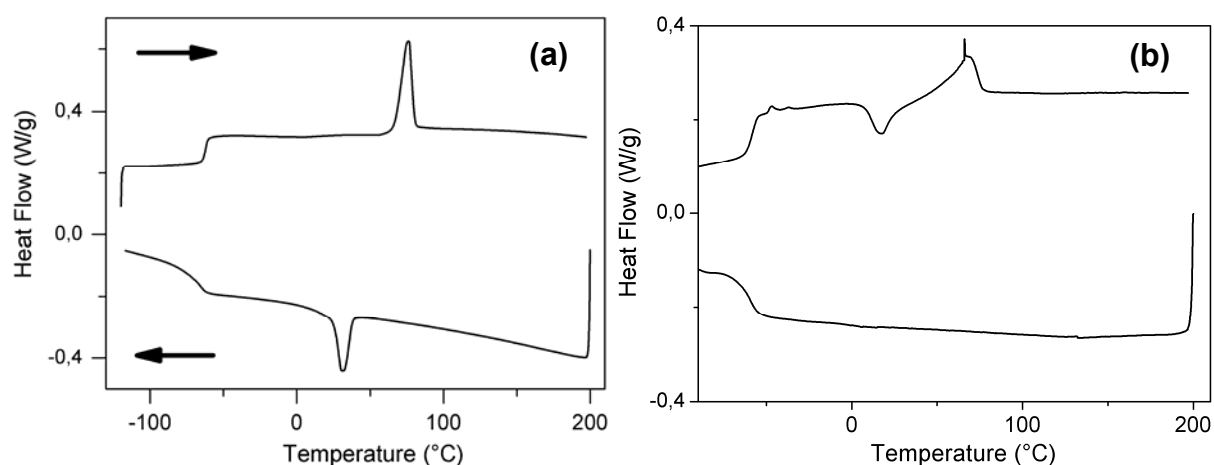
Figure IV.29. DSC at 10°C/min (exo down) of (a) Thy-PPO-2200-Thy **3a** and (b) Thy-PPO-2200-Thy **3a** containing impurities (thymine-1-acetic acid).

Possible explanations are that crystallization is hindered in Thy-PPO-250-Thy **3c** because the chain is too short to allow the thymines to position themselves for crystallization

and/or because of the presence of impurities. Indeed, if free (ungrafted) thymine is present in Thy-PPO-2200-Thy **3a**, the crystallization no longer happens during the cooling cycle, but during the next heating cycle, illustrating that impurities slow down the crystallization process (Figure IV.30).

(iii) Can long-range order and ODT be observed in a telechelic supramolecular polymer with no crystallization ?

Finally, whether the long-range order and ODT can be observed in a main-chain supramolecular polymer with no crystallization remains an open question. As the temperature is decreased, Thy-PPO-X-Thy **3a-b** go directly from the disordered state to a lamellar structure because of thymine crystallization. However, it should be possible to obtain BCC, lamellar or cylindrical morphologies in main-chain telechelic supramolecular polymers with no crystallization and very high χ (*i.e.* very low affinity) between the stickers and the spacers (Figure IV.5). Development of models taking into account dispersion forces as well as directional associations[28] should pave the way to better control of supramolecular polymers organization and properties.

(iv) Application to nanolithography ?

Block copolymers are considered to be the future of nanolitography. Indeed, block copolymers with a cleavable block may be used to manufacture regular nano-patterns. However, to obtain the wanted size features, below 10 nm, short chains are needed, but phase separation is usually not as efficient for short chains, except if the incompatibility is very high, but then difficulties of synthesis arise. If something related to our system could be applied to this, its size features might be smaller (6 nm for Thy-PPO-2200-Thy **3a** and 2 to 3 nm for Thy-PPO-460-Thy **3b**) than anything done today. A challenge that would need to be addressed for the application to nanolithography concerns the alignment, which needs to be of very long-range order and perpendicular to the surface. Magnetic field alignment[29] or solvent alignment may be used.

---

[28] Hoy, R. S.; Fredrickson, G. H.; **Thermoreversible associating polymer networks. I. Interplay of thermodynamics, chemical kinetics, and polymer physics**; *J. Chem. Phys.* **2009**, *131*, 224902.

[29] Majewski, P. W.; Gopinadhan, M.; Osuji, C. O.; **Magnetic field alignment of block copolymers and polymer nanocomposites: Scalable microstructure control in functional soft materials**; *J. Polym. Sci. B: Polym. Phys.* **2012**, *50*, 2.

2. Disorder in supramolecular polymers

In this part, we study supramolecular polymers which, contrary to Thy-PPO-*X*-Thy **3a-b**, do not exhibit long-range order and do not crystallize. This part was partially published in reference 42.

(i) Supramolecular polymers used in this study: glassy DAT-PPO-*X*-DAT **2a-b**

The supramolecular polymers used in this study consist of low glass transition temperature (T_g), low-molecular-weight and noncrystalline poly(propylene oxide) (PPO) oligomers functionalized on each end with diaminotriazine (DAT) groups (Chart IV.2a). They are denoted as DAT-PPO-*X*-DAT **2a-b** (**a**: *X* = 2200, **b**: *X* = 460), where *X* is the molecular weight (in g/mol) of the PPO spacer. Their synthesis is described in Chapter II.
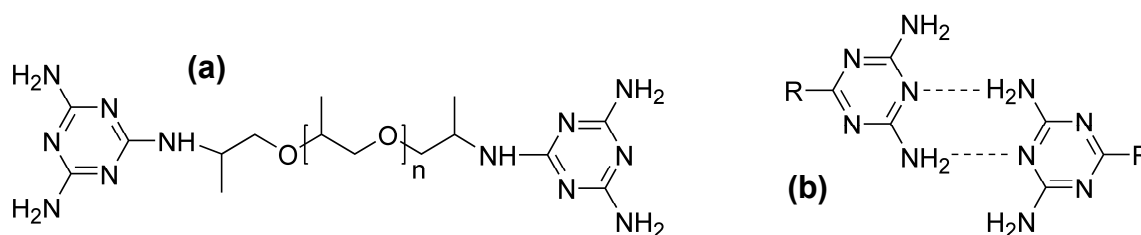

Chart IV.2. (a) DAT-PPO-*X*-DAT **2a-b** and (b) DAT self-association.

Like Thy, DAT is a very polar group that can weakly self-associate through two hydrogen bonds (Chart IV.2b, $K_{DAT-DAT} = 2.2$ M^{-1} versus $K_{Thy-Thy} = 4.3$ M^{-1}, as determined by ^{1}H NMR spectroscopy in CDCl$_3$).[49] In contrast, the PPO chain is much less polar. However, unlike Thy derivatives that readily crystallize, DAT derivatives are known for their tendency to form glasses instead of crystallizing. Indeed, they form hydrogen-bonded aggregates that pack poorly because of their multiple nonequivalent hydrogen-bonding sites.[30,31] Therefore, the DAT-PPO-*X*-DAT **2a-b** behaviors differ from that of Thy-PPO-*X*-Thy **3a-b**.

---

[30] Wang, R.; Pellerin, C.; Lebel, O.; **Role of hydrogen bonding in the formation of glasses by small molecules: a triazine case study**; *J. Mater. Chem.* **2009**, *19*, 2747-2753.

[31] Plante, A.; Mauran, D.; Carvalho, S. P.; Pagé, J. Y. S. D.; Pellerin, C. ; Lebel, O.; **Tg and Rheological Properties of Triazine-Based Molecular Glasses: Incriminating Evidence Against Hydrogen Bonds**; *J. Phys. Chem. B* **2009**, *113*, 14884.

(ii) DAT-PPO-*X*-DAT **2a-b** are <u>not</u> crystalline and <u>not</u> ordered

Indeed, unlike Thy-PPO-*X*-Thy **3a-b**, DAT-PPO-*X*-DAT **2a-b** show no ordering, neither crystalline nor lamellar. Indeed, they display only a glass transition step in DSC (Figure IV.30) and show no birefringence in polarized optical microscopy images. Their X-ray scattering spectra at 25°C (Figure IV.31 and Figure IV.32) are composed of a broad band between 11 and 2 Å characteristic of nearest-neighbor' correlations in amorphous phases. This broad halo does not contain any sharp peaks characteristic of crystallinity. These results indicate that DAT-PPO-*X*-DAT **2a-b** are amorphous (noncrystalline). This confirms the ability of DAT derivatives to form glasses because of their lack of efficient packing.[30,31]
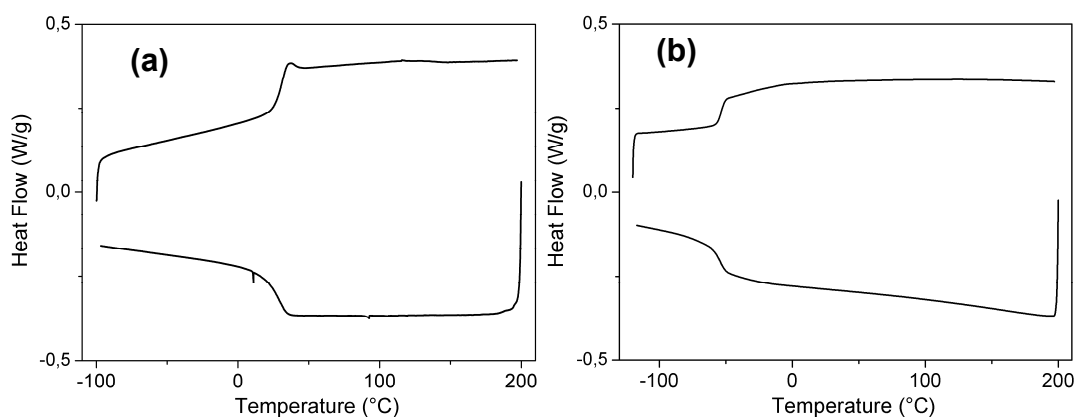
Figure IV.30. DSC at 10°C/min (exo down) of (a) DAT-PPO-460-DAT **2b** and (b) DAT-PPO-2200-DAT **2a**.
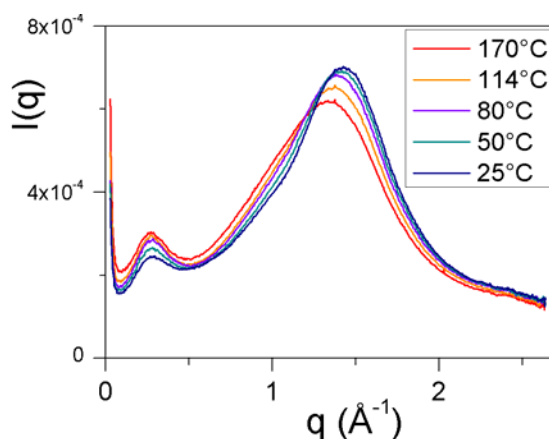
Figure IV.31. X-ray scattering spectra of DAT-PPO-460-DAT **2b** at different temperatures.[32]

---

[32] Performed at the SOLEIL synchrotron source with the beamline SWING allowing simultaneous acquisition of small-angle and wide-angle X-ray scattering (SAXS and WAXS).
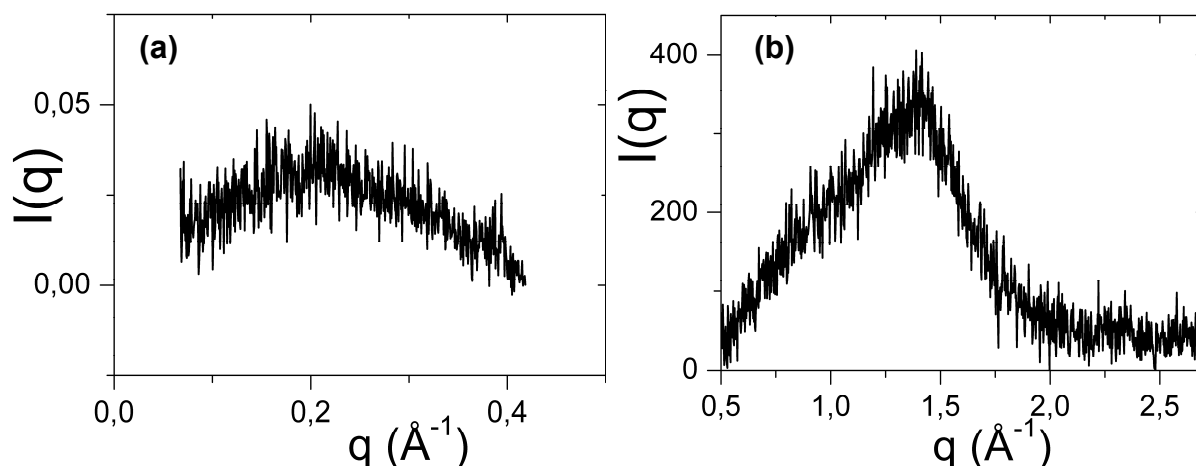
Figure IV.32. (a) SAXS and (b) WAXS spectra, of DAT-PPO-2200-DAT **2a** at room temperature.[33]

(iii) DAT-PPO-*X*-DAT **2a-b** are simple viscous liquids above T_g

The rheology of DAT-PPO-2200-DAT **2a** from -10°C to 120°C (Figure IV.33a) is characteristic of a viscous fluid in the terminal flow regime, with a complex viscosity that is independent of the angular frequency ω, a loss modulus G'' that is higher than the storage modulus G', $G''(\omega) \sim \omega$ and $G'(\omega) \sim \omega^2$. The same behavior is observed for DAT-PPO-460-DAT **2b** from 40°C to 120°C (Figure IV.33b).
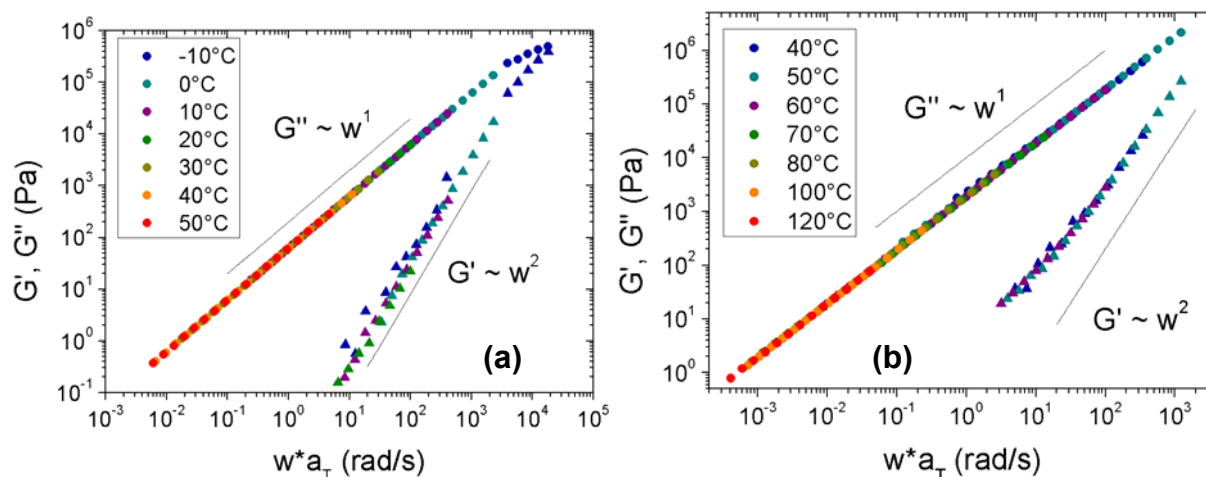

Figure IV.33. Frequency sweeps at different temperatures, shifted according to time-temperature superposition of (a) DAT-PPO-2200-DAT **2a** and (b) DAT-PPO-460-DAT **2b**.

---

[33] Performed with a sealed tube X-ray generator radiation.

(iv) Is DAT-PPO-*X*-DAT **2a-b** uniformly distributed or microphase-separated (with liquid clusters of DAT) ?

A low-intensity peak that scales with the chain length is also observed in the X-ray spectra of DAT-PPO-*X*-DAT **2a-b** (Figure IV.31 and Figure IV.32). We interpret this peak as resulting from the correlation hole effect (see previous part for a detailed explanation).[2a,21] If this peak is indeed a result of the correlation hole effect, it reflects the typical distance between the strongly scattering polar stickers separated by the PPO chain (resulting in the chain length scaling) but does not indicate mesoscopic organization or microphase-separation (clusters). In any case, since there are no harmonics to this peak, DAT-PPO-*X*-DAT **2a-b** are in a disordered state.

However, distinguishing between a "homogeneous" state with strong composition fluctuations and a "microphase-separated" state with no long-range order, but with transient clusters of stickers, is not trivial.[34] Some methods are developed in reference 34 but they are hardly applicable here.

Besides, similar low-intensity and low-frequency peaks observed in the X-ray and neutron scattering spectra of imidazolidium-based room-temperature ionic liquids have often been experimentally interpreted as indicative of nanoscale segregation.[35] Although this hypothesis has not been disproved, it is also possible to explain this peak by simpler consideration (namely by the intrinsic anisotropy of the cations resulting from the long cationic alkyl tail, because the tails are the spacer between the strong scattering polar groups).[35]

Moreover, Wunderlich and Chen reported that amphiphilic molecules may still show some remnants of phase separation in the form of what they call "cybotactic domains" in the isotropic state, which results in an X-ray reflection at low angle with spacing of 6 to 25 Å comparable to the length of the molecules. This means that even in the isotropic state the amphiphilic molecules are not uniformly distributed.[36]

---

[34] Velankar, S.; Cooper, S. L.; **Microphase Separation and Rheological Properties of Polyurethane Melts. 2. Effect of Block Incompatibility on the Microstructure**; *Macromolecules* **2000**, *33*, 382.

[35] Annapureddy, H. V. R.; Kashyap, H. K.; De Biase, P. M.; Margulis, C. J.; **What is the Origin of the Prepeak in the X-ray Scattering of Imidazolium-Based Room-Temperature Ionic Liquids?**; *J. Phys. Chem. B* **2010**, *114*, 16838-16846.

[36] Chen, W.; Wunderlich, B.; **Nanophase separation of small and large molecules**; *Macromol. Chem. Phys.* **1999**, *200*, 283.

Furthermore, X-ray measurements and computer simulation of common amphiphilic liquids such as octan-1-ol show that besides the nearest-neighbor' correlation halo there is a peak below 0.5 Å^{-1}.[35,37] Whether this peak carry relevant information about the structure has been a source of extensive debate, although "perhaps much of the controversy is simply semantics".[35]

Indeed, the knots of the issue are questions of time-scale and length-scale. If clusters form transiently, on very short length scale and time scale, is it fluctuations or nanophase-segregation?

(v) Why is DAT-PPO-*X*-DAT **2a-b** not ordered like Thy-PPO-*X*-Thy **3a-b** ?

To understand why long-range ordering is found for Thy-PPO-*X*-Thy **3a-b** but not for DAT-PPO-*X*-DAT **2a-b**, estimates of the Flory-Huggins interaction parameters (χ) for PPO/DAT ($\chi_{PPO/DAT}$ between 0.5[38] and 3.5[39]) and PPO/Thy ($\chi_{PPO/Thy}$ between 3[38] and 11[39]) can be compared. χ reflects the affinity between two molecules. It can be roughly estimated from the Hildebrand solubility parameters determined by Fedor's or Hansen's method.[40,41] PPO appears to have a weaker affinity for Thy than for DAT, so the microphase segregation driving force is stronger in Thy-PPO-*X*-Thy **3a-b** than in DAT-PPO-*X*-DAT **2a-b**. This could explain why Thy-PPO-*X*-Thy **3a-b** are ordered and DAT-PPO-*X*-DAT **2a-b** are not.

However, the truly important explanation is that the crystallization driving force is not present in DAT-PPO-*X*-DAT **2a-b** as it is in Thy-PPO-*X*-Thy **2a-b**. In addition, Thy crystallization could be promoted by hydrogen bonding between the amide junctions, which are present in Thy-PPO-*X*-Thy but absent in DAT-PPO-*X*-DAT.

---

[37] Morineau, D.; Alba-Simionesco, C.; **Hydrogen-bond-induced clustering in the fragile glass-forming liquid m-toluidine: Experiments and simulations**; *J. Chem. Phys.* **1998**, *109*, 8494.

[38] determined by Hansen's method.

[39] determined by Fedor's method.

[40] Barton, Allan F.M.; *Handbook of Solubility Parameters and Other Cohesion Parameters*; CRC Press: Boca Raton, FL, **1991**.

[41] Van Krevelen, D.W.; *Properties of Polymers - Their Estimation and Correlation with Chemical Structure*; Elsevier: Amsterdam, **1976**.

3. Suppression of mesoscopic order by complementary interactions in supramolecular polymers

In this part, we report that optimization of the directional interactions by strong complementary associations can paradoxically suppress mesoscopic order in telechelic supramolecular polymers with flexible spacers. This effect is due to modifications of the stickers' ability to crystallize and of the sticker-backbone dispersion forces. Consequently, supramolecular polymers having the same backbone but self-complementary or complementary stickers show very different mechanical behaviors (Figure IV.34). When the stickers are weakly self-complementary and mesoscopic order is absent, the material is a liquid (Figure IV.34a). When the stickers are weakly self-complementary and mesoscopic order is present, the material is a solid (Figure IV.34b). When the stickers are strongly complementary and mesoscopic order is absent, the material is a liquid (Figure IV.34c).
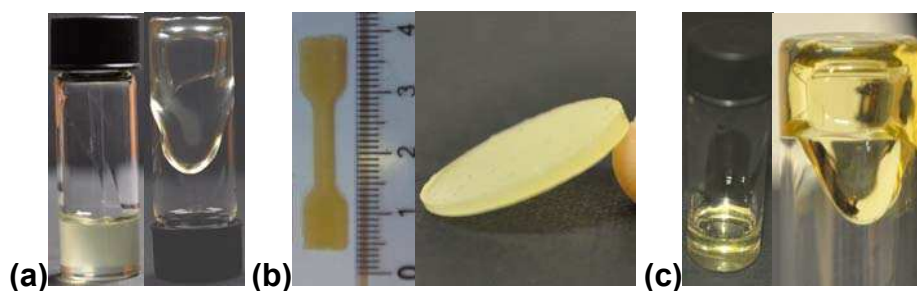
Figure IV.34. Pictures of: (a) a supramolecular polymer with weakly self-complementary stickers (DAT), DAT-PPO-2200-DAT **2a**, which is a liquid, (b) a supramolecular polymer with weakly self-complementary stickers (Thy) and mesoscopic order, Thy-PPO-2200-Thy **3a**, which is a solid, and (c) a supramolecular polymer with strongly complementary stickers (Thy and DAT), 50/50-M-2200 **4a** (i.e., a stoichiometric mixture of Thy-PPO-2200-Thy **3a** and DAT-PPO-2200-DAT **2a**), which is a liquid.

We also report that above the ODT temperature (T_{ODT}), where all of the supramolecular polymers are disordered, their behavior is controlled by the directional interactions. In that case, the viscosities of the supramolecular polymers depend on the association constants.

This part was partially published in reference 42.[42]

---

[42] Cortese, J.; Soulié-Ziakovic, C; Tencé-Girault, S.; Leibler, L.; **Suppression of Mesoscopic Order by Complementary Interactions in Supramolecular Polymers**; *J. Am. Chem. Soc.* **2012**, *134*, 3671.

a. Mesoscopic order and disorder in supramolecular polymers

(i) Supramolecular interactions often lead to ordering

Supramolecular interactions are employed to induce mesoscopic order by self-assembly, as in crystals,[43] liquid crystals,[6,44] bolaamphiphiles,[45] or polymer-surfactant systems.[46] We described above the long-range order and ODT of a homoditopic telechelic supramolecular polymer.[1] Homoditopic telechelic supramolecular polymers (A-spacer-A and B-spacer-B) consist of bifunctional molecular units linked together through directional and reversible noncovalent bonds (such as hydrogen bonds or π-π stacking) between the A and B stickers.[7] In our system described in part 1 of this chapter (A = B = Thy),[1] the long-range order was driven by dispersion forces between the stickers and the spacer, crystallization of the stickers, and directional interactions between the stickers.

(ii) Yet textbook supramolecular polymers are disordered

When only the directional interactions dictate their behavior, telechelic supramolecular polymers [(A-spacer-A=B-spacer-B)$_n$] are disordered. They may display reversible polymer-like properties in solution and in the bulk. Their viscosity increases with the average degree of polymerization (DP = n), which increases with the thermodynamic association constant (K_{AB}) of the A and B stickers.[7] For hydrogen-bonded supramolecular polymers, the viscosity

---

[43] (a) ***The Crystal as a Supramolecular Entity***; Desiraju, G. R., Ed.; Persepectives in Supramolecular Chemistry Vol. 2*; Wiley: Chichester, England, **1996**. (b) Cao, Y. W.; Chai, X. D.; Li, T. J.; Smith, J.; Li, D.; **Self-patterned H-bond supramolecular self-assembly**; *Chem. Commun.* **1999**, 1605. (c) Manzano, B. R.; Jalon, F. A.; Soriano, M. L.; Rodriguez, A. M.; de la Hoz, A.; Sanchez-Migallon, A.; **Multiple Hydrogen Bonds in the Self-Assembly of Aminotriazine and Glutarimide. Decisive Role of the Triazine Substituents**; *Cryst. Growth Des.* **2008***, 8*, 1585.

[44] Brienne, M.-J.; Gabard, J.; Lehn, J.-M.; Stibor, I.; **Macroscopic expression of molecular recognition. Supramolecular liquid crystalline phases induced by association of complementary heterocyclic components**; *J. Chem. Soc., Chem. Commun.,* **1989***, 24*, 1868.

[45] (a) Fuhrhop, J.-H. ; Wang, T.; **Bolaamphiphiles**; *Chem. Rev.* **2004***, 104*, 2901. (b) Iwaura, R.; Iizawa, T.; Minamikawa, H.; Ohnishi-Kameyama, M. ; Shimizu, T.; **Diverse Morphologies of Self-Assemblies from Homoditopic 1,18-Nucleotide-Appended Bolaamphiphiles: Effects of Nucleobases and Complementary Oligonucleotides**; *Small* **2010***, 6*, 1131.

[46] (a) Ruokolainen, J.; Mäkinen, R.; Torkkeli, M.; Mäkelä, T.; Serimaa, R.; ten Brinke, G.: Ikkala, O.; **Switching Supramolecular Polymeric Materials with Multiple Length Scales**; *Science* **1998***, 280*, 557. (b) Ikkala, O.; ten Brinke, G.; **Functional Materials Based on Self-Assembly of Polymeric Supramolecules**; *Science* **2002***, 295*, 2407.

decreases as the temperature increases because the hydrogen bonds are released and the association lifetime decreases.[7]

(iii) But many supramolecular polymers are organized

However, incompatibility between the spacers and the stickers and crystallization of the stickers can induce organization. Clusterization[11,12,13,14,15] - with[14,15] or without[12a,12i] crystallization of the stickers - as well as long-range order[1,11] have been evidenced in many supramolecular polymers based on self-complementary associations (A = B). The organization controls the mechanical properties: stickers domains act as physical cross-links, causing behavior typical of thermoplastic elastomers.[11,12,13,14,15]

Organization has also been reported in supramolecular polymers based on complementary[47] associations (A ≠ B). Lehn, Rowan, and their coworkers obtained liquid crystals from telechelic supramolecular polymers where A and B are two different stickers that strongly associate with one another but weakly self-associate.[48] Liquid crystallinity was obtained in part because the spacers used were rigid.

## b. Suppression of mesoscopic order by complementary interactions in supramolecular polymers

(i) Supramolecular polymers used in this study: $\phi/(100-\phi)$-M-X

The supramolecular polymers used in this study are based on noncrystalline and low-molecular-weight poly(propylene oxide) (PPO) chains functionalized on both ends with

---

[47] Park, T.; Zimmerman, S. C.; **Formation of a Miscible Supramolecular Polymer Blend through Self-Assembly Mediated by a Quadruply Hydrogen-Bonde Heterocomplex**; *J. Am. Chem. Soc.* **2006**, *128*, 11582.

[48] (a) Fouquey, C.; Lehn, J.-M.; Levelut, A.-M.; **Molecular recognition directed self-assembly of supramolecular liquid crystalline polymers from complementary chiral components**; *Adv. Mater.* **1990**, *2*, 254. (b) Kotera, M.; Lehn, J.-M.; Vigneron, J.-P.; **Self-assembled Supramolecular Rigid Rods**; *J. Chem. Soc.*, **1994**, *2*, 197-199. (c) Gulik-Krzywicki, T.; Fouquey, C.; Lehn, J.-M.; **Electron microscopic study of supramolecular liquid crystalline polymers formed by molecular-recognition-directed self-assembly from complementary chiral components**; *Proc. Natl. Acad. Sci. U.S.A.* **1993**, *90*, 163. (d) Sivakova, S.; Rowan, S. J.; **Fluorescent supramolecular liquid crystalline polymers from nucleobase-terminated monomers**; *Chem. Commun.* **2003**, *19*, 2428. (e) Sivakova, S.; Wu, J.; Campo, C. J.; Mather, P. T. ; Rowan, S. J.; **Liquid-Crystalline Supramolecular Polymers Formed through Complementary Nucleobase-Pair Interactions**; *Chem. Eur. J.* **2006**, *12*, 446.

thymine (Thy) or diaminotriazine (DAT) groups (Chart IV.3a,b). They are denoted as ϕ/(100-ϕ)-M-X **4a-b**, **5a**, **6a** (**a**: X = 2200, **b**: X = 460; **4**: ϕ = 50, **5**: ϕ = 25, **6**: ϕ = 75). X is the molecular weight (in g.mol^{-1}) of the PPO spacer, and ϕ/(100-ϕ)-M-X **4a-b**, **5a**, **6a** indicates a mixture (M) of ϕ % Thy-PPO-X-Thy **4a-b** and (100-ϕ) % DAT-PPO-X-DAT **4a-b**. The preparation of ϕ/(100-ϕ)-M-X **4a-b**, **5a**, **6a** is described in Chapter II.
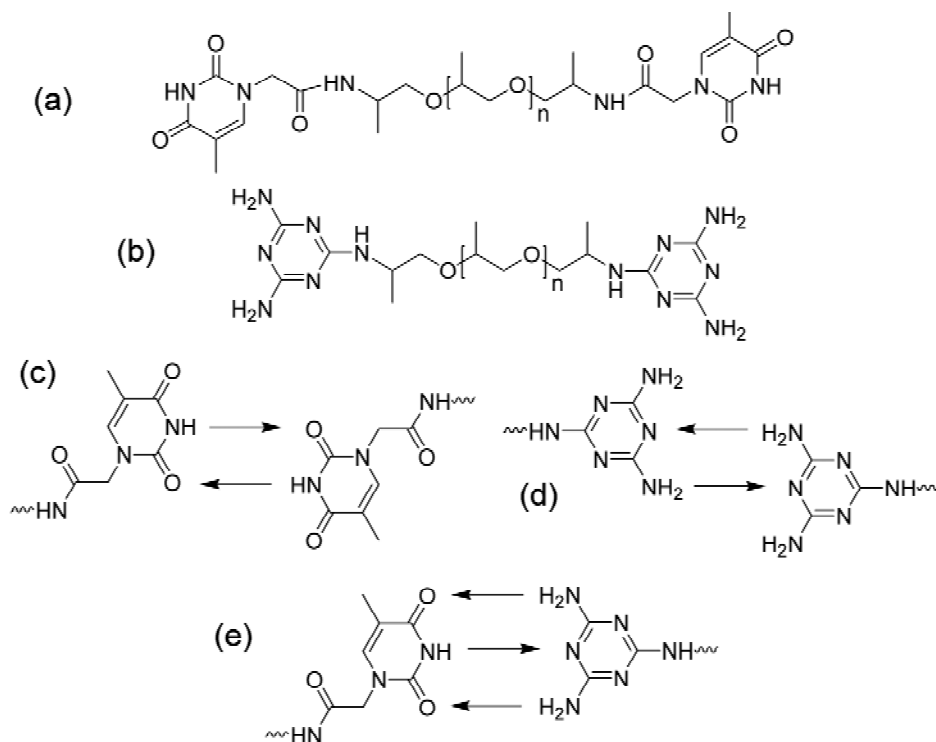
Chart IV.3. (a) Thy-PPO-X-Thy **3a-b**, (b) DAT-PPO-X-DAT **2a-b**, (c) Thy-Thy self-association, (d) DAT-DAT self-association, and (e) Thy-DAT complementary association.

Thy and DAT can associate with one another through self- and hetero-complementary hydrogen bonding (Chart IV.3c,d,e).[49] Thy-DAT complementary association is much stronger than the Thy-Thy and DAT-DAT self-association, as evidenced by the differences in the thermodynamic binding constants: $K_{\text{Thy-DAT}}$ = 890 M^{-1} versus $K_{\text{DAT-DAT}}$ = 2.2 M^{-1} and $K_{\text{Thy-Thy}}$ = 4.3 M^{-1} (as determined by ^{1}H NMR spectroscopy in CDCl$_3$).[49]

Therefore, three different phenomena can concur and compete in the bulk: hydrogen bonding between the stickers, phase segregation between the PPO chains and the stickers, and crystallization of the thymines into microdomains. This system can then be used to underline

---

[49] Beijer, F. H.; Sijbesma, R. P.; Vekemans, J. A. J. M.; Meijer, E. W.; Kooijman, H.; Spek, A. L.; **Hydrogen-Bonded Complexes of Diaminopyridines and Diaminotriazines: Opposite Effect of Acylation on Complex Stabilities**; *J. Org. Chem.* **1996**, *61*, 6371.

the respective effects of hydrogen bonding, phase segregation, and the ability of the stickers to crystallize on the structure.

The bulk behaviors of our homoditopic compounds Thy-PPO-*X*-Thy **3a-b** and DAT-PPO-*X*-DAT **2a-b** and their mixtures 50/50-M-*X* **4a-b**, 75/25-M-2200 **5a**, 25/75-M-2200 **6a** were investigated by structural (X-ray scattering, polarized optical microscopy), thermal (differential scanning calorimetry [DSC]), rheological and mechanical characterizations.

(ii) Thy-PPO-*X*-Thy **3a-b** is ordered at room temperature, but not DAT-PPO-*X*-DAT **2a-b**

As described in detail in the first part of this chapter, Thy-PPO-*X*-Thy **3a-b** exhibit two distinct orderings below T_{ODT} (67°C for $X = 2200$, 109°C for $X = 460$): a crystalline ordering and a lamellar ordering (of *d*-spacing of 60 Å for $X = 2200$ and 28 Å for $X = 460$). The lamellar structure consists of alternating two-dimensional crystallized thymine planes and amorphous PPO layers. This microphase segregation seems to be crystallization-driven. As a result, these materials are solid below T_{ODT} (Figure IV.34a), even above their glass transition temperature ($T_g = 24$°C for $X = 460$ and -62°C for $X = 2200$). At T_{ODT}, a transition to a disordered state occurs, and these materials become liquid.

In contrast, DAT-PPO-*X*-DAT **2a-b** show no order, as detailed in the second part of this chapter.

## (iii) 50/50-M-*X* **4a-b** is not ordered

DSC (Figure IV.35a and Figure IV.36), polarized optical microscopy, rheology (Figure IV.37a) and X-ray-scattering (Figure IV.35b) of 50/50-M-*X* **4a-b** show that these mixtures behave exactly as neat DAT-PPO-*X*-DAT **2a-b**. Indeed, their X-ray scattering spectra at 25 °C (Figure IV.35b) display a broad halo between 11 and 2 Å resulting from nearest-neighbor correlations, without any sharp peak characteristic of crystallinity. They also display a low-intensity peak resulting from correlation hole effect that scales with the chain length. Moreover, they display only a glass transition step in DSC (Figure IV.35a and Figure IV.36), show no birefringence in polarized optical microscopy images, and their rheology (Figure IV.37a) is characteristic of a viscous fluid in the terminal flow regime.
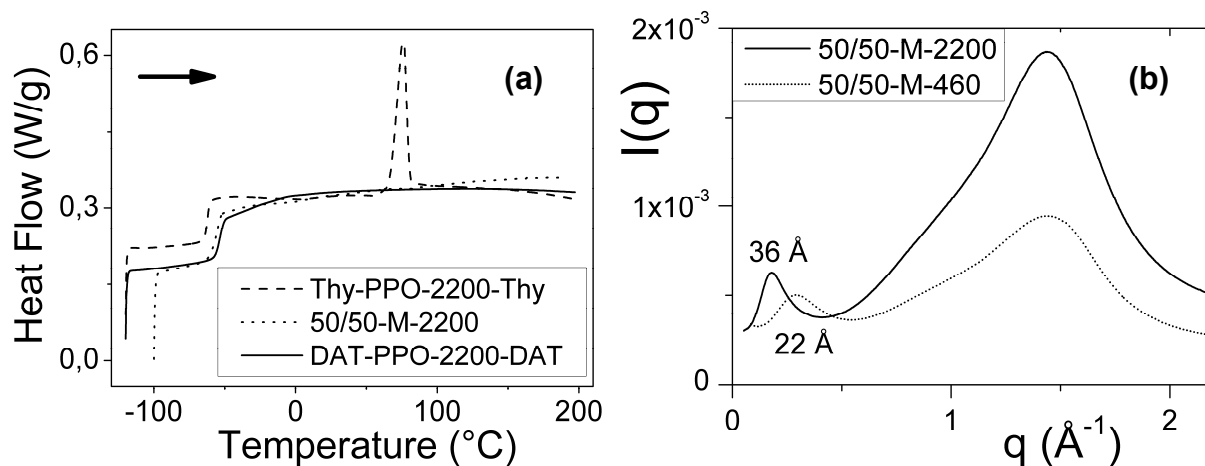
Figure IV.35. (a) DSC at 10°C/min (exo down) of DAT-PPO-2200-DAT **2a**, 50/50-M-2200 **4a**, Thy-PPO-2200-Thy **3a**; (b) X-ray scattering at 25°C of 50/50-M-*X* **4a-b**.
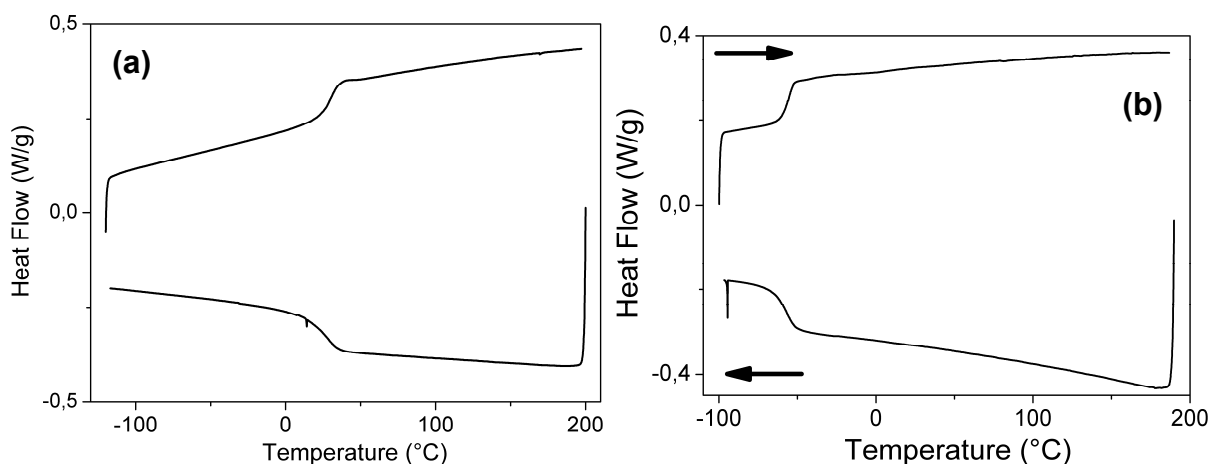

Figure IV.36. DSC at 10°C/min (exo down) of (a) 50/50-M-460 **4b** and (b) 50/50-M-2200 **4a**.
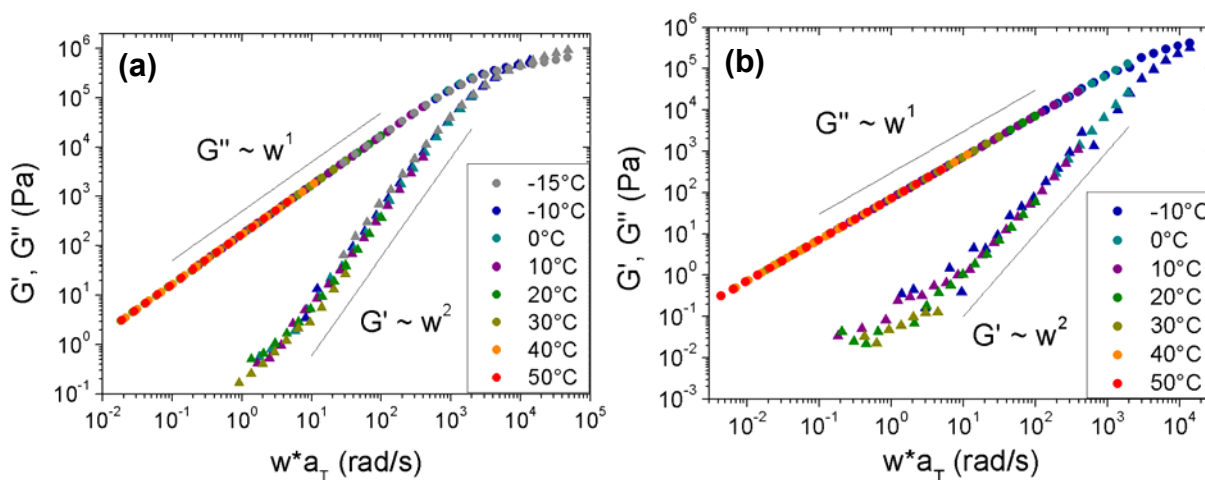

Figure IV.37. Frequency sweeps at different temperatures, shifted according to time-temperature superposition of (a) 50/50-M-2200 **4a** and (b) 25/75-M-2200 **5a**.

Thus, 50/50-M-*X* **4a-b** are amorphous (noncrystalline) and do not present well ordered structure, in contrast to Thy-PPO-*X*-Thy **3a-b**. The presence of the DAT groups seems to inhibit the crystallization of thymine and the subsequent formation of the lamellar structure of crystallized thymine planes and PPO layers. This underlines the existence of a selective Thy-DAT interaction in the bulk state. In fact, the disorder in 50/50-M-*X* **4a-b** stems from the strong directional interactions between the Thy and DAT stickers: Thy no longer crystallizes when it is linked to DAT, and the dispersions interactions are weaker because DAT has more affinity with PPO than Thy ($\chi_{DAT/PPO} < \chi_{Thy/PPO}$).

The existence of a selective Thy-DAT interaction in the bulk state is further confirmed by bulk ^{1}H NMR measurements. Indeed, 2D correlation of simple and double quanta ^{1}H show that, in Thy-PPO-460-Thy **3b**, Thy NH **D** protons correlate with other Thy NH **D** protons (Figure IV.38a), which means that a Thy NH **D** proton is in close proximity of another Thy NH **D** proton. That is achieved when Thy groups are self-associated (see representation of Thy self-association in Figure IV.38a). Similarly, in DAT-PPO-460-DAT **2b**, DAT NH$_2$ **Ψ** protons correlate with other DAT NH$_2$ **Ψ** protons (Figure IV.38b), so a DAT NH$_2$ **Ψ** proton is in close proximity of another DAT NH$_2$ **Ψ**, is achieved when DAT groups are self-associated (see representation of DAT self-association in Figure IV.38b). In contrast, in 50/50-M-460 **4b** Thy NH **D** protons do not correlate with other Thy NH **D** protons and DAT NH$_2$ **Ψ** protons do not correlate with other DAT NH$_2$ **Ψ** protons, but Thy NH **D** protons correlate with DAT NH$_2$ **Ψ** protons (Figure IV.39). Therefore, Thy and DAT are associated with one another and not self-associated.
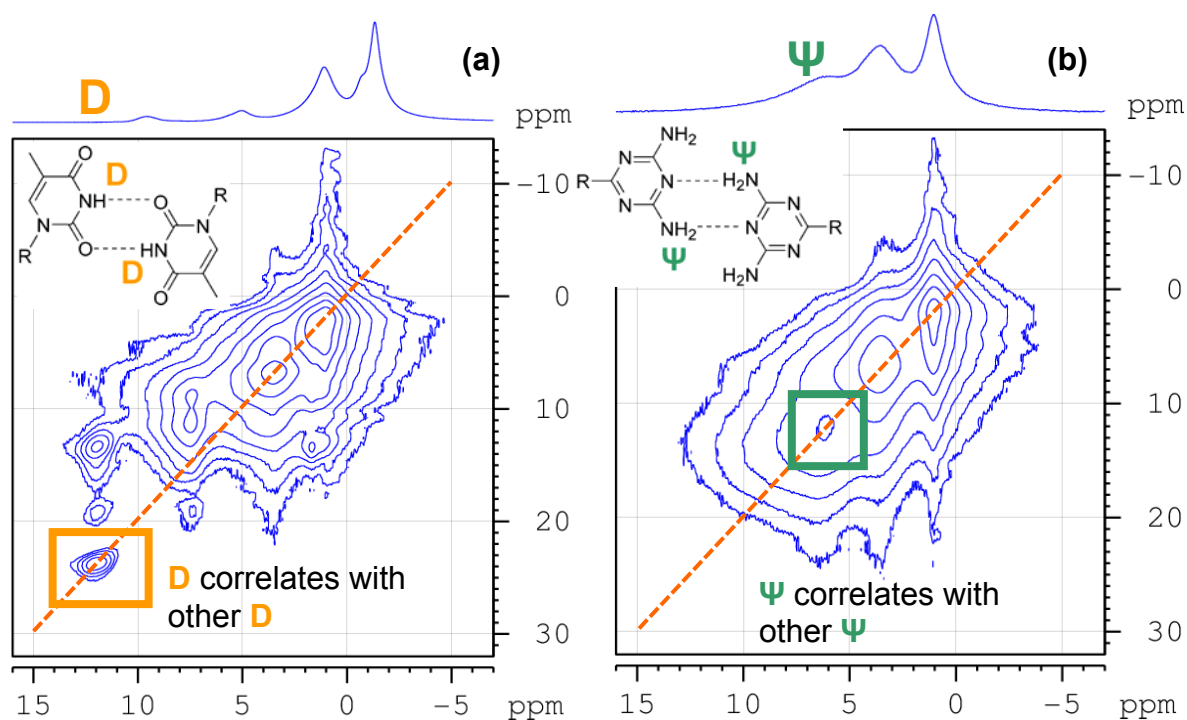
Figure IV.38. 2D bulk ^{1}H NMR at 25°C (correlation simple quanta ^{1}H – double quanta ^{1}H) of:
(a) Thy-PPO-460-Thy **3b** and (b) DAT-PPO-460-DAT **2b**. Rotation speed is 60 kHz.
On the horiontal axis and on the spectra above the card is the simple quanta ^{1}H NMR (simple impulsion).
On the vertical axis is the double quanta ^{1}H NMR ("BaBa" excitation of double quanta,
one rotation, excitation time = 16.6 µs).
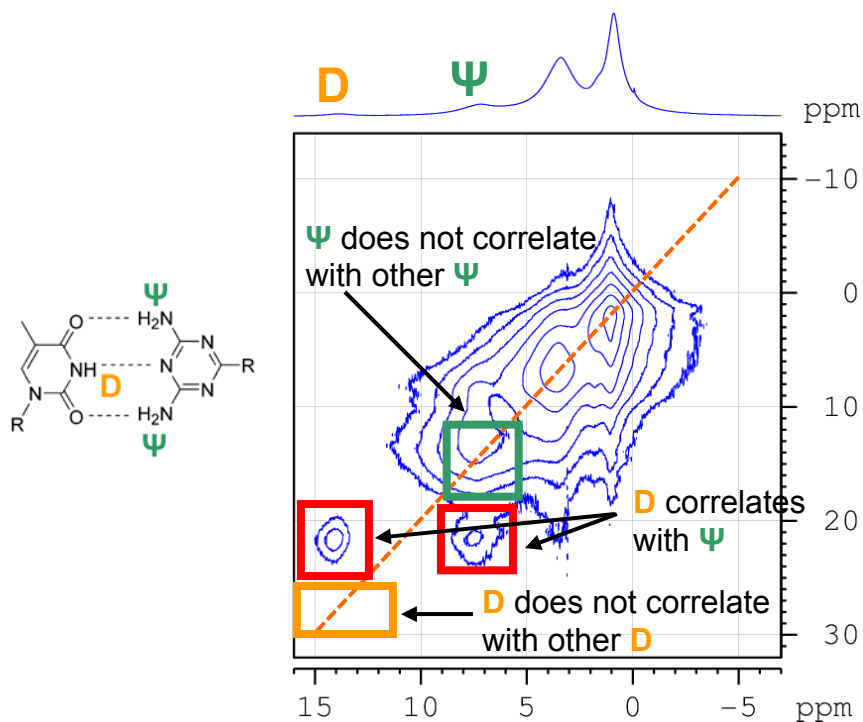
Figure IV.39. 2D bulk ^{1}H NMR at 25°C (correlation simple quanta ^{1}H – double quanta ^{1}H) of 50/50-PPO-460
4b. On the horiontal axis and on the spectra above the card is the simple quanta ^{1}H NMR (simple impulsion).
On the vertical axis is the double quanta ^{1}H NMR ("BaBa" excitation of double quanta,
one rotation, excitation time = 16.6 µs). Rotation speed is 60 kHz.

(iv) 25/75-M-2200 **5a** is not ordered

Again, DSC (Figure IV.40a), polarized optical microscopy, rheology (Figure IV.37b) and X-ray-scattering (Figure IV.40b) of 25/75-M-2200 **5a** (25% Thy-PPO-2000-Thy **3a** and 75% DAT-PPO-2000-DAT **2a**), indicate that this mixture behaves like DAT-PPO-2200-DAT **2a** and 50/50-M-2200 **4a**. Thus, 25/75-M-2200 **5a** is amorphous (noncrystalline), as expected since the DAT moieties are in excess relative to the Thy moieties. Therefore, all the Thy moieties are associated with DAT and cannot crystallize.
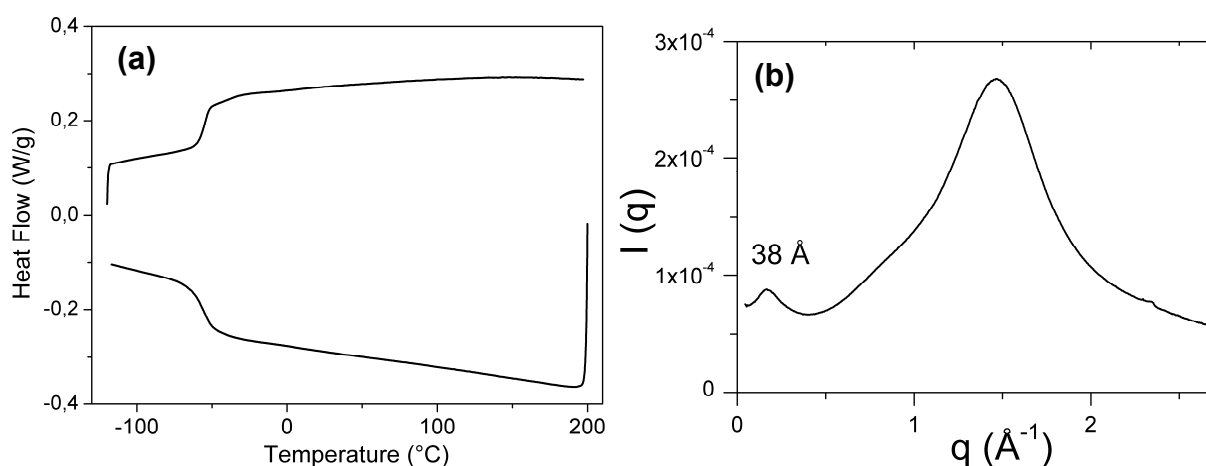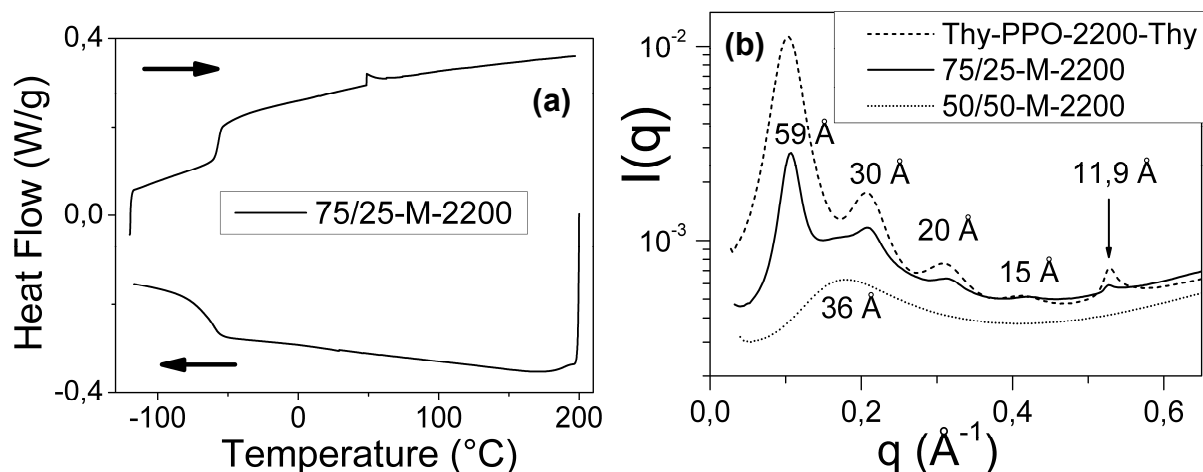

Figure IV.40. (a) DSC at 10°C/min (exo down) and (b) X-ray scattering spectra at 25°C, of 25/75-M-2200 **5a**.

(v) 75/25-M-2200 **6a** is somewhat ordered

In contrast, 75/25-M-2200 **6a** (the mixture containing 75% Thy-PPO-2200-Thy **3a** and 25% DAT-PPO-2200-DAT **2a**), displays in the heating cycle of DSC (Figure IV.41a) a 'melting' endotherm, in addition to a glass transition step. This 'melting' endotherm has a very low intensity but is reproducible. Its enthalpy of fusion (2 J/g) is quite low compared with that of Thy-PPO-2200-Thy **3a** (15 J/g). Polarized optical microscopy images of 75/25-M-2200 **6a** show that it is birefringent, with Maltese crosses and spherulites (Figure IV.42).

Its X-ray scattering spectrum at 25°C (Figure IV.41b) reveals a sharp peak at 11.9 Å characteristic of the Thy crystallinity in Thy-PPO-2200-Thy **3a**. It also reveals peaks corresponding to a lamellar structure at the same positions as for Thy-PPO-2200-Thy **3a**. Moreover, the X-ray pattern shows what seems to be a correlation hole peak, surimposed with the lamellar peaks, at the same position as the one for 50/50-M-2200 **4a**.

Figure IV.41. (a) DSC at 10°C/min (exo down) of 75/25-M-2200 **6a**; (b) X-ray scattering at 25°C of 75/25-M-2200 **6a**, 50/50-M-2200 **4a** and Thy-PPO-2200-Thy **3a**.
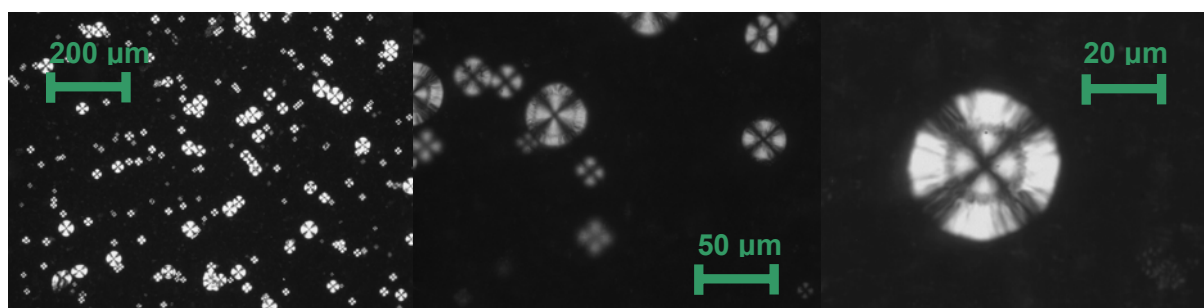

Figure IV.42. Polarized optical microscopy of 75/25-M-2200 **6a**.

These results suggest that 75/25-M-2000 **6a** is semicrystalline as a result of crystallization of the excess Thy moieties. While DAT groups are available, Thy groups associate with them and result in non-crystallizable Thy-DAT units. Excess of Thy functionalities is free to crystallize in 2D-planes and form a lamellar structure, with the PPO chains in between the crystallized thymine planes. Therefore, there is a coexistence of disordered and ordered phases.

(vi) Viscosities above T_{ODT}

At high temperatures, crystallization and mesoscopic structuration are no longer present in Thy-PPO-2200-Thy **3a**. In that temperature range, the viscosity of 50/50-M-2200 **4a** is higher than those of Thy-PPO-2200-Thy **3a** and DAT-PPO-2200-DAT **2a** (Figure IV.43). This viscosity effect can be attributed to the higher DP of the mixture because of the higher association constant between Thy and DAT than between Thy and Thy or DAT and DAT. The classical vision of telechelic supramolecular polymers in bulk can then be applied.

Since the chain extension is due to hydrogen bonding, the viscosity decreases as the temperature increases, as observed in Figure IV.43. Indeed, the hydrogen bonds are released as the temperature increases, in agreement with FT-IR data (Figure IV.44 and Figure IV.45). These effects are traditional supramolecular polymer effects.
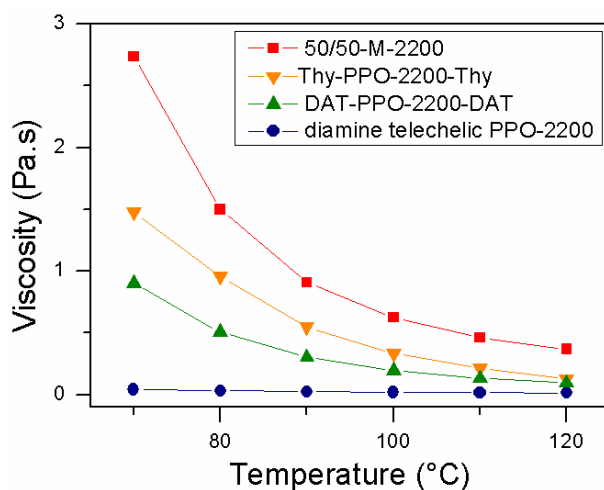
Figure IV.43. Viscosity as a function of temperature for diamine telechelic NH_2-PPO-2200-NH_2 **1a**, DAT-PPO-2200-DAT **2a**, Thy-PPO-2200-Thy **3a**, and 50/50-M-2200 **4a**.
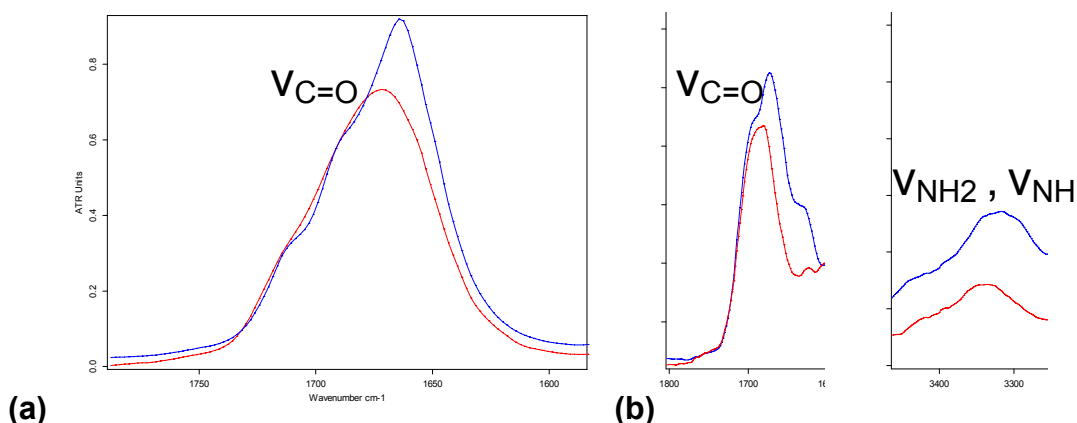
Figure IV.44. FT-IR of stickers' bonds involved in hydrogen bonding (a) Thy-PPO-460-Thy **3b** at 60°C (in blue) and 120°C (in red) and (b) 50/50-M-460 **4b** at 30°C (in blue) and 180°C (in red).
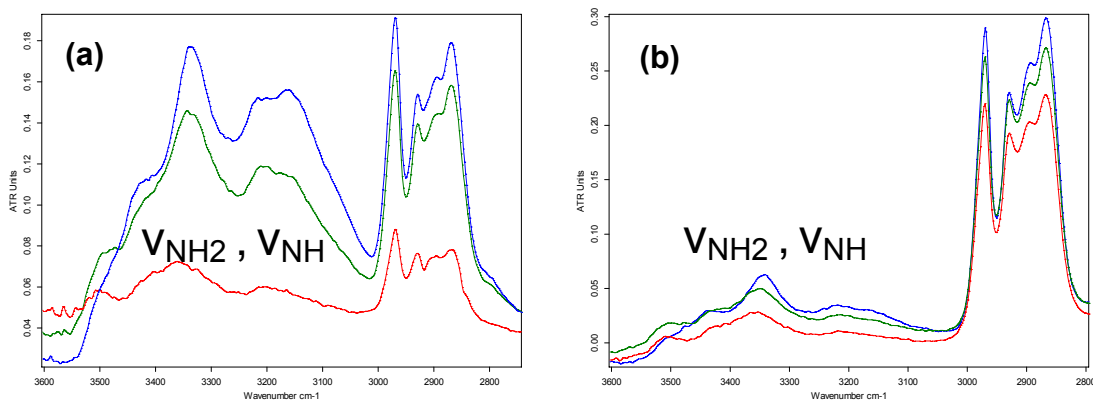
Figure IV.45. FT-IR of stickers' bonds involved in hydrogen bonding at 30°C (in blue), 100°C (in green) and 180°C (in red) of (a) DAT-PPO-460-DAT **2b** and (b) DAT-PPO-2200-DAT **2a**.

(vii) Conclusion and Perspectives

To conclude, contrary to Thy-PPO-*X*-Thy **3a-b**, DAT-PPO-*X*-DAT **2a-b** (*X* = 460, 2200) show no long-range organization because the crystallization driving force is not present in DAT derivatives and the phase segregation is weaker. In the 50:50 Thy-PPO-*X*-Thy / DAT-PPO-*X*-DAT mixtures **4a-b**, the complementary association between Thy and DAT is strong enough to control the structure by inhibiting the Thy crystallization and the lamellar organization. The impact on the mechanical properties is crucial.

For amorphous and flexible spacers, the main factor to take into account for long-range order seems to be the crystallization of the stickers. Indeed, if it takes place, the ordering can appear whatever the segregation force between the spacer and the stickers

.

However, if there is no crystallization of the stickers, long-range order may also occur if the segregation is strong enough. Binder and his co-workers evidenced the long-range order of a supramolecular amphiphile consisting of monofunctional poly(isobutylene) (PIB) bearing a diaminotriazine chain-end (PIB-3500-DAT).[11] $\chi_{PPO/DAT}$ = 3.5 is lower than $\chi_{PIB/DAT}$ = 6.1,[39,40] illustrating that DAT has a weaker affinity for PIB than for PPO, and possibly justifying why PIB-3500-DAT is ordered while DAT-PPO-*X*-DAT **2a-b** are not.[50] Hence, for polar functional groups, when the backbone is also rather polar, little tendency for long-range mesoscopic organization is expected in comparison with less polar backbones such as PPO.

To complete the understanding of the interplay between mesophase formation and thermomechanical behavior, it will be interesting to explore the structure and dynamics of systems in which incompatibility between the spacers and the stickers can induce long-range order but the stickers do not crystallize.

---

[50] The control parameter actually is (χ.n) / z where n is the degree of polymerization and z is the functionality:
n ~ 70, z = 1 for PIB-3500-DAT;
n ~ 40, z = 2 for DAT-PPO-2200-DAT **2a**;
n ~ 8, z = 2 for DAT-PPO-460-DAT **2b**.

Chapter V

Glass transition
of supramolecular polymers
in the bulk

Grafting Thy and DAT stickers on telechelic PPO oligomers induces a glass transition temperature (T_g) increase that plays an important role on the materials properties. Indeed, as a result DAT-PPO-X-DAT **2b-c**, Thy-PPO-X-Thy **3b-c**, and 50/50-M-X **4b-c** (**b**: X = 460, **c**: X = 250) are solids at room temperature whereas homologues with longer spacer (**a**: X = 2200) are liquids at room temperature. This increase of T_g can be ascribed either to the presence of hydrogen bonds and/or aromatic interactions (π-stacking) slowing down the chain dynamics or to the stiffness of the Thy and DAT stickers.

Chapter V. Glass transition of supramolecular polymers in the bulk

a. Glass transition temperature (T_g) of supramolecular polymers

Grafting hydrogen-bonding stickers on polymeric or oligomeric backbones can induce an increase in the glass transition temperature (T_g) of the backbones. For instance, Long and his coworkers reported an important increase of the T_g of stickers-end-functionalized compared to nonfunctionalized or hydroxyl-terminated polymers.[1] Similar increase of T_g for side-chain functionalized polymers were reported by Long and his coworkers,[2] by Feldman *et al.*,[3] both for UPy stickers, and by Kuo and Tsai for Thy and DAT stickers.[4] Moreover, T_g increased linearly as the UPy content increased.[2,3] This increase of T_g was ascribed either to the presence of hydrogen bonds slowing down the chain dynamics or to more straightforward steric effects.[3]

b. Supramolecular polymers used in this study

The supramolecular polymers used in this study consist of low-molecular-weight poly(propylene oxide) (PPO) oligomers functionalized on both ends with thymine (Thy) or diaminotriazine (DAT) groups. They are denoted as Thy-PPO-*X*-Thy **3a-c** (Chart V.1a), DAT-PPO-*X*-DAT **2a-c** (Chart V.1b), and 50/50-M-*X* **4a-c** for the 50/50 mixture of **3a-c** and **2a-c**, with *X* the molecular weight of the PPO chain (**a**: $X = 2200$, **b**: $X = 460$, **c**: $X = 250$). Their synthesis is described in Chapter II.

---

[1] Yamauchi, K.; Lizotte, J. R.; Hercules, D. M.; Vergne, M. J.; Long, T. E.; **Combinations of microphase separation and terminal multiple hydrogen bonding in novel macromolecules** *J. Am. Chem. Soc.* **2002**, *124*, 8599.

[2] Yamauchi, K.; Lizotte, J. R. ; Long, T. E.; **Thermoreversible poly(alkyl acrylates) consisting of self-complementary multiple hydrogen bonding**; *Macromolecules* **2003**, *36*, 1083.

[3] Feldman, K. E.; Kade, M. J.; Meijer, E.; Hawker, C. J.; Kramer, E. J.; **Model transient networks from strongly hydrogen-bonded polymers**; *Macromolecules* **2009**, *42*, 9072.

[4] Kuo, S.-W.; Tsai, H.-T.; **Complementary multiple hydrogen-bonding interactions increase the glass transition temperatures to PMMA copolymer mixtures**; *Macromolecules* **2009**, *42*, 4701.

Thy and DAT can associate with one another through self- and hetero-complementary hydrogen bonding (Chart V.1c,d,e).[5] The Thy-DAT complementary association has a much higher thermodynamic binding constant than the Thy-Thy and DAT-DAT self-associations, in chloroform, in toluene (see Chapter III) and in the bulk (see Chapter IV).

Three lengths of PPO chain are used: 250, 460 and 2200 g/mol. The percentage of stickers in the material decreases when the chain length increases. Therefore, this system can be used to evaluate the effects of the Thy and DAT stickers on the T_g.
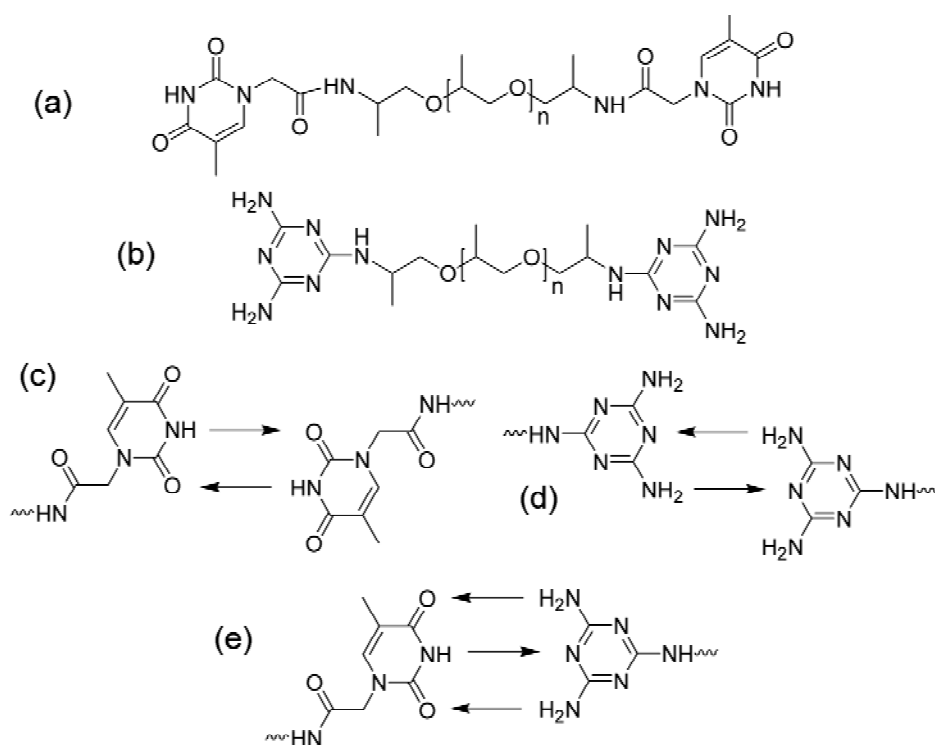
Chart V.1. (a) Thy-PPO-*X*-Thy **3a-c**, (b) DAT-PPO-*X*-DAT **2a-c**, (c) Thy-Thy self-association, (d) DAT-DAT self-association, and (e) Thy-DAT complementary association.

c. Effect of the Thy and DAT stickers on the T_g

(i) T_g determined by DSC and DRS

Glass transition temperatures (T_g) were determined by differential scanning calorimetry (DSC) and/or dielectric relaxation spectroscopy (DRS) (Table V.1).

---

[5] Beijer, F. H.; Sijbesma, R. P.; Vekemans, J. A. J. M.; Meijer, E. W.; Kooijman, H.; Spek, A. L.; **Hydrogen-bonded complexes of diaminopyridines and diaminotriazines: opposite effect of acylation on complex stabilities**; *J. Org. Chem.* **1996**, *61*, 6371.

Compound	T_g (°C) from DSC	T_g (°C) from DRS
NH₂-PPO-2200- NH₂ **1a**	- 72	- 72
NH₂-PPO-460- NH₂ **1b**	- 82	-
NH₂-PPO-250- NH₂ **1c**	- 85	-
DAT-PPO-2200-DAT **2a**	- 54	- 53
DAT -PPO-460-DAT **2b**	30	-
DAT-PPO-250-DAT **2c**	93	-
Thy-PPO-2200-Thy **3a**	- 62	- 63
Thy-PPO-460-Thy **3b**	28	-
Thy-PPO-250-Thy **3c**	98	-
Thy-PPO-250-Thy **3c** with 10% impurities (salt and DIEA)	77	-
50/50-M-2200 **4a**	- 55	- 55
50/50-M-460 **4b**	30	-
50/50-M-250 **4c**	98	-

Table V.1. T_g determined by DSC and DRS.

(ii) T_g can also be determined by IR

Thy-PPO-250-Thy **3c**'s glass transition can also be evidenced by temperature-dependent FT-IR spectroscopy. Indeed, the elongation vibration $\nu_{C=O}$ of a C=O bond is shifted towards smaller wavenumbers if the C=O bond is implicated in hydrogen bonds (because the bond is then stretched). Thy-PPO-250-Thy **3c** contains three types of C=O bonds, two from the thymine cycle and one from the amide linker. When free C=O and implicated in hydrogen bonds C=O coexist, six $\nu_{C=O}$ bands are thus expected. However, the spectra are not resolved enough to distinguish them, but the global trend can be studied. The broad signal shifts towards smaller wavenumbers as the temperature is decreased, from 1662 cm⁻¹ at 190°C to 1656 cm⁻¹ at 30°C (Figure V.1), indicating that there are more hydrogen bonds. Moreover, a modification of slope is observed at temperatures corresponding to the T_g previously determined by DSC and DRS.
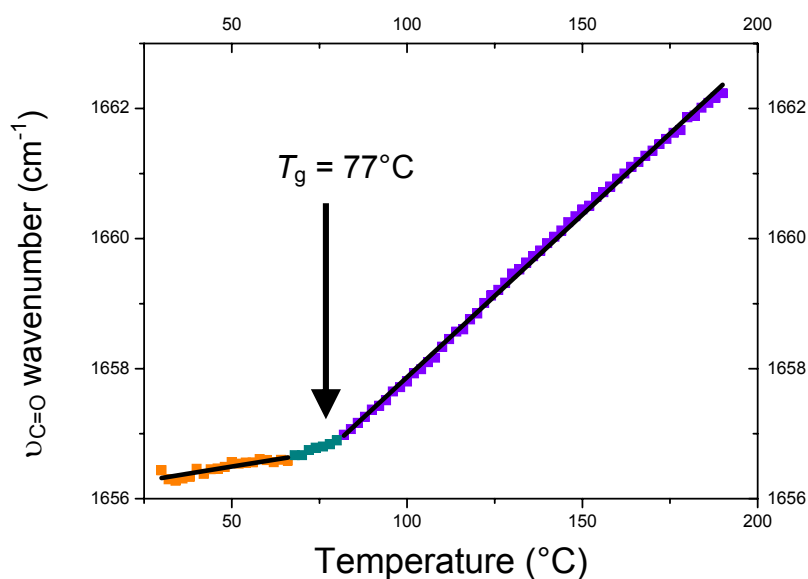
Figure V.1. T_g determination of Thy-PPO-250-Thy **3c** by temperature-dependant FT-IR in ATR mode (this sample contained impurities so T_g was lower than for the more pure Thy-PPO-250-Thy **3c** discussed in the following pages).

(iii) Free-end effect for polymers and oligomers

For polymers and oligomers, decreasing the molecular weight decreases the T_g because of the free-end effect.[6] Indeed, a sample of shorter chains contains more free-ends than a (same-volume) sample of longer chains, and end-chain units have more free volume than units within the chain. Therefore, samples of shorter chains have more free volume and thus lower T_g's, since T_g is reached when the free space available for molecular motions becomes very low. The empirical Flory-Fox equation modelizes the free-end effect by relating the T_g to the number-average molecular weight M_n, the maximum glass transition T_g^{∞} for a theoretical infinite chain, and an empirical parameter k [equation (1)].

$$T_g = T_g^{\infty} - \frac{k}{M_n} \tag{1}$$

As expected according to the free-end effect, the T_g of CH_3-PPO-CH_3 increases with its molar mass (Figure V.2).[7]

---

[6] Sperling, L. H.; ***Introduction to physical polymer science***, Wiley-Interscience, **1996**.

[7] Yoon, S.; MacKnight, W. J.; Hsu, S. L.; **End-group effect on chain conformation of poly(propylene glycol) and poly(ethylene glycol)**; *J. Appl. Polym. Sci.* **1997**, *64*, 197.

(iv) Reduction of free-end effect for dihydroxy and diamino telechelic PPO

However, the T_g of HO-PPO-OH depends very weakly on the molecular weight (Figure V.2).[8] This absence of the free-end effect is ascribed to hydrogen bonding of the hydroxyl end groups, which reduces mobility of the chain ends.[8,9,10] The T_g of NH_2-PPO-NH_2 **1a-c** increases weakly with the molecular weight (Figure V.2). The free-end effect is reduced here because of hydrogen bonding, but not absent maybe because NH_2 hydrogen bonds are weaker than OH hydrogen bonds.

(v) Inversion of free-end effect for **2a-c**, **3a-c**, and **4a-c**: ⬚Anchor Effect⬚

The T_g of DAT-PPO-X-DAT **2a-c**, Thy-PPO-X-Thy **3a-c**, and 50/50-M-X **4a-c** are much higher than that of NH_2-PPO-NH_2 **1a-c** and decrease when the molar mass increase (Figure V.2). The fact that T_g decreases when the molecular weight increases, in contradiction with the free-end effect, is related to the Thy and DAT stickers. Indeed, the two grafted stickers represent 15 % of the molecular volume for the 2200 chains, 40 % for the 460 chains and 55 % for the 250 chains, whose T_g is the highest. When the volumic fraction of sticker increases, the T_g increases and the mobility decreases. As a result, DAT-PPO-X-DAT **2b-c**, Thy-PPO-X-Thy **3b-c**, and 50/50-M-X **4b-c** (**b**: $X = 460$, **c**: $X = 250$) are solids at room temperature whereas homologues with longer spacer (**a**: $X = 2200$) are liquids at room temperature.

[8] Nicolai, T.; Floudas, G.; **Dynamics of linear and star poly(oxypropylene) studied by dielectric spectroscopy and rheology**; *Macromolecules* **1998**, *31*, 2578.

[9] Nicol, E.; Nicolai, T.; Durand, D.; **Dynamics of poly(propylene sulfide) studied by dynamic mechanical measurements and dielectric spectroscopy**; *Macromolecules* **1999**, *32*, 7530.

[10] Nicol, E.; Durand, D.; Nicolai, T.; **Influence of chain-end relaxation on the primary and secondary relaxation of supercooled polymeric liquids**; *Europhys. Lett.* **2001**, *53*, 598.
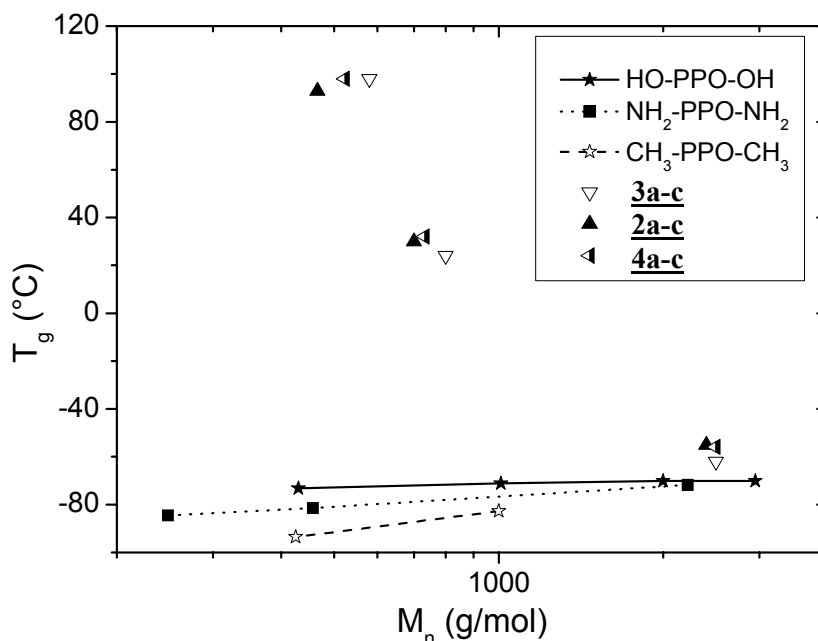
Figure V.2. T_g as a function of M_n, for HO-PPO-OH (from ref 8), NH$_2$-PPO-X-NH$_2$ **1a-c**, CH$_3$-PPO-CH$_3$ (from ref 7), Thy-PPO-X-Thy **3a-c**, DAT-PPO-X-DAT **2a-c**, and 50/50-M-X **4a-c**.

There are several ways to account for this. First of all, the introduction of relatively stiff chemical groups (such as aromatic rings, Thy and DAT) can interfere with the flowing process and hence increase T_g.[11] Furthermore, the hydrogen bonding and aromatic interactions (π-π stacking) of chain ends could increase the rigidity of the system.

Besides, these molecules can be seen as triblock copolymers with a soft central block and two rigid end blocks. Triblock copolymers of thermodynamically compatible chain segments display only one T_g, between the T_g of the two polymers. When the proportion of one polymer increases, the T_g of the triblock copolymer gets closer to the T_g of that polymer.[12] In our case, as the molar mass increases, the rigid end blocks remain identical whereas the soft central block gets longer. Therefore the mobility increases and T_g decreases.

Therefore, the increase of T_g must be related to the stiffness of the end groups and/or to the terminal moieties interchain interactions (by H-bonding and/or π-stacking), which rigidify the system.

---

[11] Cowie, J.M.G.; Arrighi, V.; *Polymers: chemistry and physics of modern materials*, CRC Press, **2007**.

[12] Nagelsdiek, R.; Keul, H.; Hocker, H.; **Synthesis of block copolymers with thermodynamically compatible chain segments: di- and triblock copolymers of polystyrene and poly(2,6-dimethyl-1,4-phenylene oxide)**; *Polym. Internation.* **2006**, *55*, 108.

196

However, if the mere existence of hydrogen bonding was sufficient to reduce so immensely the mobility to have this huge T_g increase, then the T_g of HO-PPO-OH should be much higher. If it was a question of strength of the association (measured by the association constant and/or the lifetime of the association), then since $K_{Thy-DAT}$ is much higher than $K_{Thy-Thy}$ and $K_{DAT-DAT,}$ the T_g of 50/50-M-X **4a-c** should be higher than the T_g of Thy-PPO-X-Thy **3a-c** and DAT-PPO-X-DAT **2a-c** and it is not the case. So, the effect of rigidity must be preponderant, which would explain why there is so little difference between the T_g's of 50/50-M-X **4a-c** and Thy-PPO-X-Thy **3a-c**, DAT-PPO-X-DAT **2a-c**. This "anchor effect" affects the segmental motion of the chain, the more so if the chains are shorter.

(vi) Influence of order on Thy-PPO-X-Thy **3a-c**'s T_g?

T_g is higher for the amorphous phases of semi-crystalline polymers because of the constraints exerted by the crystallites.[13,14] Crystallites act as a solid wall on which the amorphous chains connected to them are firmly anchored, which restrains chain motion.[15] The higher the crystalline fraction is, the higher the T_g of the amorphous fraction. Could Thy crystallization be responsible for Thy-PPO-X-Thy **3a-c** high T_g? It is very unlikely since Thy-PPO-250-Thy **3c** is neither ordered nor crystallized, and DAT-PPO-X-DAT **2a-c** are amorphous and yet display the same increase of T_g compared to NH$_2$-PPO-NH$_2$ **1a-c** than Thy-PPO-X-Thy **3a-c**.

Moreover, the T_g of Thy-PPO-2200-Thy **3a** is 6°C higher after a very fast cooling at 60°C/min, where crystallization and lamellar structuration did not have time to occur, than after a slow cooling at 10°C/min (where crystallization and lamellar structuration took place) (Figure V.3). This could be interpreted as a sign that mobility is higher when there are crystallites and lamellas, because then the PPO chains are phase separated from the stiff Thy groups. Furthermore, after the very fast cooling at 60°C/min, Thy-PPO-2200-Thy **3a**'s T_g is

[13] Doi, M. et Edwards, S.F.; *The theory of polymer dynamics*; Oxford University Press: USA, **1986**.

[14] Aref-Azar, A.; Arnoux, F.; Biddlestone, F.; Hay, J. N.; **Physical ageing in amorphous and crystalline polymers. Part 2. Polyethylene terephthalate**; *Thermochimica Acta* **1996**, *273*, 217.

[15] (a) Vaia, R.; Sauer, B.; Tse, O.; Giannelis, E.; **Relaxations of confined chains in polymer nanocomposites: Glass transition properties of poly(ethylene oxide) intercalated in montmorillonite**; *J. Polym. Sci B: Polym. Phys.* **1997**, *35*, 59. (b) Cheng, S. Z. D.; Cao, M. Y.; Wunderlich, B.; **Glass transition and melting behavior of poly(oxy-1,4-phenyleneoxy-1,4-phenylenecarbonyl-1,4-phenylene) (PEEK)**; *Macromolecules* **1986**, *19*, 1868. (c) Cheng, S. Z. D.; Wu, Z. Q.; Wunderlich, B.; **Glass transition and melting behavior of poly(thio-1,4-phenylene)**; *Macromolecules* **1987**, *20*, 2802.

equal to that of DAT-PPO-2200-DAT **2a**, which is disordered (see Chapter IV) because the DAT groups do not crystallize and do not microphase-separate from the PPO chains. However, this decrease in T_g could just be due to the slower cooling rate. Indeed, the history of the material, and thus its cooling rate, can have an influence on the T_g.
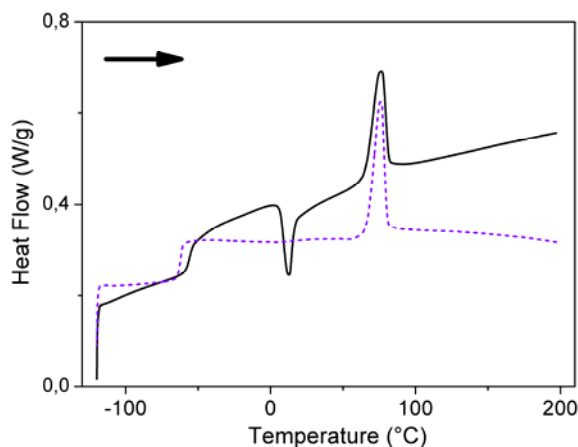
Figure V.3. DSC on heating of Thy-PPO-2200-Thy **3a** at 10°C/min (exo down) after cooling at:
(a) 10°C/min (dot-line) and (b) 60°C/min (full line).

d. Conclusion: viscosities depend on T_g as well as association

We have shown that adding Thy and/or DAT supramolecular groups on the chain-ends of PPO oligomers strongly increase their T_g, especially for short chains. Moreover, T_g's of 50/50-M-2200 **4a**, DAT-PPO-2200-DAT **2a** and Thy-PPO-2200-Thy **3a**, are equal (when there are no crystallite and no mesocopic structuration **3a**, which is the case above 67°C). Therefore, above 67°C, their viscosities can be compared, as we have done in Chapter IV (Figure V.4). Indeed, even at 100°C over the T_g, the T_g influences the viscosities of materials. Since these compounds have the same T_g, the fact that 50/50-M-2200 **4a** viscosity is higher than that of Thy-PPO-2200-Thy **3a** and DAT-PPO-2200-DAT **2a** can indeed be attributed to the higher DP of the mixture because of the higher association constant between Thy and DAT than between Thy and Thy or DAT and DAT.
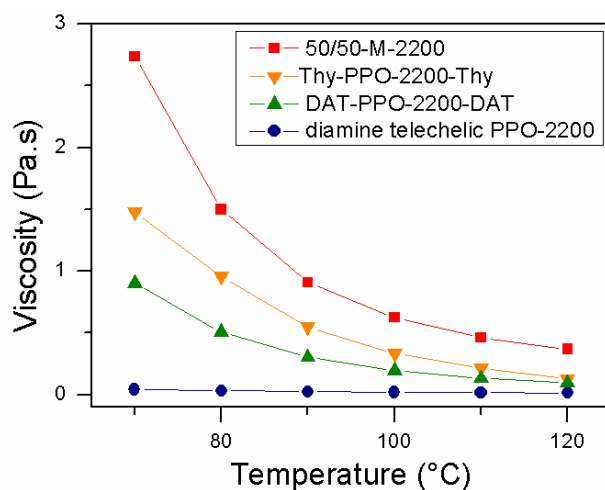
Figure V.4. Viscosity as a function of temperature for diamine telechelic NH$_2$-PPO-2200-NH$_2$ **1a**, DAT-PPO-2200-DAT **2a**, Thy-PPO-2200-Thy **3a**, and 50/50-M-2200 **4a**.

However, since the T_g of the precursor NH$_2$-PPO-2200-NH$_2$ **1a** is 16°C lower than **2a**, **3a** and **4a**'s T_g, its lower viscosity is not only due to differences in association, but also to the lower T_g and to the differences in friction coefficients of PPO, NH$_2$, Thy and DAT.

General conclusion

In this thesis, we have studied, in solution and in the bulk, a model system consisting of noncrystalline poly(propylene oxide) (PPO) chains end-functionalized with complementary stickers: thymine derivative (Thy) and diaminotrozaine (DAT). This system combines weak (Thy/Thy and DAT/DAT self-associations) and strong (Thy/DAT complementary association) hydrogen bonding, aromaticity of the stickers, strong repulsion between the polar stickers and the PPO spacers, and very different tendency towards crystallization for Thy and DAT. Homoditopic and heteroditopic compounds were synthesized. This system modelizes supramolecular polymers, which are cited as a field of research in macromolecular science with many challenges and opportunities for the next decade.[1]

We have shown that, in solution, the solvent influences the association constants and the organizations observed. In the bulk, all materials show a relatively complex behavior, as three different phenomena concur and compete: hydrogen bonding between the stickers, phase segregation between the polymer backbone (less polar) and the stickers (more polar), and crystallization of thymines into microdomains. These phenomena impact the mesoscopic organization of the materials and thus their mechanical properties.

We presented the different organizations observed in solution and in the bulk and discussed the new insight our studies bring for understanding the role played respectively by hydrogen bonding, phase segregation, solvation and crystallization.

---

[1] Ober, C. K.; Cheng, S. Z. D.; Hammond, P. T.; Muthukumar, M.; Reichmanis, E.; Wooley, K. L.; Lodge, T. P.; **Research in Macromolecular Science: Challenges and Opportunities for the Next Decade**; *Macromolecules* **2009**, *42*, 465.

Appendix I. Material and methods

Reagents and solvents

Jeffamine® D Series, T Series and M Series were kindly provided by Huntsman. The other reagents were purchased from Sigma-Aldrich, Acros or Alfa-Aesar. All chemicals were used as received unless otherwise stated.

^{1}H, ^{13}C, COSY and HMQC NMR

The NMR spectra were recorded on a Bruker AC300 400 MHz spectrometer. The solvents used are: CDCl$_3$, DMSO-d$_6$, or toluene-d$_8$. The chemical shifts (δ) are expressed in ppm relative to TMS, the solvent signal being used as an intern reference (^{1}H: δ_{CDCl3} = 7.26 ppm, $\delta_{DMSO-d6}$ = 2.50 ppm, and $\delta_{toluene-d8}$ = 2.09 ppm; ^{13}C: δ_{CDCl3} = 77.16 ppm, $\delta_{DMSO-d6}$ = 39.52 ppm, and $\delta_{toluene-d8}$ = 20.4 ppm). The signals multiplicity is indicated as follows: s : singulet; d : doublet; t : triplet; q : quadruplet; m : multiplet. The numerotation of atoms, used to attribute the NMR signals, does not correspond to the nomenclature.

Determination of association constants by NMR

The association constants K_{AA} of an AA complex (A + A $\leftrightarrows$ AA) and K_{AB} of an AB complex (A + B $\leftrightarrows$ AB) can be determined by ^{1}H NMR titration, assuming isodesmic mechanisms.[1, 2] Indeed, the chemical shifts of the A protons implicated in the hydrogen bonds vary greatly between the free, self-associated, and AB associated states. If the equilibria are faster than the NMR spectroscopic time scale, the observed chemical shift is a weighted average between the chemical shifts of the associated δ_{AB}, self-associated δ_{AA}, and free states δ_A. Thus, at a given temperature, K_{AA} and K_{AB} can be measured by monitoring the A protons implicated in the hydrogen bonds chemical shift as a function of species concentration. The

---

[1] Fielding, L.; **Determination of Association Constants (Ka) from Solution NMR Data**; *Tetrahedron* **2000**, *56*, 6151.

[2] Steed, J. W.; Atwood, J. L.; ***Supramolecular Chemistry***, *2nd Edition*; Wiley: Chippenham, UK, **2009**.

titration curves are then analyzed by computer fitting with least-squares methods (EQNMR program).[3]

For solutions containing only A's:

$$\delta = \delta_A \frac{[A]}{C_A} + 2\delta_{AA} \frac{[AA]}{C_A} \tag{1}$$

$$C_A = [A] + 2[AA] \tag{2}$$

$$K_{AA} = \frac{[AA]}{[A]^2} \tag{3}$$

$$\delta^A = \delta_{AA} + (\delta_{AA} - \delta_A)\frac{1 - \sqrt{1 + 8K_{AA}C_A}}{4K_{AA}C_A} \tag{4}$$

For solutions containing A and B, and where the AA dimerization can be neglected:

$$\delta = \delta_A \frac{[A]}{C_A} + \delta_{AB} \frac{[AB]}{C_A} \tag{5}$$

$$C_A = [A] + [AB] \tag{6}$$

$$K_{AB} = \frac{[AB]}{[A][B]} \tag{7}$$

$$\delta^A = \delta_{AB} + (\delta_A - \delta_{AB})\frac{C_A - 1/K_{AB} - C_B + \sqrt{(C_A + 1/K_{AB} + C_B)^2 - 4C_A C_B}}{2C_A} \tag{8}$$

FT-IR

FT-IR spectra were recorded on a Bruker Tensor 37 equipped with an ATR block or in transmission with KBr pellets. Wavenumber are expressed in cm^{-1}.

GC-MS

Gas chromatograms and mass spectra *(electronic impact)* were recorded in ethanol, or methanol, or ethyl acetate on a Hewlett Packard 6890 Series GC System - 5973 Mass Selective Detector or on a Shimadzu GC-MS equipped with a 12m capillary column coupled to a mass spectrometer Shimadzu 5971 at 70 eV. The MS analysis of the principal GC signals (retention time in minutes) is given: molecular peak M or M-1 or M+1, when visible, and base peak.

---

[3] Hynes, M. J.; **EQNMR: A Computer Program for the Calculation of Stability Constants from Nuclear Magnetic resonance Chemical Shift Data**; J. Chem. Soc. Dalton Trans. **1993**, 2, 311.

Chromatography

Purification by column chromatography was performed on silica 60 (0.063 - 0.200 mm) from Merck. Qualitative thin-layer chromatography (TLC) was done on precoated aluminium sheets silical gel 60 F_{254} from Merck. Compounds were detected either with $KMnO_4$ or 254 nm UV light.

Differential scanning calorimetry (DSC)

DSC experiments were performed under helium on a TA Q1000 instrument. Two or three heating cycles were recorded at 10 °C/min. The glass transition temperature (T_g) is taken as the inflexion point of the glass transition step on the last heating.

Rheometer

The rheological properties were investigated on a Anton Paar Physica MCR 501, equipped with a Peltier oven and a cone and plate geometry (diameter 25 mm or 50 mm) for the bulk samples, and equipped with a double-gap Couette cell (external diameter: 26.7 mm; gap: 0.45 mm, sample volume: 3.8 mL) for the solutions.

X-ray Scattering

X-ray scattering were performed at the SOLEIL Synchrotron source in France with the beamline SWING enabling simultaneous small-angle and wide-angle X-ray scattering measurements.

Dynamic mechanical analysis (DMA)

DMA experiments were conducted on a TA Q800 apparatus in the film tension geometry. Heating ramps were applied at 3 °C/min. Rectangular samples of 5.7 mm × 1.8 mm cross-section and about 9.5 mm length were tested at 1 Hz and 0.5 μm amplitude.

Tensile tests

Tensile tests were performed at room temperature on dog bone samples (10 mm x 3 mm x 1.4 mm) using an Instron 5564 tensile machine, with a strain rate of 2 mm/min.

Appendix II. Synthesis and characterization

1. N-(2-(4,6-diamino-1,3,5-triazine))-dodecylamine DAT-C$_{12}$

(i) Synthesis protocol of DAT-C$_{12}$

Dodecylamine (1.89 g - 10 mmol - 1 eq.) was dissolved in 80 mL of a water / absolute ethanol mixture (v/v 50/50). NaHCO$_3$ (1.01 g – 12 mmol - 1.1 eq.) and 2-chloro-4,6-diamino-1,3,5-triazine (DAT-Cl, 1.65 g – 11 mmol - 1.1 eq.) were added, and the resulting suspension was stirred under reflux for 20 hrs. Since DAT-Cl was only partially soluble in this solvent, the reaction mixture started as a white suspension that transformed into a transparent solution as the reaction progressed. The reaction mixture was then allowed to cool to room temperature. White crystals precipitated and were recovered by filtration, washed with distilled water, and dried under vacuum at 120°C, affording N-(2-(4,6-diamino-1,3,5-triazine))-dodecylamine (DAT-C$_{12}$, 2.40 g - 80 %).

(ii) Synthesis of DAT-C$_{12}$ followed by GC-MS

After 2 hrs, GC of the reaction mixture (Figure 1a) shows three peaks attributed to dodecylamine, DAT-Cl and DAT-C$_{12}$ by the MS spectra. Indeed, MS of the first GC peak at 4.4 min is comprised of dodecylamine's molecular peak at m/z 185, as well as a peak correponding to the loss of a CH$_3$ group at m/z 170, followed by several peaks correponding to the extra loss of a CH$_2$ (at m/z 156, 142, 128, 114, 100, 86). MS of the second GC peak at 4.8 min contains DAT-Cl's two molecular peaks at m/z 145 (for ^{35}Cl) and 147 (for ^{37}Cl), as well as a peak at m/z 110 corresponding to DAT without Cl. Finally, MS of the last GC peak at 9.2 min consist of DAT-C12's molecular peak at m/z 294, of peaks corresponding to the loss of a CH$_3$ (at m/z 279) and of an extra CH$_2$ (at m/z 265, 251, 237, 223, 209, 195, 181, 167, 153, 139, 125), as well as a peak at m/z 111 corresponding to DAT.

After 20h, GC of the reaction mixture (Figure 1b) shows that all the dodecylamine has been consumed, that DAT-C12 has been formed, and that only traces amount of impurities (2-hydroxy-4,6-diamino-1,3,5-triazine (DAT-OH) and reactive DAT-Cl) remain.
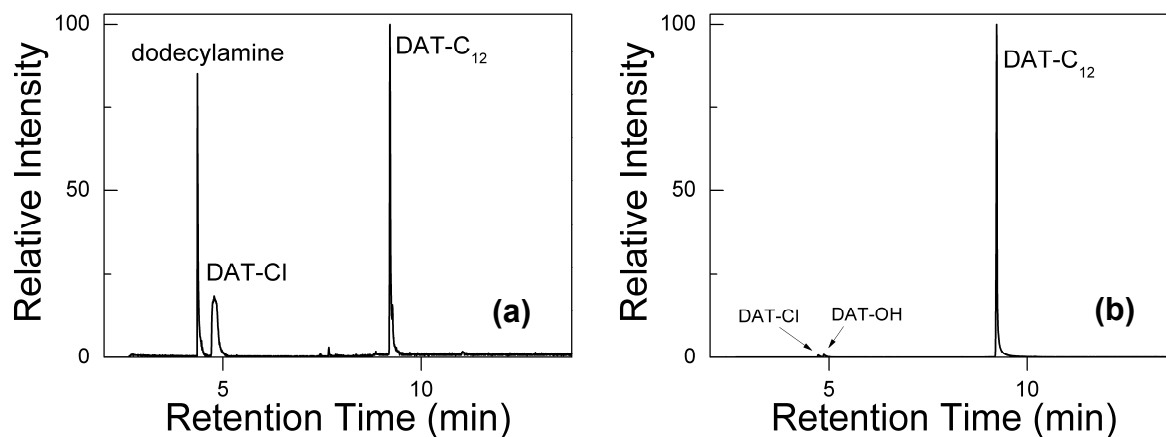
Figure 1. GC of reaction mixture: (a) after 2h, and (b) after 20h.

GC-MS in ethyl alcohol (reaction mixture after 2 hrs) : **4.4 min** : m/z (185 - 170 - 156 - 142 - 128 - 114 - 100 - 86 - 55) [$C_{12}H_{25}NH_2$]; **4.8 min** : m/z (147 - 145 - 110 - 68) [**DAT-Cl**] ; **9.2 min** : m/z (294 - 279 - 265 - 251 - 237 - 223 - 209 - 195 - 181 - 167 - 153 - 140 - 139 - 125 - 111 - 85 - 68) [**DAT-C$_{12}$**]).

GC-MS in ethyl alcohol (reaction mixture after 20 hrs) : **4.7 min** : m/z (147 - 145 - 110 - 68) [**DAT-Cl**, traces] ; **4.9 min** : m/z (127 - 111 - 85 - 69) [**DAT-OH**, traces] ; **9.2 min** : m/z (294 - 279 - 265 - 251 - 237 - 223 - 209 - 195 - 181 - 167 - 153 - 140 - 139 - 125 - 111 - 85 - 68) [**DAT-C$_{12}$**]

(iii) Characterization of DAT-C$_{12}$ by ^{1}H and ^{13}C NMR

^{1}H, ^{13}C, COSY and HMQC NMR of the final product in DMSO-d$_6$ showed that DAT-C$_{12}$ was obtained, and was pure at 98% (Table 1). For instance, on the ^{1}H spectrum of the product, the CH$_2$ closest to the amino terminal group was shifted downfield above 3 ppm, and the NH$_2$ on the DAT aromatic ring were shifted upfield from around 7 ppm to around 6 ppm.

	NMR ^{1}H	NMR ^{13}C
Φ H₂N Λ N Γ Cl N Ψ H₂N Σ δ/ppm (DMSO-d₆ / TMS) =	**7.12** (s, 2H, **Φ**) **7.21** (s, 2H, **Ψ**)	**150.05** (**Γ**) **167.12** (**Λ**) **168.72** (**Σ**)
ζ ε δ γ β α H₂N−CH₂−CH₂−(CH₂)₈−CH₂−CH₃ δ/ppm (CDCl₃ / TMS) =	**0.86** (t, 3H, **α**) **1.19 - 1.32** (m, 20H, **β, γ, ζ**) **1.41** (m, 2H, **δ**) **2.66** (t, 2H, **ε**)	**14.23** (**α**) **22.81** (**β**) **27.03, 29.47, 29.64,** **29.70 - 29.85, 32.04** (**γ**) **34.03** (**δ**) **42.41** (**ε**)
Φ H₂N Λ N Ω ε δ γ β α N Γ−NH−CH₂−CH₂−(CH₂)₈−CH₂−CH₃ H₂N Σ Ψ δ/ppm (DMSO-d₆ / TMS) =	**0.85** (t, 3H, **α**) **1.23** (m, 18H, **β, γ**) **1.42** (m, 2H, **δ**) **3.15** (m, 2H, **ε**) **5.90** (s, 1.7H, **Φ**) **6.06** (s, 1.7H, **Ψ**) **6.39** (t, 1H, **Ω**) impurities 2% DAT-Cl: **7.13** (s, 0.03H, **Φ** of DAT-Cl) **7.22** (s, 0.03H, **Ψ** of DAT-Cl)	**14.00** (**α**) **22.15** (**β**) **26.56, 28.77, 28.99,** **29.08, 29.09, 29.13,** **29.15, 29.49** (**γ**) **31.35** (**δ**) **39.83** (**ε**) **166.39** (**Γ**) **~ 167** (**Λ, Σ**)
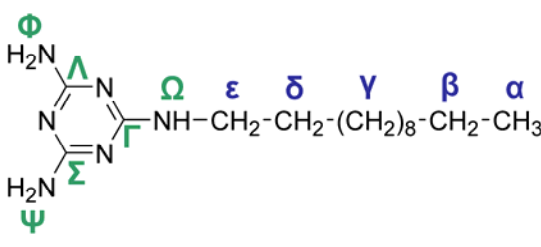
Table 1. NMR data of reactants (DAT-Cl and *n*-dodecylamine) and product (DAT-C₁₂).

2. N-alkyl-(thymine-1)-acetamide Thy-C$_n$ (n = 4, 12, 18)

a. N-butyl-(thymine-1)-acetamide Thy-C$_4$

(i) Synthesis protocol of Thy-C$_4$

Thymine-1-acetic acid (0.20 g - 1.1 mmol - 1 eq.) was dissolved in DMF (8 mL). *n*-Butylamine (0.08 g - 1.1 mmol - 1 eq.), followed by TBTU (0.35 g - 1.1 mmol - 1 eq.), and DIEA (0.4 mL - 0.28 g - 2.2 mmol - 2 eq.) were then added. The reaction mixture was stirred at room temperature for 3h. Crystals precipitated from the solution, were recovered by filtration, washed with water, and dried under vacuum at 100°C, affording N-butyl-(thymine-1)-acetamide (Thy-C$_4$, 0.201 g - 77 %).

(ii) Characterization of Thy-C$_4$ by GC-MS

GC-MS of Thy-C$_4$ show that the desired product was obtained in pure form. The MS spectra contains the molecular peak at m/z 239, as well as peaks corresponding to thymine fragments (at m/z 183, 167, 140, 126).

GC-MS in methyl alcohol: **7.56 min** : m/z (239 - 197 - 183 - 167 - 140 - 126 - 96 - 69 - 57) [**Thy-C$_4$**].

(iii) Characterization of Thy-C$_4$ by ^{1}H and ^{13}C NMR

^{1}H, ^{13}C, COSY and HMQC NMR of the final products in DMSO-d$_6$ also showed that Thy-C$_4$ was obtained in pure form (Table 2). For instance, compared to the reactants ^{1}H spectrum, on the product spectra, the amide group NH appears around 8 ppm, the CH$_2$ on the thymine side is shielded, and the CH$_2$ on the aliphatic chain side is deshielded.

	NMR ^{1}H	NMR ^{13}C
  δ/ppm (DMSO-d$_6$ / TMS) =	**1.74** (d, 3H, ^{4}J = 1.2 Hz, **A**) **4.36** (s, 2H, **B**) **7.48** (q, 1H, ^{4}J = 1.2 Hz, **C**) **11.34** (s, 1H, **D**) **13.11** (s, 1H, **J**)	**11.98** (**A**) **48.49** (**B**) **108.45** (**E**) **141.88** (**C**) **151.07** (**F**) **164.46** (**G**) **169.77** (**H**)
  δ/ppm (CDCl$_3$ / TMS) =	**0.76** (t, 3H, **α**) **0.93** (s, 2H, **ζ**) **1.13 - 1.31** (m, 4H, **β**, **δ**) **2.53** (t, 2H, **ε**)	**13.74** (**α**) **19.81** (**β**) **35.89** (**δ**) **41.78** (**ε**)
  δ/ppm (DMSO-d$_6$ / TMS) =	**0.85** (t, 3H, **α**) **1.27** (m, 2H, **β**) **1.37** (m, 2H, **δ**) **1.74** (m, 3H, **A**) **3.06** (dt, 2H, **ε**) **4.25** (s, 2H, **B**) **7.41** (m, 1H, **C**) **8.07** (t, 1H, **I**) **11.24** (s, 1H, **D**)	**11.95** (**A**) **13.69** (**α**) **19.57** (**β**) **31.22** (**δ**) **38.40** (**ε**) **49.44** (**B**) **108.00** (**E**) **142.54** (**C**) **151.10** (**F**) **164.58** (**G**) **166.73** (**H**)

Table 2. NMR data of reactants (thymine-1-acetic acid and *n*-butylamine) and product (Thy-C$_4$).

b. N-dodecyl-(thymine-1)-acetamide Thy-C$_{12}$

(i) Synthesis Protocol of Thy-C$_{12}$

Thymine-1-acetic acid (2.07 g - 11 mmol - 1.1 eq.) was dissolved in DMF (100 mL). *n*-Dodecylamine (1.89 g - 10 mmol - 1 eq.), followed by TBTU (4.54 g - 14 mmol - 1.7 eq.), and DIEA (5.2 mL - 3.87 g - 30 mmol - 3.3 eq.) were then added. The reaction mixture was stirred at room temperature for 15 h. Water (50 mL) was then added, and the reaction mixture was extracted with toluene (2 x 30mL, if necessary emulsions were destabilized by filtering on Celite®), washed with water (2 x 30 mL), dried over anhydrous magnesium sulfate, filtered, evaporated and dried under vacuum at 120°C, affording N-dodecyl-(thymine-1)-acetamide (Thy-C$_{12}$, 3.15 g - 90 %).
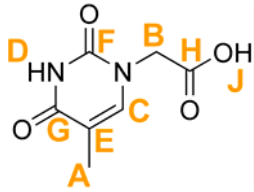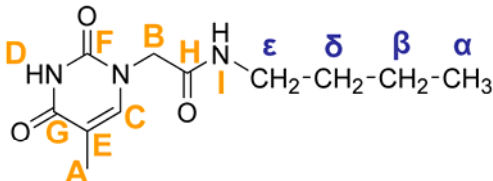
(ii) Characterization of Thy-C$_{12}$ by GC-MS

GC-MS of Thy-C$_{12}$ show that the desired product was obtained in pure form. The MS spectra contains the molecular peak at m/z 351, as well as peaks corresponding to thymine fragments (at m/z 183, 167, 140, 126). Thy-C$_{12}$'s MS also contains several peaks corresponding to the extra loss of a CH$_2$ (at m/z 281, 266, 252, 238, 225, 212).

GC-MS in ethyl alcohol: **10.79 min** : m/z (351 - 294 - 281 - 266 - 252 - 238 - 225 - 212 - 197 - 183 - 167 - 140 - 127 - 96 - 69 - 57) [**Thy-C$_{12}$**].

(iii) Characterization of Thy-C$_{12}$ by ^{1}H and ^{13}C NMR
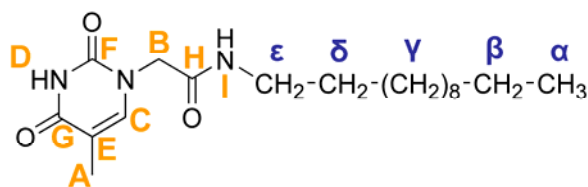
Chart 1. Thy-C$_{12}$.

^{1}H, ^{13}C, COSY and HMQC NMR of the final products in DMSO-d$_6$ also showed that Thy-C$_{12}$ was obtained in pure form. For instance, compared to the reactants ^{1}H spectrum, on

the product spectra, the amide group NH appears around 8 ppm, the CH_2 on the thymine side is shielded, and the CH_2 on the aliphatic chain side is deshielded.

RMN ^{1}H δ/ppm (DMSO-d$_6$ / TMS) = **0.85** (t, 3H, **α**) - **1.24** (m, 18H, **β**, **γ**) - **1.38** (m, 2H, **δ**) - **1.75** (s, 3H, **A**) - **3.04** (dt, 2H, **ε**) - **4.24** (s, 2H, **B**) - **7.41** (s, 1H, **C**) - **8.06** (t, 1H, **I**) - **11.23** (s, 1H, **D**) - impurities 0.7% DMF: **2.73** (s, 0.02H) - **2.89** (s, 0.02H).

RMN ^{13}C δ/ppm (DMSO-d$_6$ / TMS) = **11.93** (**A**) - **13.99** (**α**) - **22.14** (**β**) - **26.39**, **28.76**, **28.78**, **29.01-29.13** (**γ**) - **31.34** (**δ**) - **38.43** (**ε**) - **49.35** (**B**) - **107.91** (**E**) - **142.46** (**C**) - **151.04** (**F**) - **164.52** (**G**) - **166.64** (**H**).

c. N-octadecyl-(thymine-1)-acetamide Thy-C$_{18}$

(i) Synthesis protocol of Thy-C$_{18}$

Thymine-1-acetic acid (1.03 g - 5.5 mmol - 1.1 eq.) was dissolved in 100 mL of a DMF / toluene mixture (v/v 50/50) heated to 60°C. Octadecylamine (1.39 g - 5 mmol - 1 eq.), followed by TBTU (2.27 g - 7 mmol - 1.7 eq.), and DIEA (2.6 mL - 1.94 g - 15 mmol - 3 eq.) were then added. The reaction mixture was stirred at 60°C for 15 h, and then allowed to cool to room temperature. Crystals precipitated from the solution, were recovered by filtration, washed with water, and dried under vacuum at 120°C, affording N-octadecyl-(thymine-1)-acetamide (Thy-C$_{18}$, 2.03 g - 93 %).

(ii) Characterization of Thy-C$_{18}$ by ^{1}H and ^{13}C NMR
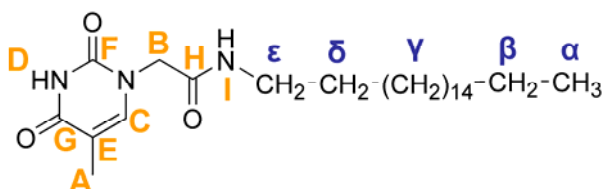
Chart 2. Thy-C$_{18}$

RMN ^{1}H δ/ppm (DMSO-d$_6$ / TMS) = **0.86** (3H, **α**) - **1.24** (30H, **β**, **γ**) - **1.38** (2H, **δ**) - **1.74** (3H, **A**) - **3.04** (2H, **ε**) - **4.24** (2H, **B**) - **7.41** (1H, **C**) - **8.07** (1H, **I**) - **11.23** (1H, **D**).

3. Diamine telechelic PPO (Jeffamine ® D series, NH$_2$-PPO-X-NH$_2$ **1a-c**)
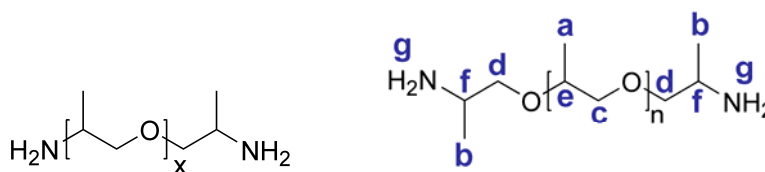
Chart 3. Jeffamine ® D series (NH$_2$-PPO-X-NH$_2$ **1a-c** [**a**: X = 2200, **b**: X = 460, **c**: X = 250], n = x-1), provided by Huntsman.

(i) Characterization of NH$_2$-PPO-X-NH$_2$ **1a-c** by ^{1}H and ^{13}C NMR

	NMR ^{1}**H**	NMR ^{13}**C**
NH$_2$-PPO-2200-NH$_2$ **1a** δ/ppm (CDCl$_3$ / TMS) =	**0.99** (m, 6H, **b**) **1.10** (m, 109H, **a**) **1.78** (s, 4H, **g**) **3.0 à 3.8** (m, 117H, **d**, **f**, **c**, **e**)	**17.4** (**a**) **19.6** (**b**) **46.6** and **47.1** (**f**) **75.4** (**e**) **73.0** and **73.4** (**c**) **76.4** (**d**)
NH$_2$-PPO-460-NH$_2$ **1b** δ/ppm (CDCl$_3$ / TMS) =	**0.95** (d, $^3J_{b,f}$ = 6.3 Hz, 6H, **b**) **1.07** (d, $^3J_{a,e}$ = 6.2 Hz, 17H, **a**) **1.46** (s, 4H, **g**) **2.9 à 4** (m, 23H, **d**, **f**, **c**, **e**)	**17.3** (**a**) **19.7** (**b**) **46.5** and **47.0** (**f**) **74.7** and **75** (**e**) **73.0**, **73.3** and **75.4** (**c**) **76.3** and **78.4** (**d**)
NH$_2$-PPO-250-NH$_2$ **1c** δ/ppm (CDCl$_3$ / TMS) =	**0.95** (m, 6H, **b**) **1.07** (m, 6H, **a**) **1.43** (s, 4H, **g**) **2.9 à 4.0** (m, 12H, **d**, **f**, **c**, **e**)	**17.2** (**a**) **19.7** (**b**) **46.4** and **46.9** (**f**) **74.7** and **75** (**e**) **73.1**, **75.3** and **78.3** (**c**) **76.2** and **78.3** (**d**)
NH$_2$-PPO-250-NH$_2$ **1c** δ/ppm (DMSO-d$_6$ / TMS) =	**0.91** (m, 6H, **b**) **1.05** (d, $^3J_{a,e}$ = 6.3 Hz, 6.1H, **a**) **1.57** (s, 4H, **g**) **2.8 à 3.8** (m, 12H, **d**, **f**, **c**, **e**).	**17.1** (**a**) **19.9** (**b**) **46.0**, **46.2** and **46.4** (**f**) **72.3**, **73.9**, **74.2**, **74.5**, **75.8** and **78.0** (**c**,**d**,**e**)

Table 3. NMR data of NH$_2$-PPO-X-NH$_2$ **1a-c**.

(ii) Characterization of NH_2-PPO-X-NH_2 **1b-c** by GC-MS

GC-MS of NH_2-PPO-460-NH_2 **1b** in methyl alcohol: **3.59** mn : m/z (75 - 58) [**x = 2**; 0.15%]; **5.14** mn : m/z (247 - 75 - 58) [**x = 3**; 2.10%]; **6.44** mn : m/z (305 - 75 - 58) [**x = 4**; 6.70%]; **7.52** mn : m/z (363 - 58) [**x = 5**; 16.12%]; **8.51** mn : m/z (421 - 58) [**x = 6**; 33.02%]; **9.42** mn : m/z (479 - 58) [**x = 7**; 28.33%]; **10.80** mn : m/z (523 - 58) [**x = 8**; 12.05%]; **13.11** mn : m/z (58) [**x = 9**; 1.53%]

GC-MS of NH_2-PPO-250-NH_2 **1c** in methyl alcohol: **3.68** mn : m/z (189 - 75 - 58) [**x = 2**; 28.3%]; **5.19** mn : m/z (247 - 75 - 58) [**x = 3**; 51.1%]; **6.45** mn : m/z (305 - 75 - 58) [**x = 4**; 19.4%]; **7.68** mn : m/z (363 - 75 - 58) [**x = 5**; 1.1%].

(iii) Characterization of NH_2-PPO-250-NH_2 **1c** by FT-IR

IR ATR of NH_2-PPO-250-NH_2 **1c** (cm^{-1}) : **3368**, **3306** (NH_2), **2970**, **2930**, **2870** (CH_3, CH_2), **1467** (CH_2, scissoring), **1373** (CH_3), **1306** (CH_2, torsion), **1201** (C-N), **1099** (C-O).

4. DAT-PPO-X-DAT **2a-c** (**a**: X = 2200, **b**: X = 460, **c**: X = 250)

a. Synthesis protocol of DAT-PPO-X-DAT **2a-c**

(i) General Procedure for DAT-PPO-X-DAT **2a-c**

NH_2-PPO-X-NH_2 **1a-c** (5 mmol - 1 eq.) was dissolved in 80 mL of a water / absolute ethanol mixture (v/v 50/50). $NaHCO_3$ (11 mmol - 0.93 g - 2.2 eq.) and 2-chloro-4,6-diamino-1,3,5-triazine (11 mmol - 1.60 g - 2.2 eq.) were added, and the resulting suspension was stirred under reflux for 20 hrs. Since DAT-Cl was only partially soluble in this solvent, the reaction mixture started as a white suspension that transformed into a transparent solution as the reaction progressed. Ethanol was removed in vacuo from the transparent reaction mixture. After extraction with toluene (2 x 30mL), the combined organic layers were washed with water (2 x 30 mL, emulsions can be destabilized by filtering on Celite®, adding sodium chloride salt or waiting long enough), dried over anhydrous magnesium sulfate, filtered, evaporated, and dried under vacuum at 100°C, affording DAT-PPO-X-DAT **2a-c**.

	yield (%)
DAT-PPO-2200-DAT **2a**	93
DAT-PPO-460-DAT **2b**	68
DAT-PPO-250-DAT **2c**	61

Table 4. Synthesis yields of DAT-PPO-X-DAT **2a-c**.

(ii) Synthesis protocol specificities for DAT-PPO-250-DAT **2c**

The reaction suspension was stirred under reflux for 26h. The solvent was removed *in vacuo* from the transparent reaction mixture. The product was then solubilized in a chloroform / methanol mixture (v/v 50/50) under reflux (~ 60°C) and filtered to eliminate a precipitate (composed of $NaHCO_3$ and hydroxydiaminotriazine (DAT-OH)). This evaporation / solubilization / filtration process was repeated twice. The final filtrate was dried over anhydrous magnesium sulfate, filtered, evaporated, and dried under vacuum at 180°C, affording DAT-PPO-250-DAT **2c**.

b. Characterization of DAT-PPO-X-DAT *2a-c* by ^{1}H and ^{13}C NMR
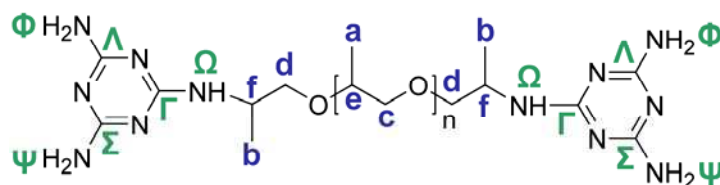
Chart 4. DAT-PPO-X-DAT **2a-c**.

	NMR ^{1}H		NMR ^{13}C	
	DAT	PPO	DAT	PPO
DAT-PPO-2200-DAT **2a** δ/ppm (DMSO-d$_6$ / TMS) =	**5.8** to **6.2** (m, 10H, **Φ**, **Ψ**, **Ω**)	**1.04** (m, 148H, **a**, **b**) **2.8 to 3.8** (m, 148H, **d**, **c**, **e**) **4.04** (m, 2H, **f**)	**165.9** (**Γ**) **167.2** (**Λ**, **Σ**)	**17.3** (**a**) **17.9** (**b**) **45.0** (**f**) **72.2, 74.6** (**c,d,e**)
DAT-PPO-460-DAT **2b** δ/ppm (DMSO-d$_6$ / TMS) =	**5.8** to **6.3** (m, 10H, **Φ**, **Ψ**, **Ω**)	**1.04** (m, 29H, **a**, **b**) **2.8 to 3.8** (m, 29H, **d**, **c**, **e**) **4.04** (m, 2H, **f**)	**165.9** (**Γ**) **167.2** (**Λ**, **Σ**)	**17.3** (**a**) **18.0** (**b**) **45.0** (**f**) **72.2, 74.5, 79.2** (**c, d, e**)
DAT-PPO-250-DAT **2c** δ/ppm (DMSO-d$_6$ / TMS) =	**5.9 à 6.6** (m, 10H, **Φ**, **Ψ**, **Ω**)	**1.03** (m, 12H, **a**, **b**) **3.0 à 3.8** (m, 10H, **d**, **c**, **e**) **4.07** (m, 2H, **f**)	**165.9** (**Γ**) **167.2** (**Λ**, **Σ**)	**17.1** (**a**) **17.95** (**b**) **45.1** (**f**) **71.9, 74.1, 79.3** (**c, d, e**)

Table 5. NMR data of DAT-PPO-X-DAT **2a-c**.
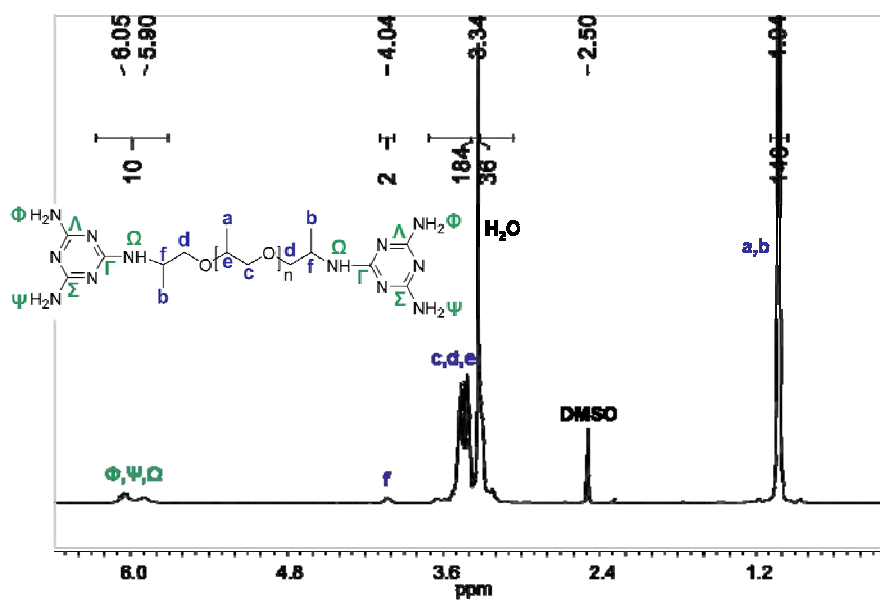
Figure 2. ^{1}H NMR in DMSO-d_6 of DAT-PPO-2200-DAT **2a**.
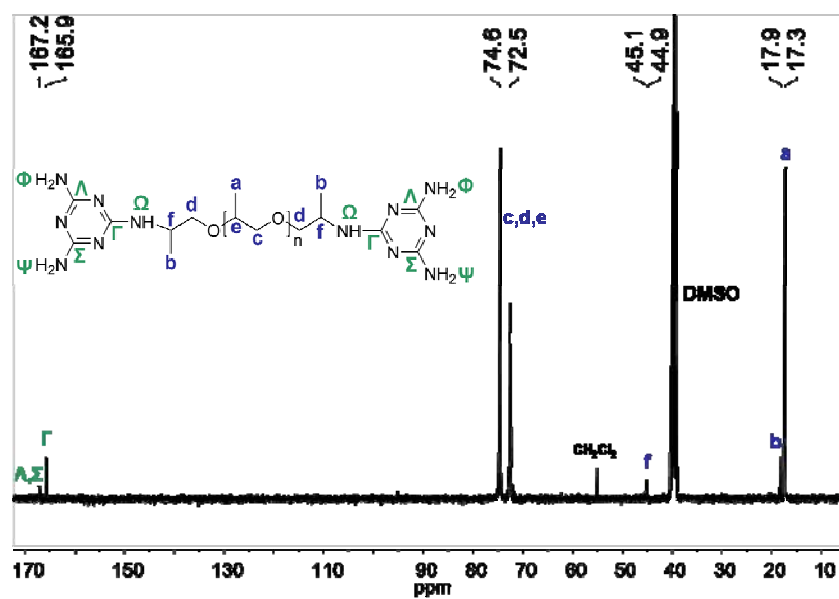
Figure 3. ^{13}C NMR in DMSO-d_6 of DAT-PPO-2200-DAT **2a**.

5. Thy-PPO-X-Thy **3a-c** (**a**: X = 2200, **b**: X = 460, **c**: X = 250)

a. Synthesis protocols of Thy-PPO-X-Thy **3a-c**

(i) General procedure with TBTU

Thymine-1-acetic acid (2.05 g - 10.9 mmol - 2.2 eq.) was dissolved in DMF (25 mL). NH_2-PPO-X-NH_2 **1a,c** (5.0 mmol - 1 eq.), TBTU (4.14 g - 12.8 mmol - 2.5 eq.) and DIEA (7 mL - 40.1 mmol - 8 eq.) were then added. The reaction stirred at room temperature for one day and was subsequently quenched by adding water (25 mL). The reaction mixture was extracted with toluene (2 x 50mL), washed with water (2 x 50 mL), dried over anhydrous magnesium sulfate, filtered, evaporated, and dried under vacuum at 100°C, affording Thy-PPO-X-Thy **3a,c**.

	yield (%)	
	with TBTU	by heating
Thy-PPO-2200-Thy **3a**	96	60
Thy-PPO-460-Thy **3b**	-	70
Thy-PPO-250-Thy **3c**	20	50

Table 6. Synthesis yields of Thy-PPO-X-Thy **3a-c**.

(ii) Synthesis protocol specificities for Thy-PPO-250-Thy **3c** (with TBTU)

After stirring for one day, the reaction was subsequently partially evaporated. Water was added and the solution filtered to eliminate a precipitate (composed of hydrated HOBt). Water was removed in vacuo, and the product was purified by column chromatography (MeOH/CHCl$_3$: 1/9 v/v), and dried under vacuum at 160°C, affording Thy-PPO-250-Thy **3c** (0.2 eq., with 16% of DIEA).

(iii) General procedure by heating

Thymine-1-acetic acid (2 eq.) was added progressively to NH_2-PPO-X-NH_2 **1a-c** (1 eq.) at 160°C under a stream of nitrogen gas. The reaction stirred for 24h, until completion of the reaction (followed by ATR FT-IR and ^1H NMR). The product was purified by column chromatography (MeOH/CHCl$_3$: 1/9 v/v), and dried under vacuum at 170°C, affording Thy-PPO-X-Thy **3a-c**.

(iv) Synthesis protocol specificities for **3b-c** (by heating)

For Thy-PPO-460-Thy **3b**, the reaction stirred for 48h. DMF was added dropwise if stiring became difficult. The product was purified by column chromatography (MeOH/CHCl$_3$: 2/8 v/v), and dried under vacuum at 170°C, affording Thy-PPO-460-Thy **3b**.

For Thy-PPO-250-Thy **3c**, the reaction stirred for 96h. DMF was also added dropwise if stiring became difficult. The product was purified by column chromatography (MeOH/CHCl$_3$: 3/7 v/v), and dried under vacuum at 170°C, affording Thy-PPO-250-Thy **3c**.

b. Characterization of Thy-PPO-250-Thy 3c by FT-IR

IR (ATR, 30°C, cm^{-1}) : **3306.2**, **3179.5** (NH bonded), **3060.3** (=CH), **2969.6**, **2930.0**, **2870.6** (CH$_3$, CH$_2$), **1687.4** (NH-**CO** thymine), **1670.7** (C=O amide I), **1646.8** (C=C), **1550.0** (NH amide II), **1484.9** (CH$_2$, scissoring), **1418.4** (C-N), **1372.5** (CH$_3$), **1233.2** (NH amide III), **1092.4** (C-O), **792** (NH amide IV).

c. Characterization of Thy-PPO-X-Thy $\underline{\textbf{3a-c}}$ by ^{1}H and ^{13}C NMR
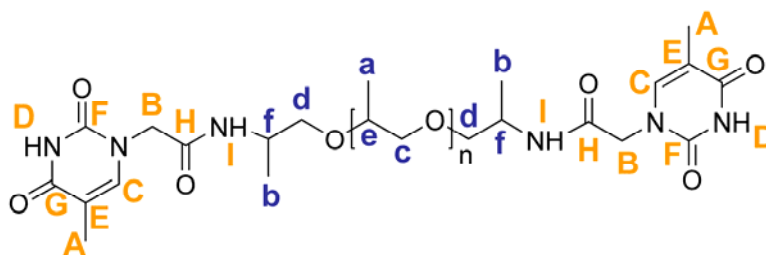
Chart 5. Thy-PPO-X-Thy $\underline{\textbf{3a-c}}$.

	NMR ^{1}H		NMR ^{13}C	
	Thy	PPO	Thy	PPO
Thy-PPO-2200-Thy **3a** δ/ppm (DMSO-d$_6$ / TMS) =	**1.74** (s, 6H, **A**) **4.25** (s, 4H, **B**) **7.40** (s, 2H, **C**) **7.97** (qdd, 2H, **I**) **11.24** (s, 2H, **D**)	**1.03** (d, 121H, **a, b**) **3 to 4** (m, **c, d, e**) **3.83** (m, 2H, **f**)	**11.9** (**A**) **49.2** (**B**) **107.8** (**E**) **142.5** (**C**) **151.0** (**F**) **164.4** (**G**) **166.2** (**H**)	**17.3** (**a, b**) **44.7** and **45.0** (**f**) **71 to 76** (**c, d, e**)
Thy-PPO-460-Thy **3b** δ/ppm (DMSO-d$_6$ / TMS) =	**1.74** (s, 6H, **A**) **4.25** (s, 4H, **B**) **7.40** (s, 2H, **C**) **7.99** (qdd, 2H, **I**) **11.21** (s, 2H, **D**)	**1.05** (d, 26H, **a, b**) **3 to 4** (m, **c, d, e**) **3.85** (m, 2H, **f**)	**12.0** (**A**) **49.3** (**B**) **107.9** (**E**) **142.6** (**C**) **151.1** (**F**) **164.5** (**G**) **166.3** (**H**)	**17.4** (**a, b**) **44.8** and **45.0** (**f**) **71 to 76** (**c, d, e**)
Thy-PPO-250-Thy **3c** δ/ppm (DMSO-d$_6$ / TMS) =	**1.74** (s, 6H, **A**) **4.25** (s, 4H, **B**) **7.39** (s, 2H, **C**) **7.98** (qdd, 2H, **I**) **11.20** (s, 2H, **D**)	**1.05** (d, 10.5H, **a, b**) **3 to 4** (m, 11.8H, **c, d, e**) **3.88** (m, 2H, **f**)	**11.86** (**A**) **49.23** (**B**) **107.84** (**E**) **142.49** (**C**) **151.01** (**F**) **164.47** (**G**) **166.31** (**H**)	**17.1** (**a**) **17.31** (**b**) **44.5, 44.8** and **45.0** (**f**) **71.3, 71.6, 73.6, 74.2, 74.3** (**c, d, e**)

Table 7. NMR data of Thy-PPO-X-Thy $\underline{\textbf{3a-c}}$.
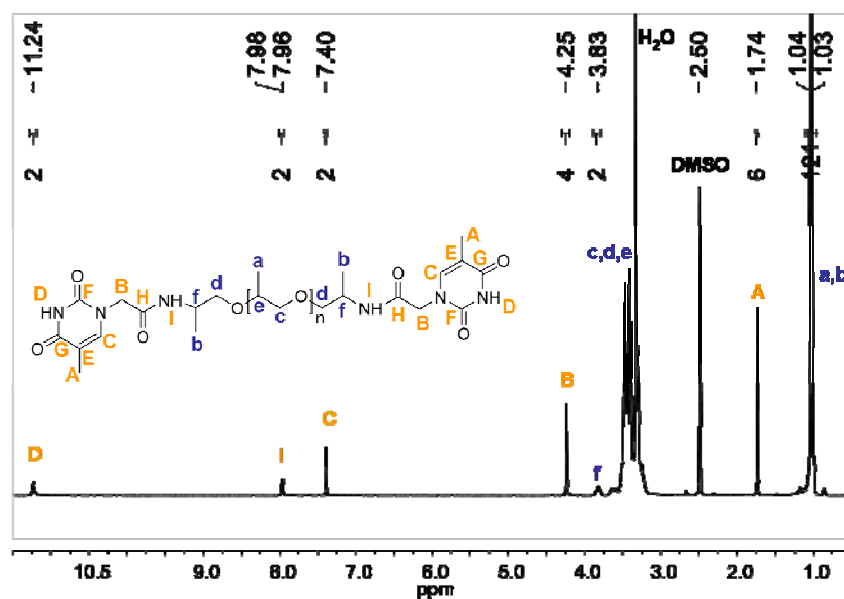
Figure 4. ^{1}H NMR in DMSO-d_6 of Thy-PPO-2200-Thy **3a**.
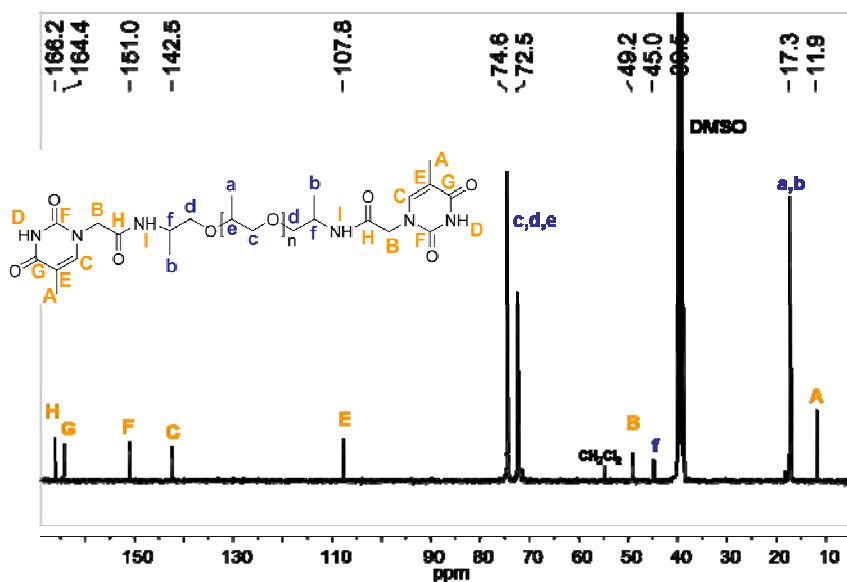
Figure 5. ^{13}C NMR in DMSO-d_6 of Thy-PPO-2200-Thy **3a**.

6. $\phi/(100-\phi)$-M-X **4a-b**, **5a**, **6a** (**a**: X = 2200, **b**: X = 460; **4**: ϕ = 50, **5**: ϕ = 25, **6**: ϕ = 75)

a. Preparation of $\phi/(100-\phi)$-M-X **4a-b**, **5a**, **6a**

$\phi/(100-\phi)$-M-X **4a-b**, **5a**, **6a** (**a**: X = 2200, **b**: X = 460; **4**: ϕ = 50, **5**: ϕ = 25, **6**: ϕ = 75) were prepared by separately solubilizing Thy-PPO-X-Thy **3a-b** and DAT-PPO-X-DAT **2a-b** in a good solvent (CHCl$_3$/MeOH 1:1 blend or CH$_2$Cl$_2$), before mixing the two solutions. $\phi/(100-\phi)$-M-X **4a-b**, **5a**, **6a** were then obtained in the bulk by solvent casting and annealing under vacuum at 120°C for 3 hrs.

b. Characterization of 50/50-M-X **4a-b** by ^{1}H and ^{13}C NMR
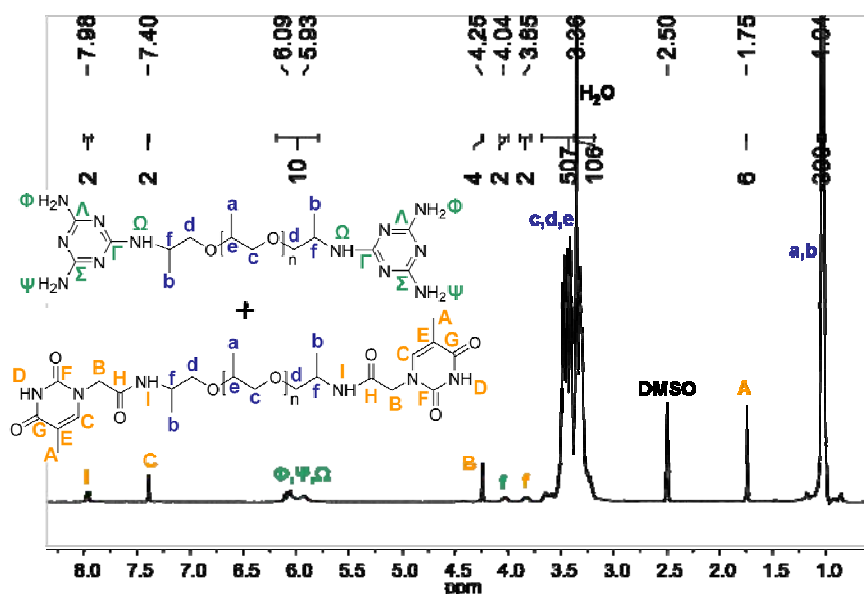
Figure 6. ^{1}H NMR in DMSO-d$_6$ of 50/50-M-2200 **4a**.
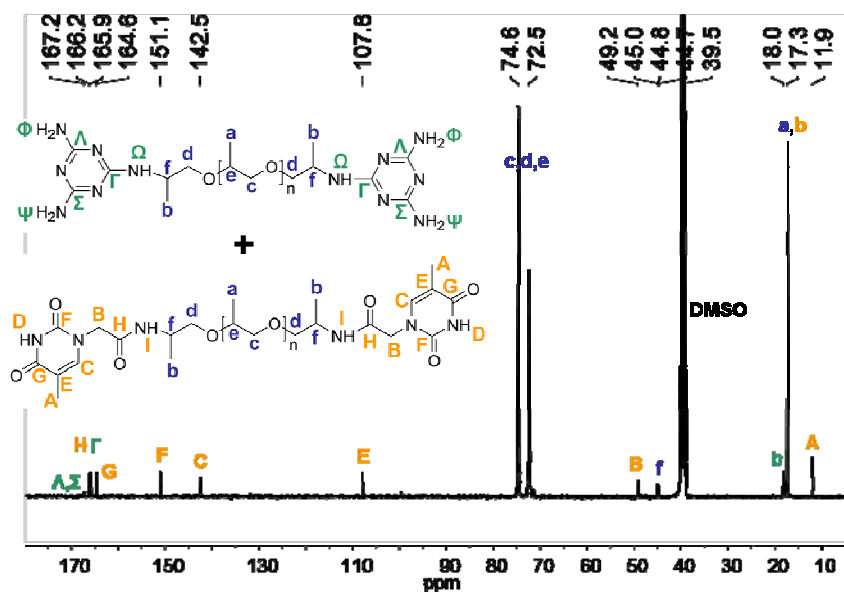
Figure 7. ^{13}C NMR in DMSO-d$_6$ of 50/50-M-2200 **4a**.

	NMR ^{1}**H**		NMR ^{13}**C**	
	Thy / DAT	PPO	Thy / DAT	PPO
50/50-M-2200 **4a** δ/ppm (DMSO-d$_6$ / TMS) =	**1.75** (s, 6H, **A**) **4.25** (s, 4H, **B**) **5.93, 6.09** (m, 10H, **Φ, Ψ, Ω**) **7.40** (s, 2H, **C**) **7.98** (m, 2H, **I**) **~11** (s, **D**)	**1.04** (d, 390H, **a, b**) **3.1 to 3.7** (m, 401H, **d, c, e**) **3.85** (m, 2H, **f**) **4.04** (m, 2H, **f**)	**11.9** (**A**) - **49.2** (**B**) **107.8** (**E**) - **142.5** (**C**) **151.1** (**F**) - **164.6** (**G**) **165.9** (**Γ**) **166.2** (**H**) **167.2** (**Λ, Σ**)	**17.3** (**a, b**) **18.0** (**b**) **44.8, 45.0** (**f, f, f**) **72.5, 74.6** (**c, d, d, e**)
50/50-M-2200 **4b** δ/ppm (CDCl$_3$ / TMS) =	**1.87** (s, 6H, **A**) **4.29** (s, 4H, **B**) **6.17** (m, 10H, **Φ, Ψ, Ω**) **7.10** (s, 2H, **C**)	**1.10** (d, 55H, **a, b**) **3.0 to 4.0** (m, 50H, **d, c, e**) **4.06** (m, 2H, **f**) **4.13** (m, 2H, **f**)	**12.3** (**A**) - **50.4** (**B**) **110.9** (**E**) - **141.3** (**C**) **152.7** (**F**) - **165.8** (**G**) **166.1** (**Γ**) **166.3** (**H**) **167.1** (**Λ, Σ**)	**17.4** (**a, b**) **18.0** (**b**) **46.1** (**f, f, f**) **71.7, 72.5, 73.1, 73.4, 75.4, 77.4** (**c, d, d, e**)
50/50-M-2200 **4c** δ/ppm (DMSO-d$_6$ / TMS) =	**1.74** (s, 6H, **A**) **4.26** (s, 4H, **B**) **6.2 to 6.8** (m, 10H, **Φ, Ψ, Ω**) **7.43** (s, 2H, **C**) **8.05** (m, 2H, **I**) **11.50** (s, 2H, **D**)	**1.04** (d, 24H, **a, b**) **3.1 to 3.8** (m, 401H, **d, c, e**) **3.87** (m, 2H, **f**) **4.09** (m, 2H, **f**)	**11.8** (**A**) - **49.3** (**B**) **107.8** (**E**) - **142.6** (**C**) **151.1** (**F**) - **164.5** (**G**) **164.6** (**Γ**) **166.22** (**H**) **166.24** (**Λ, Σ**)	**17.3** (**a, b**) **17.7** (**b**) **45.0** (**f, f, f**) **71 to 75, 79.2** (**c, d, d, e**)

Table 8. NMR data of 50/50-M-*X* **4a-c**.

7. Thy-PPO-X-DAT **10a-c** (**a**: X = 2200, **b**: X = 460, **c**: X = 250)
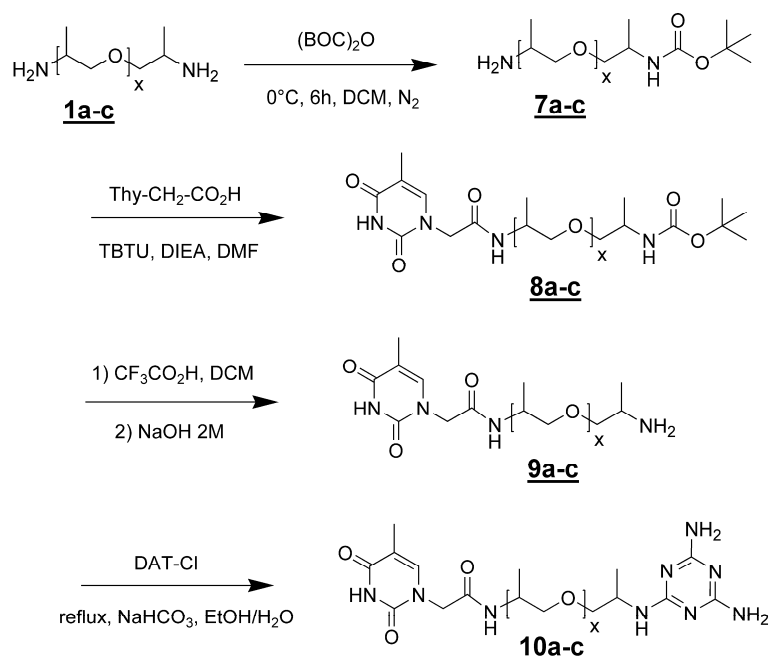
Scheme 1. Synthesis of heterotelechelic units Thy-PPO-X-DAT **10a-c** (a: X = 2200, b: X = 460, c: X = 250).

a. First step: synthesis protocol of N-BOC monoprotection

(i) General procedure for NH_2-PPO-2200-BOC **7a-c**

A solution of di-*tertio*-butyl dicarbonate (BOC_2O, 4.94 g - 22.6 mmol - 1 eq.) in dichloromethane (DCM, 100 mL) was added dropwise to a solution of NH_2-PPO-X-NH_2 (**1a-c**, 22.6 mmol - 1 eq.) in DCM (100 mL), under nitrogen flow, and cooled in an ice bath (0°C). The reaction mixture was allowed to stir, under nitrogen flow, for 6 hrs, in the ice bath, and was subsequently purified by liquid-liquid extractions. The final organic phase was dried over anhydrous magnesium sulfate, filtered, and evaporated, affording BOC-PPO-X-NH_2 **7a-c**.

	yield (%)
NH_2-PPO-2200-BOC **7a**	31
NH_2-PPO-460-BOC **7b**	14 - 37
NH_2-PPO-250-BOC **7c**	37

Table 9. Synthesis yields of BOC-PPO-X-NH_2 **7a-c**.

(ii) Synthesis protocol specificities for NH$_2$-PPO-2200-BOC **7a**

The reaction mixture was washed with a 0.1 M acetic acid solution (pH ~ 3; 2 x 200 mL) to extract the unreacted diamine. The combined organic phases were evaporated, a 0.1 M acetic acid solution (150 mL) was added to the resultant oily material, and the solution was filtered. A 2 M sodium hydroxide solution was added to the pH ~ 4 filtrate until pH reached ~ 10. The mixture was then extracted with DCM, yielding the final organic phase.

(iii) Synthesis protocol specificities for NH$_2$-PPO-2200-BOC **7b**

The reaction mixture was washed with a 0.1 M acetic acid solution (pH ~ 3, 3 x 200 mL) to extract the unreacted diamine. The solvent was then removed by rotary evaporation. Water (150 mL) was added to the resultant oily material. Non solubilized di-BOC-protected diamine was filtered from the mixture (filter pores diameter = 0.45 μm). A 2N sodium hydroxide solution was added to the aqueous filtrate (pH ~ 4) until pH reached 10. The mixture was then extracted with DCM, yielding the final organic phase.

To increase the yield and purity, NH$_2$-PPO-460-NH$_2$ can be purified before the reaction, by liquid-liquid extraction, in order to eliminate the bigger molecules which prefer the organic phase to the acidic aqueous phase. With this, the yield increases from 14% to 37% and the purity from 78% of NH$_2$-PPO-460-BOC (with x ~ 9) to 94% of NH$_2$-PPO-460-BOC (with x ~ 6).

(iv) Synthesis protocol specificities for NH$_2$-PPO-2200-BOC **7c**

The reaction was carried in THF instead of DCM and 3 eq. of NH$_2$-PPO-250-NH$_2$ for 1eq. of (BOC)$_2$O was used. After stirring for 6 hrs, the solvent was removed by rotary evaporation. A 2N sodium hydroxide solution (100 mL) was added to the resultant oily material and the mixture was extracted with methyl-*tertio*-butylether (MTBE, 3 x 60 mL). Combined organic extracts were evaporated, solubilized in dichloromethane (DCM, 60 mL) and washed with a 2N sodium hydroxide solution (3 x 60 mL), yielding the final organic phase.

(v) Characterization of NH_2-PPO-X-BOC **7a-c** by ^1H and ^{13}C NMR
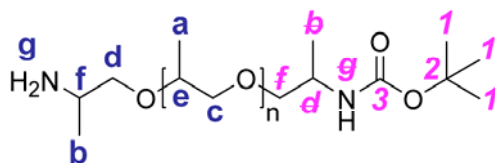
Chart 6. NH_2-PPO-X-BOC **7a-c** (n = x - 1).

	NMR ^1H		NMR ^{13}C	
	BOC	PPO	BOC	PPO
NH₂-PPO-2200-BOC **7a** δ/ppm (CDCl₃ / TMS) =	1.42 (s, 9H, *1*)	0.99 (m, 3H, **b**) 1.11 (m, 109H, **a**, *b*) 1.74 (s, 2H, **g**) 2.9 à 3.8 (m, **c**, **d**, *d*, **e**, **f**, *f*) 4.89, 5.18 (s, 0.6H, *g*)	28.6 (*1*) 155.6 (*3*)	17.5 (**a**) 18.3 (*b*) 19.8 (**b**) 46.5, 47.0 (**f**, *f*) 72 to 78 (**d**, *d*, **c**, **e**, *2*)
NH₂-PPO-460-BOC **7b** δ/ppm (CDCl₃ / TMS) =	1.38 (s, 14H, *1*)	0.97 (d, 3H, **b**) 1.08 (m, 28H, **a**, *b*) 1.92 (s, 2.2H, **g**) 2.8 à 4.0 (m, 31H, **f**, *f*, **d**, *d*, **c**, **e**) 3.69 (s, 2H, *f*) 4.87 (s, 0.8H, *g*)	28.5 (*1*) 155.6 (*3*)	17.1 (**a**) 18.1 (*b*) 19.8 (**b**) 46.5 et 47.0 (**f**, *f*) 72.3 to 79.0 (**d**, **c**, **e**, *d*, *2*)
NH₂-PPO-250-BOC **7c** δ/ppm (CDCl₃ / TMS) =	1.40 (s, 9H, *1*)	0.98 (m, 3.6H, **b**) 1.09 (m, 10H, **a**, *b*) 1.55 (s, 2.4H, **g**) 2.8 à 4.0 (m, 13.5H, **f**, *f*, **d**, *d*, **c**, **e**) 3.71 (s, 1H, *f*) 4.86 (s, 0.7H, *g*)	28.5 (*1*) 155.6 (*3*)	17.1 (**a**) 18.1 (*b*) 19.8 (**b**) 46.5 et 47.0 (**f**, *f*) 72.3 to 79.0 (**d**, **c**, **e**, *d*, *2*)

Table 10. NMR data of NH_2-PPO-X-BOC **5a-c**.

(vi) Characterization of NH_2-PPO-250-BOC **7c** by GC-MS

GC-MS : 5.90 mn : m/z (291 - 75 - 58) [**NH₂-PPO-250-BOC-x=2**] ; 7.02 mn : m/z (349 - 58) [**NH₂-PPO-250-BOC-x=3**] ; 7.52 mn : m/z (75 - 58) [**NH₂-PPO-250-BOC-x=4**].

b. Second step: synthesis protocol of Thy grafting

(i) Synthesis protocol for Thy-PPO-X-BOC **8a-c**: general procedure

Thymine-1-acetic acid (0.88 g - 4.8 mmol - 1 eq.) was dissolved in DMF (15 mL). NH_2-PPO-X-BOC **7a** (4.8 mmol - 1 eq.), TBTU (3.08 g - 9.6 mmol - 2 eq.) and triethylamine (TEA, 2.7 mL - 19.4 mmol - 4 eq.) were then added. The reaction stirred at room temperature for 2.5 days, and was subsequently quenched by adding water (100 mL). The reaction mixture was extracted with toluene (2 x 100 mL), washed with water (100 mL), dried over anhydrous magnesium sulfate, filtered, and evaporated, affording Thy-PPO-X-BOC **8a-c**.

	yield (%)
Thy-PPO-2200-BOC **8a**	100
Thy-PPO-460-BOC **8b**	100
Thy-PPO-250-BOC **8c**	100

Table 11. Synthesis yields of Thy-PPO-X-BOC **8a-c**.

(ii) Synthesis protocol specificities for Thy-PPO-X-NH_2 **8a-c**

For Thy-PPO-250-NH_2 **8c**, only 1 eq. of TBTU was used and DIEA (2 eq.) was used instead of TEA. After stirring at room temperature for 15 hrs, the reaction mixture was partially evaporated, quenched by adding water (90 mL), and filtered to remove 1-hydroxybenzotriazol (HOBt), an hydrolyse product of TBTU. The filtrate was extracted with chloroform (2 x 80 mL), washed with water (2 x 60 mL), dried over anhydrous magnesium sulfate, filtered, evaporated and dried under vacuum, affording Thy-PPO-X-BOC **8c**. For Thy-PPO-250-NH_2 **8c**, DIEA (4 eq.) was used instead of TEA.

8a contains 92.3 wt% of Thy-PPO-2200-BOC and BOC-PPO-2200-BOC, 7.2 wt% of toluene and 0.5 wt% of tetramethylurea. Indeed, the product was not dried under vacuum and heat, to avoid BOC deprotection. The impurities, such as toluene and tetramethylurea have no impact on the next reaction and will be extracted after the third or fourth step.

(iii) Characterization of Thy-PPO-X-BOC <u>**8a-c**</u> by ^{1}H and ^{13}C NMR
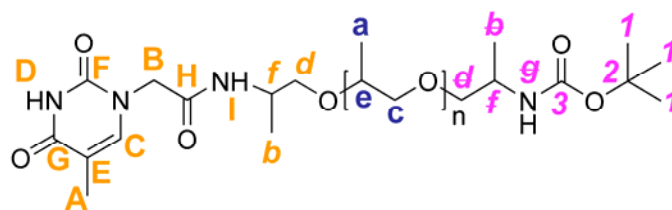
Chart 7. Thy-PPO-X-BOC <u>**8a-c**</u>.

	NMR ^{1}**H**		NMR ^{13}**C**	
	Thy / BOC	PPO	Thy / BOC	PPO
Thy-PPO-2200-BOC <u>**8a**</u> δ/ppm (DMSO-d$_6$/TMS) =	**1.37** (s, 10.3H, *1*) **1.75** (s, 3H, **A**) **4.25** (s, 2H, **B**) **7.40** (s, 1H, **C**) **7.98** (m, 1H, **I**) **11.24** (s, 1H, **D**)	**1.04** (m, 132H, **a**, *b*, ~~b~~) **3.1 to 3.7** (m, **c**, *d*, ~~d~~, e, *f*) **3.84** (m, 1H, *f*) **6.51** (d, 0.8H, ~~g~~)	**11.9** (**A**) **28.2** (*1*) **49.2** (**B**) **107.7** (**E**) **142.4** (**C**) **151.0** (**F**) **154.9** (*3*) **164.4** (**G**) - **166.2** (**H**)	**17.2** (**a**) **17.9 to 18.4** (*b*, ~~b~~) **44.7, 45.0, 45.6, 45.9** (*f*,*f*) **71 to 75, 77.5** (**c**, *d*, ~~d~~, e, *2*)
Thy-PPO-460-BOC <u>**8b**</u> δ/ppm (DMSO-d$_6$/TMS) =	**1.37** (s, 12H, *1*) **1.75** (s, 3H, **A**) **4.26** (s, 2H, **B**) **7.40** (s, 1H, **C**) **7.99** (m, 1H, **I**) **11.24** (s, 1H, **D**)	**1.04** (m, 30H, **a**, *b*, ~~b~~) **3.1 to 3.8** (m, **c**, *d*, ~~d~~, e, *f*) **3.84** (m, 1H, *f*) **6.54** (d, 1H, *g*)	**11.9** (**A**) **28.2** (*1*) **49.2** (**B**) **107.8** (**E**) **142.5** (**C**) **151.0** (**F**) **155.0** (*3*) **164.5** (**G**) - **166.2** (**H**)	**17.0 to 18.5** (**a**, *b*, ~~b~~) **44.8, 45.8** (*f*,*f*) **71 to 75, 77.4** (**c**, *d*, ~~d~~, e, *2*)
Thy-PPO-250-BOC <u>**8c**</u> δ/ppm (DMSO-d$_6$/TMS) =	**1.36** (s, 5.6H, *1*) **1.74** (s, 3H, **A**)	**1.04** (m, 13.3H, **a**, *b*, ~~b~~) **3 to 4** (m, 14.2H, *f*, ~~f~~, *d*, ~~d~~, **c**, e) **3.85** (m, 1.4H, *f*) **4.26** (s, 2H, **B**) **7.40** (s, 1H, **C**) **8.03** (m, 0.8H, **I**)	**11.93** (**A**) **28.3** (*1*) **49.24** (**B**) **107.82** (**E**) **142.54** (**C**) **151.03** (**F**) **155.0** (*3*) **164.50** (**G**) - **166.30** (**H**)	**17.2** (**a**) **17.9 to 18.4** (*b*, ~~b~~) **44.5, 44.8, 45.0** (*f*, *f*) **71 to 72.5, 73.6, 74.3, 74.4, 77.5** (**c**, *d*, ~~d~~, e)

Table 12. NMR data of Thy-PPO-X-BOC <u>**8a-c**</u>.

^{1}H and ^{13}C NMR in DMSO-d_6 of **8c** show that Thy-PPO-250-BOC was formed. However, **8c** also contains non negligible amounts of Thy-PPO-250-Thy **3c** and BOC-PPO-250-BOC. Given the small sizes of these oligomers, purification by column chromatography can be envisaged, but has not be performed.

c. Third step: Synthesis protocol of BOC deprotection

(i) Synthesis protocol for Thy-PPO-X-NH$_2$ **9a-c**: general procedure

Thy-PPO-X-BOC **8a-c** (8.1 mmol - 1 eq.) was dissolved in DCM (20 mL) at 0°C. Trifluoroacetic acid (TFA, 25 mL - 337 mmol - 42 eq.) was then added. The reaction stirred at room temperature for 2 days, and the solvents were subsequently removed by rotary evaporation.[1] The amino functions were then neutralized by adding a 2M sodium hydroxyde solution saturated with sodium chloride until pH reached 14. The product was extracted with toluene (3 x 20 mL), dried over anhydrous magnesium sulfate, filtered, and evaporated, affording Thy-PPO-X-NH$_2$ **9a-c**.

	yield (%)
Thy-PPO-2200-NH$_2$ **9a**	85
Thy-PPO-460-NH$_2$ **9b**	23
Thy-PPO-250-NH$_2$ **9c**	?

Table 13. Synthesis yields of Thy-PPO-X-NH$_2$ **9a-c**.

(ii) Synthesis protocol specificities for Thy-PPO-X-NH$_2$ **9a,c**

For Thy-PPO-2200-NH$_2$ **9a**, 100 eq. of TFA was used. The reaction mixture stirred at room temperature for 1 day, was evaporated, and treated with a 2 M sodium hydroxyde solution (15 mL). Toluene was added to extract the product, but a very stable emulsion was formed. After evaporation of the organic solvent, the product was recovered by phase separation. Toluene was added, and the resulting solution was dried over anhydrous magnesium sulfate, filtered, and evaporated, affording Thy-PPO-2200-NH$_2$ **9a**

---

[1] The rotavapor needs to be equipped with anti-corrosive tubes, since TFA is very corrosive.

For Thy-PPO-250-NH$_2$ **9c**, 6 eq. of TFA was used. After neutralization, the solution was washed with DCM, affording Thy-PPO-250-NH$_2$ **9c** in the basic aqueous phase.

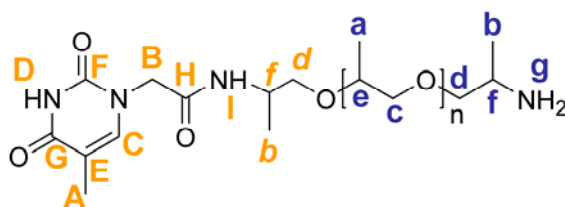## (iii) Characterization of Thy-PPO-X-NH$_2$ **9a-c** by ^{1}H and ^{13}C NMR

Chart 8. Thy-PPO-X-NH$_2$ **9a-c**.

	NMR ^{1}**H**		NMR ^{13}**C**	
	Thy	PPO	Thy	PPO
Thy-PPO-2200- NH$_2$ **9a** δ/ppm (DMSO-d$_6$ /TMS) =	1.74 (s, 3H, **A**) 4.25 (s, 2H, **B**) 7.40 (s, 1H, **C**) 7.99 (d, 1H, **I**)	1.03 (m, 142H, **a**, **b**, *b*) 3.1 to 3.7 (m, **c**, **d**, *d*, **e**, **f**) 3.83 (m, 1H, *f*)	11.9 (**A**) ~ 49 (**B**) 107.8 (**E**) ~ 143 (**C**) 151.0 (**F**) 164.5 (**G**) 166.2 (**H**)	17.3 (**a**) ~ 18 (**b**, *b*) ~ 45 (*f*, **f**) 71.5 to 75.0 (**c**, **d**, *d*, **e**)
Thy-PPO-460- NH$_2$ **9b** δ/ppm (DMSO-d$_6$ /TMS) =	1.68 (s, 3H, **A**) 4.15 (s, 2H, **B**) 6.99 (s, 1H, **C**) 7.81 (d, 1H, **I**)	0.89 (d, 4H, **b**) 1.04 (m, 27H, **a**, *b*) 3.0 to 3.7 (m, **c**, **d**, *d*, **e**, **f**) 3.80 (m, 1H, *f*)		
Thy-PPO-250- NH$_2$ **9c** δ/ppm (DMSO-d$_6$ /TMS) =	1.69 (s, 3H, **A**) 3.66 (s, 2H, **B**) 7.10 (s, 1H, **C**)	0.88 (m, 2.4H, **b**) 0.95 (m, 3H, *b*) 1.02 (m, 5.8H, **a**) 2.7 to 3.6 (m, 10H, **f**, **d**, *d*, **c**, **e**) 3.80 (m, 1H, *f*)	13.6 (**A**) 49.24 (**B**) 108.6 (**E**) 143.1 (**C**) 158.6 (**F**) 168.2 (**G**) 171.1 (**H**)	17.1 (**a**) 18.5 (**b**) 20.0 (*b*) 46 (*f*, **f**) 74 to 76 (**c**, **d**, *d*, **e**)

Table 14. NMR data of Thy-PPO-X-NH$_2$ **9a-c**.

d. Final step: Synthesis protocol of DAT Grafting

(i) Synthesis protocol for Thy-PPO-X-DAT **10a-c**: general procedure

Thy-PPO-NH$_2$ **9a-c** (2.4 mmol - 1 eq.) was dissolved in 60 mL of a water / absolute ethanol mixture (v/v 50/50). NaHCO$_3$ (0.47 g - 4.9 mmol - 2 eq.) and 2-chloro-4,6-diamino-1,3,5-triazine (0.43 g - 2.9 mmol - 1.2 eq.) were added, and the resulting suspension was stirred under reflux for 48h. Since DAT-Cl was only partially soluble in this solvent, the reaction mixture started as a white suspension that transformed into a transparent solution as the reaction progressed. Ethanol was removed *in vacuo* from the reaction mixture. After extraction with DCM (60 mL), the organic phase was dried over anhydrous magnesium sulfate, filtered, evaporated, and dried under vacuum at 100°C, affording Thy-PPO-X-DAT **10a-c**.

	yield (%)
Thy-PPO-2200-DAT **10a**	92
Thy-PPO-460-DAT **10b**	66
Thy-PPO-250-DAT **10c**	?

Table 15. Synthesis yields of Thy-PPO-X-NH$_2$ **10a-c**.

(ii) Synthesis protocol specificities for Thy-PPO-X-DAT **10b-c**

For Thy-PPO-460-DAT **10b**, water, as well as ethanol, was removed *in vacuo* from the transparent reaction mixture. DCM (50 mL) was added, the suspension was filtered, dried over anhydrous magnesium sulfate, filtered, evaporated, and dried under vacuum at 100°C, affording Thy-PPO-460-NH$_2$ **10b**.
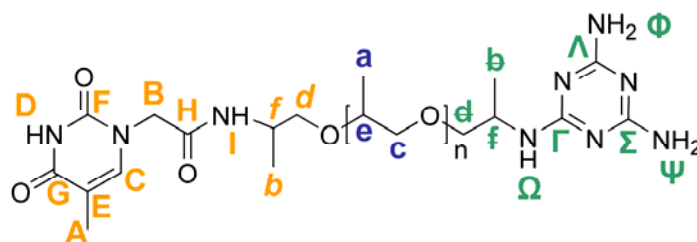
For Thy-PPO-250-DAT **10c**, Thy-PPO-250-NH$_2$ **7c** in 20 mL basic water was added to the water / absolute ethanol mixture.

(iii) Characterization of Thy-PPO-X-DAT **10a-c** by NMR

Chart 9. Thy-PPO-X-DAT **10a-c**.

	NMR ^{1}**H**		NMR ^{13}**C**	
	Thy / DAT	PPO	Thy / DAT	PPO
Thy-PPO-2200-DAT **10a** ^{1}H δ/ppm (DMSO-d$_6$/TMS) = ^{13}C δ/ppm (CDCl$_3$/TMS) =	**1.75** (s, 3H, **A**) **4.25** (s, 2H, **B**) **5.8 to 6.2** (m, 5H, **Φ, Ψ, Ω**) **7.40** (s, 1H, **C**) **7.97** (d, 1H, **I**)	**1.04** (m, 142H, a, b, *b*) **3.1 to 3.7** (m, c, d, *d*, e) **3.83** (m, 1H, *f*) **4.04** (m, 1H, f)	**12.4 (A) - 50.3 (B)** **71 to 79** (c, d, *d*, e) **104.6 (E)** **141.3 (C)** **152.5 (F) - 165.0 (G)** **165.8 (Γ)** **166.0 (H)** **170.0 (Λ, Σ)**	**17 to 19** (a, b, *b*) **46.2** (f, f, *f*)
Thy-PPO-460-DAT **10b** δ/ppm (DMSO-d$_6$/TMS) =	**1.75** (s, 3H, **A**) **4.26** (s, 2H, **B**) **5.8 to 6.3** (m, 5H, **Φ, Ψ, Ω**) **7.42** (s, 1H, **C**) **7.98** (d, 1H, **I**)	**1.04** (m, 29H, a, b, *b*) **2.9 to 3.7** (m, c, d, *d*, e) **3.84** (m, 1H, *f*) **4.04** (m, 1H, f)	**11.9 (A) - 49.3 (B)** **71 to 75** (c, d, *d*, e) **107.8 (E)** **142.6 (C)** **151.1 (F) - 164.6 (G)** **165.9 (Γ)** **166.1 (H)** **168.3 (Λ, Σ)**	**17 to 19** (a, b, *b*) **44.8** (f, f, *f*)
Thy-PPO-250-DAT **10c** δ/ppm (DMSO-d$_6$/TMS) =	**1.74** (s, 3H, **A**) **4.26** (s, 2H, **B**) **5.8 to 6.2** (m, 5H, **Φ, Ψ, Ω**) **7.40** (s, 1H, **C**) **8.01** (m, 1H, **I**) **11.26** (s, 1H, **D**)	**1.04** (m, 12H, a, b, *b*) **3.1 to 3.8** (m, c, d, *d*, e) **3.85** (m, 1H, *f*) **4.04** (m, 1H, f)	**12.0 (A) - 49.3 (B)** **69 to 77** (c, d, *d*, e) **107.9 (E)** **142.6 (C)** **151.1 (F) - 164.6 (G)** **166.2 (Γ)** **166.3 (H)** **168.7 (Λ, Σ)**	**16 to 21** (a, b, *b*) **44.8** (f, f, *f*)

Table 16. NMR data of Thy-PPO-X-DAT **10a-c**.

Appendix III. Résumé en français

Organisations dans les polymères supramoleculaires : du comportement en solution au comportement en masse

Introduction

Les polymères sont de longues chaînes d'atomes liés entre eux par des liaisons covalentes. Les enchevêtrements et la viscoélasticité des polymères résultent directement de leur grande taille et leur procurent des propriétés intéressantes. Ces propriétés sont spécifiques aux polymères et expliquent leurs succès dans de nombreuses applications, des cosmétiques aux automobiles, en passant par les emballages, le bâtiment, le médical, ou encore l'électronique. Toutefois, la longueur des chaînes de polymères peut également rendre difficile leur mise en forme ou leur recyclage.

La chimie supramoléculaire, définie comme la chimie des interactions non covalentes, permet d'introduire de la réversibilité et une sensibilité aux stimuli dans les liens entre atomes. Les liaisons hydrogène en particulier, sensibles à la température, sont très utilisées.

Le concept des polymères supramoléculaires est de construire de grands objets à partir de petites molécules reliées entre elles par des interactions non covalentes et directionnelles. Cette approche permet d'obtenir des matériaux alliant réversibilité et propriétés propres aux polymères. Par exemple, pour des matériaux maintenus par des liaisons hydrogène, une élévation de la température permet de rompre ces liaisons et d'obtenir un liquide peu visqueux : le matériau peut alors être remis en forme.

Par ailleurs, des propriétés originales comme l'auto-réparation peuvent également être observées. Ainsi, un élastomère supramoléculaire auto-réparant a été mis au point au

237

laboratoire de Matière Molle et Chimie.[1] Dans ce matériau, les liaisons hydrogène entre molécules de relativement faible masse molaire leur permettent de s'assembler en un réseau tridimensionnel rappelant les polymères réticulés.[1] Les associations formées sont faibles mais nombreuses. Par ailleurs, les propriétés uniques de ces matériaux semblent être fortement influencées par leur nanostructuration pressentie. Cette nanostructuration proviendrait d'une ségrégation entre les groupements à liaisons hydrogène polaires (les « motifs collants ») et les liens apolaires entre ces motifs (les « espaceurs »).[2,3] La ségrégation de phase peut faciliter les liaisons hydrogène en augmentant localement la concentration des motifs collants.[4] De plus, les nanodomaines sont associés à de lents processus de diffusion, comme dans les copolymères à bloc,[5] et jouent un rôle dans la réparation après fracture qui implique une reconstruction de la nanostructure.[2,3] Par ailleurs, ces élastomères auto-cicatrisants sont construits de sorte que la cristallisation des motifs à liaisons hydrogène soit inhibée (en exploitant le désordre des espaceurs). En effet, la cristallisation des motifs collants dans les polymères supramoléculaires est un phénomène courant.[6,7]

Pour examiner les interactions entre les liaisons directionnelles telles que les liaisons hydrogène entre les motifs collants, la ségrégation de phase entre les espaceurs et les motifs collants, et la cristallisation des motifs collants, nous avons choisi d'étudier un système modèle. Ce système consiste en des chaînes non cristallines de poly(oxyde de propylène) (PPO) fonctionnalisées en bout de chaîne par des motifs complémentaires, inspirés des bases de l'ADN : un dérivé de thymine (Thy) et la diaminotriazine (DAT). Ce système combine des liaisons hydrogène faibles (auto-associations Thy-Thy [Schéma A.III.1a] et DAT-DAT

[1] Cordier, P.; Tournhilhac, F.; Soulié-Ziakovic, C.; Leibler, L.; **Self-healing and thermoreversible rubber from supramolecular assembly**; *Nature* **2008**, *451*, 977.

[2] Montarnal, D.; *Mise en oeuvre de liaisons réversibles covalentes et non-covalentes pour de nouveaux matériaux polymères recyclables et retransformables*; PhD Thesis, *Université Paris 6*, **2011**.

[3] Maes, F.; Montarnal, D.; Cantournet, S.; Tournilhac, F.; Corte, L.; Leibler, L.; **Activation and deactivation of self-healing in supramolecular rubbers**; *Soft Matter* **2012**, *8*, 1681.

[4] Sivakova, S.; Bohnsack, D. A.; Mackay, M. E.; Suwanmala, P.; Rowan, S. J.; **Utilization of a Combination of Weak Hydrogen-Bonding Interactions and Phase Segregation to Yield Highly Thermosensitive Supramolecular Polymers**; *J. Am. Chem. Soc.* **2005**, *127*, 18202.

[5] Yokoyama, H.; **Diffusion of block copolymers**; *Mater. Sci. Engineer.: R* **2006**, *53*, 199.

[6] Lillya, C. P.; Baker, R. J.; Hutte, S.; Winter, H. H.; Lin, Y. G.; Shi, J.; Dickinson, L. C.; Chien, J. C. W.; **Linear chain extension through associative termini**; *Macromolecules* **1992**, *25*, 2076.

[7] Wietor, J.-L.; van Beek, D. J. M.; Peters, G. W.; Mendes, E.; Sijbesma, R. P.; **Effects of Branching and Crystallization on Rheology of Polycaprolactone Supramolecular Polymers with Ureidopyrimidinone End Groups**; *Macromolecules* **2011**, *44*, 1211.

[Schéma A.III.1b]) et fortes (association complémentaire Thy-DAT [Schéma A.III.1c]), l'aromaticité des motifs collants, une forte répulsion entre les motifs collants polaires et les espaceurs peu polaires PPO, et des tendances à la cristallisation très différentes pour Thy et DAT. Effectivement, les dérivés de Thy sont sujets à la cristallisation, tandis que les dérivés de DAT sont enclins à former des verres au lieu de cristalliser. Ils forment des agrégats liés par liaisons hydrogène qui ne peuvent s'empiler efficacement du fait de la multiplicité des sites non équivalents de liaisons hydrogène.[8,9] Ce système combine donc plusieurs caractéristiques, et nous nous demandons si l'une prendra le dessus ou si un compromis sera trouvé.
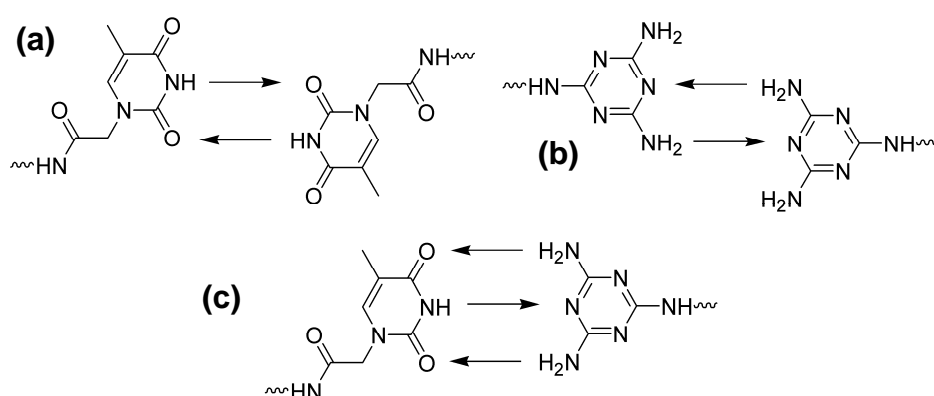
Schéma A.III.1. (a) auto-association Thy-Thy, (b) auto-association DAT-DAT, et (c) association complémentaire Thy-DAT.

Dans cette thèse, nous nous sommes concentrés sur l'étude de la structuration et des propriétés rhéologiques de ce système, en solution et en masse. Dans un premier temps, la synthèse de ces matériaux est présentée. Puis, nous décrivons le comportement de ces polymères supramoléculaires en solution, où l'influence du solvant est cruciale. Ensuite, nous nous intéressons à l'organisation de ces produits en masse. Finalement, nous étudions leur transition vitreuse, avant de conclure.

---

[8] Wang, R.; Pellerin, C.; Lebel, O.; **Role of hydrogen bonding in the formation of glasses by small molecules: a triazine case study**; *J. Mater. Chem.* **2009**, *19*, 2747-2753.

[9] Plante, A.; Mauran, D.; Carvalho, S. P.; Pagé, J. Y. S. D.; Pellerin, C. ; Lebel, O.; **Tg and Rheological Properties of Triazine-Based Molecular Glasses: Incriminating Evidence Against Hydrogen Bonds**; *J. Phys. Chem. B* **2009**, *113*, 14884.

Synthèse de polymères supramoléculaires par greffage de Thy et DAT sur chaînes PPO

Les produits préparés dans le cadre de cette thèse sont des chaînes oligomères de poly(oxyde de propylène) (PPO) fonctionnalisées aux extrémités par un dérivé de thymine (Thy) et/ou de diaminotriazine (DAT). Les chaînes PPO précurseurs sont de faible masse moléculaire et sont notés NH$_2$-PPO-X-NH$_2$ **1a-c** avec X la masse molaire en g.mol^{-1} de la chaîne PPO (**a**: $X = 2200$, **b**: $X = 460$, **c**: $X = 250$).

DAT est greffé par substitution nucléophile aromatique, tandis que Thy est greffé par amidation, par simple chauffage ou à l'aide d'un agent couplant (TBTU). Les composés homoditopiques auto-associatifs sont synthétisés en une étape (pour DAT-PPO-X-DAT **2a-c** : Schéma A.III.2; pour Thy-PPO-X-Thy **3a-c** :Schéma A.III.3). Les mélanges de ces composés en solution permettent d'obtenir après évaporation du solvant ϕ/(100-ϕ)-M-X **4a-c**, **5a**, **6a** (avec ϕ le pourcentage de Thy-PPO-X-Thy **3a-c** et (100-ϕ) celui de DAT-PPO-X-DAT **2a-c** ; **4**: $\phi = 50$, **5**: $\phi = 25$, **6**: $\phi = 75$). Les composés hétéroditopiques (Thy à l'une extrémité et DAT à l'autre) sont synthétisés en trois étapes après une première étape de monoprotection par un groupe protecteur hydrophobe permettant une purification plus aisée (Thy-PPO-X-DAT **10a-c** : Schéma A.III.4).
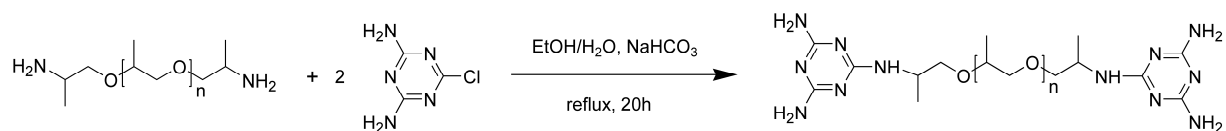
Schéma A.III.2. Synthèse de DAT-PPO-X-DAT **2a-c** *via* une substitution nucléophile aromatique de diamino poly(oxyde de propylène) NH$_2$-PPO-X-NH$_2$ **1a-c** par 2-chloro-4,6-diamino-1,3,5-triazine.
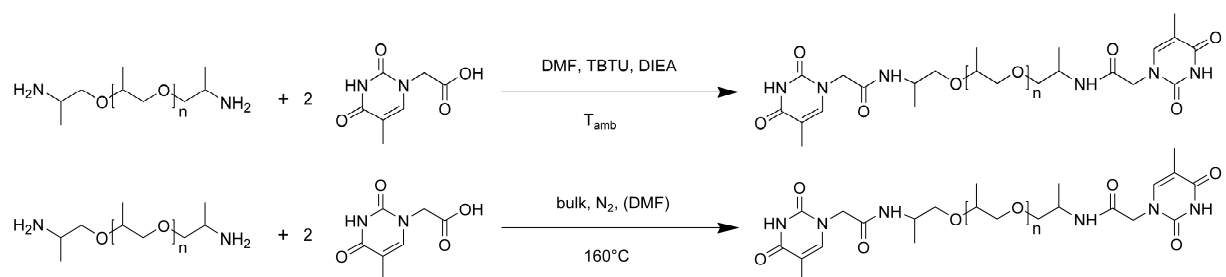
**Schéma A.III.3.** Synthèse de Thy-PPO-X-Thy **3a-c** par amidation de NH$_2$-PPO-X-NH$_2$ **1a-c** par l'acide thymine-1-acétique réalisée (a) en solution avec un agent couplant, ou (b) en masse à 160°C sous azote.
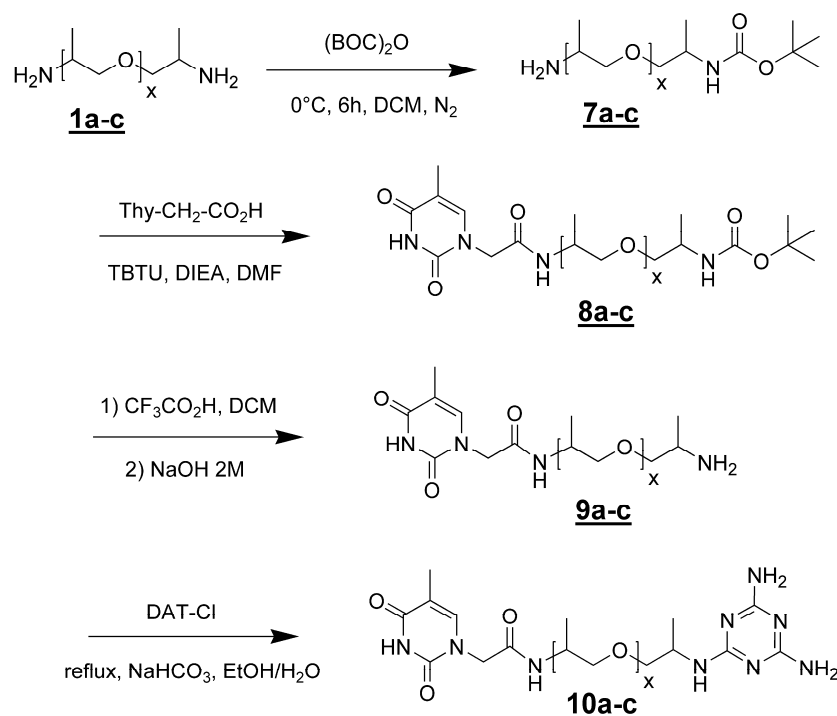
**Schéma A.III.4.** Synthèse des unités hétérotéléchéliques Thy-PPO-*X*-DAT **10a-c**.

Polymères supramoléculaires en solution : comportement dépendant du solvant

Le comportement de nos composés en solution dans trois solvants de différente polarité (DMSO, chloroforme et toluène) a été étudié par des mesures spectroscopiques et rhéologiques (Figure A.III.1). Le solvant influence fortement la valeur des constantes d'association entre les motifs Thy et DAT (Schéma A.III.5, Table A.III.1), ainsi que leur structuration. Le DMSO est un solvant dissociant des liaisons hydrogène entre Thy-DAT, tandis que le chloroforme et le toluène sont des solvants non dissociants à basse température et dissociants à haute température. De plus, le DMSO est un mauvais solvant des chaînes PPO et un bon solvant des motifs Thy et DAT, tandis que le toluène est un mauvais solvant des motifs collants et un bon solvant des chaînes PPO. Par conséquent, nos polymères supramoléculaires semblent former des micelles avec un cœur de PPO et une couronne de Thy, DAT dans le DMSO ; des micelles inverses avec une couronne de PPO et un cœur de Thy, DAT dans le toluène; et des chaînes linéaires par liaisons hydrogène entre Thy et DAT dans le chloroforme (Figure A.III.2). Les différences d'organisation et de constantes d'association ($K_{Thy-DAT}^{25°C,toluene} \approx 22 * K_{Thy-DAT}^{25°C,chloroform}$) entre le toluène et le chloroforme peuvent être

attribuées d'une part, à une meilleure solvatation des motifs collants par le chloroforme et, d'autre part, aux interactions aromatiques entre cycles aromatiques Thy et DAT prenant place dans le toluène, en plus des liaisons hydrogène.
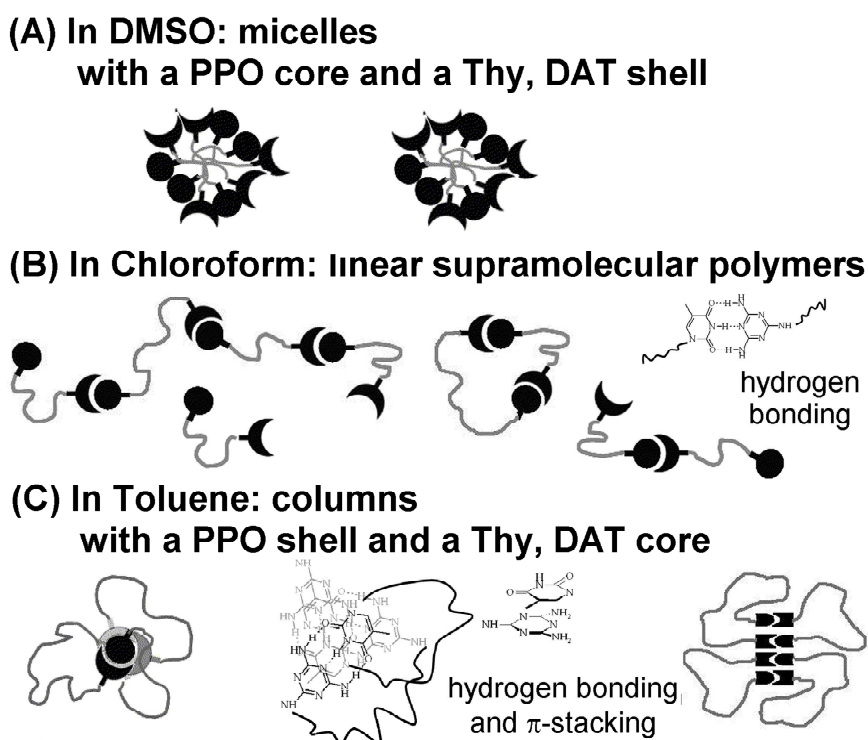
10a	Thy-PPO-2200-DAT
4a	50/50-M-2200
2a	DAT-PPO-2200-DAT
3a	Thy-PPO-2200-Thy
1a	NH2-PPO-2200-NH2
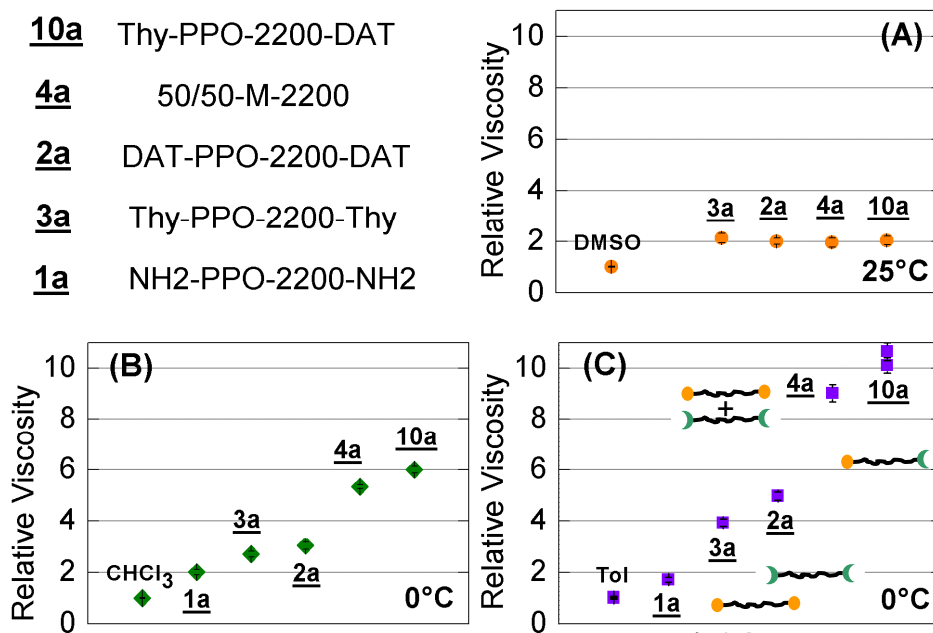
Figure A.III.1. Viscosité relative de solutions à $9.6*10^{-2}$ g/mL de NH_2-PPO-2200-NH_2 **1a**, Thy-PPO-2200-Thy **3a**, DAT-PPO-2200-DAT **2a**, 50/50-M-2200 **4a** et Thy-PPO-2200-DAT **10a**, dans : (A) DMSO à 25°C (à 10%wt), (B) chloroforme à 0°C, and (C) toluène à 0°C.
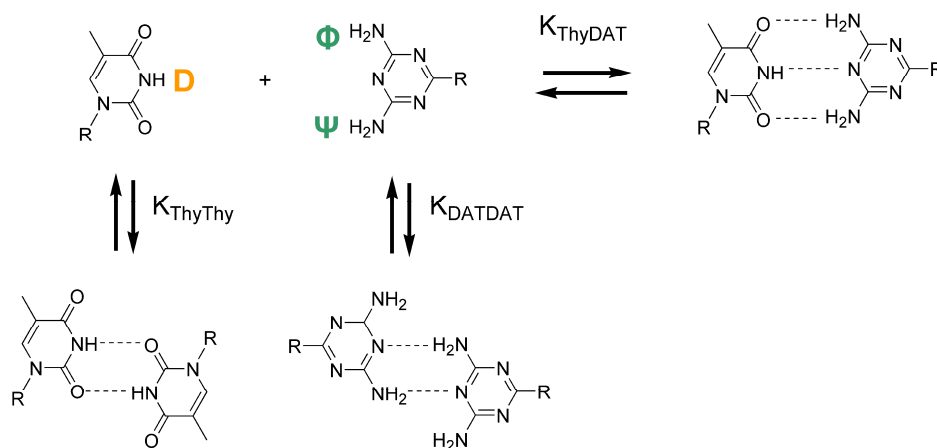
Schéma A.III.5. Définitions des constantes d'associations.

	DMSO-d_6	CDCl$_3$	toluene-d_8
$K_{Thy-Thy}$	-	2.0	26.5
$K_{DAT-DAT}$	-	2.8	42.5
$K_{Thy-DAT}$	1.3	~ 1000	~ 22 000

Table A.III.1. Constantes d'association (en L/mol).

(A) In DMSO: micelles
with a PPO core and a Thy, DAT shell

(B) In Chloroform: linear supramolecular polymers

hydrogen
bonding

(C) In Toluene: columns
with a PPO shell and a Thy, DAT core

hydrogen bonding
and π-stacking

Figure A.III.2. Structuration de Thy-PPO-2200-DAT **10a** dans le : (A) DMSO, (B) chloroforme, (C) toluène.

## *Ordre et désordre dans les polymères supramoléculaires en masse*

Dans les polymères supramoléculaires, les interactions directionnelles contrôlent la connectivité des unités, mais les forces de dispersions et la cristallisation peuvent conduire à des organisations complexes. Ainsi, en masse, les composés Thy-PPO-*X*-Thy **3a-b** présentent un ordre à longue distance à température ambiante and une transition ordre-désordre (ODT) à plus haute température (Figure A.III.3). En-dessous de la température de transition ordre-désordre (T_{ODT}), ces composés sont semicristallins avec une structure lamellaire résultant d'une nano-séparation de phase entre des plans cristallisés de Thy et des couches de PPO amorphes (Schéma A.III. 6). Au-dessus de T_{ODT}, ces composés sont amorphes et homogènes, bien que leur spectre de diffraction des rayons X présente une bande. Cette bande est due à l'effet de trou de corrélation dû au contraste entre les motifs collants et les espaceurs. Macroscopiquement, la transition s'accompagne d'une modification dramatique des propriétés mécaniques et d'écoulement (Figure A.III.5). Quand aux composés DAT-PPO-*X*-DAT **2a-b**, ils sont désordonnés à toute température.
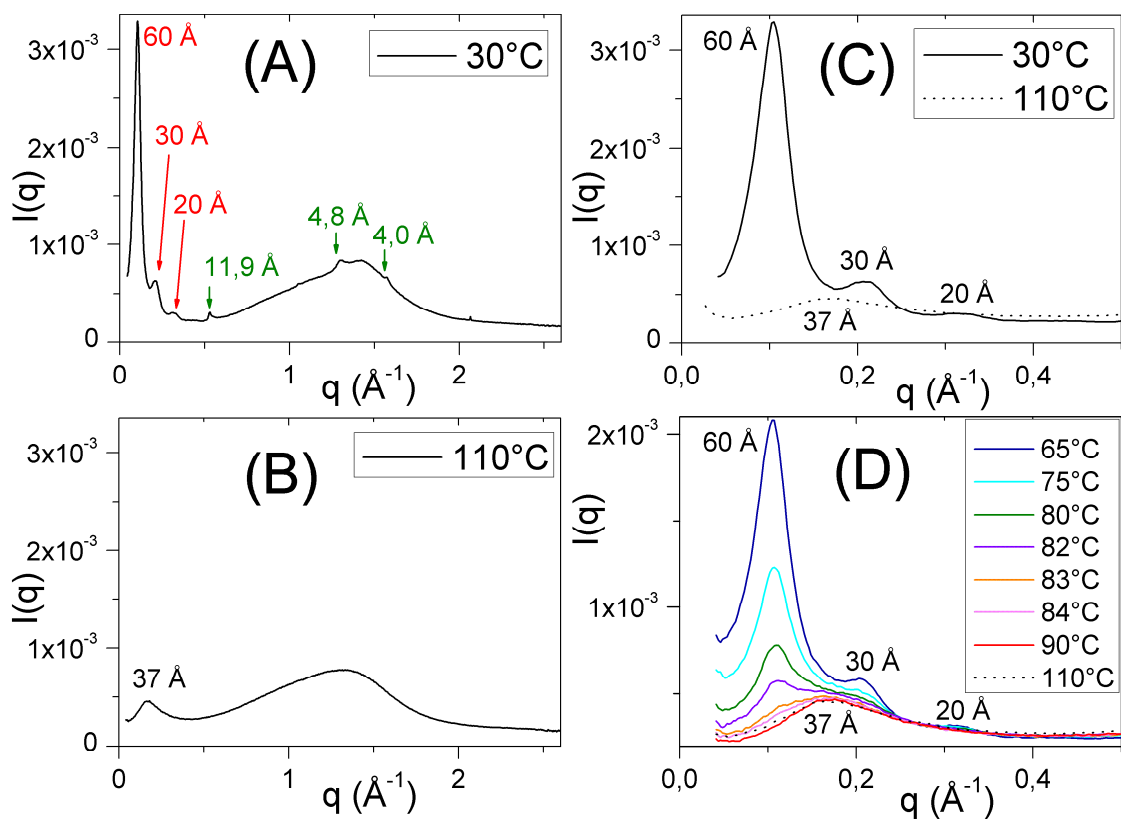
Figure A.III.3. Spectres de diffraction des rayons X de Thy-PPO-2200-Thy **3a** à 30°C (A), 110°C (B); élargissement de la zone faible q à 30°C et 110°C (C) et autour de l'ODT ($T_{ODT} = 85$°C) (D).
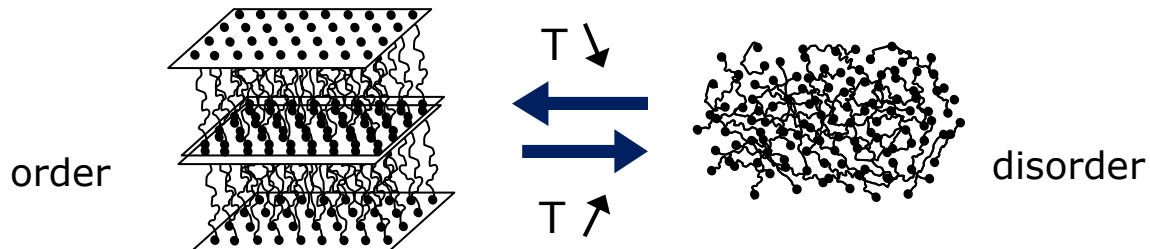
Schéma A.III. 6. ODT: ordre lamellaire et semi-cristallin en-dessous de T_{ODT}, désordre au-dessus de T_{ODT}.
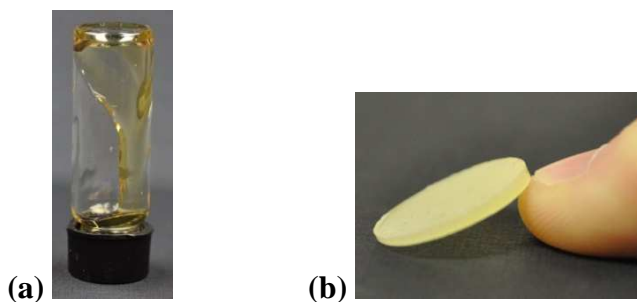
Figure IV.4. Photos de Thy-PPO-2200-Thy **3a** (a) au-dessus de T_{ODT} et (b) en-dessous de T_{ODT}.

Par ailleurs, nous montrons que l'optimisation des interactions directionnelles dans ces systèmes par des associations complémentaires fortes supprime l'ordre mésoscopique. En conséquence, un changement contre-intuitif, au premier abord, des propriétés est observé. En effet, la ségrégation de microphase observée pour Thy-PPO-2200-Thy **3a** est inhibée par ajout de DAT-PPO-2200-DAT **2a** : la forte interaction complémentaire Thy-DAT inhibe la cristallisation de Thy en microdomaines et la structuration en lamelles. Par conséquent, le polymère supramoléculaire basé sur des associations faibles, Thy-PPO-2200-Thy **3a**, est un solide, tandis que le polymère supramoléculaire reposant sur des associations complémentaires fortes, 50/50-M-2200 **4a**, est un liquide (Figure A.III.5). Au-dessus de T_{ODT}, le comportement classique est rétabli, avec une plus forte viscosité de 50/50-M-2200 **4a** par rapport à Thy-PPO-2200-Thy **3a** (Figure A.III.6).
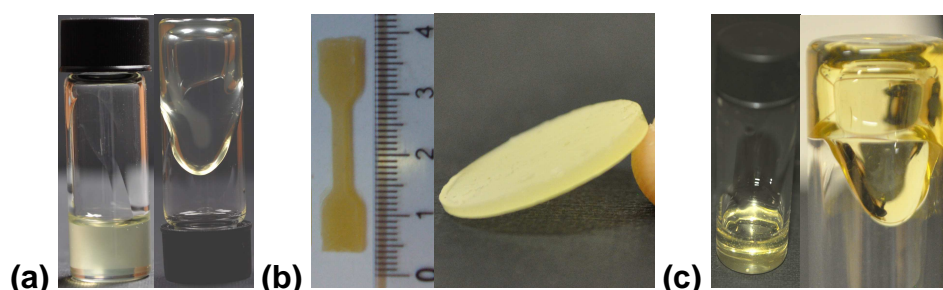

Figure A.III.5. Photos de : (a) DAT-PPO-2200-DAT **2a**, (b) Thy-PPO-2200-Thy **3a**, et (c) 50/50-M-2200 **4a**.
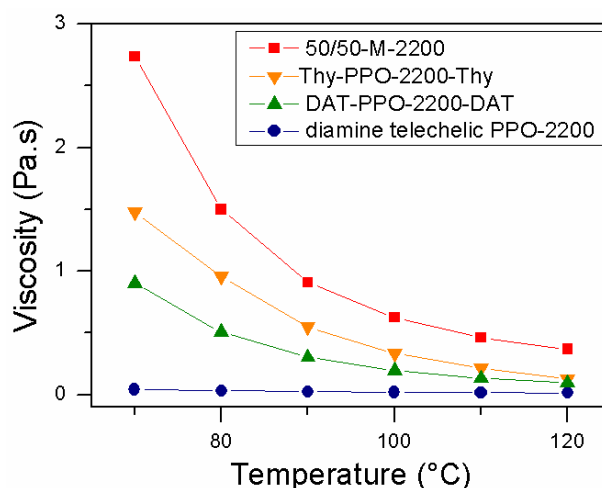

Figure A.III.6. Viscosité en fonction de la température de PPO-2200 **1a**, DAT-PPO-2200-DAT **2a**, Thy-PPO-2200-Thy **3a**, et 50/50-M-2200 **4a**.

Transition vitreuse dans les polymères supramoléculaires en masse

Greffer les motifs Thy et DAT sur des chaînes telecheliques PPO induit une augmentation de la température de transition vitreuse (T_g) d'autant plus grande que la chaîne PPO est courte. Par conséquent, DAT-PPO-*X*-DAT **2b-c**, Thy-PPO-*X*-Thy **3b-c**, et 50/50-M-*X* **4b-c** (**b**: *X* = 460, **c**: *X* = 250) sont solides à température ambiante tandis que 50/50-M-2200 **4a**, Thy-PPO-2200-Thy **3a**, et DAT-PPO-2200-DAT **2a** sont liquides à température ambiante. Cette augmentation de T_g peut être attribuée soit à la présence de liaisons hydrogènes et/ou d'intéraction aromatiques (π-stacking) qui ralentissent la dynamique des chaînes, soit à la rigidité des motifs Thy et DAT.

Conclusion

Finalement, dans cette thèse nous avons étudié, en solution et en masse, un système modèle de polymères supramoléculaires, qui sont cités comme un domaine de recherche de la science macromoléculaire porteur de nombreux défis et opportunités pour la prochaine décennie.[10]

Nous avons montré qu'en solution le solvant influence les constantes d'association et les organisations observées. En masse, un comportement relativement complexe est observé, avec une compétition entre les liaisons hydrogène entre les motifs collants, la ségrégation de phase entre les chaînes espaceurs (peu polaires) et les motifs collants (assez polaires), et la cristallisation des thymines en microdomaines. Ces phénomènes influencent l'organisation mésoscopique de ces matériaux et donc leurs propriétés mécaniques.

Nous avons présenté les différentes organisations observées en solution et en masse, et avons discuté les idées que notre étude apporte pour comprendre les rôles joués respectivement par les liaisons hydrogènes, la ségrégation de phase, la solvatation et la cristallisation.

---

[10] Ober, C. K.; Cheng, S. Z. D.; Hammond, P. T.; Muthukumar, M.; Reichmanis, E.; Wooley, K. L.; Lodge, T. P.; **Research in Macromolecular Science: Challenges and Opportunities for the Next Decade**; *Macromolecules* **2009**, *42*, 465.